The localization of mTORC1 signaling

By

Timothy Richard Peterson
B.S. Biochemistry
University of Michigan-Ann Arbor

SUBMITTED TO THE DEPARTMENT OF BIOLOGY IN PARTIAL FULFILLMENT OF THE REQUIREMENTS FOR THE DEGREE OF

DOCTOR OF PHILOSOPHY IN BIOLOGY
AT THE
MASSACHUSETTS INSTITUTE OF TECHNOLOGY

May 2010
[June 2010]

Signature of Author: _____
Department of Biology
April 30, 2010

Certified by: _____
David M. Sabatini
Member, Whitehead Institute
Associate Professor of Biology
Thesis Supervisor

Accepted by: _____
Stephen P. Bell
Professor of Biology
Chair, Committee for Graduate Studies

The localization of mTORC1 signaling

By

Timothy Richard Peterson

Submitted to the Department of Biology
on May 19, 2010 in Partial Fulfillment of the
Requirements for the Degree of Doctor of Philosophy in Biology

Abstract

Cells sense and respond to their environment by maintaining appropriate activity levels and localizations of key signaling proteins. In eukaryotic cells, cell size is increasingly appreciated as being coordinated by the Target of Rapamycin (TOR) Pathway. TOR is a serine/threonine kinase that resides in two distinct protein complexes which in mammals are referred to as mTORC1 and mTORC2. While significant emphasis has been placed on defining which pathways TOR controls and on how TOR activity is set, less is known about where TOR is positioned or positions its effectors to control growth. In the work described here, we identify and characterize three distinct aspects of the localization of mTORC1 signaling: the redistribution of the mTORC1 effectors, lipin 1 and SREBP, in controlling sterol- and lipogenesis; mTORC1-mediated regulation of actin-myosin contractility during cytokinesis; the regulation of mTORC1 localization in response to amino acids. Through these studies, we provide not only insights into the topology of cell growth, but also reveal how derangements of these localizations might contribute to conditions such as cancer and metabolic disease.

Thesis supervisor: David M. Sabatini
Title: Member, Whitehead Institute; Associate Professor of Biology

Acknowledgements

I remember first e-mailing my thesis advisor, David Sabatini, when I was still in medical school. I had just learned about a rare tumor syndrome, Birt-Hogg-Dube, and became convinced that the pathophysiology underlying this disease involved mTOR. Without knowing who I was, David took immediate interest in me as we discussed this idea as well as other scientific topics. That David was so approachable and enthusiastic about research was pivotal in my decision to apply to graduate school at MIT and is still a powerful memory for me. During my time working with David, his scientific adventurousness has continually inspired me to take on projects which have pushed my knowledge in many exciting and unexpected directions. Though perhaps most importantly, I am grateful to David for setting an example of how to be a rigorous scientist. David has a rare attention to detail that I hope to emulate throughout my scientific career.

Complimenting David's role, I would like to thank the members of my thesis committee– Harvey Lodish and Michael Yaffe. Despite their busy schedules and my frequently changing projects, they have continually provided insightful advice over the last few years that has contributed greatly to the success of my work.

I have many members of the lab to thank for their friendship and collaboration. Mathieu Laplante, for sharing with me a curiosity in DEPTOR and for introducing me to the value in testing ideas on the tangent. Carson Thoreen and Yasemin Sancak, I would like to acknowledge for bonding with me through the Sabatini lab rite of passage, the identification of protein-protein interactions. Tony Kang, whose energy is impressive and whose generosity with his time isn't any less superlative. Kathleen Ottina, for being the lab's steadying presence. And finally, to all the other past and present members of the Sabatini lab, Dos, Xana, Steve, Dave, Nada, Joon-Ho, Shomit, Liron, Nora, Peggy, Heather, Kris, Jan, Jason, Mat, Lahra, Dos, Rob, Doug, Deanna, Kalyani, Do-Hyung, Yoav, Jacob, Pekka, Rich, and Dudley, all of whom have made the lab a great place to work.

When I started at the Whitehead Institute, I was fortunate to meet Thijn Brummelkamp, who was also starting at the Whitehead as a Fellow at the time. I

learned pretty quickly how exceptional Thijn is as a scientist and feel deeply grateful for the mentorship he has provided me over the years.

My parents Deborah and Alan, and my brother David, have always provided the unquestioning support that inspires and allows me to follow my interests. Still, just to be clear, I am done with formal education, I think. I also owe a debt of gratitude to my wife's family: Patty, John, Julie, Lauren, Kim, Lance, who have embraced and supported me truly like a son and brother. I'd also like to thank Grace DaCunha for being my wife's and my family away from home.

Finally, I would not have made it through these last few years without my wife, Melissa. She has endured my increasing application of the scientific method to admittedly too many areas of our lives, and has persevered through many years of long days in lab. She brings me the joy that makes my work possible. I will always be grateful for her devotion.

Table of Contents

Chapter 5

mTORC1 regulates cytokinesis through activation of Rho-ROCK signaling

.

Chapter 6

Future Directions

Chapter 1

I. Introduction to cell growth

Growing cells have the challenge of building the molecules that will comprise them at both the right time and place. The issue of synthesizing the right molecules at the right time and the right place are relevant to seemingly all aspects of a cell's existence: its replication, differentiation, migration, and defense against various insults. One way a cell ensures that a given synthetic pathway occurs at the right time is by synchronizing the levels of the input and output of that pathway. This can be accomplished by coordinating the uptake of a given precursor with the synthesis of its product. It is also challenging to determine the 'right place' for cell growth because molecules can diffuse or, on the other hand, are restricted in space. Compared with eukaryotes, prokaryotes simplify many of these production decisions by being less compartmentalized, e.g., unlike eukaryotes, they lack internal membranes that surround their transcriptional as well as major ATP-producing machinery. That eukaryotes have these membranes suggests that they have likely evolved mechanisms to coordinate their growth across their compartments. Once such key coordinator we discuss the importance of below is the TOR signaling pathway.

II. The TOR pathway

A. The origins of the Target Of Rapamycin (TOR) pathway

The history of TOR signaling originates with the isolation of rapamycin from the bacteria *Streptomyces hygroscopicus* taken from soil samples in Easter Island (Rapa nui) in the 1970s and subsequent attempts to understand the molecular mechanism behind its antifungal (*1*) and anti-tumor properties (*2*). The discovery that rapamycin is also a potent immunosuppressant with low toxicity (*3*) accelerated investigation of this molecule. The budding yeast, *Saccharomyces cerevisiae,* was a key tool for unlocking

the first major mystery of how rapamycin works. To identify intracellular targets of rapamycin, two groups conducted mutagenesis screens for mutations that conferred resistance to the G1 arrest caused by rapamycin (*4, 5*). Both groups identified mutations in FPR1, the homologue for the mammalian FKBP12, though the observation that loss of FPR1 had no obvious consequences made it not likely to be the sole target of rapamycin. The other two classes of mutations were dominant gain-of-function defects in two similar genes, which were named the target of rapamycin (TOR1 and TOR2).

Although this work established a solid rationale for the TOR proteins as the direct targets of rapamycin, that idea wasn't elucidated until a few years later. In independent approaches to isolate proteins which interact with the FKBP12-rapamycin complex, several groups identified a large protein with homology to the yeast TORs (*6-9*). This protein was given several names upon its discovery, including FRAP, RAFT1, and RAPT1, but is now referred to simply as mammalian TOR, or mTOR. The high degree of sequence similarity between the mammalian and yeast homologues provided an early indication that many of features of TOR signaling were preserved between these highly diverged species.

Despite its catalytic site having strong sequence similarity to the better known at the time lipid kinase, phosphatidylinositide 3-kinase (PI3K), it was soon realized that TOR is a protein kinase. This was first suggested by experiments which showed that mTOR autophosphorylates in a rapamycin-sensitive manner (*10, 11*). Comparison of the genomes of divergent species further revealed that TOR belongs to a family of PI3K-related, protein kinases (PIKK) that includes ATM, ATR, DNA-PK and SMG1 (*12*). The similarity between the PIKKs is concentrated in their C-terminal kinase domains, which is similar to the kinase domain of PI3K and gives this family its name.

B. Components of the TOR complexes, TORC1 and TORC2

In large part to rapamycin, our understanding of TOR signaling has progressed quickly since the discovery of the TOR genes over almost two decades ago. Since then, one of the most revealing features of TOR signaling is that has separable functions which are attributable to two physically distinct complexes, called TORC1 and TORC2 (mTORC1 and mTORC2 in mammalian cells). The early genetic studies of TOR

function hinted at this complexity. Loss of TOR1 severely hindered cell growth, but it failed to recapitulate the G1 arrest caused by rapamycin treatment (*13*). By contrast, TOR2 was found to be an essential gene and its deletion caused a random cell cycle arrest (*13*). Curiously, the combined deletion of TOR1 and TOR2 caused a G1 arrest that was similar to rapamycin treatment (*13*). Later work showing that rapamycin-resistant alleles of TOR1 could support normal growth in the presence of rapamycin suggested that the essential function of TOR2 was rapamycin-insensitive (*14*). While these studies of TOR2 gave us early hints of rapamycin-insensitive functionality in TOR signaling, it was the biochemical purification of TORC1- and TORC2-specific binding partners that provided the key evidence to support this claim (*15, 16*). Fittingly, only one complex, TORC1, was shown to bind the rapamycin-FKBP12 complex, and these two complexes are now often referred to as the rapamycin-sensitive and rapamycin-insensitive pathways (*15, 16*).

mTORC1 has four components in addition to mTOR (Fig. 1): regulatory associated protein of mTOR (raptor); mammalian lethal with Sec13 protein 8 (mLST8, also known as GβL); proline-rich AKT substrate 40 kDa (PRAS40); and DEP-domain-containing 6 mTOR interacting protein (DEPTOR, also known as DEPDC6). The functional role for each of these proteins within mTORC1 is being actively researched. Raptor is crucial for mTORC1 assembly and is thought to recruit mTORC1 substrates such as the translational regulators, S6 kinase 1 (S6K1) and the eIF4E-binding protein 1 (4E-BP1) (*17-19*). The role of mLST8 in mTORC1 remains unclear, for deletion of the gene has no affect on mTORC1 activity *in vivo* (*20, 21*). PRAS40 and DEPTOR both inhibit mTORC1 kinase activity, though their modes of inhibition likely differ (*22-25*) (Chapter 3).

Regarding the conservation of TORC1 components, in some species of yeast including S. cerevisiae, TORC1 contains two TOR proteins, TOR1 and TOR2, whereas most other eukaryotes contain only one TOR protein (*26*). Homologs of raptor, mTOR, and mLST8 are present in all eukaryotes. PRAS40 and DEPTOR homologs are found as early in evolution as Arthropoda and Chordata, respectively (*26*)(Chapter 3). On the other hand, in yeast, TORC1 contains TCO89 which does not appear to be conserved in higher eukaryotes.

mTORC2 shares several proteins with mTORC1 such as mTOR, mLST8 and DEPTOR (Fig. 1). However, mTORC2 also contains several unique components: rapamycin insensitive companion of mTOR (rictor), stress-activated protein kinase interacting protein (SIN1), and protein observed with Rictor-1 (Protor-1), which is also known as PRR5 or PRRL5. Rictor, SIN1, mLST8 stabilize each other and are required for mTORC2 to phoshorylate the substrate, Akt/PKB (*21, 27, 28*). To date, there has been no unified mTORC2 function ascribed to Protor-1/PRR5/PRR5L other than its interaction with mTORC2 components (*29-31*). Similar to its effects on mTORC1, DEPTOR serves as an inhibitor of mTORC2 (Chapter 3). All mTORC2 components with the exception of DEPTOR have clear homologs in yeast (*26*).

The research results described in this thesis primarily focus on mTORC1 biology, therefore the remainder of the introduction will focus on the signaling upstream and downstream of mTORC1, as well as its role in growth, metabolism and disease.

C. TORC1 prologue

The defining member of the TORC1 complex is referred to as raptor in mammals and kog1 or mip1 in yeast. The first reference to the function of this gene was in S. *pombe,* were it was characterized in a screen for high-copy suppressors of ectopic meiosis caused by expression of the meiotic regulator mei2 (*32*). Mei2p normally induces meiosis only in response to starvation conditions, and loss of Mip1p interfered with this process. However, it was not until the identification of the human homologue, raptor, by immunoprecipitation and mass-spectrometry that this protein was associated with TOR signaling (*17, 18*). Soon after, the raptor homolog kog1p was found to associate with both TOR1 and TOR2, thus defining TORC1 in budding yeast (*15*). In cells, raptor has a clear positive role in mTORC1 activity, and depletion of it by RNAi leads to inhibition of downstream targets, S6K1 and 4E-BP1, similar to rapamycin treatment (*17, 18*). Interestingly, TORC1 is known to have activity towards S6K1 *in vitro* even in the absence of raptor (*33*). Although potentially an artifact, this observation suggests that raptor might activate mTOR in cells through a mechanism that doesn't directly alter its kinase activity, such as localization or substrate recognition. On the subject of substrate binding, several groups have suggested that a conserved, short

TOR-signaling (TOS) motif which appears in many TORC1 substrates is key for their recognition by raptor (*19, 34*).

mTORC1 also contains three other components: mLST8/GβL and DEPTOR, which bind directly to mTOR, and PRAS40, which binds raptor. mLST8/GβL was first identified as a TORC1 component in budding yeast (*15*) and shortly after in mammalian cells (*20*). Although there is some debate concerning the function of mLST8 in mammalian cells, in yeast, LST8 has been shown to negatively regulate amino acid biosynthesis and uptake, phenocopying some of the effects of rapamycin (*35*).

PRAS40 and DEPTOR are the most recently described mTORC1 components. PRAS40 was recently identified as a raptor-binding protein and a negative regulator of the pathway (*22, 23*). Its homolog in the fruit fly, *Drosophila melanogaster*, Lobe, has long been known to regulate developmental processes (*36*), but if and how those phenotypes might connect with TORC1 signaling has only been recently begun to be assessed (*37*). A more detailed discussion of the functions of DEPTOR and the signaling downstream of TORC1 follows in later sections.

D. On the activation of TORC1

TORC1 is controlled by a constellation of signals that reflect the overall metabolic state of the cell. Most famously, TORC1 is thought to act as an intracellular sensor of nitrogen availability. However, numerous inputs including glucose sufficiency, oxygen availability, energy status, membrane composition, and in metazoans, growth factors such as insulin, have been shown be potently regulate TORC1 output (*38*). Impressively, all of these inputs likely converge upon the heterodimer Tuberous Sclerosis Complex (consisting of TSC1, also known as hamartin; and TSC2, also known as tuberin) and the small GTPase Rheb (Ras homolog enriched in brain).

Rheb was first associated with cell growth in *S. pombe*, where its loss causes a growth arrest with a terminal phenotype similar to that caused by nitrogen starvation (*39*). However, it was studies in *Drosophila melanogaster* and mammalian cells which directly connected Rheb and TSC1/2 genes to the TOR pathway (*40-44*). How Rheb and TSC1/2 act on TORC1 has recently begun to be elucidated. The TSC1/2 heterodimer catalyzes the conversion of Rheb-GTP to Rheb-GDP Rheb, and in its GTP-

bound state, Rheb directly binds and activates mTORC1 (*23, 45, 46*). Only the TSC2 protein contains a GAP domain, but its activity toward mTORC1 is dependent on its association with TSC1, perhaps by localizing TSC2 to endomembranes where Rheb resides (*47-50*).

Kinases stimulated by upstream signals such as insulin or glucose regulate mTORC1 by phosphorylating a collection of sites on TSC2 and/or raptor (*51-55*). The effects of these phosphorylations have been shown or are presumed to change of the activities of the TSC1/2 or mTORC1 complexes, respectively thereby regulating S6K and 4E-BP1 phosphorylation. One of the kinases that acts on TSC2 is the PI3K-regulated kinase, Akt, which phosphorylates TSC2 in response to insulin (*51, 52*). This phosphorylation is thought to provide a critical piece of the mechanism by which this growth factor stimulates mTORC1. More recently, this mechanism has been elucidated further by Cai et al. who show that TSC2 phosphorylation by Akt maintains the GTP-bound state of Rheb by dissociating TSC2 from membranes where Rheb resides (*50*). AMPK, which is activated by rising intracellular AMP in response to glucose deprivation or energetic stress, also phosphorylates TSC2 and raptor and regulates mTORC1 activity (*54, 55*). Under what circumstances this kinase acts on either or both of these mTORC1 pathway components is not yet well understood.

Lastly, the *Drosophila* hypoxia-induced proteins, Scylla and Charybdis, as well as the Scylla mammalian homolog Redd1/RTP801 are also thought to act on the TSC1/2 complex to inhibit TORC1 (*56*) (*57*). Recently it has been posited that Redd1 might inhibit mTORC1 by controlling the release of TSC2 from its growth-factor-induced association with 14-3-3 proteins (*58, 59*).

Despite many attempts to connect amino acids to TORC1 through any of the aforementioned upstream regulators, the view on this longstanding question remains murky. For instance, some groups had proposed that loss of TSC1 and TSC2 rendered TORC1 signaling resistant to amino acid deprivation (*41*). However, it is now widely believed that, although loss of TSC1/2 hyperactivates TORC1 signaling and can overcome the effects of growth factor withdrawal, it cannot overcome the effects of amino acid deprivation (*60*) (*61*). Other groups have shown that overexpression of Rheb can overcome the effects of amino acid starvation on mTORC1 signaling in cultured

cells and that overexpression in drosophila embryonic tissue causes overgrowth regardless of amino acid availability (*43*). However, these results are complicated by the likelihood that ectopic overexpression of Rheb might not reflect a physiological state comparable to the manipulation of intracellular amino acid levels. Moreover, it is worth noting that TORC1 signaling is strongly regulated by amino acids in S. cerevisiae despite the lack of TSC1/2 homologs and that the loss of Rheb in this species does not cause as significant a growth defect as it does in most other organisms (*62*). These results suggest that if the sensory mechanism were to be conserved, it likely involves additional or distinct pathways from the TSC/Rheb axis.

One attractive candidate amino acid-regulated pathway that is conserved in S. cerevisiae is the vacuolar membrane-associated protein complex (EGO), composed of EGO1, EGO3 and the GTPases Gtr1 and Gtr2 (*63, 64*). This complex has been shown to be required for the resumption of growth following a rapamycin-induced G1 arrest (*63*) and to have synthetic interactions with a TOR1 mutation (*64*). Moreover, comparable to the effects of amino acid starvation, Gtr1 and Gtr2 are known to regulate the sorting of the general amino acid permease Gap1p (*65, 66*). Dubouloz et al. suggested that the EGO proteins might act upstream of TORC1 in amino acid sensing because diverse readouts which are negatively controlled by TORC1, e.g., glycogen accumulation, phosphorylation of eIF2α on Ser 51, and macroautophagy, depend on the presence of Ego1, Gtr2, and Ego3 during recovery from rapamycin treatment for resetting to their initial status. In further support of this idea, overproduction of Gtr2 or Ego3 enhances rapamycin resistance (*63*) and an engineered molecule that was found to bind Ego3 directly in cells could overcome the effects of rapamycin, possibly by causing a gain of function of Ego3 (*67*).

III. TORC1 controls growth-associated processes

A. TORC1, protein synthesis, and ribosome biogenesis

Studies in mammalian cells on the cell cycle inhibitory effects of rapamycin first suggested the signaling cascade that is perhaps most commonly associated with TOR,

i.e., the regulation of protein synthesis through p70 S6 kinase (a 70kDa protein also known as S6K). S6K received its name fittingly after being found to be a major kinase of the ribosomal protein, S6 (*68*). S6, is a protein of the 40s ribosomal subunit long known to be phosphorylated upon stimulation of cells with mitogens (e.g., growth promoting stimuli that are present in serum including insulin, EGF, IL-2, erythropoietin) (*69*). mTOR came into the protein synthesis picture when rapamycin was shown to prevent the phosphorylation and activation of S6K (*70-74*). In addition to growth factors, depletion of amino acids from cells profoundly inhibits protein synthesis (*75*). Therefore, it was an exciting discovery that rapamycin also abolished amino acid stimulation of S6K phosphorylation and activation (*76*).

As with short term fasting in animals (where growth factors such as insulin become depleted from the blood) (*77*), amino acid withdrawal from cells is characterized by a loss of polysomes and an increase in monomeric ribosomes (*78, 79*). These findings both point to growth factors and nutrients controlling translation at its initiation. The rapamycin-sensitive S6K pathway is thought to participate in regulating translation initiation by controlling the translational efficiency of a specific subset of transcripts, namely elongation factor and ribosomal protein mRNAs which possess an unusual pyrimidine-rich sequence at their 5′ end, referred to as a 5′ TOP (terminal oligopyrimidine) (*80-82*). In addition to its role in 5' TOP-mediated translation, mTORC1-S6K signaling has also recently been shown to control translation by regulating pre-mRNA splicing (*83*).

mTORC1 regulates S6K by directly phosphorylating it on a highly conserved residue, threonine 389, that is essential for its activity (*84, 85*). Recently, Sch9 was shown to be a direct substrate of TORC1 and thus likely represents the yeast S6K homolog (*86*). Regarding the localization of Sch9, it has been shown to be enriched at the vacuole (*87, 88*), which interestingly, is a cellular compartment in eukaryotic cells that serves as the major storage vesicle of amino acids (*89*). However, how Sch9 localizes to this compartment is still not well understood.

Entry of yeast cells into the G0 or stationary phase in cells lacking TOR function is accompanied by loss of cell proliferation including a reduction in translation initiation. That loss of TOR function is suppressed by altering the translational control of the G1

cyclin, CLN3, suggested that TOR likely controls G1 progression by regulating translation initiation (*90*). Subsequent investigation into the effects of TOR on CLN3 centered on the translation initiation factor, eIF4E. The justification for this is because CDC33 (eIF4E) and TOR mutants are known to have remarkably similar phenotypes, including a G1-specific function as well as an essential function that is not G1 specific (*90*). Also, in mammalian cells, similar to that found with S6K, rapamycin was shown to block the serum-stimulated phosphorylation of a key repressor of eIF4E-mediated translation, eIF4E-binding protein 1 (4E-BP1/PHAS-I) (*91, 92*). The phosphorylation of 4E-BP1 controls cap-dependent translation of mRNAs with extensive secondary structure including the G1-regulating, CLN3 homolog, cyclin D1 (*93-95*). Initiation factor 4F complexes with these mRNAs through the interaction of its eIF-4G subunit with eIF-4E, which is the cap-binding protein that recognizes the N^7-methyl-GpppN structure of the 5′ end of all nonorganellar mRNAs. In quiescent cells, 4E-BP1 competes with eIF-4G for binding to eIF-4E and represses translation by displacing the initiation factor 4F from the mRNA. Growth stimuli activate phosphorylation of 4E-BP1, which decreases its affinity for eIF-4E and releases the block on cap-dependent translation (*95*). Interestingly, regulation of 4E-BP1 phosphorylation by serum starvation or rapamycin treatment has been shown to redistribution of eIF4E from the cytoplasm to the nucleus (*96*). However, the significance of this regulation in translational control has not yet been investigated.

Regarding the mechanism of 4E-BP1 phosphorylation, mTORC1 has been shown to direct phosphorylate 4E-BP1 on multiple residues, including threonines 37 and 46 (T37/T46) (*84, 97*). The significance of mTORC1 in regulating translation via 4E-BP1 is highlighted by the finding that the T37/T46 residues are critical for its association with eIF4E (*98*). Interestingly, mTORC1 kinase activity towards 4E-BP1 has been shown to be aided by its increased binding to raptor in mTORC1 (*99*). Because S6K has not been demonstrated to interact with mTORC1 in a similar manner, it remains to be determined whether or not this finding will apply to other mTORC1 substrates.

In addition to controlling translation initiation, TORC1 is known to regulate ribosome biogenesis (*100*), which refers to the transcription of ribosomal protein and rRNA genes. TORC1 regulates the expression of these genes by controlling the

nuclear-cytoplasmic translocation of multiple transcriptional regulators, including Sfp1 and CRF1, which in the absence of TORC1 function, are recruited or prevented from interacting with, respectively, the promoters of ribosomal and/or rRNA genes (*101, 102*). TORC1 controls CRF1 indirectly by repressing the activity of the PKA target, YAK1, whose phosphorylation of CRF1 promotes its nuclear accumulation (*102*). The mechanism of Sfp1 translocation was recently explored by Lempianinen et al. (*103*). In contrast to CRF1, Sfp1 localization is regulated by its direct interact with TORC1 in a manner dependent on TORC1-catalyzed phosphorylation (*103*).

Because of their functional similarities, the protooncogene, c-myc, is thought to be the homolog of Sfp1 in multicellular eukaryotes (*104*). Notably, c-myc has previously been functionally linked to mTORC1 signaling and its overexpression increases cell size and increased ribosomal and nucleolar gene expression similar to that of Sfp1 overexpresion (*88, 105, 106*).

B. TORC1 and autophagy

Considering the prevalence of feedback loops in biological systems, it is intuitive to think that because TORC1 promotes protein synthesis it would also inhibit protein degradation. Indeed, when TORC1 activity is reduced in cells, organelles and proteins are degraded en masse via a catabolic processed termed autophagy (*107*). Autophagy involves the *de novo* synthesis of membrane bound vesicles, termed autophagosomes, which sequester intra-cellular components and deliver them to the vacuole/lysosomes via membrane fusion. Vacuole/lysosomal degradation of these components liberate biological material to sustain macromolecule biosynthesis and energy production. The inhibition of TORC1 by inactivation of TORC1 components, amino acid deprivation, or rapamycin treatment triggers autophagy, whereas stimulation of TORC1 prevents this process (*108*). Analogous to the mechanism of TORC1-mediated 4E-BP1 phosphorylation and activation of translation, TORC1 represses autophagy by binding and/or directly phosphorylating multiple components of a protein complex that initiates autophagosome formation, unc-51-like kinase 1 (ULK1, Atg1/Apg1 in yeast), autophagy-related gene 13 (ATG13, Atg13/Apg13 in yeast), and focal adhesion kinase [FAK] family-interacting protein of 200 kDa (FIP200, Atg17/Apg17 in yeast) (*109-114*).

C. TORC1 regulates sterol-lipogenesis

In one of the first studies into the antifungal properties of rapamycin in *C. albicans*, it was noted that this agent prevented the synthesis of lipids from the carbon-containing precursor, acetate (*1*). Another early work pertaining to the role of TORC1 in lipogenesis found that during amino acid starvation of fruit fly larvae, lipids mobilized from adipose cells of the larval fat body became visible as lipid vesicle aggregates and that this effect was indistinguishable from that caused by loss of the *Drosophila* TOR homolog, dTOR (*115*). Despite these interesting findings, a thorough demonstration of the involvement of TORC1 in lipid synthesis has only more recently been made. It was shown in mammalian cells that Akt-dependent lipogenesis requires positive input from mTORC1 to control *de novo* lipid synthesis as well as the levels of sterol regulatory element binding protein 1 (SREBP1) (*116*). SREBP1 is a member of a transcription factor family that plays a critical role in promoting fatty acid and cholesterol biosynthetic gene expression (*117*). Further stating a case for SREBP functioning as a conserved growth regulator, Porstmann et al. found that silencing of the *Drosophila* homolog of SREBP, dSREBP1, results in reduced cell and organ size in a manner refractory to dPI3K-induced growth (*116*).

Conversion of mouse 3T3-LI preadipocytes (fibroblasts) to fully developed adipocytes under the influence of dexamethasone, 1-methyl-3-isobutyl xanthine, and insulin has been an invaluable approach to investigate differentiation-related changes in lipid metabolism (*118, 119*). In this system, inhibition of either mTORC1 by rapamycin or amino acid deprivation inhibits 3T3-L1 preadipocyte differentiation by suppressing the expression and transactivation activity of peroxisome proliferator activated receptor-gamma (PPARγ)- a master regulator of adipogenesis (*120, 121*). Additionally, rapamycin has been shown to reduce the phosphorylation of lipin-1 (*122*), a phosphatidic acid (PA) phosphatase that is key for preadipocyte differentiation, likely due to its coactivation of many transcription factors linked to lipid metabolism, including PPARγ, peroxisome proliferator-activated receptor-alpha (PPARα), and peroxisome proliferative activated receptor gamma coactivator-alpha (PGC1α) (*123*). Consistent with lipin 1 having a conserved key role in sterol and lipid homeostasis, mutation of its

S. cerevisiae homolog, Pah1, have been shown to strongly perturb intracellular neutral lipid and phospholipid levels in stationary and active growing cells (*124*).

The ability of yeast to sense the availability of inositol and to adjust the expression of genes required for lipid biosynthesis, in particular the *INO1* gene, has been studied as a model for the integration of transcriptional signaling pathways. The *INO1* gene encodes inositol-1-phosphate synthase, which converts glucose-6-phosphate to inositol-1-phosphate for its subsequent use in phospholipid synthesis (*125, 126*). Consistent with a role for TORC1 in promoting phospholipid synthesis, rapamycin represses INO1 expression (*127*). Also, deletion of the S. cerevisiae lipin 1 homolog, Pah1/smp2, or the phosphatase complex which is known to dephosphorylates Pah1/smp2, Nem1/Spo7, promotes INO1 expression (*124, 128*). That deletion of either Nem1 or Spo7 confers rapamycin sensitivity suggest that TORC1 might have a conserved role in regulating lipin 1/Pah1 phosphorylation (*129*). However, whether lipin-1/Pah1 are direct substrates of mTORC1/TORC1 and whether lipin-1/Pah1 might regulate the aforementioned lipid-regulating transcriptional regulators in a manner dependent on mTORC1/TORC1 is still unclear.

D. TORC1 and the cytoskeleton

Tor1p and Tor2p, both present in TORC1, are kinase homologs which have structurally and functionally similar, but not identical functions (*130*). One critical Tor2p-unique activity is known to be signaling to components required for proper remodeling of actin and the integrity of the cell wall (*131-134*). These components include the Rho1p GTPase and its associated regulatory partners Rom2p and Sac7p, which function in part by regulating protein kinase C (Pkc1p), an upstream activator of the mitogen-activated protein kinase (MAPK) Slt2p/Mpk1p. Because the Tor2p-dependent actin and cell wall phenotypes found in this early work were rapamycin-insensitive, much of the attention on the Tor2p-Rho1p-actin cascade subsequently focused on TORC2 (*135, 136*). However, more recently, the role of TORC1 in regulating cell structure has begun to receive some attention. Using a combined proteomic and genomic approach, it was found that a large number of yeast genes involved in actin polarization possessed altered sensitivities to inhibition of the TORC1 components, TOR1 and TCO89 (*137*).

Also as rapamycin treatment and inhibition of the TORC1-controlled, Tap42p/Sit4p phosphatase system were recently shown to alter actin polarization and cell wall integrity, in contrast to previous reports, the role of the TORC1 in controlling the cytoskeleton remains controversial (*138, 139*).

There is also evidence in mammalian cells that TORC1-relevant inputs, such as amino acids, rapamycin, and raptor regulate various aspects of actin organization (*140-142*). As with yeast, a common effector in these processes is thought to be the Rho pathway. However, the involvement of Rho in mediating these mTORC1-dependent effects has yet to be functionally tested.

Mitosis and cytokinesis rely heavily on cytoskeletal rearrangements to coordinate cleavage of the cytoplasm of a dividing cell (*143, 144*). While the role of TORC2 in completing the cell cycle has begun to be directly addressed (*145*), this information on TORC1 is still largely through inference. The inhibition of translation observed during mitosis results from a global decrease in cap-dependent translation, however the cap-independent translation of some mRNAs are upregulated (*146, 147*). Wilker et al. showed that a defective switch in this mechanism results in reduced mitotic-specific expression of the endogenous internal ribosomal entry site (IRES)-dependent form of the cyclin-dependent kinase Cdk11 (p58 PITSLRE) (*148*). PITLSRE is known to regulate the cytoskeleton by promoting centrosome maturation and bipolar spindle formation (*149, 150*). That TORC1 might be important in these PITLSRE-dependent cytoskeletal events was suggested by the finding that impairing PITLSRE translation during mitosis lead to impaired cytokinesis and the accumulation of binucleate cells, both of which can be rescued using rapamycin (*148*). Additional observations of a putative important role for TORC1 in regulating centrosomes and the mitotic spindle have likewise been made only recently (*151, 152*).

E. TORC1 and mitochondria

Given that the bulk of cellular ATP synthesis occurs in the mitochondria, and that anabolic processes require significant energy consumption, the notion that mTORC1 regulates mitochondrial metabolism is not surprising. Inhibition of mTORC1 by rapamycin lowers mitochondrial membrane potential, oxygen consumption and cellular

ATP levels, and profoundly alters the mitochondrial phosphoproteome (*153*). Conversely, hyper-activation of mTORC1 results in increased expression of PGC-1∝, which is known to promote increased mitochondrial abundance (as measured by mitochondrial DNA copy number), as well as the expression of many genes encoding proteins involved in oxidative metabolism (*154*). Additionally, conditional deletion of raptor in the skeletal muscle of mice reduces the expression of genes involved in mitochondrial biogenesis (*155*).

While PGC-1α lacks an obvious homolog in yeast, it is clear that TOR pathway is a conserved important determinant of mitochondrial function. *In S. cerevisiae*, regulators of TORC1 signaling (i.e., TOR1/2, LST8, rapamycin) control the transcription of specific tricarboxylic acid (TCA) and glyoxylate cycle genes through a circuit referred to as the retrograde (RTG) pathway (*156*). As early reactions of the tricarboxylic acid cycle, retrograde gene products (encoded by the *CIT2, ACO1, IDH1/2*, and *DLD3 genes*) are particularly involved in regulating the balance of carbon and nitrogen utilization by cells. TOR and nutrient based signals are thought to interface with the RTG system by controlling the phosphorylation and/or nuclear-cytoplasmic distribution of multiple RTG gene transcriptional regulators: RTG1, RTG2, RTG3, and Mks1 (*156*). For example, rapamycin treatment of cells grown under rich nutrient conditions causes Rtg1p and Rtg3p proteins to translocate from the cytoplasm into the nucleus and activate their target genes (*157, 158*). Several proteins have been identified that are important for these TORC1-regulated nucleocytoplasmic trafficking events, including two cytoplasmic proteins, Rtg2p (*157-159*) and Mks1p (*158, 160, 161*). Dynamic interactions between Rtg2p and Mks1p that involve TORC1-mediated, Mks1 phosphorylation-dependent interactions with Bmh1p and Bmh2p, the latter being the yeast homologues of mammalian 14-3-3 proteins, play critical roles in regulating the localization and activity of the Rtg1p·Rtg3p complex (*162, 163*).

Because the glyoxylate cycle, which is an anabolic pathway that allows yeast, plants, and several microorganisms to use fats for carbohydrate synthesis, is thought to be absent in most animals (*164*), the conserved relevance of RTG pathway to TORC1 signaling has remained ambiguous. Regardless, that genetic screens continue to detect many of these RTG enzymes as synthetic interactors with TORC1 signaling

components suggests that continued dissection of the relationship between these systems is warranted (*165*).

F. TORC1 and protein sorting

The delivery to the plasma membrane of the general amino acid permease, Gap1p, of Saccharomyces cerevisiae is regulated by the quality of the nitrogen source in the growth medium. Gap1p sorting is thought to occur at either the endosome or trans-Golgi compartments (*166, 167*) and one major class of mutations that influences Gap1p sorting is known to be in ubiquitination genes (*168, 169*). Because polyubiquitination of Gap1p is a signal for its sorting to the vacuole, mutation of genes required for Gap1p polyubiquitination (e.g., *bul1 bul2*, *rsp5*, or *doa4*) causes Gap1p to be sorted to the plasma membrane more efficiently. While rapamycin curiously does not regulate GAP1p sorting, mutations in the TORC1 pathway components, Lst8 and the EGO complex do, though in the case of the EGO complex there are clearly strain-specific effects (*66, 166, 170*). Gln3 is also sorted in an TORC1- and ubiquitin-dependent manner. This regulation occurs through a phosphorylation cascade involving TOR, SIT4, Npr1, and Rsp5 whose details are still under investigation (*171-173*) (*174*).

TORC1 also appears to regulate microtubule-dependent protein trafficking. TSC2 deficient mouse cells alters the distribution of several proteins whose microtubule-based trafficking has been well-studied, VSV-g, caveolin, and GLUT4 (*175-177*). Though it is thought that mTORC1 controls this trafficking through the microtubule associated protein, CLIP-170/Restin, and that in yeast TORC1 controls the CLIP-170 homolog, Bik1p, in regulating nuclear positioning, (*178, 179*), delineation of the core elements of this microtubule-based TORC1 trafficking pathway still seems in a early stage relative to other TORC1 pathways.

IV. mTORC1 signaling in disease

A. mTORC1 and Cancer

The TSC complex is a heterodimer of the proteins tuberin (TSC1) and hamartin (TSC2). Before the TSC complex was associated with TOR signaling, they had already been appreciated as tumor suppressor genes, and inactivation of either causes a familial autosomal dominant disorder tuberous sclerosis complex (TSC) that affects approximately 1:6000 individuals (*180*). A defining feature of TSC is the development of hamartomous tumors in multiple tissues that can be severely disrupt tissue function but are rarely metastatic (*181*). Loss of TSC2 is also strongly associated with lymphangioleiomyomatosis (LAM), a rare multi-systemic disease that causes cystic destruction of the lung parenchyma and abdominal tumors (*182*). LAM occurs almost exclusively in young women, and the mechanistic connection to TSC is still not well understood. There are several additional hamartoma syndromes that share pathological features with TSC, including Cowden Disease, Peutz-Jeghers Syndrome, neurofibromatosis and Birt-Hogg-Dube Syndrome (*183*). Like TSC1 and TSC2, the tumor suppressor genes linked to these diseases (PTEN, LKB1, NF1 and FLCN respectively) encode proteins that restrict mTORC1 signaling.

An interesting aside on TSC1/2 function concerns the benign nature of TSC tumors. Due to downregulation of growth factor signaling, via S6K-mediated downregulation of the insulin receptor substrate 1 (IRS-1) (*184, 185*) and/or downregulation of platelet-derived growth factor receptor (PDGFR) (*186*), TSC1 or TSC2 loss is known to inactivate signaling through PI3K/Akt (*186, 187*), a kinase which is known to be hyperactivated in most malignant tumors (*188, 189*). As a consequence, it has been hypothesized that TSC tumors are less aggressive because of this impaired PI3KAkt signaling (*186*).

While TSC1/2 mutations are relatively uncommon cause of tumors in humans, mTORC1 also sits at the nexus of many classical oncogenic signaling pathways. Its most prominent connection is to the PTEN/PI3K pathway, which is activated by growth factor signaling and is mutationally deregulated in a wide spectrum of sporadic cancers (*190, 191*). PTEN alone is disrupted in 50-80% of sporadic cancers, which includes endometrial carcinoma, glioblastoma and prostate, and 30-50% of breast, colon and lung cancers (*192*). Both mTORC1 and mTORC2 pathways are hyperactivated by

PTEN inactivation and are increasingly blamed for many of its subsequent signaling defects, such as deregulation of Akt (*193*).

A second class of cancers that have close connections with mTORC1 are those characterized by hyperactive functioning of the translation initiation factor, eIF4E. In an mTOR-dependent manner, eIF4E coordinates the translation of a subset of mRNAs with extensive structure in the 5' untranslated region, including cyclin D1 and c-myc (*194*). Highlighting the importance of eIF4E, cyclin D1, and c-myc in cancer, this translational control is frequently lost or deregulated due to alteration of the 5' mRNA sequences or amplification of genomic DNA including their genes in various tumors (*195-197*).

mTORC1 can also contribute to tumor growth by promoting angiogenesis. Activation of mTORC1 increases levels of the transcription factor hypoxia-inducible factor 1 alpha (HIF1α) by driving its expression and suppressing its degradation (*198, 199*). As HIF1α accumulates, it drives angiogenesis through expression of the vascular endothelial growth factor (VEGF) (*200*). Kaposi's sarcoma and certain sporadic or hereditary kidney cancers show elevated VEGF signaling and increased HIF1α levels, respectively (*193, 201, 202*).

B. mTORC1, insulin sensitivity, and diet-induced obesity

Concurrent with the work in mouse fibroblasts showing that TSC1/ TSC2 deficiency negatively regulates PI3K/Akt signaling, a similar role for TSC1/TSC2 in regulating Akt was shown in fruit flies (*203*). Moreover, this *Drosophila* work established that dTSC1/dTSC2-dependent negative regulation of dAkt/PKB activity could be reserved by the simultaneous loss of dS6K. Fittingly, when S6K1 knockout mice were generated (*204*), these mice were also shown to have increased Akt phosphorylation (*184*). The increased Akt in these mice was also shown to correlate with decreased turnover of the insulin receptor substrate 1 (IRS-1). IRS-1 is known to promote Akt phosphorylation by initiating a cascade whereby IRS-1 binding contributes to PI3K activation which promotes PIP3 formation and PIP3-mediated recruitment of Akt to membranes where it can be phosphorylated by membrane-bound kinases (*205, 206*). It has been the assembly of this pathway with the concurrent work with S6K-deficient flies

and mice that led to the now well-appreciated idea of a negative feedback loop from TORC1-S6K to PI3K-Akt signaling (*207*).

Despite decreased β-cell mass which lead to hypoinsulinemia (*204*), the S6K1 knockout mice also had increased glucose uptake upon insulin administration indicating that these mice had increased insulin sensitivity, again consistent with increased Akt phosphorylation in the tissues of these animals (*184*). Compared to age matched controls, Um et al. also found in these S6K1-null mice a five-fold increase in the rate of fat lipolysis as well as an increase in metabolic rate as measured by oxygen consumption. Loss of S6K1 converted white adipose tissue into an energy-consuming tissue by increasing mitochondria number and expression of uncoupling protein 1 (UCP1), carnitine palmitoyltransferase 1 (Cpt1) and PGC1α. Interestingly, though opposite to what one might expect, similar changes in gene expression to those of the S6K1-deficient adipocytes where seen in 4E-BP1-deficient adipocytes (*208*). The changes in Cpt1 gene expression in S6K1-deficient adipocytes also occurred in S6K1-deficient skeletal muscle leading to marked increase in fatty-acid β-oxidation in the muscle. Consistent with this increased oxidative function, these mice were also resistant to age-associated and high fat diet-induced obesity.

To directly study mTORC1 in mice, white adipose and skeletal muscle tissue specific knockouts of raptor, an essential component of mTORC1, have also recently been engineered (*155, 209*). Satisfyingly, these knockout mice have confirmed many of the S6K1 knockout mice phenotypes. Loss of raptor in adipocytes led to decreased adipocyte size and number (*209*). Similar to the S6K1 knockout mouse, the decrease in fat storage upon loss of raptor was due to increased oxidative metabolism within the white adipose tissue driven by increased expression of UCP1 (*209*). Both the fat- and muscle-specific raptor knockout mice also had decreased PGC-1α expression in their respective mTORC1-deficient tissues. Adipocyte-specific raptor deficient mice had lower circulating levels of insulin, but were more insulin sensitive than wild type controls resulting in lowered blood glucose, also similar to S6K1 knockout mice (*209*). Loss of raptor in the fat also changed whole body metabolism in response to a high-fat diet. As expected in the raptor mutant mice, fat deposition was countered by increased oxidative

capacity (Polak et al., 2008). Moreover, raptor mutant mice continued to be more insulin sensitive under a high fat diet (*209*).

In summary, these studies show that mTORC1 has important energy storage and utilization functions; in its absence in adipose tissue, there is both increased energy uncoupling and fatty acid oxidation. Loss of mTORC1 signaling also leads to increased insulin sensitivity and accompanying glucose uptake by muscle and prevents the onset of insulin resistance on a high-fat diet.

C. mTORC1, hyperlipidemia, and hypercholesterolemia

Before mTOR had shown to be a key piece of the mechanism for the growth-inhibitory effects of rapamycin, rapamycin was already in use as an immune suppressive agent in transplantation settings (*210, 211*). Currently, rapamycin, which is known by trade names, sirolimus, everolimus, and temsirolimus, is a common therapeutic strategy for the prevention of kidney transplant rejection, restenosis in coronary stents, and in the treatment of renal cell carcinoma, respectively (*212-214*). While rapamycin has typically been shown to be a well-tolerated drug, it is also known for common side effects, namely, hyperlipidemia and less commonly, hypercholesterolemia (*215, 216*). The effects of rapamycin on plasma lipids and cholesterol in human patients have also been found in experimental animal models. Long-term treatment of mice with rapamycin has been shown to decrease muscle PGC1α expression and mitochondrial function and this was associated with these mice developing hyperlipidemia as well as insulin resistance (*154*). These mice also developed hypercholesterolemia though the mechanism for this effect was not clear.

To begin to think about why rapamycin might increase plasma cholesterol levels in humans and mice, two key regulators of cholesterol homeostasis are important to discuss, the low density lipoprotein receptor (LDLR) and 3-hydroxy-3-methylglutaryl coenzyme A reductase (HMGCR). LDLR is a cholesterol receptor prominently expressed by liver cells that is critical for clearing the blood of plasma cholesterol (which in the blood are complexed with proteins referred to as lipoproteins) (*217*). HMGCR is the rate-liming enzyme in cholesterol biosynthesis and incidentally is the target of the commonly used cholesterol-lowering drug, statins. Early studies by Brown and

Goldstein found that HMGCR activity is strongly reduced when cells are grown in media containing cholesterol and the opposite is true when cholesterol is depleted (*217*). These results suggested a feedback mechanism that involved coordination of cellular cholesterol uptake and biosynthesis. Over the ensuing years, this feedback was shown to occur because cells control cholesterol uptake and biosynthesis through a circuit controlled by a transcription factor, SREBP, which potently regulates both LDLR and HMGCR gene expression levels. The feedback works as follows: 1) in the presence of cholesterol in the media, SREBP activity becomes downregulated which lowers HMGCR and LDLR expression and cholesterol is subsequently not taken up by nor made in cells. 2) the ensuing absence of cholesterol within cells causes the activation of SREBP which then restores cholesterol uptake and biosynthesis. A recent study suggests that this feedback regulation might be broken by rapamycin. In hepatocyte cell line, it was shown that rapamycin downregulates LDLR expression while not perturbing the levels of HMGCR (*218*). Therefore, one explanation for why rapamycin might induce high blood cholesterol levels in humans and mice might be because their livers do not clear the cholesterol (due to downregulated LDLR expression) and subsequently don't downregulate its synthesis accordingly (HMGCR expression is maintained).

These effects of rapamycin in humans and in mice on plasma lipids and cholesterol stand in contrast those recently observed with selective inhibiton of mTORC1 by deleting raptor in adipose tissue of mice. Here, raptor loss specifically in fat protects these animals from high fat diet-induced hyperlipidemia and hypercholesterolemia (*209*). Importantly, these effects are similar to those seen in SREBP1 knockout mice fed a western-diet (*219*). The above data suggests that further investigation into how distinct mTOR inhibitors might differentially regulate these key SREBP targets will be valuable in evaluating the utility of these agents in treating/preventing hyperlipidemia and hypercholesterolemia.

D. mTORC1-based therapies

Cancer: The best rationale for therapeutic inhibition of mTOR in cancer is in the hamartoma syndromes such as tuberous sclerosis complex (TSC). The constitutive activation of mTORC1 that results from loss of TSC1/TSC2 function is thought to drive

many of the pathological features of TSC, thus establishing a compelling argument for the therapeutic use of rapamycin (*220*). Clinical trials to treat TSC patients are currently underway and early results have been promising (*221*). NF1 mutant cells also strongly respond to rapamycin (*222*), and accordingly, preclinical studies to test the utility of rapamycin in treating these tumors are ongoing (*223*). In sporadic cancers rapamycin has been less successful. Indeed, the use of rapamycin and its analogues has had modest successes in the treatment of mantle cell lymphoma, endometrial cancer, and renal cell carcinoma (*224*). In these cases, it is possible that other modes of mTORC1 inhibition, such as using ATP-competitive mimetics to the active site of mTOR, might prove more successful (*225*).

Metabolic disease: In addition to testing the utility of rapamycin as well as other classes of mTOR inhibitors in treating cancer, these molecules also have emerging potential for the treatment of metabolic diseases. Because metabolic disease and aging are intertwined concepts, it would be first useful to briefly discuss what we know about the mechanisms of aging. As a key regulator of growth-associated metabolism, TORC1 has gained notice as a potentially important regulator of aging (*226*). This role has recently been substantiated in studies mice and humans. For example, S6K1 knockout mice have been shown to live longer and are resistant to age-related pathologies such as bone, immune and motor dysfunction as well as loss of insulin sensitivity. This result is a genetic confirmation of another recent report describing the ability of oral rapamycin treatment to extend lifespan in both male and female mice (*227*). As more studies suggest the importance of TORC1 in aging, two metabolically-related themes begin to emerge on the mechanisms for its effects: insulin signaling and mitochondrial metabolism.

Insulin signaling was first implicated in aging through the isolation of mutant worms which lived twice as long as normal worms (*228*). Subsequent work has not only confirmed the importance of the insulin signaling as a conserved regulator of aging, but has also placed TORC1 firmly as part of this pathway (*226*). While few genomic alterations in canonical insulin signaling pathway components have been linked to longevity of humans (*229*), mutations that are suspected to be causative in premature

aging of humans have been identified. Virtually all of these known mutations reside in a gene which encodes a component of the nuclear matrix, lamin A (*230*). Lamin A mutations are associated with a condition known as progeria, which is a premature aging syndrome that is often associated with the deregulation of metabolically active tissues such as fat and muscle (e.g., progeria patients often develop lipodystrophy (alterations in adipose tissue distribution/accumulation) and insulin resistance). Lamin A is farnesylated protein, therefore one approach to treat progeria patients has been to use farnesyl transferase inhibitors (FTIs) which block maturation of the lamin A protein. Though the initial studies are preliminary, early indications of the use of FTIs in progeria appear to be encouraging. (*231*).

Whether FTIs might hold promise as a treatment for aging-related diseases besides those caused by lamin A mutations is debatable. However, one practical approach that could be useful to a wide variety of insulin/mTORC1-related metabolic diseases is the use of dietary restriction. The validity of dietary restriction as a means to improve human health has received increased focus due to its profound effects in multiple organisms in extending lifespan (*232*). That dietary restriction has been shown to increase lifespan comparable to, or in a manner-dependent on TOR inhibition in multiple organisms puts TORC1 at the center of this therapeutic strategy (*233-235*). Therefore, it seems reasonable to suggest that dietary restriction could be considered a viable alternative to mTOR-targeting pharmaceuticals for the treatment of mTORC1-related metabolic diseases.

V. Conclusions

One may reasonably assume that our understanding of disease is limited by the experiments we are actually capable of performing. While model organisms such as mice, fruit flies, and worms, have proven valuable for investigating mechanisms of TORC1 signaling, it is worth considering that their applicability to treating human disease can be limited and their implementation in the lab time-consuming. Because the TORC1 pathway sits at the center of many clinically-relevant pathologies, immune

dysfunction, cancer, aging, it is important to continue to think of how we can approach this pathway in novel ways. That the TORC1 pathway is highly conserved should enable us to make connections across a growing number of eukaryotic species whose genomes are being characterized. Recognizing 'deep homology' of TORC1 function in diverse eukaryotic species is one such promising approach (*236*). By considering a greater assortment of organisms, one may appreciate which shared or unique platforms are utilized by TORC1 to control species with diverse signaling requirements. With this knowledge more in mind, we should be better able to explain the logic of TORC1 and provide better rationales for treating TORC1-related diseases.

In the following document, we address in particular three key questions of how mTORC1 signaling is controlled by its localization:

1) How is mTORC1 activated?
2) How does mTORC1 regulate cell division?
3) How does mTORC1 promote sterol/lipogenesis?

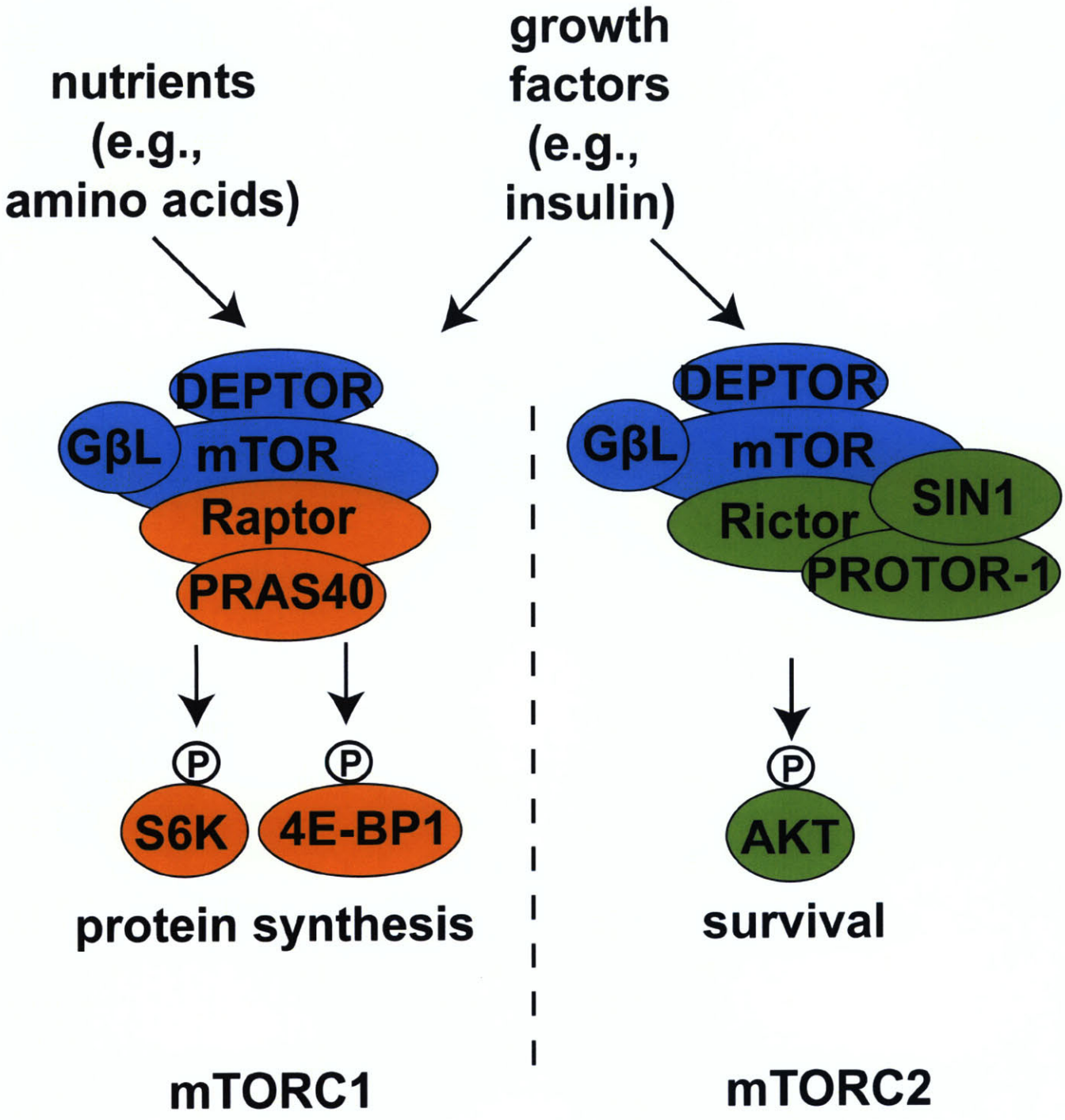
nutrients
(e.g.,
amino acids)
growth
factors
(e.g.,
insulin)
DEPTOR
GβL
mTOR
Raptor
PRAS40
P
P
S6K
4E-BP1
protein synthesis
mTORC1
DEPTOR
GβL
mTOR
SIN1
Rictor
PROTOR-1
P
AKT
survival
mTORC2

References

1. K. Singh, S. Sun, C. Vezina, *J Antibiot (Tokyo)* **32**, 630 (Jun, 1979).
2. C. P. Eng, S. N. Sehgal, C. Vezina, *J Antibiot (Tokyo)* **37**, 1231 (Oct, 1984).
3. R. E. Morris, E. G. Hoyt, M. P. Murphy, R. Shorthouse, *Transplant Proc* **21**, 1042 (Feb, 1989).
4. J. Heitman, N. R. Movva, P. C. Hiestand, M. N. Hall, *Proc Natl Acad Sci U S A* **88**, 1948 (Mar 1, 1991).
5. Y. Koltin *et al.*, *Mol Cell Biol* **11**, 1718 (Mar, 1991).
6. E. J. Brown *et al.*, *Nature* **369**, 756 (Jun 30, 1994).
7. D. M. Sabatini, H. Erdjument-Bromage, M. Lui, P. Tempst, S. H. Snyder, *Cell* **78**, 35 (Jul 15, 1994).
8. M. I. Chiu, H. Katz, V. Berlin, *Proc Natl Acad Sci U S A* **91**, 12574 (Dec 20, 1994).
9. C. J. Sabers *et al.*, *J Biol Chem* **270**, 815 (Jan 13, 1995).
10. E. J. Brown *et al.*, *Nature* **377**, 441 (Oct 5, 1995).
11. G. J. Brunn *et al.*, *Embo J* **15**, 5256 (Oct 1, 1996).
12. H. Lempiainen, T. D. Halazonetis, *Embo J* **28**, 3067 (Oct 21, 2009).
13. J. Kunz *et al.*, *Cell* **73**, 585 (May 7, 1993).
14. X. F. Zheng, D. Florentino, J. Chen, G. R. Crabtree, S. L. Schreiber, *Cell* **82**, 121 (Jul 14, 1995).
15. R. Loewith *et al.*, *Mol Cell* **10**, 457 (Sep, 2002).
16. D. D. Sarbassov *et al.*, *Curr Biol* **14**, 1296 (Jul 27, 2004).
17. D. H. Kim *et al.*, *Cell* **110**, 163 (Jul 26, 2002).
18. K. Hara *et al.*, *Cell* **110**, 177 (Jul 26, 2002).
19. H. Nojima *et al.*, *J Biol Chem* **278**, 15461 (May 2, 2003).
20. D. H. Kim *et al.*, *Mol Cell* **11**, 895 (Apr, 2003).
21. D. A. Guertin *et al.*, *Dev Cell* **11**, 859 (Dec, 2006).
22. E. Vander Haar, S. I. Lee, S. Bandhakavi, T. J. Griffin, D. H. Kim, *Nat Cell Biol* **9**, 316 (Mar, 2007).

23. Y. Sancak *et al.*, *Mol Cell* **25**, 903 (Mar 23, 2007).
24. L. Wang, T. E. Harris, R. A. Roth, J. C. Lawrence, Jr., *J Biol Chem* **282**, 20036 (Jul 6, 2007).
25. N. Oshiro *et al.*, *J Biol Chem* **282**, 20329 (Jul 13, 2007).
26. A. Soulard, A. Cohen, M. N. Hall, *Curr Opin Cell Biol* **21**, 825 (Dec, 2009).
27. M. A. Frias *et al.*, *Curr Biol* **16**, 1865 (Sep 19, 2006).
28. E. Jacinto *et al.*, *Cell* **127**, 125 (Oct 6, 2006).
29. S. Y. Woo *et al.*, *J Biol Chem* **282**, 25604 (Aug 31, 2007).
30. L. R. Pearce *et al.*, *Biochem J* **405**, 513 (Aug 1, 2007).
31. K. Thedieck *et al.*, *PLoS ONE* **2**, e1217 (2007).
32. S. Shinozaki-Yabana, Y. Watanabe, M. Yamamoto, *Mol Cell Biol* **20**, 1234 (Feb, 2000).
33. S. M. Ali.
34. S. S. Schalm, J. Blenis, *Curr Biol* **12**, 632 (Apr 16, 2002).
35. E. J. Chen, C. A. Kaiser, *J Cell Biol* **161**, 333 (Apr 28, 2003).
36. A. G. Steinberg, *Proc Natl Acad Sci U S A* **30**, 5 (Jan 15, 1944).
37. Y. H. Wang, M. L. Huang, *Mech Dev* **126**, 781 (Oct, 2009).
38. A. Efeyan, D. M. Sabatini, *Curr Opin Cell Biol*, (Nov 27, 2009).
39. K. E. Mach, K. A. Furge, C. F. Albright, *Genetics* **155**, 611 (Jun, 2000).
40. A. R. Tee *et al.*, *Proc Natl Acad Sci U S A* **99**, 13571 (2002).
41. X. Gao *et al.*, *Nat Cell Biol* **4**, 699 (2002).
42. H. Stocker *et al.*, *Nat Cell Biol* **5**, 559 (Jun, 2003).
43. L. J. Saucedo *et al.*, *Nat Cell Biol* **5**, 566 (Jun, 2003).
44. Y. Zhang *et al.*, *Nat Cell Biol* **5**, 578 (Jun, 2003).
45. K. Inoki, Y. Li, T. Xu, K. L. Guan, *Genes Dev* **17**, 1829 (Aug 1, 2003).
46. X. Long, Y. Lin, S. Ortiz-Vega, K. Yonezawa, J. Avruch, *Curr Biol* **15**, 702 (Apr 26, 2005).
47. K. Takahashi, M. Nakagawa, S. G. Young, S. Yamanaka, *J Biol Chem* **280**, 32768 (Sep 23, 2005).
48. K. Saito, Y. Araki, K. Kontani, H. Nishina, T. Katada, *J Biochem (Tokyo)* **137**, 423 (Mar, 2005).

49. C. Buerger, B. DeVries, V. Stambolic, *Biochem Biophys Res Commun* **344**, 869 (Jun 9, 2006).
50. S. L. Cai *et al.*, *J Cell Biol* **173**, 279 (Apr 24, 2006).
51. B. D. Manning, A. R. Tee, M. N. Logsdon, J. Blenis, L. C. Cantley, *Mol Cell* **10**, 151 (Jul, 2002).
52. K. Inoki, Y. Li, T. Zhu, J. Wu, K. L. Guan, *Nat Cell Biol* **12**, 12 (2002).
53. P. P. Roux, B. A. Ballif, R. Anjum, S. P. Gygi, J. Blenis, *Proc Natl Acad Sci U S A* **101**, 13489 (Sep 14, 2004).
54. K. Inoki *et al.*, *Cell* **126**, 955 (Sep 8, 2006).
55. D. M. Gwinn *et al.*, *Mol Cell* **30**, 214 (Apr 25, 2008).
56. J. H. Reiling, E. Hafen, *Genes Dev* **18**, 2879 (Dec 1, 2004).
57. J. Brugarolas *et al.*, *Genes Dev* **18**, 2893 (Dec 1, 2004).
58. M. P. DeYoung, P. Horak, A. Sofer, D. Sgroi, L. W. Ellisen, *Genes Dev* **22**, 239 (Jan 15, 2008).
59. S. Vega-Rubin-de-Celis *et al.*, *Biochemistry* **49**, 2491 (Mar 23).
60. T. Nobukuni *et al.*, *Proc Natl Acad Sci U S A* **102**, 14238 (Oct 4, 2005).
61. E. M. Smith, S. G. Finn, A. R. Tee, G. J. Browne, C. G. Proud, *J Biol Chem* **280**, 18717 (May 13, 2005).
62. J. Urano, A. P. Tabancay, W. Yang, F. Tamanoi, *J Biol Chem* **275**, 11198 (Apr 14, 2000).
63. F. Dubouloz, O. Deloche, V. Wanke, E. Cameroni, C. De Virgilio, *Mol Cell* **19**, 15 (Jul 1, 2005).
64. S. A. Zurita-Martinez, R. Puria, X. Pan, J. D. Boeke, M. E. Cardenas, *Genetics* **176**, 2139 (Aug, 2007).
65. E. J. Chen, C. A. Kaiser, *Proc Natl Acad Sci U S A* **99**, 14837 (Nov 12, 2002).
66. M. Gao, C. A. Kaiser, *Nat Cell Biol* **8**, 657 (Jul, 2006).
67. J. Huang *et al.*, *Proc Natl Acad Sci U S A* **101**, 16594 (Nov 23, 2004).
68. G. Thomas, *Biochem Soc Trans* **20**, 678 (Aug, 1992).
69. A. M. Gressner, I. G. Wool, *Nature* **259**, 148 (Jan 15, 1976).
70. C. J. Kuo *et al.*, *Nature* **358**, 70 (1992).
71. J. Chung, C. J. Kuo, G. R. Crabtree, J. Blenis, *Cell* **69**, 1227 (1992).

72. D. J. Price, J. R. Grove, V. Calvo, J. Avruch, B. E. Bierer, *Science* **257**, 973 (1992).
73. N. Terada *et al.*, *Biochem Biophys Res Commun* **186**, 1315 (1992).
74. S. Ferrari, R. B. Pearson, M. Siegmann, S. C. Kozma, G. Thomas, *J Biol Chem* **268**, 16091 (1993).
75. V. M. Pain, *Biochimie* **76**, 718 (1994).
76. K. Hara *et al.*, *J Biol Chem* **273**, 14484 (Jun 5, 1998).
77. F. J. Kelly, L. S. Jefferson, *J Biol Chem* **260**, 6677 (Jun 10, 1985).
78. K. A. Scorsone, R. Panniers, A. G. Rowlands, E. C. Henshaw, *J Biol Chem* **262**, 14538 (Oct 25, 1987).
79. V. M. Pain, *Eur J Biochem* **236**, 747 (Mar 15, 1996).
80. H. B. Jefferies, C. Reinhard, S. C. Kozma, G. Thomas, *Proc Natl Acad Sci U S A* **91**, 4441 (1994).
81. N. Terada *et al.*, *Proc Natl Acad Sci U S A* **91**, 11477 (Nov 22, 1994).
82. H. B. Jefferies *et al.*, *Embo J* **16**, 3693 (1997).
83. X. M. Ma, S. O. Yoon, C. J. Richardson, K. Julich, J. Blenis, *Cell* **133**, 303 (Apr 18, 2008).
84. P. E. Burnett, R. K. Barrow, N. A. Cohen, S. H. Snyder, D. M. Sabatini, *PNAS* **95**, 1432 (1998).
85. R. B. Pearson *et al.*, *Embo J* **14**, 5279 (1995).
86. J. Urban *et al.*, *Mol Cell* **26**, 663 (Jun 8, 2007).
87. W. K. Huh *et al.*, *Nature* **425**, 686 (Oct 16, 2003).
88. P. Jorgensen *et al.*, *Genes Dev* **18**, 2491 (Oct 15, 2004).
89. D. J. Klionsky, P. K. Herman, S. D. Emr, *Microbiol Rev* **54**, 266 (Sep, 1990).
90. N. C. Barbet *et al.*, *Mol Biol Cell* **7**, 25 (1996).
91. A. Pause *et al.*, *Nature* **371**, 762 (1994).
92. L. Beretta, A. C. Gingras, Y. V. Svitkin, M. N. Hall, N. Sonenberg, *EMBO J* **15**, 658 (1996).
93. Y. Xiong, T. Connolly, B. Futcher, D. Beach, *Cell* **65**, 691 (May 17, 1991).
94. C. J. Sherr, *Trends Biochem Sci* **20**, 187 (May, 1995).
95. N. Sonenberg, A. G. Hinnebusch, *Cell* **136**, 731 (Feb 20, 2009).

96. L. Rong *et al.*, *Rna* **14**, 1318 (Jul, 2008).
97. G. J. Brunn *et al.*, *Science* **277**, 99 (1997).
98. A. C. Gingras *et al.*, *Genes Dev* **13**, 1422 (1999).
99. L. Wang, C. J. Rhodes, J. C. Lawrence, Jr., *J Biol Chem* **281**, 24293 (Aug 25, 2006).
100. T. Powers, P. Walter, *Mol Biol Cell* **10**, 987 (Apr, 1999).
101. R. M. Marion *et al.*, *Proc Natl Acad Sci U S A* **101**, 14315 (Oct 5, 2004).
102. D. E. Martin, A. Soulard, M. N. Hall, *Cell* **119**, 969 (Dec 29, 2004).
103. H. Lempiainen *et al.*, *Mol Cell.* **33**, 704 (2009).
104. C. V. Dang *et al.*, *Semin Cancer Biol* **16**, 253 (Aug, 2006).
105. S. Kim, Q. Li, C. V. Dang, L. A. Lee, *Proc Natl Acad Sci U S A* **97**, 11198 (Oct 10, 2000).
106. F. de Nigris, M. L. Balestrieri, C. Napoli, *Cell Cycle* **5**, 1621 (Aug, 2006).
107. D. J. Klionsky, *Nat Rev Mol Cell Biol* **8**, 931 (Nov, 2007).
108. Y. Y. Chang *et al.*, *Biochem Soc Trans* **37**, 232 (Feb, 2009).
109. Y. Kamada *et al.*, *J Cell Biol* **150**, 1507 (Sep 18, 2000).
110. N. Hosokawa *et al.*, *Mol Biol Cell* **20**, 1981 (Apr, 2009).
111. C. H. Jung *et al.*, *Mol Biol Cell* **20**, 1992 (Apr, 2009).
112. I. G. Ganley *et al.*, *J Biol Chem* **284**, 12297 (May 1, 2009).
113. E. Y. Chan, A. Longatti, N. C. McKnight, S. A. Tooze, *Mol Cell Biol* **29**, 157 (Jan, 2009).
114. Y. Kamada *et al.*, *Mol Cell Biol* **30**, 1049 (Feb).
115. H. Zhang, J. P. Stallock, J. C. Ng, C. Reinhard, T. P. Neufeld, *Genes Dev* **14**, 2712 (Nov 1, 2000).
116. T. Porstmann *et al.*, *Cell Metab* **8**, 224 (Sep, 2008).
117. J. D. Horton, J. L. Goldstein, M. S. Brown, *J Clin Invest* **109**, 1125 (May, 2002).
118. H. Green, M. Meuth, *Cell* **3**, 127 (Oct, 1974).
119. H. Green, O. Kehinde, *Cell* **5**, 19 (May, 1975).
120. J. E. Kim, J. Chen, *Diabetes* **53**, 2748 (Nov, 2004).
121. M. Lehrke, M. A. Lazar, *Cell* **123**, 993 (Dec 16, 2005).

122. T. A. Huffman, I. Mothe-Satney, J. C. Lawrence, Jr., *Proc Natl Acad Sci U S A* **99**, 1047 (Jan 22, 2002).
123. K. Reue, J. R. Dwyer, *J Lipid Res* **50 Suppl**, S109 (Apr, 2009).
124. G. S. Han, W. I. Wu, G. M. Carman, *J Biol Chem* **281**, 9210 (Apr 7, 2006).
125. S. A. Henry, J. L. Patton-Vogt, *Prog Nucleic Acid Res Mol Biol* **61**, 133 (1998).
126. M. Chen, L. C. Hancock, J. M. Lopes, *Biochim Biophys Acta* **1771**, 310 (Mar, 2007).
127. M. K. Shirra, S. E. Rogers, D. E. Alexander, K. M. Arndt, *Genetics* **169**, 1957 (Apr, 2005).
128. H. Santos-Rosa, J. Leung, N. Grimsey, S. Peak-Chew, S. Siniossoglou, *Embo J* **24**, 1931 (Jun 1, 2005).
129. T. F. Chan, J. Carvalho, L. Riles, X. F. Zheng, *Proc Natl Acad Sci U S A* **97**, 13227 (Nov 21, 2000).
130. S. B. Helliwell *et al.*, *Mol Biol Cell* **5**, 105 (Jan, 1994).
131. A. Schmidt, J. Kunz, M. N. Hall, *Proc Natl Acad Sci U S A* **93**, 13780 (Nov 26, 1996).
132. A. Schmidt, M. Bickle, T. Beck, M. N. Hall, *Cell* **88**, 531 (Feb 21, 1997).
133. S. B. Helliwell, I. Howald, N. Barbet, M. N. Hall, *Genetics* **148**, 99 (Jan, 1998).
134. S. B. Helliwell, A. Schmidt, Y. Ohya, M. N. Hall, *Curr Biol* **8**, 1211 (Nov 5, 1998).
135. A. Audhya *et al.*, *Embo J* **23**, 3747 (Oct 1, 2004).
136. Y. Kamada *et al.*, *Mol Cell Biol* **25**, 7239 (Aug, 2005).
137. S. Aronova, K. Wedaman, S. Anderson, J. Yates, 3rd, T. Powers, *Mol Biol Cell* **18**, 2779 (Aug, 2007).
138. J. Torres, C. J. Di Como, E. Herrero, M. A. De La Torre-Ruiz, *J Biol Chem* **277**, 43495 (Nov 8, 2002).
139. H. Wang, Y. Jiang, *Mol Cell Biol* **23**, 3116 (May, 2003).
140. E. Jacinto *et al.*, *Nat Cell Biol* **6**, 1122 (Nov, 2004).
141. S. F. Tavazoie, V. A. Alvarez, D. A. Ridenour, D. J. Kwiatkowski, B. L. Sabatini, *Nat Neurosci* **8**, 1727 (Dec, 2005).
142. L. Liu, L. Chen, J. Chung, S. Huang, *Oncogene* **27**, 4998 (Aug 28, 2008).
143. C. E. Walczak, S. Cai, A. Khodjakov, *Nat Rev Mol Cell Biol* **11**, 91 (Feb).

144. T. D. Pollard, *Curr Opin Cell Biol* **22**, 50 (Feb).
145. A. Barquilla, J. L. Crespo, M. Navarro, *Proc Natl Acad Sci U S A* **105**, 14579 (Sep 23, 2008).
146. S. Pyronnet, L. Pradayrol, N. Sonenberg, *Mol Cell* **5**, 607 (Apr, 2000).
147. X. Qin, P. Sarnow, *J Biol Chem* **279**, 13721 (Apr 2, 2004).
148. E. W. Wilker *et al.*, *Nature* **446**, 329 (Mar 15, 2007).
149. T. Li, A. Inoue, J. M. Lahti, V. J. Kidd, *Mol Cell Biol* **24**, 3188 (Apr, 2004).
150. C. Petretti *et al.*, *EMBO Rep* **7**, 418 (Apr, 2006).
151. A. Astrinidis, W. Senapedis, E. P. Henske, *Hum Mol Genet* **15**, 287 (Jan 15, 2006).
152. G. Goshima *et al.*, *Science* **316**, 417 (Apr 20, 2007).
153. S. M. Schieke *et al.*, *J Biol Chem* **281**, 27643 (Sep 15, 2006).
154. J. T. Cunningham *et al.*, *Nature* **450**, 736 (Nov 29, 2007).
155. C. F. Bentzinger *et al.*, *Cell Metab* **8**, 411 (Nov, 2008).
156. Z. Liu, R. A. Butow, *Annu Rev Genet* **40**, 159 (2006).
157. A. Komeili, K. P. Wedaman, E. K. O'Shea, T. Powers, *J Cell Biol* **151**, 863 (Nov 13, 2000).
158. T. Sekito, J. Thornton, R. A. Butow, *Mol Biol Cell* **11**, 2103 (Jun, 2000).
159. X. Liao, R. A. Butow, *Cell* **72**, 61 (Jan 15, 1993).
160. I. Dilova, C. Y. Chen, T. Powers, *Curr Biol* **12**, 389 (Mar 5, 2002).
161. J. J. Tate, K. H. Cox, R. Rai, T. G. Cooper, *J Biol Chem* **277**, 20477 (Jun 7, 2002).
162. Z. Liu, T. Sekito, M. Spirek, J. Thornton, R. A. Butow, *Mol Cell* **12**, 401 (Aug, 2003).
163. I. Dilova, S. Aronova, J. C. Chen, T. Powers, *J Biol Chem* **279**, 46527 (Nov 5, 2004).
164. V. N. Popov, E. A. Moskalev, M. Shevchenko, A. T. Eprintsev, *Zh Evol Biokhim Fiziol* **41**, 507 (Nov-Dec, 2005).
165. M. Costanzo *et al.*, *Science* **327**, 425 (Jan 22).
166. K. J. Roberg, S. Bickel, N. Rowley, C. A. Kaiser, *Genetics* **147**, 1569 (Dec, 1997).

167. S. B. Helliwell, S. Losko, C. A. Kaiser, *J Cell Biol* **153**, 649 (May 14, 2001).
168. J. Y. Springael, B. Andre, *Mol Biol Cell* **9**, 1253 (Jun, 1998).
169. B. Magasanik, C. A. Kaiser, *Gene* **290**, 1 (May 15, 2002).
170. M. Binda *et al.*, *Mol Cell* **35**, 563 (Sep 11, 2009).
171. A. Schmidt, T. Beck, A. Koller, J. Kunz, M. N. Hall, *Embo J* **17**, 6924 (Dec 1, 1998).
172. E. Jacinto, B. Guo, K. T. Arndt, T. Schmelzle, M. N. Hall, *Mol Cell* **8**, 1017 (Nov, 2001).
173. J. L. Crespo *et al.*, *J Biol Chem* **279**, 37512 (Sep 3, 2004).
174. S. Gander *et al.*, *Rapid Commun Mass Spectrom* **22**, 3743 (Dec, 2008).
175. K. A. Jones, X. Jiang, Y. Yamamoto, R. S. Yeung, *Exp Cell Res* **295**, 512 (May 1, 2004).
176. X. Jiang, R. S. Yeung, *Cancer Res* **66**, 5258 (May 15, 2006).
177. X. Jiang *et al.*, *Am J Pathol* **172**, 1748 (Jun, 2008).
178. J. H. Choi *et al.*, *Curr Biol* **10**, 861 (Jul 13, 2000).
179. J. H. Choi *et al.*, *EMBO Rep* **3**, 988 (Oct, 2002).
180. J. Montagne, T. Radimerski, G. Thomas, *Sci STKE* **2001**, pe36 (Oct 23, 2001).
181. D. J. Kwiatkowski, B. D. Manning, *Hum Mol Genet* **14 Spec No. 2**, R251 (Oct 15, 2005).
182. D. Chorianopoulos, G. Stratakos, *Lung* **186**, 197 (Jul-Aug, 2008).
183. K. Inoki, M. N. Corradetti, K. L. Guan, *Nat Genet* **37**, 19 (Jan, 2005).
184. S. H. Um *et al.*, *Nature* **431**, 200 (Sep 9, 2004).
185. O. J. Shah, Z. Wang, T. Hunter, *Curr Biol* **14**, 1650 (Sep 21, 2004).
186. H. Zhang *et al.*, *J Clin Invest* **112**, 1223 (Oct, 2003).
187. D. J. Kwiatkowski *et al.*, *Hum Mol Genet* **11**, 525 (Mar 1, 2002).
188. J. A. Engelman, *Nat Rev Cancer* **9**, 550 (Aug, 2009).
189. L. R. Pearce, D. Komander, D. R. Alessi, *Nat Rev Mol Cell Biol* **11**, 9 (Jan).
190. M. Cully, H. You, A. J. Levine, T. W. Mak, *Nat Rev Cancer* **6**, 184 (Mar, 2006).
191. K. K. Wong, J. A. Engelman, L. C. Cantley, *Curr Opin Genet Dev* **20**, 87 (Feb).
192. L. Salmena, A. Carracedo, P. P. Pandolfi, *Cell* **133**, 403 (May 2, 2008).
193. D. A. Guertin, D. M. Sabatini, *Cancer Cell* **12**, 9 (Jul, 2007).

194. Y. Mamane *et al.*, *Oncogene* **23**, 3172 (Apr 19, 2004).
195. M. A. Bjornsti, P. J. Houghton, *Nat Rev Cancer* **4**, 335 (May, 2004).
196. P. Jares, D. Colomer, E. Campo, *Nat Rev Cancer* **7**, 750 (Oct, 2007).
197. N. Meyer, L. Z. Penn, *Nat Rev Cancer* **8**, 976 (Dec, 2008).
198. H. Zhong *et al.*, *Cancer Res* **60**, 1541 (Mar 15, 2000).
199. C. C. Hudson *et al.*, *Mol Cell Biol* **22**, 7004 (Oct, 2002).
200. N. Ferrara, *Nat Rev Cancer* **2**, 795 (Oct, 2002).
201. J. A. Bertout, S. A. Patel, M. C. Simon, *Nat Rev Cancer* **8**, 967 (Dec, 2008).
202. W. G. Kaelin, Jr., *Nat Rev Cancer* **8**, 865 (Nov, 2008).
203. T. Radimerski, J. Montagne, M. Hemmings-Mieszczak, G. Thomas, *Genes Dev* **16**, 2627 (Oct 15, 2002).
204. M. Pende *et al.*, *Nature* **408**, 994 (Dec 21-28, 2000).
205. X. J. Sun *et al.*, *Nature* **352**, 73 (Jul 4, 1991).
206. T. F. Franke, D. R. Kaplan, L. C. Cantley, A. Toker, *Science* **275**, 665 (Jan 31, 1997).
207. B. D. Manning, *J Cell Biol* **167**, 399 (Nov 8, 2004).
208. K. Tsukiyama-Kohara *et al.*, *Nat Med* **7**, 1128 (Oct, 2001).
209. P. Polak *et al.*, *Cell Metab* **8**, 399 (Nov, 2008).
210. R. Y. Calne *et al.*, *Lancet* **2**, 227 (Jul 22, 1989).
211. A. W. Thomson, J. Woo, *Lancet* **2**, 443 (Aug 19, 1989).
212. J. Steffel, F. R. Eberli, T. F. Luscher, F. C. Tanner, *Ann Med* **40**, 242 (2008).
213. R. Marcen, *Drugs* **69**, 2227 (Nov 12, 2009).
214. A. Pinto Marin *et al.*, *Urol Oncol*, (Mar 4).
215. C. Brattstrom *et al.*, *Transplantation* **65**, 1272 (May 15, 1998).
216. C. G. Groth *et al.*, *Transplantation* **67**, 1036 (Apr 15, 1999).
217. J. L. Goldstein, M. S. Brown, *Arterioscler Thromb Vasc Biol* **29**, 431 (Apr, 2009).
218. L. J. Sharpe, A. J. Brown, *Biochem Biophys Res Commun* **373**, 670 (Sep 5, 2008).
219. N. Y. Kalaany *et al.*, *Cell Metab* **1**, 231 (Apr, 2005).
220. J. R. Sampson, *Biochem Soc Trans* **37**, 259 (Feb, 2009).
221. D. N. Franz *et al.*, *Ann Neurol* **59**, 490 (Mar, 2006).

222. C. M. Johannessen *et al.*, *Proc Natl Acad Sci U S A* **102**, 8573 (Jun 14, 2005).
223. P. Bhola *et al.*, *Int J Cancer* **126**, 563 (Jan 15).
224. J. J. Gibbons, R. T. Abraham, K. Yu, *Semin Oncol* **36 Suppl 3**, S3 (Dec, 2009).
225. C. C. Thoreen *et al.*, *J Biol Chem* **284**, 8023 (Mar 20, 2009).
226. C. J. Kenyon, *Nature* **464**, 504 (Mar 25).
227. D. E. Harrison *et al.*, *Nature* **460**, 392 (Jul 16, 2009).
228. C. Kenyon, J. Chang, E. Gensch, A. Rudner, R. Tabtiang, *Nature* **366**, 461 (Dec 2, 1993).
229. M. Bonafe *et al.*, *J Clin Endocrinol Metab* **88**, 3299 (Jul, 2003).
230. B. C. Capell, F. S. Collins, *Nat Rev Genet* **7**, 940 (Dec, 2006).
231. I. S. Mehta, J. M. Bridger, I. R. Kill, *Biochem Soc Trans* **38**, 287 (Feb).
232. L. Guarente, *Cell* **132**, 171 (Jan 25, 2008).
233. T. Vellai *et al.*, *Nature* **426**, 620 (Dec 11, 2003).
234. M. Kaeberlein *et al.*, *Science* **310**, 1193 (Nov 18, 2005).
235. C. Selman *et al.*, *Science* **326**, 140 (Oct 2, 2009).
236. N. Shubin, C. Tabin, S. Carroll, *Nature* **457**, 818 (Feb 12, 2009).

Chapter 2

mTORC1 regulates lipin 1 localization to control nuclear structure and the SREBP pathway

Manuscript in preparation:

Timothy R. Peterson [1], Shomit S. Sengupta [1], Thurl E. Harris [2], David A. Guertin [3], Katherine L. Madden [4], Anne E. Carpenter [4], Brian N. Finck [5], David M. Sabatini [6].

[1] Whitehead Institute for Biomedical Research, Koch Center for Integrative Cancer Research at MIT, Department of Biology, Massachusetts Institute of Technology, Cambridge, MA 02142, USA.
[2] Department of Pharmacology, University of Virginia, Charlottesville, VA 22908, USA.
[3] Program in Molecular Medicine, University of Massachusetts Medical School, Worcester, MA 01605, USA.
[4] Imaging Platform, Broad Institute of Harvard and MIT, Cambridge, MA 02142, USA.
[5] Division of Geriatrics and Nutritional Sciences, Washington University School of Medicine, St. Louis, MO 63110, USA.
[6] Whitehead Institute for Biomedical Research, Howard Hughes Medical Institute, Koch Center for Integrative Cancer Research at MIT, Department of Biology, Massachusetts Institute of Technology, Cambridge, MA 02142, USA.

Experiments in Figure 1 were performed by T.R.P.
Experiments in Figure 2 were performed by T.R.P.
Experiments in Figure 3 were performed by T.R.P.
Experiments in Figure 4 were performed by T.R.P.
Experiments in Figure 5 were performed by T.R.P.

Summary

The mTOR Complex 1 (mTORC1) pathway regulates many processes that control growth, including protein synthesis, autophagy, and lipogenesis. Through unknown mechanisms, mTORC1 promotes the function of SREBP, a master regulator of lipo- and sterolgenic gene transcription. Here, we demonstrate that mTORC1 regulates SREBP by controlling the nuclear entry of lipin 1, a phosphatidic acid phosphatase. When coordinately phosphorylated by mTORC1 and GSK3, lipin 1 resides in the cytoplasm and mTORC1 inhibition causes its translocation to the nucleus, which is required for SREBP inhibition. Inhibition of mTORC1 in the liver significantly impairs SREBP function and makes mice resistant, in a lipin 1-dependent fashion, to the hepatic steatosis and hypercholesterolemia induced by a high fat and cholesterol diet. The phosphatase activity of nuclear localized lipin 1 promotes nuclear eccentricity and juxtaposition of SREBP with lamin A, a nuclear location that suppresses gene transcription. Like lipin 1, lamin A is required for the full downregulation of SREBP-target genes that occurs upon mTORC1 suppression. Our results establish lipin 1 and lamin A as key mediators of the effects of mTORC1 inhibition on SREBP, and suggest the existence of a novel nuclear signaling system for the epigenetic regulation of gene expression.

Introduction

mTOR is an evolutionarily conserved, PI3K-related family (PIKK) serine/threonine kinase that regulates cell growth together with multiple interacting partners. An essential component of the mTOR-containing protein complex, mTORC1, in the control of protein synthesis is raptor. Raptor is required for the mTOR-catalyzed phosphorylation of the translation regulators, S6K1 and 4E-BP1, yet the mechanism(s) by which raptor regulates mTOR phosphorylation of these substrates remain largely unknown. However, an emerging view, at least in the case of 4E-BP1, is that its binding affinity for raptor is critical in determining its ability to be phosphorylated by mTOR (*1*). Evidence that mTORC1 not only phosphorylates, but also can stably associate with 4E-BP1, has acquired further relevance as additional TORC1 substrates have been identified by virtue of their copurification with TORC1. For example, in *Saccharomyces cerevisiae*, TORC1 was found to interact in a rapamycin-sensitive manner with and directly phosphorylate Sfp1 (*2*), findings which filled a prominent gap in our understanding of how this transcription factor controls TORC1-dependent ribosome biogenesis.

Previously, lipin 1, which generates the rate limiting precursor in triacylglycerol synthesis, diacylglycerol (*3, 4*), was shown to be phosphorylated in an amino-acid and growth factor-stimulated, rapamycin-sensitive manner (*5*). This result, following the identification of lipin 1 as the gene responsible for the phenotype of the fatty liver dystrophy (fld) mouse (*6*), generated considerable interest as a potential connection between mTOR and lipid homeostasis. However, since these results preceded the identification of raptor (*7, 8*) and because subsequent investigation into the function of lipin 1 using rapamycin failed to identify a role for mTOR in regulating lipin 1 activity (*9*), the significance of the mTOR-dependent phosphorylation of lipin 1 has remained elusive.

Results

In revisiting a potential functional link between mTOR and lipin 1, we noted that cell cycle-regulated phosphorylations of lipin 1, the related protein, lipin 2, and their yeast homolog, Pah1/Smp2, negatively regulate their Mg^{2+}-dependent phosphatidic acid phosphatase (a.k.a., PAP1) activities (*10*). However, because rapamycin lacked an effect on PAP1 activity, we explored the possibility that mTORC1 might regulate some other aspect of Lipin 1 function, such as its intracellular localization. Strikingly, treatment of cells with the ATP-competitive mTOR inhibitor, Torin1 (*11*), which potently inhibits mTORC1, as measured by T37/T46 and S65 4E-BP1 phosphorylation, caused a complete redistribution of lipin 1 from the cytoplasm to the nucleus (Fig. 1A and B). This complete redistribution was also seen with LY294002 at a concentration, 25 μM, which also potently inhibits mTORC1 signaling (Fig. 1A and B) (*12*). Rapamycin, on the other hand, while abolishing the phosphorylation of the mTORC1 target, S6K1, largely lacked an effect on lipin 1 localization and did not affect 4E-BP1 phosphorylation at the time point examined (Fig. 1A and B). That rapamycin lacked an effect on lipin 1 localization is in disagreement with that recently observed by another group in a different cell type, 3T3-L1 adipocytes (*13*). However, as it is known that the completeness of inhibition of rapamycin on mTORC1 signaling varies considerably between cell types (*14*), we reasoned that the discrepancy on lipin 1 localization might be explained by the differing rapamycin sensitivities of mTORC1 in the cell types assessed. In support of this, in HEK-293T cells, unlike in NIH3T3 fibroblasts (Fig. 1A and B), lipin 1 nuclear translocation was partially sensitive to rapamycin and this correlated with partial inhibition of S65 4E-BP1 phosphorylation (Fig. S1A and S1B). Consistent with lipin 1 nuclear translocation correlating with the extent of mTORC1 inhibition, a PI3K inhibitor, PI-103, caused only a partial accumulation of lipin 1 in the nucleus and this correlated with the extent of 4E-BP1 and S6K1 dephosphorylation caused by this agent (Fig. 1A and B). Torin1 also caused lipin 1 nuclear translocation in cells lacking mTORC2 (i.e., rictor deficient), consistent with

mTORC1 regulating lipin 1 localization (Fig. 1C). Reminiscent of the effects of mTORC1 inhibition on 4E-BP1 phosphorylation and the regulation of cap-dependent translation as recently reported (*11, 14*), the above data suggest that lipin 1 cytoplasmic-nuclear distribution is controlled in a largely rapamycin-resistant, yet mTORC1-dependent manner.

We next tested known physiological inputs into mTORC1 signaling for their effect on lipin 1 localization. Growth factors, such as insulin, strongly promote mTORC1 activation (*15*), therefore it was surprising that serum deprivation only caused partial lipin 1 nuclear accumulation (Fig. 1D). However, because this partial effect was similar to that caused by the effects of the PI3K inhibitor, PI-103 (Fig. 1A), we wondered whether serum deprivation might activate a signaling event that precludes the full nuclear accumulation of lipin 1. The GSK3α/β kinases were attractive candidates to mediate this resistance because these kinases are activated by growth factor deprivation/PI3K inhibition by loss of phosphorylation at a site, (Ser9/Ser21 in GSK3α/β, respectively) which is catalyzed by the growth-factor/PI3K-activated kinase Akt (*16*). GSK3α/β inhibition with the specific ATP competitive GSK3α/β (hereafter referred to as GSK3) inhibitor, GSK3-IX (a.k.a. BIO), did not cause redistribution of lipin 1 (Fig. 1D), consistent with these kinases already being inactivated by the presence of serum. However, when GSK3 was inhibited concomitantly with growth factor deprivation, lipin 1 fully accumulated in the nucleus (Fig. 1D). The assertion that combined PI3K/GSK3 inhibition phenocopies the effects of mTORC1 inhibition on lipin 1 nuclear translocation was further supported by a time course of Torin1 treatment. After acute (1 hour) treatment, lipin 1 partially accumulated in the nucleus, which correlated with the downregulation of PI3K signaling, as judged by T308 Akt phosphorylation, yet the activation of GSK3β, as judged by loss of S9 phosphorylation, at this early time point (Fig. 1D and E). However, at later times ($\geq$3 hours), lipin 1 became fully retained in the nucleus, and this then correlated with the restoration of PI3K signaling and the inhibition of both mTORC1 and GSK3β activities (Fig. 1E and F).

Because mTORC1 is also regulated by nutrient status, we assessed whether glucose and amino acids regulated lipin 1 localization. Unlike with serum deprivation, serum deprivation combined with glucose deprivation promoted the full nuclear accumulation of lipin 1, an effect which correlated with a greater degree of 4E-BP1 dephosphorylation caused by this treatment in comparison to serum alone (Fig. S1C and S1D). Similar to the effect of glucose deprivation, complete amino acid deprivation, which abolishes the activation of mTORC1 by growth factors (*17*), caused a complete nuclear accumulation of lipin 1 (Fig. S1E). Lastly, because the phosphorylation state of lipin 1, lipin 2, and Pah1/Smp2 is regulated by cell cycle activity (*18, 19*), we tested whether various cell cycle perturbations would affect lipin 1 localization. Neither G1 arrest by a double thymidine block, nor CDK or MEK inhibition affected lipin 1 localization (Fig. S1F). Taken together, these results suggest that lipin 1 cytoplasmic retention is positively promoted, albeit in a hierarchal manner, by the mTORC1 and GSK3 kinases: inputs which promote mTORC1 activity prevent lipin 1 nuclear localization regardless of the presence of growth factors, whereas GSK3 requires a „priming" signal provided by the absence of serum to regulate lipin 1 cytoplasmic-nuclear distribution.

We next sought to gain insight into the mechanisms by which lipin 1 translocation is regulated by mTORC1 and GSK3. Because mTORC1 and GSK3 are protein kinases, we focused on the lipin 1 phosphorylation state and the 19 phosphorylation sites previously identified on it (*9*). In our mass spectrometry analysis, we detected 17 of the 19 published sites as well as 2 novel sites, S237 and T335 and observed that most of these 21 sites could be categorized into two phosphorylation motif groups (Fig. 2A). Nine of the sites fell within "proline-directed" motifs (S/T-P) like those in 4E-BP1 (Fig. 2A) (*20-22*), which are known to be phosphorylated by mTOR (*20*), whereas 7 sites are part of a phosphorylation cassette conforming to the canonical GSK3 motif, ((Ser/Thr)-XXX-(Ser(P)/Thr(P))) (Fig. 2A). This motif is unique in that GSK3 is known to require its substrates with this motif, such as glycogen synthase, to be first

primed by phosphorylation by a distinct kinase on a residue 4 amino acids c-terminal to the site GSK3 phosphorylates (*23, 24*).

Rapamycin is known to regulate the insulin-stimulated phosphorylation of the proline-directed lipin 1 site, S106, (*9*), therefore we assessed whether this phosphorylation was also sensitive to Torin1. Indeed, insulin-stimulated phosphorylation of S106 lipin 1 was blocked by both rapamycin and Torin1 (Fig. 2B). Using a phospho-specific antibody we raised to the proline-directed S472 residue of lipin 1, we also detected a pattern of S472 phosphorylaton that was similar to that of S106 lipin 1 (Fig. 2B). Interestingly, treatment with Torin1, but not rapamycin, reduced phosphorylation of S106 and S472 lipin 1 and S65 4E-BP1 to levels below those seen in serum-depleted cells, suggesting that the insulin-independent phosphorylations of S106 and S472 lipin 1 and S65 4EBP1 occur in a rapamycin-resistant, yet mTORC1-dependent manner. Because S106 and S472 phosphorylation were partially sensitive to acute (1 hour) rapamycin treatment (Fig. 2B), we next sought to determine whether the lipin 1 phosphorylation state would be regulated by prolonged inhibition of mTORC1. Analogous to the lack of effect of prolonged rapamycin treatment on 4E-BP1 phosphorylation (*25*), S237 and S472 lipin 1 phosphorylation were not impaired by a prolonged course (12 hours) of rapamycin, but were sensitive to Torin1 (Fig. S2A). Therefore, similar to 4E-BP1 phosphorylation (*11, 25*), this result suggests that multiple proline-directed lipin 1 phosphorylation sites are regulated in a rapamycin-resistant, yet mTORC1-dependent manner.

To determine if lipin 1 can be directly phosphorylated at S106 and S472 in an mTORC1-dependent manner, we isolated mTOR via mLST8/GβL from control or raptor knockdown cells and performed in vitro kinase assays on purified lipin 1. An mTORC1-containing mLST8/GβL purification, but not one where raptor was depleted in cells by RNAi, readily phosphorylated S106 and S472 lipin 1 (Fig. 2C). Importantly, this activity was lost when mTOR kinase activity was inhibited with Torin1 (Fig. 2C). These findings were similar to those seen with the established mTORC1 substrate 4E-BP1 (Fig. 2C) and suggest that mTORC1 is a bona fide lipin 1 kinase.

As multiple TORC1 substrates have been shown to remain bound to TORC1 when purified from cells (*2, 26, 27*) we assessed lipin 1 for this behavior. Indeed, raptor and co-expressed raptor and mTOR copurified with lipin 1 but not with the metap2 or rap2a control proteins (Fig. 2D). That lipin 1 did not interact with mTOR alone and that mTOR did not increase the abundance of raptor copurifying with lipin 1 suggested that lipin 1 interacts with mTORC1 via raptor. Overexpressed lipin 1 also interacted with endogenous mTOR and raptor, but not rictor, in a manner sensitive to inhibition of mTOR kinase activity (Fig. S2B), a finding also in common with other established TORC1 substrates (*2, 26, 28*).

To test the involvement of GSK3 in regulating lipin 1 phosphorylation, we focused on the S468/S472 phosphorylation cassette sites because: 1) we previously established regulation of its putative GSK3 priming site, S472 (Fig. 2B and C); 2) we could not readily detect phosphorylation of the doubly phosphorylated species, which again would putatively require GSK3, in the presence of serum (a condition which activates PI3K-Akt signaling and thus represses GSK3 activity (*16*)) (Fig. 2E). To investigate if GSK3 regulates the doubly phosphorylated S468/S472 form of lipin 1, we exploited the fact that Torin1 and PI-103 differentially inhibit mTORC1 and PI3K signaling. At 250 nM, both Torin1 and PI-103 inhibited PI3K and activated GSK3 signaling, as judged by T308 Akt and S9 GSK3β phosphorylation, respectively (Fig. 2E). However, only Torin1 significantly downregulated mTORC1 signaling, as judged by T37/T46 4E-BP1 phosphorylation, and affected the abundance of the singly phosphorylated S472-containing peptide (Fig. 2E). On the other hand, PI-103 induced S468/S472 phosphorylation, and this doubly phosphorylated species was eliminated by GSK3 IX (Fig. 2E). These results suggest that GSK3 regulates one of these two sites in cells and does so only under the condition that the other site is already phosphorylated. To determine if GSK3 directly regulates lipin 1 by this mechanism, we purified GSK3β and performed in vitro kinase assays on purified lipin 1. Using a phospho-specific antibody we raised to the doubly phosphorylated S468/S472 cassette, we detected robust GSK3β-catalyzed S468/S472 lipin 1 phosphorylation only when GSK3β was obtained from cells

pretreated with Torin1 and not vehicle (Fig. 2F). This is consistent with GSK3β kinase activity being indirectly regulated by mTORC1 through S6K1-dependent regulation of GSK3β S9 phosphorylation (*29*). As a reflection of the specificity of our S468/S472 phospho-antibody, mutating the S468/S472 sites to alanine (as part of a mutant where 15 of the 19 other lipin 1 phosphorylation sites, including S106, were mutated to alanine, hereafter referred to as "17xS/T->A"), abolished Torin1-stimulated, GSK3β-dependent S468/S472 phosphorylation. Additionally, Torin1-stimulated, GSK3β-mediated phosphorylation of S468/S472 lipin 1 was significantly decreased by in cell pretreatment of lipin 1 with Torin1 suggesting that mTORC1-dependent lipin 1 phosphorylation (likely of S472) serves as a „priming" event for its phosphorylation by GSK3β (likely at S468) (Fig. 2F). In aggregate, these data establish GSK3β as a kinase for the S468/S472 phosphorylation cassette and is consistent with mTORC1 regulating GSK3β activity toward lipin 1 by two mechanisms: 1) indirectly by controlling GSK3β through its regulatory site phosphorylation; 2) directly likely by controlling the priming phosphorylation of lipin 1 for its subsequent phosphorylation by GSK3β.

Because mTORC1 and GSK3 signaling regulate lipin 1 localization, we reasoned that a mechanism through which lipin 1 localization might be regulated is by its phosphorylation at mTORC1- and GSK3-catalyzed sites. Indeed, the 17xS/T->A lipin 1 mutant, which renders most of the proline-directed as well as GSK3 motif sites non-phosphorylatable, including the S106, S468, and S472 sites, was sufficient to promote the full nuclear accumulation of lipin 1 in multiple cell types (Fig 2G). Mutation only of the mTORC1-catalyzed site, S106, to alanine lacked an effect on lipin 1 localization (Fig. S2C). Therefore, coordinated inactivation of mTORC1 and GSK3 leads to nuclear sequestration of lipin 1 by a mechanism which requires its dephosphorylation at numerous mTORC1- and GSK3-catalyzed sites.

Previously, it was shown that mTORC1 positively regulates the activity of SREBP1 (*30, 31*), a member of the SREBP family of transcription factors that critically regulate fatty acid and cholesterol biosynthetic gene expression (*32*). Studies by Brown, Goldstein, and colleagues elucidated key parts of the

mechanism by which cholesterol sensing is coupled to the activity of SREBP (*33*). However, the mechanism(s) by which mTORC1 promotes SREBP function remains largely unknown. Because lipin 1 has been shown to regulate the expression of many genes involved in lipid homeostasis in divergent organisms (*34-36*), we were interested in whether lipin 1 might contribute to the effects of mTORC1 on the SREBP pathway. We first determined to what extent rapamycin and Torin1 regulated the mRNA expression of numerous genes which are known to be induced by SREBP1 and/or SREBP2 (*37*), such as fatty acid synthase (FASN), ATP-citrate lyase (ACLY), acetyl-CoA carboxylase alpha (ACACA), stearoyl CoA-desaturase (SCD1), HMG-CoA reductase (HMGCR), farnesyl diphosphate synthase (FDPS). In a time-dependent manner, Torin1 strongly down-regulated the gene expression of all SREBP targets we examined, yet rapamycin was largely ineffective at decreasing the expression levels of these same targets at the latest time point (Fig. 3A). On the contrary, neither Torin1 nor rapamycin decreased SREBP1 mRNA expression under the same conditions (Fig. S3). Correlating with the differential effects of rapamycin and Torin1 on lipin 1 localization, these results suggest that the redistribution of cytoplasmic lipin 1 to the nucleus might be important in the regulation of SREBP-target gene expression by mTORC1. To test this, we monitored SREBP-target mRNA levels over a time course of Torin1 in wild-type and lipin 1 deficient cells (fld) (*6*). At time points after which Torin1 caused lipin 1 to fully enter the nucleus (Fig. 1E), fld cells were completely refractory to the effects of Torin1 on SREBP-target expression (Fig. 3B). We observed similar results with combined PI3K/GSK3 inhibition (Fig. 3C), which taken together with the effects of Torin1 (Fig. 3B), indicate that lipin 1 is required for the downregulation of the SREBP pathway caused by loss of either input from mTORC1 or GSK3. To assess whether mTORC1- and GSK3-catalyzed lipin 1 phosphorylation sites are critical in the repression SREBP-target gene expression caused by loss of mTORC1 and GSK3 activities, we stably expressed either the wild-type or the 17xS/T->A mutant lipin 1 in fld cells. While wild-type lipin 1 had no effect on SREBP-target mRNA levels, the 17xS/T->A lipin 1 mutant repressed, in a manner dependent on

its catalytic activity, all SREBP targets examined (Fig. 3D). In total, these results establish nuclear lipin 1 as both necessary and sufficient for mediating the effects of mTORC1 and GSK3 inhibition on the SREBP pathway.

Because the aforementioned studies were performed in cultured cells, we wanted a more physiologically meaningful context to test a role for mTORC1 and lipin 1 in the regulation of the SREBP pathway. For this purpose, we developed a conditional null (LoxP) allele (*38*) of the raptor gene to ablate raptor expression in mice in a temporally-defined, tissue-specific manner (Fig. S4A and S4B). We deleted raptor in the post-natal liver in floxed raptor mice by expressing Cre recombinase under the control of the Albumin promoter (*39*). The liver appeared to be a particularly relevant organ in which to manipulate mTORC1 and lipin 1 function because it plays a vital role in maintaining whole body fatty acid and cholesterol homeostasis (*32*). We first confirmed that raptor expression, mTORC1, and PI3K/Akt signaling were altered specifically in the liver (Fig. 4A). Surprisingly, despite strongly perturbing mTORC1/PI3K signaling in their livers, liver-specific raptor knock-out ($raptor^{Li-/-}$) mice developed normally and at 4 months of age were of comparable body weight and glycemia as control mice (Fig. 4B and S4C). Therefore, we challenged the wild-type and $raptor^{Li-/-}$ mice with a high fat and high cholesterol "western" diet. The effects of raptor loss were now clear: unlike with chow-feeding, where both groups gained weight at a similar rate over the course of our study, western diet-fed $raptor^{Li-/-}$ mice were fully protected from hyperglycemia and gained substantially less weight than wild-type animals despite similar food intake (Fig. S4C, 4B, and S4D). Gross and microscopic examination of the livers of both groups also revealed striking western diet-specific effects. Namely, the livers of western diet, but not chow-fed $raptor^{Li-/-}$ were substantially reduced in size and were less yellowish in appearance and disorganized by intracellular droplets compared with the livers of control mice (Fig. 4C). We next measured SREBP-target gene expression in chow and western diet-fed wild-type and $raptor^{Li-/-}$ mice. As expected, the expression of FASN and HMGCR were repressed by raptor loss, though the degree of inhibition was substantially greater on the western diet, particularly for

FASN (Fig. 4D). The elevations in liver triglycerides and plasma cholesterol in wild-type animals on the western compared with the chow diet were also largely blocked by raptor loss (Fig. 4E), results which notably, phenocopy those seen in SREBP1 knock-out mice (*40*).

We suspected that lipin 1 would be important in the resistance of raptor$^{Li-/-}$ animals to some of the phenotypic consequences caused by the western-diet because fld fibroblasts were resistant to the effects of Torin1 on SREBP- target gene expression (Fig. 3B). Indeed, using two distinct adenovirally-delivered shRNAs to lipin 1, we depleted lipin 1 from the livers of western diet-fed raptor$^{Li-/-}$ mice (Fig. 4F) and this largely restored SREBP-target gene expression to the levels seen in control mice (Fig 4G). Correspondingly, the levels of liver triglycerides and plasma cholesterol in western diet-fed raptor$^{Li-/-}$ mice were also re-elevated, after the lipin 1 knock-down, to the levels seen in raptor$^{Li+/+}$ mice (Fig. 4H). Therefore, the SREBP pathway in the liver is positively regulated by mTORC1 in a manner that is opposed by lipin 1 and this regulation is critical for the development of hepatic steatosis and hypercholesterolemia caused by prolonged high fat and high cholesterol feeding.

In trying to understand how the nuclear localization of lipin 1 regulates SREBP-target gene expression, we noticed a strong correlation between the inputs which promoted lipin 1 nuclear accumulation and downregulated the SREBP pathway (i.e., inhibited mTORC1 and GSK3 signaling) and those which changed the circumference shape of the DNA and/or lipin 1 distribution in the nucleus (Fig. 1A, C and D; Fig. 2G; Fig. S1A, S1C, and S1E). More specifically, in cells where lipin 1 was redistributed from the cytoplasm to the nucleus, the nuclei appeared to be noticeably more eccentric, a term which when applied to circular objects indicates that the major and minor axes (the apopasis and periapsis, respectively) of the circle differ in length (Fig. 5A). Interestingly, it has previously been shown that overexpression of the lipin 1 homolog, Ned1, in *Schizosaccharomyces pombe* causes nuclear eccentricity, though the physiological relevance of this finding has not been determined (*41*). To pursue this phenotype, we focused on the shape of the nuclear matrix and in particular

on one of its core components, lamin A, for two reasons: 1) lamin A has previously been shown to physically interact with SREBP1 and SREBP2 and its overexpression downregulates the mRNA expression of the adipogenic SREBP target, PPARγ2 (*42, 43*); 2) lamin A mutations in humans commonly result in a lipodystrophy, a condition characterized by abnormal adipose tissue that is also seen in adipocyte-specific SREBP1 transgenic mice (*44, 45*). By visual inspection or with automated image analysis-based quantification, it was evident that either mTORC1 or combined PI3K/GSK3 inhibition increased the eccentricity of the lamin A matrix (Fig. 5B and C). Moreover, either Torin1 or combined serum and glucose deprivation increased lamin A eccentricity in a time-dependent manner (Fig. 5D). The time-dependent, increased lamin A eccentricity caused by Torin1 was absent in fld cells indicating that lipin 1 was necessary for this effect (Fig. S5A). Lastly, the expression of the catalytically active 17xS/T->A mutant lipin 1, but not its catalytic dead or the wild-type form, was sufficient to increase lamin A eccentricity, suggesting that the effects of mTORC1 and GSK3 on lamin A eccentricity are driven, at least in part, by nuclear localized lipin 1 (Fig. 5B and C).

As mTORC1/GSK3/lipin 1-mediated increases in lamin A eccentricity correlated with the repression of SREBP-target gene expression, we next focused on whether lamin A was required for this regulation. In cells with lamin A, Torin1 or the expression of the 17xS/T->A lipin 1 mutant strongly repressed SREBP targets as expected, yet cells lacking lamin A were resistant to these effects (Fig. 5E and F). As a measure of the specificity of the effects of lamin A on mTORC1-dependent gene expression, the mRNA levels of Cytochrome C (CytC), a PGC1α target whose mRNA expression is promoted by mTORC1 signaling (*46*), were equally repressed by Torin1 in lamin A wild-type and null cells (Fig. 5E). We then tested the converse of the aforementioned findings, i.e., whether the mTORC1-dependent induction of SREBP-target gene expression was impaired in Hutchison Gilford Progeria Syndrome (HGPS) cells which harbor a lamin A mutation that, as with other lipodystrophy-causing lamin A mutations, dominantly interferes with SREBP-target expression (Fig. S5B) (*43*). Loss of

TSC2 function, which stimulates the TORC1-S6K1 pathway (*47-50*), obtained using two independent shRNAs targeted to TSC2, activated SREBP-target gene expression as expected in unaffected cells, however HGPS cells were fully resistant to these effects (Fig. 5G). This result, together with those using lamin A-deficient cells, suggests that the integrity of the nuclear matrix is critical in the regulation of the SREBP pathway in response to activating or inhibitory inputs to mTORC1.

A growing body of work suggests that A- and B-type lamins physically interact with both transcriptional regulators and regions of transcriptionally inactive chromatin (*44, 51-54*), however less is known if and how these interactions might be regulated. Because mTORC1/lipin 1 signaling strongly altered the structure of the lamin A-containing nuclear matrix and because lamin A is known to bind SREBP in cells (*42*), this raised the possibility that SREBP and/or its target gene promoters might bind lamin A in a lipin 1-regulated manner. To test this, we immunoprecipitated lamin A from chemically cross-linked cells containing or lacking nuclear lipin 1 and quantified the abundance of genomic fragments containing the FASN gene promoter that copurified with it (*55*). The amount of FASN sterol response element (SRE)-containing DNA present in lamin A immunoprecipitates was enriched in wild-type cells above the background signal obtained in lamin A null cells and was reproducibly increased by either Torin1 treatment or with expression of 17xS/T->A lipin 1 compared with their respective controls (Fig. S5C and S5D). To determine whether SREBP itself might be localized to the nuclear lamina in a regulated fashion, we assessed its localization upon manipulating mTORC1 activity. In untreated cells, full-length SREBP1 appeared diffusely localized, but was more prominently extranuclear consistent with that previously reported (Fig. 5H) (*56*). Strikingly, in the presence of Torin1, SREBP1 rapidly redistributed to the nucleus and became strongly co-localized with lamin A (Fig. 5H). Interestingly, this localization of SREBP1 is similar to that seen in cells expressing mutant forms of lamin A that are impaired in their proteolytic processing (*57*). Therefore, one explanation for the mTORC1/lipin 1/lamin A-dependent effects on SREBP-target gene expression

could be that nuclear localized lipin 1 promotes the association(s) of the lamin A-containing nuclear matrix with SREBP and/or SREBP-target gene promoters in a manner that inhibits the function of the SREBP transcriptional machinery.

Discussion

In summary: 1) mTORC1 and GSK3 coordinately phosphorylate lipin 1 which prevents its nuclear entry; 2) inhibited mTORC1/nuclear lipin 1 repress SREBP-target gene expression in a manner dependent on lamin A and that, 3) correlates with the structural alteration of the lamin A-containing matrix and the relocalization of SREBP and SREBP-target promoters into proximity to lamin A. While we have not yet established a causal role of these latter findings in regulating SREBP-target gene expression, our work does support a genetic model whereby mTORC1 and GSK3 function as positive regulators and lipin 1 and lamin A function as negative regulators of the SREBP pathway (Fig. 5I).

That mTORC1 and lipin 1 have key roles in regulating triglyceride and cholesterol homeostasis is supported by our results that liver-specific mTORC1 deletion has potent protective effects against western diet-induced, hepatic steatosis and hypercholesterolemia that are reversed by lipin 1 depletion. Surprisingly, rapamycin is known to cause numerous features of metabolic syndrome: hyperlipidemia, hypercholesterolemia, and insulin resistance in humans and in mice (*46, 58*). Considering the discrepancies between the effects of rapamycin and the phenotypes of western-diet fed raptor$^{Li-/-}$ mice (noting that rapamycin, unlike liver-specific raptor loss, perturbs mTORC1 function in many tissues) and that rapamycin is significantly less potent than Torin1 in regulating lipin 1 and SREBP pathway in cells, it is clear that further examination of the differential effects of various mTORC1 inhibitors on cellular and organismal lipid and glucose homeostasis is required. Regardless, one no longer unexpected implication from our work is that unlike rapamycin, potent mTORC1 inhibiting

drugs, such as Torin1, might eventually be useful in the treatment of metabolic syndrome.

PI3K and TOR signaling have been shown to be important determinants of lifespan in model organisms (*59-61*), though the mechanism(s) by which these pathways control aging are incompletely understood. Considering the prevalence of lamin A mutations in humans who prematurely age (*44*), it is tempting to speculate that the mTORC1/PI3K-dependent regulation we describe on lamin A by lipin 1 might make an important contribution to the effects of the PI3K and TOR pathways on eukaryotic cellular and/or organismal lifespan. The mTORC1/lipin 1-dependent interaction(s) between lamin A and the FASN promoter is, to our knowledge, a first example of TOR/PI3K-regulated interaction(s) between the nuclear matrix and chromatin. In future work, it will be interesting to test the importance of this regulation not only in cellular and organismal aging, but more generally as a mechanism in controlling gene expression.

Figure legends

Fig. 1. Effect of mTORC1 and PI3K/GSK3 inhibition on lipin 1 cytoplasmic/nuclear distribution. (A) NIH3T3 cells overexpressing FLAG-lipin 1 were treated with the indicated inhibitors (100 nM rapamycin, 250 nM Torin1, 25 μM LY294002, 250 nM PI-103) or vehicle for 8 hours. Cells were then processed in an immunofluorescence assay to detect FLAG (green), costained with DAPI for DNA content (blue), and imaged (A) or analyzed by immunoblotting (B) for the levels and phosphorylated forms of the specified proteins. (C) FLAG-lipin 1 overexpressing p53 $^{-/-}$ or rictor$^{-/-}$; p53$^{-/-}$ MEFs were treated with 250 nM Torin1 or vehicle for 8 hours and analyzed as in (A). (D) FLAG-lipin 1 overexpressing NIH3T3 cells were grown in the presence or absence of serum and treated with 1.4 μM GSK3 IX or vehicle for 8 hours. (E) FLAG-lipin 1 overexpressing NIH3T3 cells were treated with 250 nM Torin1 for the specified times. The overlap of

FLAG immunoreactivity with DAPI staining was analyzed by image analysis software (*62*) for three independent fields for each condition (>500 cells total). Error bars indicate standard error for n=3. (F) NIH3T3 treated with 250 nM Torin1 for the specified times were analyzed by immunoblotting for the phosphorylation states and levels of the specified proteins.

Fig. 2. mTOR-dependent phosphorylation of lipin 1 by mTORC1 and GSK3β. (A) Schematic of location of lipin 1 phosphorylation sites. HEK-293T cells were transfected with FLAG-lipin 1, lysed, and FLAG immunoprecipitates were prepared and lipin 1 phosphorylation sites were identified by mass spectrometry. NLIP, N-terminal lipin 1 conserved region. CLIP, C-terminal lipin 1 conserved region. NLS, Nuclear Localization Signal. Capitalized serine or threonine residues (in red) indicate that phosphorylation was detected at this site. Putative serine or threonine phosphorylation sites (in red) are in lower case. (B) HEK-293E cells were deprived of serum for 4 hours and then stimulated for 20 minutes with 150 nM insulin in the presence of 100 nM rapamycin, 250 nM Torin1, or vehicle. Cell lysates were prepared and analyzed by immunoblotting for the phosphorylation states and levels of the specified proteins. (C) HEK-293T cells overexpressing FLAG-mLST8/GβL were infected with lentivirus expressing a shRNA targeting raptor or GFP. FLAG immunoprecipitates were prepared from cell lysates and analyzed for mTOR kinase activity toward lipin 1 or 4E-BP1 in the presence of 250 nM Torin1 or vehicle. (D) HEK-293T cells were transfected with the indicated cDNAs in expression vectors, cell lysates prepared, and lysates and FLAG-immunoprecipitates were analyzed by immunoblotting for the amounts of the specified recombinant proteins. (E) HEK-293T cells were transfected with FLAG-lipin 1 and treated with the indicated inhibitors (250 nM Torin1, 1.4 μM GSK3 IX and/or 250 nM PI-103) for 1 hour, and cell lysates and FLAG immunoprecipitates were prepared. FLAG immunoprecipitates were trypsin digested and the ratio of peptides containing the phosphorylated versus non-phosphorylated forms of S468 and S472 lipin 1 were quantified by mass spectrometry. „-„ indicates the phosphorylated form is absent, „+" indicates the

phosphorylated form is present, the number of „+"s indicate the relative abundance of the phosphorylated form. Cell lysates were immunoblotted for the levels and phosphorylation states of the specified proteins. (F) HEK-293T cells were transfected with myc-GSK3β, myc-rap2a, or FLAG-lipin 1 and treated Torin1 or vehicle for 1 hour. Myc and FLAG immunoprecipitates were prepared from cell lysates and myc immunoprecipitates were analyzed for kinase activity toward lipin 1 or for the levels and phosphorylated forms of the specified proteins. (G) FLAG-Wt or 17xS/T->A lipin 1 overexpressing NIH3T3 or AML12 cells were processed in an immunofluorescence assay to detect FLAG and imaged.

Fig. 3. Effect of lipin 1 on mTORC1- and PI3K/GSK3-dependent regulation of SREBP-target gene expression. (A) NIH3T3 cells were treated with 100 nM rapamycin, 250 nM Torin1, or vehicle for the indicated times. All mRNAs were measured by qRT-PCR and normalized to 36B4 mRNA levels. Error bars indicate standard error for n=4. * indicates $p<0.04$ in comparing Torin1 to vehicle treated cells. # indicates $p<0.02$ in comparing Torin1 to rapamycin treated cells. (B) Wild-type or fld MEFs were treated with 250 nM Torin1 or vehicle for the indicated times. All mRNAs were analyzed as in (A). * indicates $p<0.04$ in comparing equivalently treated fld to wild-type cells. (C) Wild-type or fld MEFs were treated with 250 nM PI-103, 250 nM PI-103 in addition to 1.4 μM GSK3 IX, or vehicle for the indicated times. All mRNAs were analyzed as in (A). * indicates $p<0.02$ in comparing equivalently treated fld to wild-type cells. (D) Indicated lipin 1 lentiviral expression vectors were stably introduced into fld cells and RNA was isolated 5 days post-infection. All mRNAs were analyzed as in (A). * indicates $p<0.01$ in comparing catalytically active, 17xS/T->A and wild-type lipin 1 expressing cells.

Fig. 4. Response of liver-specific raptor knock-out ($raptor^{Li-/-}$) mice to a high fat and high cholesterol (western) diet is lipin 1-dependent. (A) $Raptor^{Li+/+}$ (floxed raptor; Albumin-CRE-) and $raptor^{Li-/-}$ (floxed raptor; Albumin-CRE+) were starved of chow overnight and re-fed for 45 minutes. Liver and muscle tissue were

isolated from which cell lysates prepared and analyzed by immunoblotting for the phosphorylation states and levels of specified proteins. (B) 4 month old male raptor$^{Li+/+}$ and raptor$^{Li-/-}$ mice were fed chow or a western diet for two months. Body weights were measured bi-monthly. Error bars indicate standard error for n=6. (C) Representative 1x or 20x images of raptor$^{Li+/+}$ and raptor$^{Li-/-}$ livers taken from chow and western diet-fed mice. (D) Liver tissue was isolated and RNA was extracted from the indicated mice fed their respective diets for 6-8 weeks. All mice were starved for 4 hours prior to liver harvesting. All mRNAs were measured by qRT-PCR and normalized to 36B4 mRNA levels. Error bars indicate standard error for n=4-6. C, Chow, W, Western. * indicates $p<0.02$, # $p<0.04$ ^ $p<0.05$, respectively. (E) Liver tissue, from which lipids were extracted, and plasma for cholesterol measurements were obtained from mice fed the indicated diets for 6-8 weeks. All mice were starved for 4 hours prior to liver and plasma harvesting. Error bars indicate standard error for n=4 (liver triglycerides), n=6 (plasma cholesterol). * indicates $p<0.004$, # indicates $p<0.05$. (F) Western diet-fed raptor$^{Li+/+}$ and raptor$^{Li-/-}$ were infected with adenovirus expressing shRNAs targeting lacZ or lipin 1. Liver was harvested 5 days after infection and lysates prepared and immunoblotting was performed for the indicated proteins and (G) mRNA was isolated and analyzed as in (D). * indicates $p<0.01$, # indicates $p<0.05$ in comparing LacZ shRNA versus lipin 1 shRNA treated raptor$^{Li-/-}$ mice. (H) Liver triglycerides and plasma cholesterol were measured as in (E). * indicates $p<0.05$, # indicates $p<0.05$.

Fig. 5. Inhibition of SREBP-target gene expression by mTORC1 and lipin 1 requires lamin A. (A) Explanation of eccentricity. The eccentricity of an elliptical object is a measure of how much the shape of the ellipse deviates from being circular. Defined mathematically, eccentricity=1-2/((a/p)+1), where a is the radius at apopasis, i.e., the farthest distance from the edge of the ellipse to its center, and p is the radius at periapsis, i.e., the closest distance to ellipse center. The eccentricity of an ellipse is necessarily between 0 and 1; a circle has an eccentricity of 0. As the eccentricity tends to 1, the ellipse becomes more

elongated, and the ratio of a/p tends to infinity. (B) NIH3T3 cells treated with the indicated inhibitors (100 nM rapamycin, 250 nM Torin1, 1.4 μM GSK3 IX, 250 nM PI-103) or vehicle for 12 hours; or fld cells overexpressing specified FLAG-lipin 1 or -metap2 constructs were processed in an immunofluorescence assay to detect lamin A and imaged. Illustrative nuclei for each condition are shown. (C) Images processed in (B) were analyzed for mean lamin A eccentricity by image analysis software (*62*) for three independent fields for each condition (>500 cells total). Error bars indicate standard error for n=3. * indicates $p<0.0003$, # indicates $p<0.02$. (D) NIH3T3 cells were treated with Torin1 or deprived of serum and glucose for indicated times and analyzed as in (C). (E) Lamin $A^{+/+}$ and $^{-/-}$ MEFs were treated with 250 nM Torin1 for 12 hours. Protein lysates were prepared and immunoblotting for lamin A was performed. All mRNAs were measured by qRT-PCR and normalized to 36B4 mRNA levels. Error bars indicate standard error for n=4. * indicates $p<0.03$. N.S., Not Significant. (F) Lamin $A^{+/+}$ and $^{-/-}$ MEFs overexpressing Wt or 17xS/T->A mutant lipin 1 were analyzed for FLAG levels and the indicated mRNAs as in (E). * indicates $p<0.005$. (G) Human fibroblasts from a Hutchinson Gilford Progeria Syndrome patient or an unaffected relative were transduced with shRNAs targeting TSC2 or GFP. Protein lysates were prepared and immunoblotting was performed for the indicated proteins. mRNAs were measured by qRT-PCR and normalized to GAPDH mRNA levels. Error bars indicate standard error for n=4. * indicates $p<0.02$. (H) NIH3T3 cells overexpressing FLAG-SREBP1 were treated with 250 nM Torin1 or vehicle for 8 hours. Cells were then processed in an immunofluorescence assay to detect lamin A (green), FLAG (red) and costained with DAPI for DNA content (blue), and imaged. (I) Schematic of the genetic interactions characterized between mTORC1, GSK3, lipin 1, lamin A and SREBP. Arrows (->) indicate positive relationships, hatched bars (-|) indicate negative relationships.

Fig. S1. Further characterization of the regulation of lipin 1 localization upon mTORC1 or cell cycle perturbation. (A) FLAG-lipin 1 overexpressing HEK-293T cells were treated with 100 nM rapamycin, 250 nM Torin1 for 8 hours. Cells were

then processed in an immunofluorescence assay to detect FLAG, and imaged (A) or analyzed by immunoblotting (B) for the levels and phosphorylation state of 4E-BP1. (C) FLAG-lipin 1 overexpressing NIH3T3 cells were starved for serum and/or glucose for 8 hours. Cells were then processed and analyzed as in (A) and (B). (E) HEK-293T cells overexpressing FLAG-lipin 1 were starved of amino acids for 2 hours. and imaged as in (A). (F) FLAG-lipin 1 overexpressing NIH3T3 were treated with the indicated compounds (14 µm roscovitine, 10 µM PD184352) or vehicle for 12 hours. Double thymidine block was performed as follows: 2 mM thymidine for 12 hours-> 12 hours re-fresh media without thymidine-> 12 hours 2 mM thymidine.

Fig. S2. Further characterization of lipin 1 phosphorylation, the mTORC1-Lipin 1 interaction, and lipin 1 localization. (A) HEK-293T cells overexpressing FLAG-lipin 1 were treated with the indicated inhibitors (100 nM rapamycin or 250 nM Torin1) or vehicle for 12 hours. FLAG immunoprecipitates were prepared, trypsin digested, and the ratio of peptides containing the phosphorylated versus non-phosphorylated forms of S237 lipin 1 were quantified by mass spectrometry („-„ indicates the phosphorylated form was not detected, „+" indicates the phosphorylated form was detected). (B) AML12 cells expressing FLAG-lipin 1 or FLAG-metap2 were treated with 250 nM Torin1 or vehicle for 12 hours. FLAG immunoprecipitates and cell lysates were analyzed by immunoblotting for indicated proteins. (C) AML12 cells overexpressing FLAG-tagged Wt or S106A lipin 1 were processed in an immunofluorescence assay to detect FLAG and imaged.

Fig. S3. Further characterization of the regulation of mTORC1 on the SREBP pathway. NIH3T3 cells were treated with 100 nM rapamycin, 250 nM Torin1, or vehicle for the indicated times. SREBP1 mRNA was measured by qRT-PCR and normalized to 36B4 mRNA levels. Error bars indicate standard error for n=4.

Fig. S4. LoxP-raptor-LoxP conditional allele design and further phenotypic characterization of raptor$^{Li-/-}$ mice. (A) Schematic of the raptor gene and targeted allele. Recombinant genomic DNA including exon 6 of the raptor gene flanked with LoxP sites (black arrows) and intronic sequence was introduced into the endogenous locus by homologous recombination. FRT sites to excise the neomycin resistance gene (neo) are indicated by white arrows. Localization and size of DNA fragment generated by Bgl II restriction digest of the targeted allele is indicated. Probe used for southern blot analysis is shown as a wavy line (~~). Localization of PCR primers („^") and size of DNA amplified using these primers on the targeted allele are indicated. (B) Genotyping assays to identify proper raptor exon 6 targeting. Bgl II genomic DNA digestion and Southern blot analysis was used to identify ES clones that had undergone a homologous recombination event between the linearized targeting vector and genomic DNA. The presence of the neo gene, FRT sites, and LoxP sites increases the size of the targeted locus by ~2 kb. PCR of mouse tail genomic DNA was performed to distinguish between untargeted raptor intronic sequence and that containing the 3" LoxP site. wt, wild-type; m, DNA marker. Representative samples are shown in the analyses in (B). (C) Liver-specific raptor knock-out mice are protected from western diet-induced hyperglycemia. Blood glucose measurements were made from 4 hour starved, 6 month old mice fed indicated diets for 2 months. Error bars indicate standard error for n=6. C, chow; W, western. * indicates $p<0.01$. (D) Daily food consumption is unaffected by raptor genotype or diet. Error bars indicate standard error for n=6.

Fig. S5. Further characterization of mTORC1/lipin 1-dependent regulation of lamin A and lamin A-dependent regulation on SREBP-target gene expression or promoter binding. (A) Wild-type or fld MEFs were treated with 250 nM Torin1 or vehicle for the indicated times. Cells were then processed in an immunofluorescence assay to detect lamin A and images were analyzed for mean lamin A eccentricity by image analysis software for three independent fields for each condition (>500 cells total). Error bars indicate standard error for

n=3. (B). SREBP-target expression levels from fibroblast cell lines from HGPS patients or matched unaffected individuals were obtained from microarray expression profiles deposited in NCBI GEO database by (*63*). mRNA from three control and affected individuals were probed in triplicate. Error bars indicate standard error for n=9. * indicates $p<0.007$ in comparing HGPS to unaffected cells. (C) Lamin $A^{+/+}$ and $^{-/-}$ MEFs were treated with 250 nM Torin1 or vehicle for 12 hours. Cell lysates and lamin A immunoprecipitates were immunoblotted for lamin A or protease digested and genomic DNA was measured by PCR. For each condition, immunoprecipitated DNA was normalized to its corresponding whole cell lysate DNA. Error bars indicate standard error for n=4. * indicates $p<0.03$. (D) Lamin $A^{+/+}$ and $^{-/-}$ MEFs overexpressing Wt or 17xS/T->A mutant lipin 1 were prepared and analyzed as in (C). * indicates $p<0.03$.

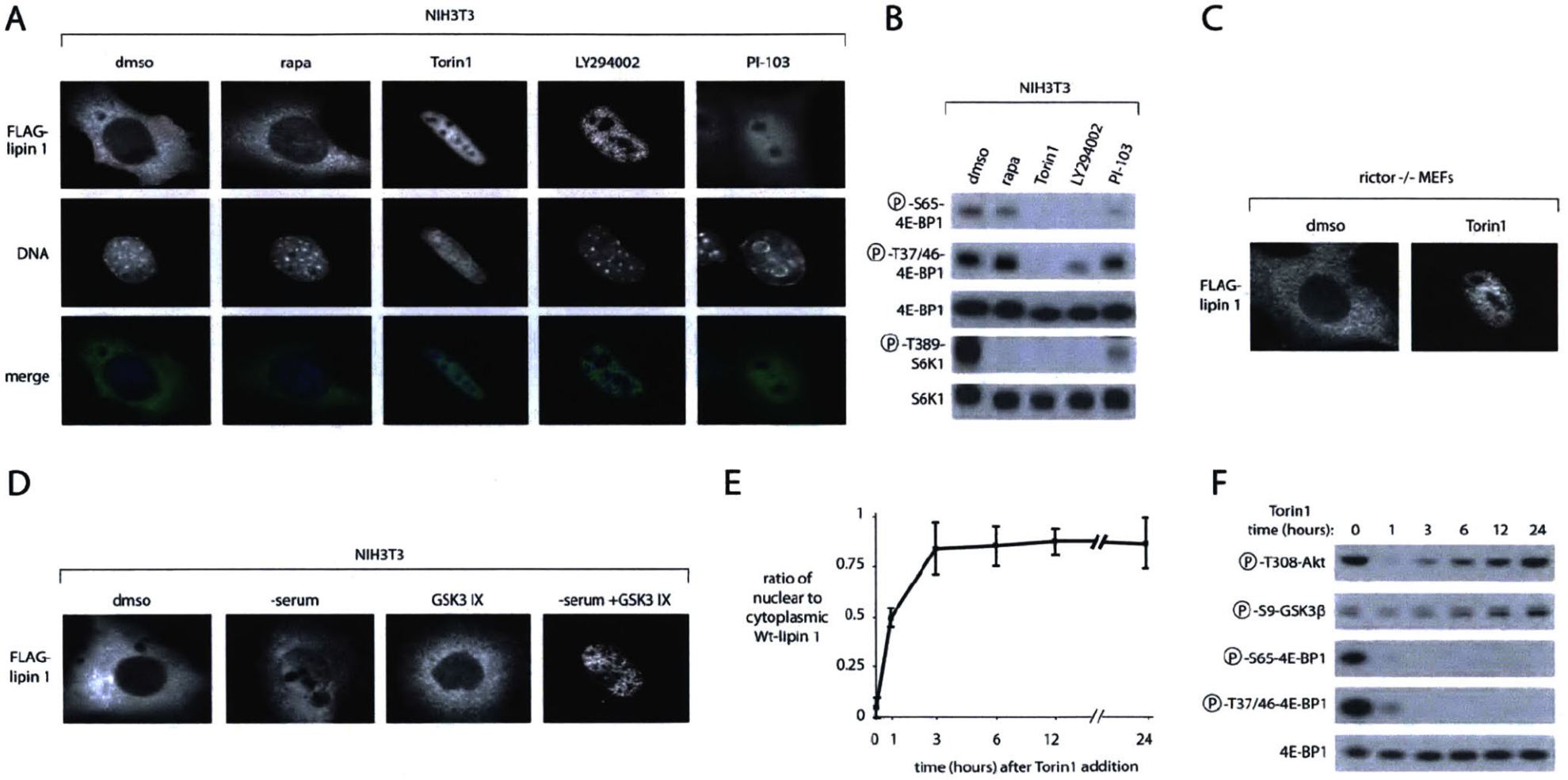
A
NIH3T3
dmso
rapa
Torin1
LY294002
PI-103
FLAG-lipin 1
DNA
merge
B
NIH3T3
dmso
rapa
Torin1
LY294002
PI-103
Ⓟ-S65-4E-BP1
Ⓟ-T37/46-4E-BP1
4E-BP1
Ⓟ-T389-S6K1
S6K1
C
rictor -/- MEFs
dmso
Torin1
FLAG-lipin 1
D
NIH3T3
dmso
-serum
GSK3 IX
-serum +GSK3 IX
FLAG-lipin 1
E
ratio of nuclear to cytoplasmic Wt-lipin 1
1
0.75
0.5
0.25
0
0 1 3 6 12 24
time (hours) after Torin1 addition
F
Torin1 time (hours): 0 1 3 6 12 24
Ⓟ-T308-Akt
Ⓟ-S9-GSK3β
Ⓟ-S65-4E-BP1
Ⓟ-T37/46-4E-BP1
4E-BP1

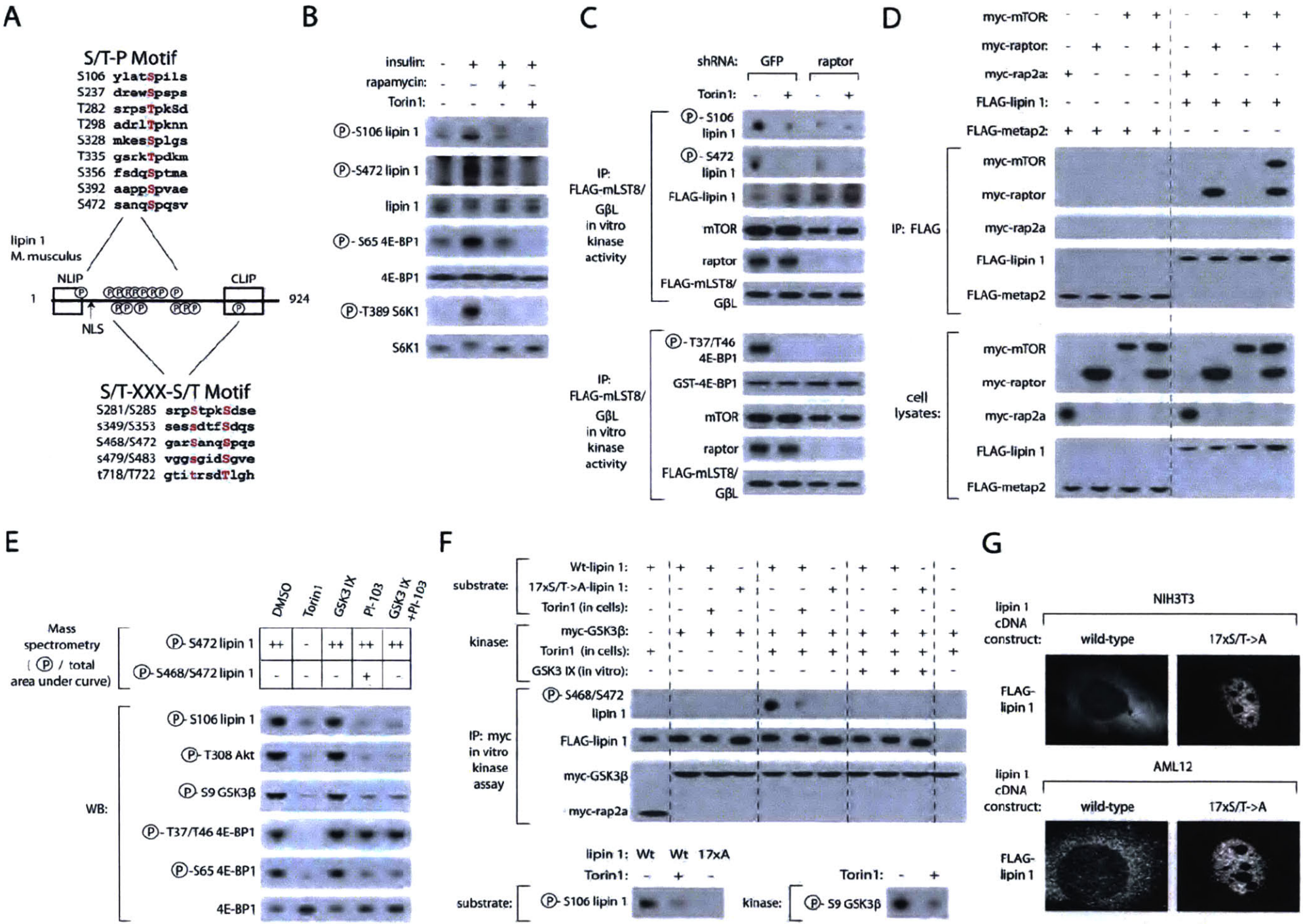
A
S/T-P Motif
S106 ylatSpils
S237 drewSpsps
T282 srpsTpkSd
T298 adrlTpknn
S328 mkesSplgs
T335 gsrkTpdkm
S356 fsdqSptma
S392 aappSpvae
S472 sanqSpqsv
lipin 1
M. musculus
NLIP
CLIP
1
924
NLS
S/T-XXX-S/T Motif
S281/S285 srpStpkSdse
s349/S353 sessdtfSdqs
S468/S472 garSanqSpqs
s479/S483 vggsgidSgve
t718/T722 gtitrsdTlgh
B
insulin:
rapamycin:
Torin1:
Ⓟ-S106 lipin 1
Ⓟ-S472 lipin 1
lipin 1
Ⓟ- S65 4E-BP1
4E-BP1
Ⓟ-T389 S6K1
S6K1
C
shRNA:
GFP
raptor
Torin1:
IP: FLAG-mLST8/ GβL in vitro kinase activity
Ⓟ- S106 lipin 1
Ⓟ- S472 lipin 1
FLAG-lipin 1
mTOR
raptor
FLAG-mLST8/ GβL
IP: FLAG-mLST8/ GβL in vitro kinase activity
Ⓟ- T37/T46 4E-BP1
GST-4E-BP1
mTOR
raptor
FLAG-mLST8/ GβL
D
myc-mTOR:
myc-raptor:
myc-rap2a:
FLAG-lipin 1:
FLAG-metap2:
IP: FLAG
myc-mTOR
myc-raptor
myc-rap2a
FLAG-lipin 1
FLAG-metap2
cell lysates:
myc-mTOR
myc-raptor
myc-rap2a
FLAG-lipin 1
FLAG-metap2
E
DMSO
Torin1
GSK3 IX
PI-103
GSK3 IX +PI-103
Mass spectrometry (Ⓟ / total area under curve)
Ⓟ- S472 lipin 1
Ⓟ- S468/S472 lipin 1
WB:
Ⓟ- S106 lipin 1
Ⓟ- T308 Akt
Ⓟ- S9 GSK3β
Ⓟ- T37/T46 4E-BP1
Ⓟ-S65 4E-BP1
4E-BP1
F
substrate:
Wt-lipin 1:
17xS/T->A-lipin 1:
Torin1 (in cells):
kinase:
myc-GSK3β:
Torin1 (in cells):
GSK3 IX (in vitro):
IP: myc in vitro kinase assay
Ⓟ- S468/S472 lipin 1
FLAG-lipin 1
myc-GSK3β
myc-rap2a
lipin 1: Wt Wt 17xA
Torin1:
substrate:
Ⓟ- S106 lipin 1
kinase:
Torin1:
Ⓟ- S9 GSK3β
G
lipin 1 cDNA construct:
NIH3T3
wild-type
17xS/T->A
FLAG-lipin 1
lipin 1 cDNA construct:
AML12
wild-type
17xS/T->A
FLAG-lipin 1

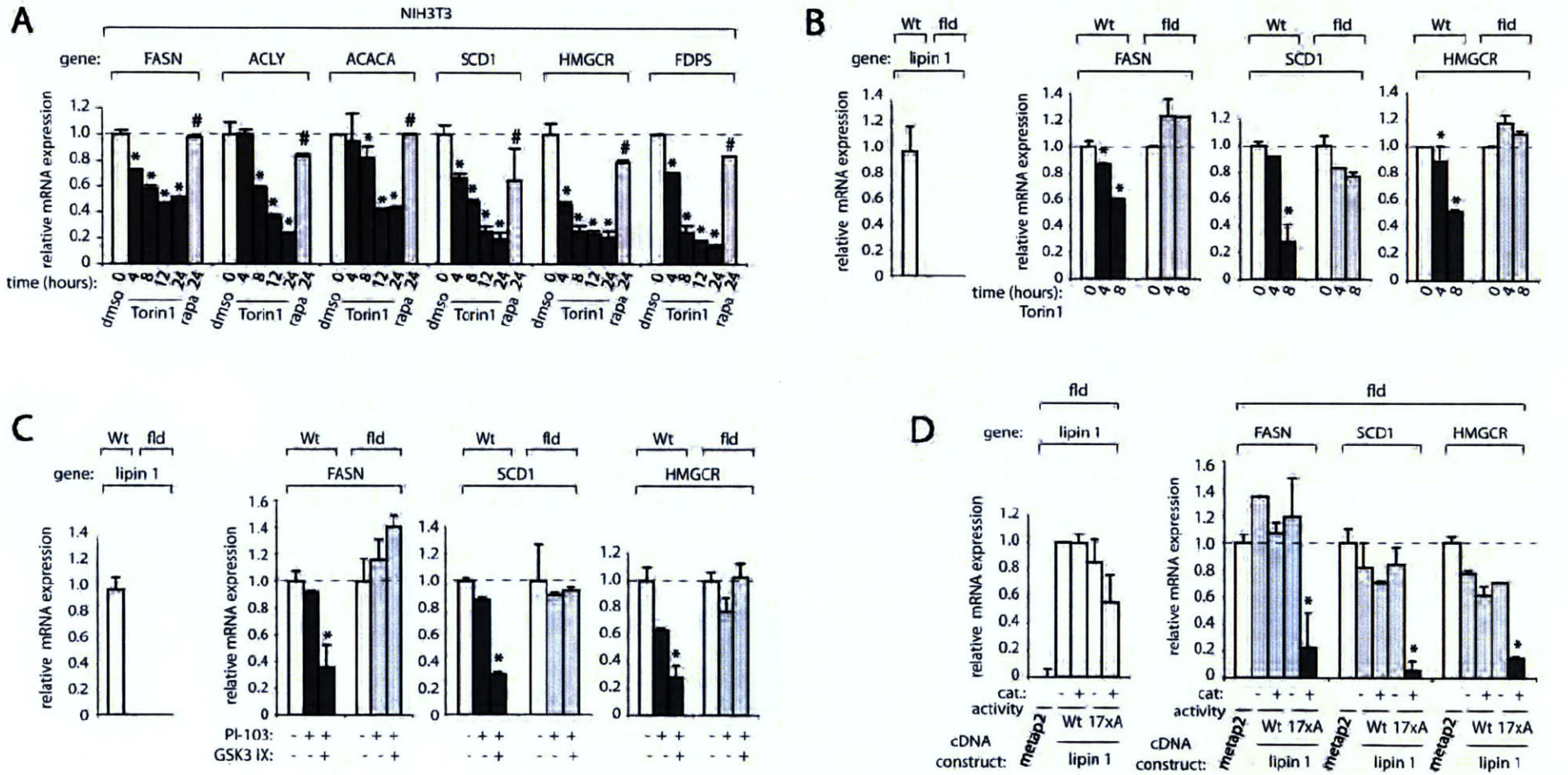
A
NIH3T3
gene:
FASN
ACLY
ACACA
SCD1
HMGCR
FDPS
relative mRNA expression
time (hours):
dmso
Torin1
rapa
B
Wt
fld
gene:
lipin 1
FASN
SCD1
HMGCR
relative mRNA expression
time (hours):
Torin1
C
Wt
fld
gene:
lipin 1
FASN
SCD1
HMGCR
relative mRNA expression
PI-103:
GSK3 IX:
D
fld
gene:
lipin 1
FASN
SCD1
HMGCR
relative mRNA expression
cat:
activity
cDNA construct:
metap2
Wt
17xA
lipin 1

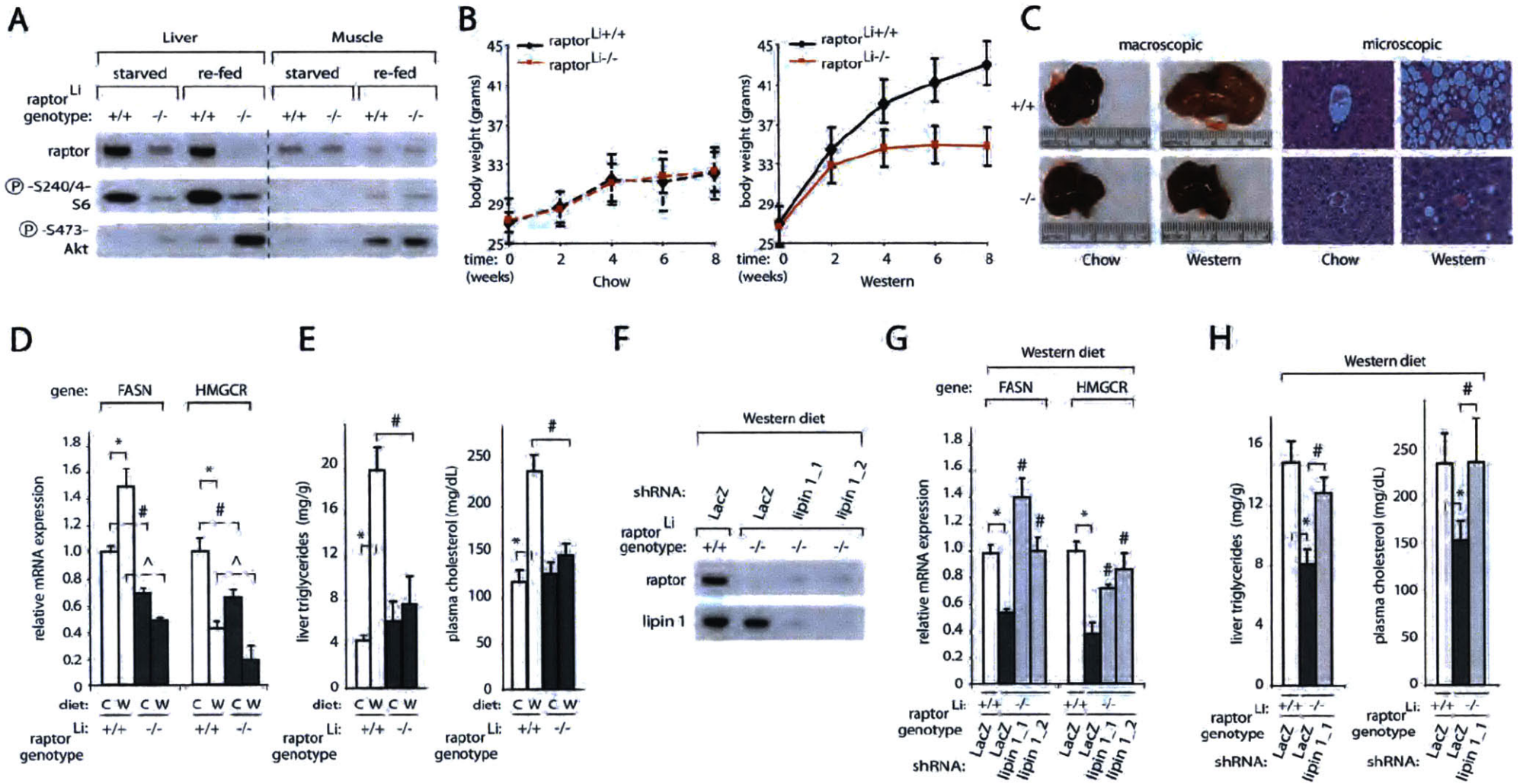
A
Liver
Muscle
starved
re-fed
starved
re-fed
raptor Li genotype: +/+ -/- +/+ -/- +/+ -/- +/+ -/-
raptor
Ⓟ -S240/4-S6
Ⓟ -S473-Akt
B
raptor Li+/+
raptor Li-/-
body weight (grams)
time: 0 2 4 6 8 (weeks)
Chow
Western
C
macroscopic
microscopic
+/+
-/-
Chow
Western
Chow
Western
D
gene: FASN HMGCR
relative mRNA expression
diet: C W C W C W C W
raptor Li genotype: +/+ -/- +/+ -/-
E
liver triglycerides (mg/g)
plasma cholesterol (mg/dL)
diet: C W C W
raptor Li genotype: +/+ -/-
F
Western diet
shRNA: LacZ LacZ lipin 1_1 lipin 1_2
raptor Li genotype: +/+ -/- -/- -/-
raptor
lipin 1
G
Western diet
gene: FASN HMGCR
relative mRNA expression
raptor Li genotype: +/+ -/- +/+ -/-
shRNA: LacZ LacZ lipin 1_1 lipin 1_2 LacZ LacZ lipin 1_1 lipin 1_2
H
Western diet
liver triglycerides (mg/g)
plasma cholesterol (mg/dL)
raptor Li genotype: +/+ -/- +/+ -/-
shRNA: LacZ LacZ lipin 1_1 LacZ LacZ lipin 1_1

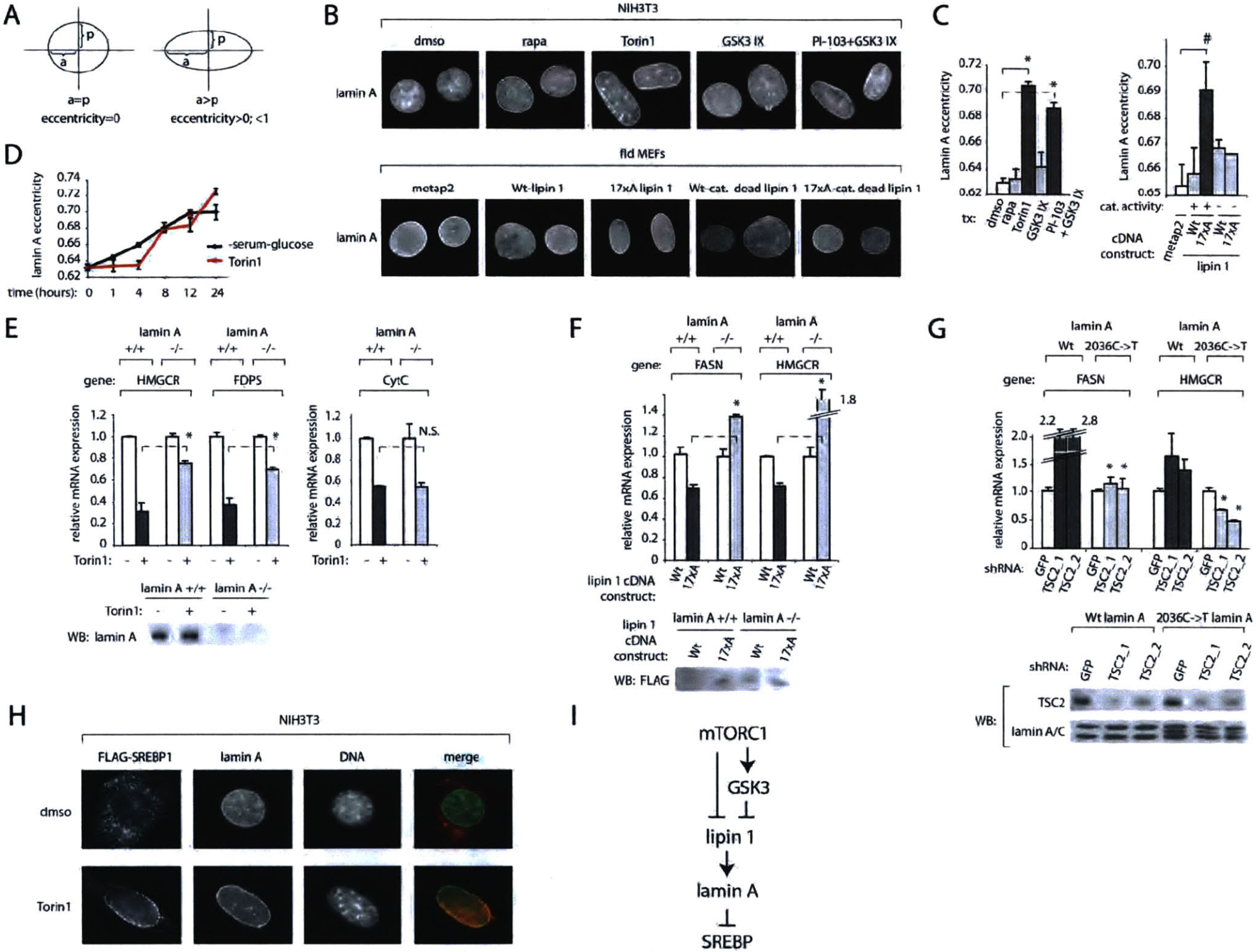
A
p
a
a=p
eccentricity=0
a>p
eccentricity>0; <1
B
NIH3T3
dmso
rapa
Torin1
GSK3 IX
PI-103+GSK3 IX
lamin A
fld MEFs
metap2
Wt-lipin 1
17xA lipin 1
Wt-cat. dead lipin 1
17xA-cat. dead lipin 1
lamin A
C
Lamin A eccentricity
tx:
dmso
rapa
Torin1
GSK3 IX
PI-103 + GSK3 IX
cat. activity:
cDNA construct:
metap2
Wt 17xA
lipin 1
D
lamin A eccentricity
-serum-glucose
Torin1
time (hours): 0 1 4 8 12 24
E
lamin A +/+
lamin A -/-
gene:
HMGCR
FDPS
CytC
relative mRNA expression
Torin1:
N.S.
lamin A +/+
lamin A -/-
WB: lamin A
F
gene:
FASN
HMGCR
relative mRNA expression
1.8
lipin 1 cDNA construct:
Wt
17xA
lipin 1 cDNA construct:
WB: FLAG
G
Wt
2036C->T
gene:
FASN
HMGCR
relative mRNA expression
2.2
2.8
shRNA:
GFP
TSC2_1
TSC2_2
Wt lamin A
2036C->T lamin A
WB:
TSC2
lamin A/C
H
NIH3T3
FLAG-SREBP1
lamin A
DNA
merge
dmso
Torin1
I
mTORC1
GSK3
lipin 1
lamin A
SREBP

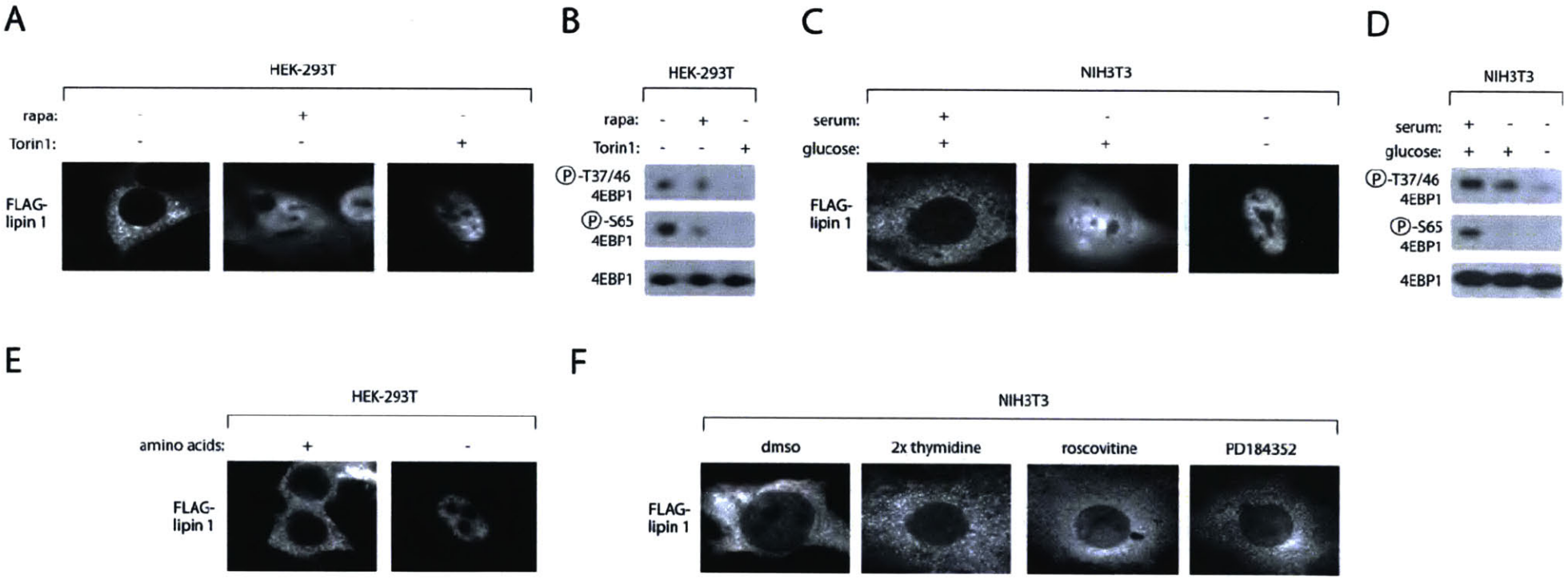
A
HEK-293T
rapa: - + -
Torin1: - - +
FLAG-lipin 1
B
HEK-293T
rapa: - + -
Torin1: - - +
Ⓟ-T37/46 4EBP1
Ⓟ-S65 4EBP1
4EBP1
C
NIH3T3
serum: + - -
glucose: + + -
FLAG-lipin 1
D
NIH3T3
serum: + - -
glucose: + + -
Ⓟ-T37/46 4EBP1
Ⓟ-S65 4EBP1
4EBP1
E
HEK-293T
amino acids: + -
FLAG-lipin 1
F
NIH3T3
dmso
2x thymidine
roscovitine
PD184352
FLAG-lipin 1

A

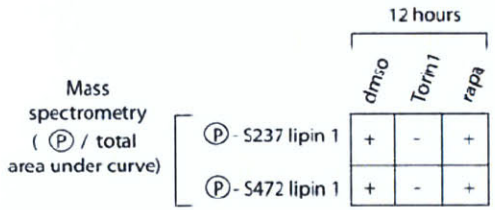
12 hours
dmso
Torin1
rapa
Mass spectrometry (Ⓟ / total area under curve)
Ⓟ - S237 lipin 1
+
-
+
Ⓟ - S472 lipin 1
+
-
+

B

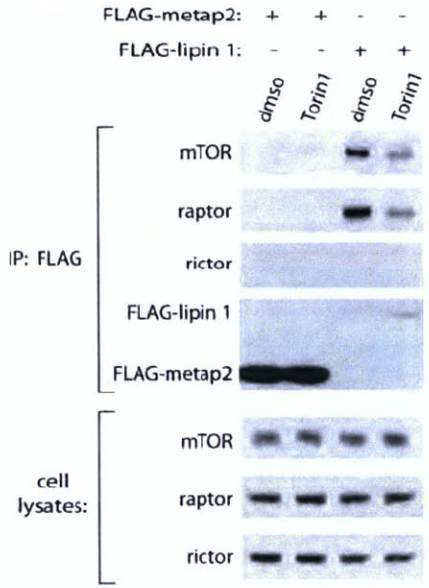
FLAG-metap2: + + - -
FLAG-lipin 1: - - + +
dmso
Torin1
dmso
Torin1
IP: FLAG
mTOR
raptor
rictor
FLAG-lipin 1
FLAG-metap2
cell lysates:
mTOR
raptor
rictor

C

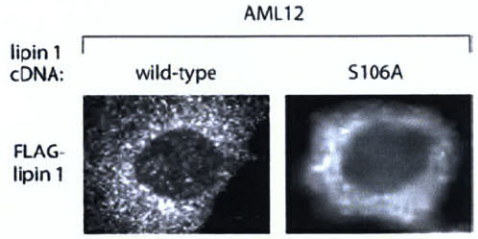
AML12
lipin 1 cDNA:
wild-type
S106A
FLAG-lipin 1

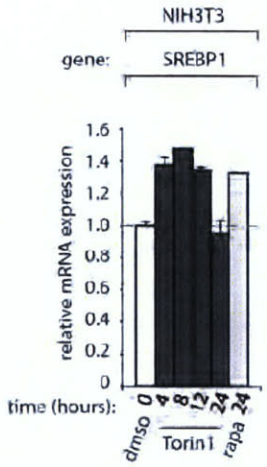
NIH3T3
gene:
SREBP1
relative mRNA expression
1.6
1.4
1.2
1.0
0.8
0.6
0.4
0.2
0
time (hours):
0
4
8
12
24
24
dmso
Torin1
rapa

A

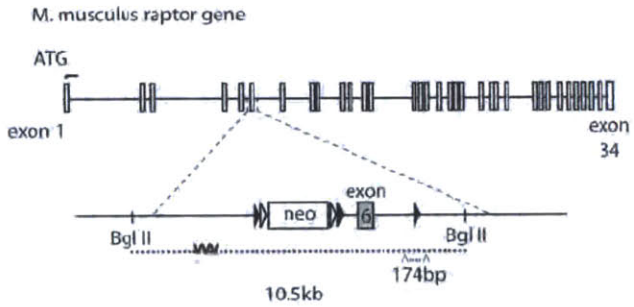
M. musculus raptor gene
ATG
exon 1
exon
34
exon
neo
6
Bgl II
Bgl II
174bp
10.5kb

B

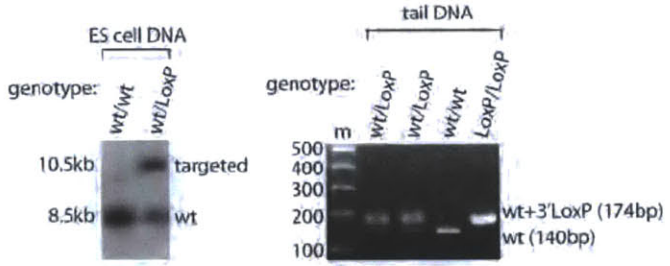
ES cell DNA
genotype:
wt/wt
wt/LoxP
10.5kb
targeted
8.5kb
wt
tail DNA
genotype:
wt/LoxP
wt/LoxP
wt/wt
LoxP/LoxP
m
500
400
300
200
100
wt+3'LoxP (174bp)
wt (140bp)

C

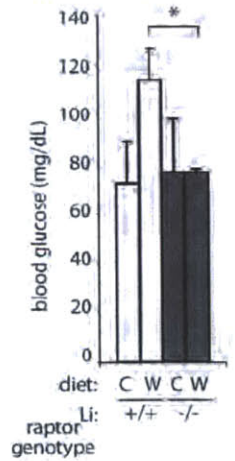
*
140
120
100
80
60
40
20
0
blood glucose (mg/dL)
diet:
C W C W
Li:
+/+ -/-
raptor genotype

D

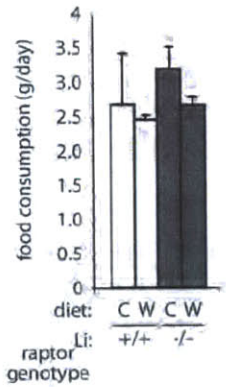
4
3.5
3.0
2.5
2.0
1.5
1.0
0.5
0
food consumption (g/day)
diet:
C W C W
Li:
+/+ -/-
raptor genotype

A

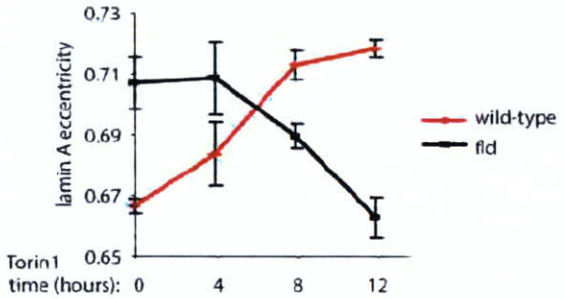
lamin A eccentricity
0.73
0.71
0.69
0.67
0.65
wild-type
fld
Torin1
time (hours): 0 4 8 12

B

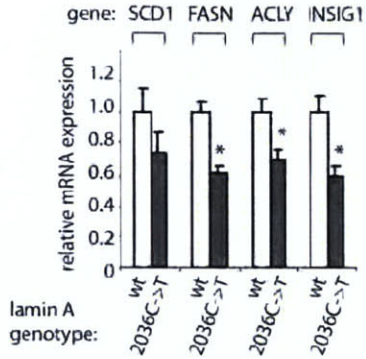
gene: SCD1 FASN ACLY INSIG1
relative mRNA expression
1.2
1.0
0.8
0.6
0.4
0.2
0
lamin A genotype:
wt
2036C->T

C

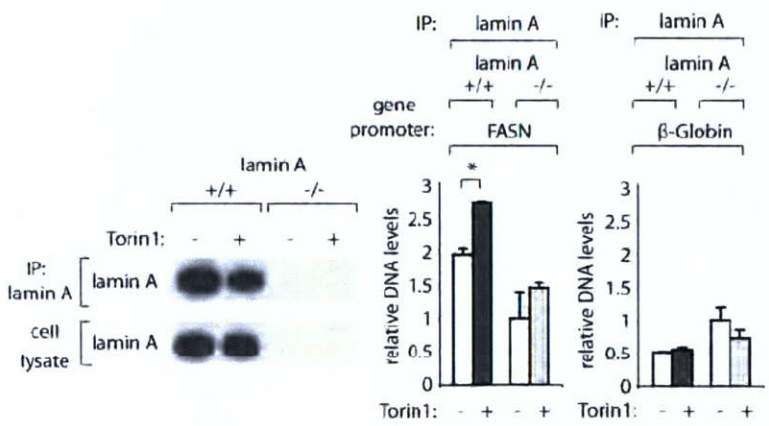
lamin A
+/+
-/-
Torin1: - + - +
IP: lamin A
lamin A
cell lysate
lamin A
IP: lamin A
gene promoter: FASN
relative DNA levels
Torin1: - + - +
IP: lamin A
gene promoter: β-Globin
relative DNA levels
Torin1: - + - +

D

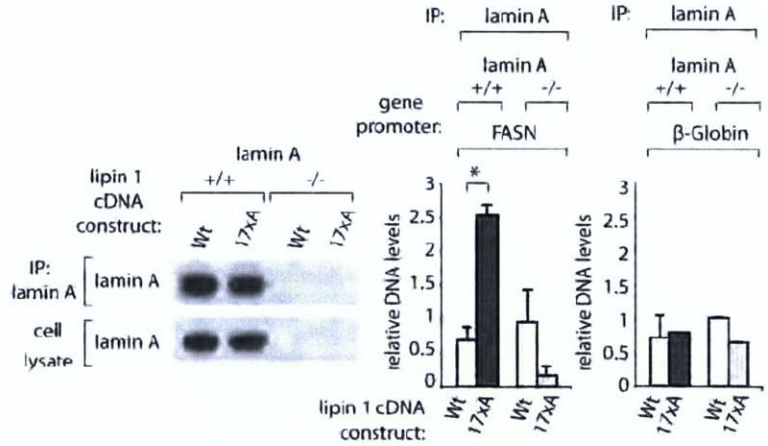
lamin A
lipin 1 cDNA construct:
Wt
17xA
IP: lamin A
cell lysate
lamin A
IP: lamin A
gene promoter: FASN
relative DNA levels
lipin 1 cDNA construct:
IP: lamin A
gene promoter: β-Globin
relative DNA levels

References

1. J. Avruch *et al.*, *Biochem Soc Trans.* **37**, 223 (2009).
2. H. Lempiainen *et al.*, *Mol Cell.* **33**, 704 (2009).
3. R. M. Bell, R. A. Coleman, *Annu Rev Biochem* **49**, 459 (1980).
4. G. S. Han, W. I. Wu, G. M. Carman, *J Biol Chem* **281**, 9210 (Apr 7, 2006).
5. T. A. Huffman, I. Mothe-Satney, J. C. Lawrence, Jr., *Proc Natl Acad Sci U S A* **99**, 1047 (2002).
6. M. Peterfy, J. Phan, P. Xu, K. Reue, *Nat Genet.* **27**, 121 (2001).
7. D. H. Kim *et al.*, *Cell* **110**, 163 (Jul 26, 2002).
8. K. Hara *et al.*, *Cell* **110**, 177 (2002).
9. T. E. Harris *et al.*, *J Biol Chem.* **282**, 277 (2007).
10. L. O'Hara *et al.*, *J Biol Chem.* **281**, 34537 (2006).
11. C. C. Thoreen *et al.*, *J Biol Chem* **15**, 15 (2009).
12. G. J. Brunn *et al.*, *EMBO Journal* **15**, 5256 (1996).
13. M. Peterfy, T. E. Harris, N. Fujita, K. Reue, *J Biol Chem* **285**, 3857 (Feb 5).
14. A. Y. Choo, S. O. Yoon, S. G. Kim, P. P. Roux, J. Blenis, *Proc Natl Acad Sci U S A* **105**, 17414 (Nov 11, 2008).
15. Y. Sancak *et al.*, *Mol Cell* **25**, 903 (Mar 23, 2007).
16. D. A. Cross, D. R. Alessi, P. Cohen, M. Andjelkovich, B. A. Hemmings, *Nature* **378**, 785 (1995).
17. K. Hara *et al.*, *J Biol Chem* **273**, 14484 (1998).
18. L. O'Hara *et al.*, *J Biol Chem* **281**, 34537 (Nov 10, 2006).
19. N. Grimsey *et al.*, *J Biol Chem* **283**, 29166 (Oct 24, 2008).
20. G. J. Brunn *et al.*, *Science* **277**, 99 (1997).
21. P. E. Burnett, R. K. Barrow, N. A. Cohen, S. H. Snyder, D. M. Sabatini, *PNAS* **95**, 1432 (1998).
22. A. C. Gingras *et al.*, *Genes Dev* **13**, 1422 (1999).
23. C. J. Fiol, A. M. Mahrenholz, Y. Wang, R. W. Roeske, P. J. Roach, *J Biol Chem.* **262**, 14042 (1987).

24. P. Cohen, M. Goedert, *Nat Rev Drug Discov.* **3**, 479 (2004).
25. A. Y. Choo, S. O. Yoon, S. G. Kim, P. P. Roux, J. Blenis, *Proc Natl Acad Sci U S A.* **105**, 17414 (2008).
26. N. Hosokawa *et al.*, *Mol Biol Cell.* **20**, 1981 (2009).
27. S. S. Schalm, D. C. Fingar, D. M. Sabatini, J. Blenis, *Curr Biol* **13**, 797 (May 13, 2003).
28. L. Wang, C. J. Rhodes, J. C. Lawrence, Jr., *J Biol Chem* **281**, 24293 (Aug 25, 2006).
29. S. H. Um *et al.*, *Nature* **431**, 200 (Sep 9, 2004).
30. T. Porstmann *et al.*, *Cell Metab.* **8**, 224 (2008).
31. S. Li, Brown, M.S., Goldstein, J.L., *Proc Natl Acad Sci U S A*, (February 1, 2010).
32. J. D. Horton, J. L. Goldstein, M. S. Brown, *J Clin Invest.* **109**, 1125 (2002).
33. M. S. Brown, J. L. Goldstein, *J Lipid Res* **50 Suppl**, S15 (Apr, 2009).
34. S. Rehnmark, C. S. Giometti, B. G. Slavin, M. H. Doolittle, K. Reue, *J Lipid Res.* **39**, 2209 (1998).
35. G. S. Han, W. I. Wu, G. M. Carman, *J Biol Chem.* **281**, 9210 (2006).
36. B. N. Finck *et al.*, *Cell Metab.* **4**, 199 (2006).
37. J. D. Horton *et al.*, *Proc Natl Acad Sci U S A.* **100**, 12027 (2003).
38. G. Friedrich, P. Soriano, *Genes Dev.* **5**, 1513 (1991).
39. C. Postic, M. A. Magnuson, *Genesis.* **26**, 149 (2000).
40. N. Y. Kalaany *et al.*, *Cell Metab.* **1**, 231 (2005).
41. Y. Tange, A. Hirata, O. Niwa, *J Cell Sci.* **115**, 4375 (2002).
42. D. J. Lloyd, R. C. Trembath, S. Shackleton, *Hum Mol Genet.* **11**, 769 (2002).
43. R. L. Boguslavsky, C. L. Stewart, H. J. Worman, *Hum Mol Genet* **15**, 653 (Feb 15, 2006).
44. B. C. Capell, F. S. Collins, *Nat Rev Genet.* **7**, 940 (2006).
45. I. Shimomura, R. E. Hammer, S. Ikemoto, M. S. Brown, J. L. Goldstein, *Nature* **401**, 73 (Sep 2, 1999).
46. J. T. Cunningham *et al.*, *Nature.* **450**, 736 (2007).

47. Y. Zhang *et al.*, *Nat Cell Biol* **5**, 578 (Jun, 2003).
48. H. Stocker *et al.*, *Nat Cell Biol* **5**, 559 (Jun, 2003).
49. L. J. Saucedo *et al.*, *Nat Cell Biol* **5**, 566 (Jun, 2003).
50. A. Garami *et al.*, *Mol Cell* **11**, 1457 (Jun, 2003).
51. D. C. Lee, K. L. Welton, E. D. Smith, B. K. Kennedy, *Exp Cell Res.* **315**, 996 (2009).
52. L. Guelen *et al.*, *Nature.* **453**, 948 (2008).
53. K. L. Reddy, J. M. Zullo, E. Bertolino, H. Singh, *Nature.* **452**, 243 (2008).
54. V. Andres, J. M. Gonzalez, *J Cell Biol* **187**, 945 (Dec 28, 2009).
55. M. K. Bennett, Y. K. Seo, S. Datta, D. J. Shin, T. F. Osborne, *J Biol Chem.* **283**, 15628 (2008).
56. X. Wang, R. Sato, M. S. Brown, X. Hua, J. L. Goldstein, *Cell* **77**, 53 (Apr 8, 1994).
57. C. Capanni *et al.*, *Hum Mol Genet* **14**, 1489 (Jun 1, 2005).
58. C. B. Blum, *Am J Transplant.* **2**, 551 (2002).
59. C. Kenyon, *Cell.* **105**, 165 (2001).
60. M. Kaeberlein *et al.*, *Science.* **310**, 1193 (2005).
61. D. E. Harrison *et al.*, *Nature.* **460**, 392 (2009).
62. A. E. Carpenter *et al.*, *Genome Biol* **7**, R100 (2006).
63. A. B. Csoka *et al.*, *Aging Cell.* **3**, 235 (2004).

Experimental procedures

Materials

Reagents were obtained from the following sources: antibodies to lamin A (sc-20680, sc-6215), as well as HRP-labeled anti-mouse, anti-goat, and anti-rabbit secondary antibodies from Santa Cruz Biotechnology; rabbit polyclonal and monoclonal antibodies to phospho-S106 lipin 1, phospho-S472 lipin 1, phospho-S468/S472 lipin 1, phospho-T389 S6K1, phospho-T37/T46 4E-BP1, phospho-S65 4E-BP1, phospho-T308 Akt, phoshpo-S473 Akt, phospho-S9-GSK3β, TSC2, 4E-BP1, raptor, rictor, and mTOR from Cell Signaling Technology; rabbit polyclonal antibody to myc from Bethyl Laboratories; Flag M2 affinity gel, Flag M2 antibody, ATP, amino acids, Thymidine, SYBR Green JumpStart Taq ReadyMix, insulin, dexamethasone, and selenium from Sigma Aldrich; protein G Sepharose from Pierce; DMEM from SAFC Biosciences; amino acid-free RPMI from US Biological; rapamycin from LC Labs; PI-103, GSK3 IX, LY294002, and Roscovitine from Calbiochem, PD184352 from Axon Medchem; FuGENE 6 and Complete Protease Cocktail from Roche; SuperScript II Reverse Transcriptase, Alexa Fluor 488 and 594 secondary antibodies, Platinum Pfx, Platinum Taq DNA Polymerase, transferrin, and inactivated fetal calf serum (IFS) from Invitrogen. Antibodies to lipin 1 (LAb-1 used in HEK-293E cells and LAb-2 used on mouse livers) were previously described (*1*). GST-4E-BP1 was previously described (*2*).

Cell Lines and Cell Culture

Lamin A null and wild-type mouse fibroblasts were kindly provided by Colin Stewart (Institute of Medical Biology, Singapore). HEK-293E were kindly provided by John Blenis (Harvard Medical School). NIH3T3 and AML12 cells were obtained from ATCC. HGPS (AG01972) and wild-type (AG08469) human fibroblasts were obtained from the Coriell Institute. HEK-293E, HEK-293T, and all fibroblast cell lines were cultured in DMEM with 10% IFS unless otherwise stated. AML12 were cultured in 50%/50% DMEM/Ham's F-12 with 10% FBS

supplemented with 5μg/ml insulin, 5μg/ml transferrin, 40ng/ml dexamethasone, 5ng/ml selenium. Fld and wild-type MEFs were generated from fld/+ mice obtained from Jackson Laboratories.

cDNA Manipulations and Mutagenesis

The cDNA for lipin 1β used was cloned by Huffman TA et al.(*1*) and has the NCBI identifier: AAL07798. The cDNA for full-length SREBP1 was cloned from a NIH3T3 fibroblast cDNA library. The cDNA for mLST8/GβL was generated as previously described (*3*). The cDNA for full-length GSK3β was cloned from a HEK-293T cDNA library. The cDNA for the control genes, rap2a and metap2, were previously described and validated (*4*). For expression studies, lipin 1, SREBP1, mLST8/GβL, GSK3β, rap2a, metap2 cDNAs were amplified by PCR and the product was subcloned into the Sal 1 and Not 1 sites of pRK5 and/or pLKO. All constructs were verified by DNA sequencing. For the catalytic site mutant analysis, the lipin 1 cDNA was mutagenized using a QuikChange mutagenesis XLII kit (Stratagene) with oligonucleotides obtained from Integrated DNA Technologies. The catalytic site residues were mutated as follows: 712 D->E, 714 D->E. The 17xS/T->A mutant encompasses the following residues: S106, S150, S281, T282, S285, S287, S293, T298, S328, S353, S356, S392, S468, S472, S483, S634, S635, S647, S648, S921, S923. The 17xS/T->A mutant has wild-type PAP1 activity (Harris TE et al., manuscript in preparation).

Cell Lysis, Immunoprecipitations, and Kinase Assays

For protein studies, all cells were rinsed twice with ice-cold PBS before lysis. All cells, with the exception of those used to isolate mTOR-containing complexes, were lysed with Triton-X 100 containing lysis buffer (40 mM HEPES [pH 7.4], 2 mM EDTA, 10 mM sodium pyrophosphate, 10 mM sodium glycerophosphate, 150 mM NaCl, 50 mM NaF, 1% Triton-X 100, and one tablet of EDTA-free protease inhibitors [Roche] per 25 ml). The soluble fractions of cell lysates were isolated by centrifugation at 13,000 rpm for 10 minutes in a microcentrifuge. For myc immunoprecipitations, primary antibodies were added

to the lysates and incubated with rotation for 1.5 hours at 4°C. A 50%/50% slurry of protein G Sepharose/lysis buffer was then added, and the incubation continued for an additional 1 hour. For FLAG purifications, cells were lysed in ice-cold CHAPS-containing lysis buffer lacking added NaCl (40 mM HEPES [pH 7.4], 2 mM EDTA, 10 mM pyrophosphate, 10 mM glycerophosphate, 0.3% CHAPS, and one tablet of EDTA-free protease inhibitors [Roche] per 25 ml). FLAG M2 resins were incubated with pre-cleared cell lysates and incubated with rotation for 1.5 hours at 4°C. FLAG immunoprecipitates were washed three times with CHAPS lysis buffer containing 150 mM NaCl. For coimmunoprecipitation experiments, immunoprecipitated proteins were then denatured by the addition of sample buffer and by boiling for 5 minutes, resolved using 4%-12% SDS-PAGE (Invitrogen), and analyzed by immunoblotting as described (*5*). For kinase assays, myc or FLAG immunoprecipitates were additionally washed twice in 25 mM HEPES (pH 7.4), 20 mM KCL after the 3 washes in their respective 150mM NaCl-containing lysis buffers. For elution of FLAG-tagged proteins, beads were incubated in elution buffer (50mM HEPES pH 7.4, 500mM NaCl, 0.1% CHAPS, 50µg/ul FLAG peptide) for 15 min at 25^0C. Kinase assays were performed as described (*6*).

Mass Spectrometric Analysis

Lipin 1 phosphorylation sites were identified by mass spectrometry of trypsin-digested FLAG-lipin 1 purified from HEK293T cells transiently overexpressing FLAG-lipin 1. The amino acid position of all lipin 1 phosphorylation sites were numbered according to NCBI M. musculus lipin 1β protein sequence NP_056578.

Label-free quantification of lipin 1 phosphorylation sites were performed with BioWorks Rev3.3 software according to the methodology utilized in (*7*).

Mammalian Lentiviral Transduction

The GFP control shRNA was previously described and validated (*4*). The raptor shRNA was previously described and validated (*8*). The TSC2 shRNAs

were obtained from the collection of The RNAi Consortium (TRC) at the Broad Institute (*9*). These shRNAs are named with the numbers found at the TRC public website:
(http://www.broad.mit.edu/genome_bio/trc/publicSearchForHairpinsForm.php)

Human TSC2_1 shRNA NM_000548.x-2330s1c1 TRCT0000001182

Human TSC2_1 shRNA NM_000548.2-4551s1c1 TRCT0000001182

To generate virus, shRNA or mRNA-encoding plasmids were co-transfected with the Delta VPR envelope and CMV VSV-G packaging plasmids into actively growing HEK-293T using FuGENE 6 transfection reagent as previously described (*8*). Virus containing supernatants were collected at 48 hours after transfection, centrifuged to eliminate cells, and target cells (100,000-400,000) infected in the presence of 8 μg/ml polybrene. 24 hours after infection, the cells were given or split into fresh media. The metap2 or lipin 1 over-expressing fld cells and HGPS and control cells expressing TSC2 or GFP shRNA were additionally selected with 1 μg/ml puromycin. shRNA or mRNA-expressing cells were analyzed 2-5 days post-infection.

Immunofluorescence Assays

25,000-100,000 cells were plated on fibronectin-coated glass coverslips in 12-well tissue culture plates, rinsed with PBS once and fixed for 15 minutes with 4% paraformaldehyde in PBS warmed to 37°C. The coverslips were rinsed three times with PBS and permeabilized with 0.2% Triton X-100 in PBS for 15 minutes. After rinsing three times with PBS, the coverslips were blocked for one hour in blocking buffer (0.25% BSA in PBS), incubated with primary antibody (FLAG M2 mouse and/or lamin A sc-20680) in blocking buffer overnight at 4°C, rinsed twice with blocking buffer, and incubated with secondary antibodies (diluted in blocking buffer 1:1000) for one hour at room temperature in the dark. The coverslips were then rinsed twice more in blocking buffer and twice in PBS, mounted on glass slides using Vectashield containing DAPI (Vector Laboratories), and imaged with a 10x or 63X objective using epifluorescence microscopy.

Nuclear/Cytoplasmic Ratio and Eccentricity Measurements

Quantification of lipin 1 nuclear/cytoplasmic ratio was performed with CellProfiler (www.cellprofiler.org) using 10x images. After illumination correction, the nuclei were automatically identified using the DAPI staining. The cytoplasmic compartment was then defined by expanding the edges of the nuclei 20 pixels in every direction. The nuclear/cytoplasmic ratio was then measured as total nuclear intensity/ total cytoplasmic intensity. Lamin A eccentricity was also quantified by CellProfiler, with the eccentricity measurement being made on nuclei identified via lamin A staining.

Gene Expression Analysis

For mRNA expression quantification, total RNA was isolated from cells or liver sections grown in the indicated conditions and reverse-transcription was performed. The resulting cDNA was diluted in DNase-free water (1:20) before quantification by real-time PCR. mRNA transcript levels were measured using Applied Biosystems 7900HT Sequence Detection System v2.3 software. All Data are expressed as the ratio between the expression of target gene to the housekeeping genes 36B4 or GAPDH. Each treated sample was normalized to the level of the vehicle controls of the same cell type. The following primers were used for quantitative real-time PCR:

FASN (M. musculus)
Forward: CAG CAG AGT CTA CAG CTA CCT
Reverse: ACC ACC AGA GAC CGT TAT GC

ACLY (M. musculus)
Forward: CTC ACA CGG AAG CTC ATC AA
Reverse: ACG CCC TCA TAG ACA CCA TC

ACACA (M. musculus)

Forward: GCC TCT TCC TGA CAA ACG AG
Reverse: TGA CTG CCG AAA CAT CTC TG

Lipin 1 (M. musculus)
Forward: CCCTCGATTTCAACGTACCC
Reverse: GCAGCCTGTGGCAATTCA

SCD1 (M. musculus)
Forward: ACGCCGACCCTCACAATTC
Reverse: CAGTTTTCCGCCCTTCTCTTT

HMGCR (M. musculus)
Forward: CTTGTGGAATGCCTTGTGATTG
Reverse: AGCCGAAGCAGCACATGAT

FDPS (M. musculus)
Forward: ATGGAGATGGGCGAGTTCTTC
Reverse: CCGACCTTTCCCGTCACA

SREBP1 (M. musculus)
AAGCAAATCACTGAAGGACCTGG
AAAGACAAGGGGCTACTCTGGGAG

CytC (M. musculus)
TGGACCAAATCTCCACGGTCTGTT
TAGGTCTGCCCTTTCTCCCTTCTT

36B4 (M. musculus)
TAAAGACTGGAGACAAGGTG
GTGTACTCAGTCTCCACAGA

FASN (H. sapiens)
Forward: GAAACTGCAGGAGCTGTC
Reverse: CACGGAGTTGAGGCGCAT

HMGCR (H. sapiens)
Forward: GGACCCCTTTGCTTAGATGAAA
Reverse: CCACCAAGACCTATTGCTCTG

GAPDH (H. sapiens)
Forward: GAAGGTGAAGGTCGGAGTC
Reverse: GAAGATGGTGATGGGATTTC

Lamin A Chromatin Immunoprecipitation (ChIP)

Protocol was adapted from (*10*). Cells were cross-linked with 1/10 volume of 11% Formaldehyde (in PBS) for 3.5 minutes at room temperature and quenched with 1/20 volume of 2.5 M glycine. Cross-linked cells were rinsed twice with PBS and lysed in RIPA buffer (40 mM HEPES [pH 7.4], 2 mM EDTA, 50mM NaF, 10mM pyrophosphate, 10 mM glycerophosphate, 1% sodium deoxycholate, 1% NP40, 0.1% SDS, and one tablet of EDTA-free protease inhibitors per 25 ml). Cell lysates were sonicated 3x10 seconds (separated by 1 minute intervals) using a Tekmar Sonic Disruptor at 35% duty cycle with power output level 3.5. Lysate protein concentrations were normalized by Bradford assay (Bio-Rad), 40µl of lamin A/C antibody (sc-6215) was added, and incubated with rotation for 2 hours at 4°C. A 50% slurry of protein G Sepharose (40 µl) was then added, and the incubation continued for an additional 1 hour. Immunoprecipitates were washed 3 times in RIPA buffer and twice in wash buffer (20mM HEPES pH 7.4, 25mM KCl). 1/5 of the immunoprecipitate was denatured with sample buffer and by boiling for 5 minutes, and analyzed by immunoblotting and the remaining 4/5 was eluted in 200µl of elution buffer (50mM Tris-HCl pH 7.4, 10mM EDTA, 1% SDS) at 65°C for 5 hours. Genomic DNA was isolated from eluates using a High Pure PCR template Purfication Kit (Roche) according to the manufacturer's

protocol. DNA was quantified by quantitative PCR using conditions described above with the following primers:

FASN
Forward: GCGCAGCCCCGACGCTCATT
Reverse: CGGCGCTATTTAAACCGCGG

β-Globin
Forward: ACCCATGATAGCAGAGGCAG
Reverse: GGTGCTTGGAGACAGAGGTC

Design of the LoxP Conditional Raptor Knock-out Mice

A BAC clone (identifier: RP24-125C11, strain: C57BL/6J) containing raptor exon 6 was obtained from the RPCI-24 mouse genomic DNA library (*11*). Standard PCR and cloning procedures were used to generate fragments spanning 4.3 kb upstream of raptor exon 6 and 2.6 kb downstream of and including raptor exon 6 (as well as a 3' LoxP site downstream of raptor Exon 6) that were subsequently assembled together into the PGKneoF2L2DTA vector (*12*). In the final targeting construct, the neomycin resistance (neo) cassette was flanked by one 5' LoxP site, a 5' and 3' Flp recognition target (Frt) recombination sites, and raptor exon 6 was flanked by a 5' and 3'-LoxP site located 111 bp or 547 bp upstream or downstream, respectively. The targeting vector was linearized and electroporated into ES cells derived from 129/SvEv mice (*13*). Clones were analyzed for correct integration by Southern blot and PCR analysis. Chimeric mice were obtained by microinjection of the correctly targeted clones into BALB/C blastocysts. Chimeric mice were crossed with C57BL/6 mice to obtain germline transmission. Mice analyzed in this study were backcrossed to C57BL/6 for 4 generations. The backcrosses involved mice constitutively expressing the FLP recombinase to excise the neo cassette from the targeted allele (*14*). Heterozygous floxed raptor mice lacking the neo cassette were then bred to albumin-CRE+ mice to obtain the final genotypes. PCR genotyping of

raptor$^{Li+/+}$ and raptor$^{Li-/-}$; Albumin-CRE-/+ mice was performed with the following primers:

3' LoxP targeted raptor allele:
Forward: CTCAGTAGTGGTATGTGCTCAG
Reverse: GGGTACAGTATGTCAGCACAG

resulting in an amplicon of 174 bp in the case of presence of the 3' LoxP site and of 140 bp in case of the wild-type allele.

Albumin-CRE transgene:
Forward: GTTAATGATCTACAGTTATTGG
Reverse: CGCATAACCAGTGAAACAGCATTGC
resulting in an amplicon of ~500 bp.

Animal Experiments

All mice were maintained in a mixed strain background (129/C57BL/6) and housed in a temperature-controlled environment with 12 hour light/dark cycles. Age-matched mice had free access to water and were fed ad libitum unless otherwise stated with either a standard chow diet (Prolab RMH 3000, 5P00) providing 3.46 kcal g^{-1}physiological fuel value, 26% of which is from protein, 14% from fat and 60% from carbohydrates or a Western-style diet (Harlan Teklad TD 88137) containing 21% (w/w) total lipid (42% calories as anhydrous milk fat [65% saturated, 32% monounsaturated, 3% polyunsaturated fats]) and 0.2% (w/w) total cholesterol (of which 0.05% is contributed by milk fat and 0.15% is added). Body weights were recorded bi-monthly, and food intake was measured tri-weekly. Blood glucose was measured from tail vein blood (Ascensia Elite). At the end of the feeding period, mice were euthanatized prior to organ harvest. Tissues were harvested for analyses as described below. All experiments were approved by the Committee on Animal Care at the Massachusetts Institute of Technology

and conform to the legal mandates and federal guidelines for the care and maintenance of laboratory animals.

Determination of Liver Triglycerides

Liver sections (25-50mg) were homogenized in 900µl of a 2/1 chloroform/methanol mixture. 300µl of methanol was added to the homogenate, which was then vortexed and centrifuged for 15 minutes at 3,000 rpm. 412.5 µl of the supernatant was transferred to a new glass tube, to which 200µl of chloroform and 137.5µl of 0.73% NaCl was added and the resulting mixture was vortexed for 30 seconds and centrifuged at 5,000 rpm for 3 minutes. The upper phase was then removed and 400ul of a 3/48/47 mixture of chloroform/methanol/NaCl(0.58%) was added to wash the lower phase and subsequently centrifuged at 5,000 rpm for 3 minutes. After 3 washes, the lower phase was evaporated and re-suspended in 1ml of isopropanol. Triglyceride levels were determined with using a standard assay kit (Infinity™ Triglycerides Reagent TR22421) from Thermo Scientific according to the manufacturer's instructions. Liver triglycerides were normalized by liver section weight.

Determination of Plasma Cholesterol Content

Mouse plasma was obtained from tail vein blood which was chelated with EDTA and centrifuged at 5,000 rpm for 10 minutes to remove red blood cells. Levels of plasma cholesterol were determined using a standard assay kit (Infinity™ Cholesterol Reagent TR13421) from Thermo Scientific according to manufacturer's instructions.

Adenoviral shRNA Delivery

Lipin 1 shRNA constructs targeting nucleotides 594–613 (lipin 1_1) or 896–915 (lipin 1_2) of the mouse lipin 1 transcript and an shRNA construct targeting LacZ were generated as previously described (*15*). Hepatic shRNA-mediated knockdown was achieved by intravenous administration of adenoviral vectors as previously described (*16*).

ACKNOWLEDGEMENTS

The authors thank the following for technical assistance: Michael Brown for histology, Steve Bilodeau for chromatin Immunoprecipitations, Seong Woo Kang and Peggy Hsu for in vitro kinase assays, Ayce Yesilatay for mouse physiology. We thank members of the Sabatini lab, Ayce Yesilatay, and Monty Krieger for helpful discussions. This work was supported by grants from the National Institutes of Health (R01 AI47389 and R01 CA103866) to D.M.S.; awards from the Keck Foundation and LAM Foundation to D.M.S.; fellowships from the American Diabetes Association and Ludwig Cancer Fund to T.R.P.; a fellowship from the Canadian Institutes of Health Research to M.L. D.M.S. is an investigator of the Howard Hughes Medical Institute. None of the authors have a conflict of interest related to the work reported in this manuscript.

Experimental procedures references

1. T. A. Huffman, I. Mothe-Satney, J. C. Lawrence, Jr., *Proc Natl Acad Sci U S A* **99**, 1047 (2002).
2. P. E. Burnett, R. K. Barrow, N. A. Cohen, S. H. Snyder, D. M. Sabatini, *PNAS* **95**, 1432 (1998).
3. D. H. Kim *et al.*, *Mol Cell* **11**, 895 (Apr, 2003).
4. T. R. Peterson *et al.*, *Cell.* **137**, 873 (2009).
5. D.-H. Kim *et al.*, *Cell* **110**, 163 (2002).
6. Y. Sancak *et al.*, *Mol Cell* **25**, 903 (Mar 23, 2007).
7. M. P. Stokes *et al.*, *Proc Natl Acad Sci U S A.* **104**, 19855 (2007).
8. D. D. Sarbassov, D. A. Guertin, S. M. Ali, D. M. Sabatini, *Science* **307**, 1098 (Feb 18, 2005).
9. J. Moffat *et al.*, *Cell* **124**, 1283 (Mar 24, 2006).
10. T. I. Lee, S. E. Johnstone, R. A. Young, *Nat Protoc.* **1**, 729 (2006).
11. K. Osoegawa *et al.*, *Genome Res.* **10**, 116 (2000).

12. R. V. Hoch, P. Soriano, *Development* **133**, 663 (Feb, 2006).
13. A. Nagy, J. Rossant, R. Nagy, W. Abramow-Newerly, J. C. Roder, *Proc Natl Acad Sci U S A.* **90**, 8424 (1993).
14. C. I. Rodriguez *et al.*, *Nat Genet.* **25**, 139 (2000).
15. B. N. Finck *et al.*, *Cell Metab.* **4**, 199 (2006).
16. C. Bernal-Mizrachi *et al.*, *Nat Med.* **9**, 1069 (2003).

Chapter 3

DEPTOR is an mTOR inhibitor frequently overexpressed in multiple myeloma cells and required for their survival.

Reprinted from Cell Press:

Timothy R. Peterson[1,2], Mathieu Laplante[1,2], Carson C. Thoreen[1,2], Yasemin Sancak[1,2], Seong A. Kang[1,2], W. Michael Kuehl[4], Nathanael S. Gray[5,6] and David M. Sabatini[1,2,3]. DEPTOR is an mTOR inhibitor frequently overexpressed in multiple myeloma cells and required for their survival. *Cell.* 2009 May 29;137(5):873-86.

[1] Whitehead Institute for Biomedical Research, Nine Cambridge Center, Cambridge, MA 02142, USA
[2] Howard Hughes Medical Institute, Department of Biology, Massachusetts Institute of Technology, Cambridge, MA 02139, USA
[3] Koch Center for Integrative Cancer Research at MIT, 77 Massachusetts Avenue, Cambridge, MA 02139, USA
[4] National Cancer Institute, 8901 Rockville Pike, Bethesda, MD 20814, USA
[5] Department of Cancer Biology, Dana Farber Cancer Institute, 250 Longwood Avenue, Boston, MA 02115, USA
[6] Department of Biological Chemistry and Molecular Pharmacology, Harvard Medical School, 250 Longwood Avenue, Boston, MA 02115, USA

Experiments in Figure 1 were performed by T.R.P
Experiments in Figure 2 were performed by T.R.P
Experiments in Figures 3A, 3B, 3E, and 3F were performed by T.R.P
Experiments in Figure 3C, 3D were performed by M.L.
Experiments in Figure 4A, 4B, 4C, 4D were performed by T.R.P
Experiments in Figures 4E, 4F, 4G were performed by M.L.
Experiments in Figure 5 were performed by T.R.P.
Experiments in Figures 6A, 6B, 6C, 6D, 6E, 6F, 6G, 6H, 6J were performed by T.R.P.
Experiments in Figure 6I were performed by M.L.

SUMMARY

The mTORC1 and mTORC2 pathways regulate cell growth, proliferation, and survival. We identify DEPTOR, also called DEPDC6, as an mTOR-interacting protein whose expression is negatively regulated by mTORC1 and mTORC2. Loss of DEPTOR activates S6K1, Akt, and SGK1; promotes cell growth and survival; and activates mTORC1 and mTORC2 kinase activities. DEPTOR overexpression suppresses S6K1 but, by relieving feedback inhibition from mTORC1 to PI3K signaling, activates Akt. Consistent with many human cancers having activated mTORC1 and mTORC2 pathways, DEPTOR expression is low in most cancers. Surprisingly, DEPTOR is highly overexpressed in a subset of Multiple Myelomas harboring Cyclin D1/D3 or c-MAF/MAFB translocations. In these cells, high DEPTOR expression is necessary to maintain PI3K and Akt activation and a reduction in DEPTOR levels leads to apoptosis. Thus, we identify a novel mTOR-interacting protein whose deregulated overexpression in Multiple Myeloma cells represents a new mechanism for activating PI3K/Akt signaling and promoting cell survival.

INTRODUCTION

Mammalian TOR (mTOR) is an evolutionarily conserved serine/threonine kinase that integrates signals from growth factors, nutrients, and stresses to regulate multiple processes, including mRNA translation, cell cycle progression, autophagy, and cell survival (reviewed in (*1*)). It is increasingly apparent that deregulation of the mTOR pathway occurs in common diseases, including cancer and diabetes, emphasizing the importance of identifying and understanding the function of the components of the mTOR signaling network. mTOR resides in two distinct multiprotein complexes referred to as mTOR complex 1 (mTORC1) and 2 (mTORC2) (reviewed in (*2*)). mTORC1 is composed of the mTOR catalytic subunit and three associated proteins, raptor, PRAS40, and mLST8/GβL. mTORC2 also contains mTOR and mLST8/GβL, but instead of raptor and PRAS40, contains the proteins rictor, mSin1, and protor.

mTORC1 controls cell growth in part by phosphorylating S6 Kinase 1 (S6K1) and the eIF-4E-binding protein 1 (4E-BP1), key regulators of protein synthesis. mTORC2 modulates cell survival in response to growth factors by phosphorylating its downstream effectors Akt/PKB and Serum/Glucocorticoid Regulated Kinase 1 (SGK1) (reviewed in (*2*)).

In addition to directly activating Akt as part of mTORC2, mTOR, as part of mTORC1, also negatively regulates Akt by suppressing the growth factor-driven pathways upstream of it. Specifically, mTORC1 impairs PI3K activation in response to growth factors by downregulating the expression of Insulin Receptor Substrate 1 and 2 (IRS-1/2) and Platelet-Derived Growth Factor Receptor-Beta (PDGFR-β) (reviewed in (*3*)). The activation of Akt that results from treating cells with the mTORC1 inhibitor rapamycin may contribute to the limited success to date of this drug and its analogs as cancer therapies.

While most information concerning the involvement of the mTOR pathway in human cancers is consistent with a role for mTOR in directly promoting tumor growth, there are also indications in the literature that mTOR possesses tumor suppressor-like properties. Thus, the tumors that develop in patients with Tuberous Sclerosis Complex (TSC), a syndrome characterized by mTORC1

hyperactivation, are thought to have a limited growth potential due to the PI3K inactivation caused by the aforementioned feedback loop (*4, 5*). In addition, partial loss of function alleles of mTOR confer susceptibility to plasmacytomas in mice, though the mechanism for this effect has not been clarified (*6*).

Here, we identify DEPTOR as an mTOR binding protein that normally functions to inhibit the mTORC1 and mTORC2 pathways. When greatly overexpressed, DEPTOR inhibits mTORC1, and, unexpectedly, this leads to the activation of the PI3K/mTORC2/Akt pathway. This indirect mode of PI3K activation is important for the viability of a subset of Multiple Myeloma cells which otherwise lack PI3K-activating mutations. We propose that DEPTOR is an endogenous inhibitor of mTOR whose deregulated overexpression promotes cell survival in a subset of Multiple Myelomas.

RESULTS

DEPTOR is an mTOR Interacting Protein

Using low-salt purification conditions designed to isolate PRAS40 (*7*), we identified within mTOR immunoprecipitates a 48 kDa protein assigned the NCBI Gene Symbol DEPDC6 (NCBI Gene ID: 64798) (Figure 1A). The gene for DEPDC6 is found only in vertebrates, and encodes a protein with tandem N-terminal DEP (Dishevelled, Egl-10, Pleckstrin) domains and a C-terminal PDZ (Postsynaptic density 95, Discs large, Zonula occludens-1) domain (reviewed in (*8, 9*) (Figure 1B). Because no previous studies refer to the function of the DEPDC6 gene product, we named it DEPTOR in reference to its DEP domains and its specific interaction with mTOR (see below). In purified preparations of recombinant DEPTOR stably expressed in HEK-293E cells, we detected via mass spectrometry endogenous mTOR, as well as raptor and rictor, mTORC1 and mTORC2-specific components, respectively. Analogous preparations of recombinant PRAS40, a raptor binding protein, contained only mTORC1 (Figure 1C). Consistent with DEPTOR being part of mTORC1 and mTORC2, endogenous DEPTOR was also detected in immunoprecipitates prepared from

HEK-293E (Figure 1D) or HeLa cells (Figure 1E) using antibodies that recognize endogenous mTOR, raptor, or rictor, but not actin. As was the case with PRAS40 (7), buffers with increased salt concentrations reduced the amounts of DEPTOR recovered in the immunoprecipitates (Figure 1D). Reciprocal experiments confirmed that endogenous mTOR specifically co-immunoprecipitates with DEPTOR (Figure 1E).

As the above results indicate that DEPTOR is part of mTORC1 and mTORC2, we expected DEPTOR to interact with mTOR and/or mLST8/GβL, the only proteins common to both mTORC1 and mTORC2. To test this, we co-overexpressed DEPTOR with epitope-tagged mTOR or mLST8/GβL and analyzed mTOR or mLST8/GβL immunoprecipitates for the presence of DEPTOR. The results indicate that DEPTOR is an mTOR interacting protein: DEPTOR co-immunoprecipitated with mTOR irrespective of whether or not mLST8/GβL was co-expressed with it, while DEPTOR co-immunoprecipitated with mLST8/GβL only when it and mTOR were expressed together (Figure 1F). DEPTOR interacts with a C-terminal portion of mTOR (a.a. 1483-2000) that is upstream of its kinase domain and does not encompass the mLST8/GβL binding site (a.a. 2001-2549) (Figure 1G, 1I), providing further evidence that, within mTORC1 and mTORC2, DEPTOR interacts specifically with mTOR and not with mLST8/GβL. Finally, reciprocal experiments showed that the PDZ domain of DEPTOR mediates its interaction with mTOR (Figure 1H, 1I).

DEPTOR Depletion Activates mTORC1 and mTORC2 signaling in Intact Cells and Enhances the In Vitro Kinase Activities of the Complexes

To test the idea that DEPTOR regulates mTOR function, we measured the activity of the mTOR pathway in cells with RNAi-mediated reductions in DEPTOR expression. Human or mouse cells expressing either of two shRNAs targeting DEPTOR, but not control proteins, had increased mTORC1 and mTORC2 signaling as judged by the phosphorylation states of the mTORC1 and mTORC2 substrates, S6K1 and Akt, respectively (Figure 2A, 2C). Concomitant with the increase in mTORC1 signaling, mTORC1 immunopurified from cells depleted of

DEPTOR had increased in vitro kinase activity towards two known substrates, S6K1 and 4E-BP1 (Figure 2B). Likewise, mTORC2 isolated from DEPTOR-depleted cells had increased in vitro kinase activity towards its substrate Akt1 (Figure 2D). Taken together, the loss of function data indicate that within cells DEPTOR is an inhibitor of mTORC1 and mTORC2 activities.

DEPTOR Depletion Increases Cell Size and Protects Cells from Apoptosis

To determine if the effects of DEPTOR loss on mTORC1/2 signaling are physiologically significant, we measured in DEPTOR-deficient cells key outputs of mTORC1 and mTORC2 function, namely cell growth and survival, respectively. Cells with reduced DEPTOR expression were larger than control cells and rapamycin treatment reversed this phenotype, consistent with DEPTOR acting upstream of mTORC1 (Figure 3A). The size of the DEPTOR-deficient cells was comparable in magnitude to, although slightly smaller than, those with reduced expression of TSC2, a well-established negative regulator of mTORC1 (reviewed in (*3*)) (Figure 3B).

Because Akt promotes cell survival (*10*) and DEPTOR suppression within cells causes an increase in Akt phosphorylation (Figure 2C), we tested whether DEPTOR-deficient cells are resistant to apoptosis induction. In HeLa cells expressing a control shRNA, reductions in the serum concentration of the media caused a dose-dependent decrease in Akt phosphorylation and a concomitant increase in the cleaved forms of caspase-3 and PARP, two hallmarks of apoptosis (*11, 12*) (Figure 3C). In contrast, DEPTOR-deficient cells were resistant to PARP and caspase-3 cleavage in a manner that correlated with the efficiency of DEPTOR suppression (Figure 3C). However, in contrast to what is observed in the presence of serum, in the absence of serum DEPTOR-deficient HeLa cells did not have higher levels of Akt phosphorylation than control cells (Figure 3C). This suggests that, despite the capacity of DEPTOR suppression to protect cells from apoptosis, the effect was unlikely to be mediated by Akt. As Akt shares some of its pro-survival functions with the related family of SGK kinases (reviewed in (*13*)) and recent evidence indicates that mTOR activates SGK1 by

directly phosphorylating it (*14, 15*), we reasoned that DEPTOR suppression might protect HeLa cells from apoptosis by promoting SGK1 activity. Consistent with this, the DEPTOR-deficient HeLa cells had, at all serum concentrations, increased phosphorylation levels of NDRG1, an established SGK1 substrate (*16*) (Figure 3C). Because it is still controversial if SGK1 is an mTORC2 and/or mTORC1 substrate (*14, 15*), we determined if DEPTOR-deficient cells could be re-sensitized to pro-apoptotic stimuli by inhibiting mTORC1 with rapamycin or by inhibiting both mTORC1 and mTORC2 with Torin1, a highly selective and potent ATP-competitive inhibitor of mTOR (*17*). Consistent with mTORC2 mediating the pro-survival effects of DEPTOR suppression, treatment of the serum-deprived and DEPTOR-deficient HeLa cells with Torin1, but not rapamycin, restored caspase-3 and PARP cleavage and reversed the hyperphosphorylation of NDRG1 caused by DEPTOR loss (Figure 3D). In accord with the results obtained with Torin1, a knockdown of rictor, but not raptor, abolished NDRG1 hyperphosphorylation and re-activated apoptosis in DEPTOR knockdown cells deprived of serum (Figure 3E). Lastly, a reduction in SGK1 levels in the DEPTOR knockdown HeLa cells reduced NDRG1 phosphorylation and re-sensitized the cells to apoptosis induction upon serum deprivation (Figure 3F). DEPTOR suppression also prevented caspase-3 cleavage in serum-deprived HT-29 cells, though in this cell type the anti-apoptotic effects of DEPTOR loss correlated with a partial rescue of Akt phosphorylation (Figure S1). Other perturbations that promote Akt activation, such as suppression of raptor expression (*18*), also protected HT-29 cells from apoptosis induced by serum withdrawal (Figure S1). Thus, analyses of DEPTOR-deficient cells indicate that DEPTOR physiologically controls cellular processes regulated by mTOR signaling.

mTOR Negatively Regulates DEPTOR Expression at the Transcriptional and Post-Translational levels

In our previous experiments, we noted that prolonged serum withdrawal caused an increase in DEPTOR protein expression (Figure 3C). To gain insight into the temporal regulation of DEPTOR expression, we starved and stimulated

HeLa cells with serum for various time intervals. Serum stimulation led to a time-dependent retardation in DEPTOR migration in SDS-PAGE until about 6 hours after serum addition, at which point DEPTOR expression began to fall, and by 12 hours, almost disappeared (Figure 4A). Interestingly, these qualitative and quantitative changes in DEPTOR correlated with inflections in mTORC1 and mTORC2 pathway activities as measured by the phosphorylations of S6K1 and Akt, respectively. As expected, the amount of DEPTOR bound to mTORC1 and mTORC2 (Figure 4B) reflected the serum-induced changes in DEPTOR expression detected in cell lysates (Figures 4A and 4B). Serum starvation and stimulation also regulated DEPTOR expression in a variety of other cancer cell lines in addition to HeLa cells (Figure 4C). We noted that cell lines known to have serum-independent mTORC1 and mTORC2 signaling, such as HEK-293T, PC3, and U87 cells (*19*) have markedly reduced levels of DEPTOR that are largely insensitive to serum (Figure 4C).

As both PC3 and U87 cells lack PTEN (SANGER COSMIC database), a negative regulator of PI3K signaling that controls the responsiveness of the mTORC1 and mTORC2 pathways to growth factors (reviewed in (*20*)), it seemed likely that PTEN loss suppresses DEPTOR expression. Consistent with this, in PTEN-null MEFs DEPTOR was virtually absent in the presence or absence of serum, while serum still regulated DEPTOR expression in MEFs that express PTEN (Figure 4D). As PTEN loss activates both mTORC1 and mTORC2 signaling we determined if DEPTOR expression is also sensitive to perturbations that only activate mTORC1. Indeed, MEFs lacking TSC2, a tumor suppressor whose loss leads to activation of only mTORC1, had reduced levels of DEPTOR even when cultured in the absence of serum (Figure 4D).

The above findings suggested that both mTORC1 and mTORC2 negatively regulate DEPTOR expression (Figures 4A-D). Supporting this idea, treatment of cells with the mTORC1 and mTORC2 inhibitor Torin1 fully blocked the mobility shift and decrease in expression of DEPTOR caused by serum stimulation, while treatment with the mTORC1 inhibitor rapamycin had only partial effects on DEPTOR mobility and expression (Figure 4E). To determine at

which regulatory level(s) cells control DEPTOR expression we measured the amounts of DEPTOR protein and mRNA in HeLa cells treated in various ways (Figure 4F and 4G). The drop in DEPTOR protein caused by serum stimulation correlated with a significant decrease in the mRNA for DEPTOR (Figure 4F), suggesting that transcriptional regulation contributes to the control of DEPTOR expression. However, it was clear that post-transcriptional mechanisms are also in play because the partial rescue by rapamycin treatment of the serum-induced decrease in DEPTOR protein amounts occurred in the absence of any change in DEPTOR mRNA levels (Figure 4F). Moreover, treatment of cells with the proteasome inhibitor MG132 (*21*) blocked the serum-induced decrease in DEPTOR protein without increasing the DEPTOR mRNA, indicating that the degradation of DEPTOR is a key step in the regulation of its expression (Figure 4F). Treatment of cells with Torin1 blocked the serum-induced drop in DEPTOR protein levels and, in contrast to rapamycin, also partially prevented the decrease in the DEPTOR mRNA (Figure 4F).

A comparison of the effects of rapamycin with those of Torin1 on DEPTOR expression suggested that both mTORC1 and mTORC2 negatively regulate DEPTOR protein expression, but that only mTORC2 negatively regulates DEPTOR mRNA expression. To further test this, we depleted mTORC1 or mTORC2 using shRNAs targeting raptor or rictor, respectively, and examined DEPTOR protein and mRNA levels. As expected, both the raptor and rictor knockdowns increased DEPTOR protein levels in serum-replete cells (Figure 4G). However, both knockdowns also increased DEPTOR mRNA (Figure 4G), indicating that the regulation of DEPTOR mRNA expression by mTORC1 is rapamycin resistant, consistent with the increasing evidence that only some mTORC1 functions are sensitive to rapamycin (*17, 22, 23*). Thus, both mTOR complexes negatively regulate DEPTOR mRNA expression, explaining why cell lines with high mTORC1 and mTORC2 activity, such as the PTEN-null PC3 or U87 cells, have low levels of DEPTOR mRNA (Figure S2A). In aggregate, these results suggest that the regulation of DEPTOR expression is complex and

involves post-translational and transcriptional mechanisms mediated by both mTORC1 and mTORC2.

DEPTOR is Phosphorylated in an mTOR-dependent Fashion

Because the mTOR inhibitor Torin 1 prevents the serum-induced degradation and SDS-PAGE mobility shift of DEPTOR, we reasoned that a mechanism through which mTORC1 and mTORC2 might regulate DEPTOR is by controlling its phosphorylation. To investigate this, we purified DEPTOR from serum-stimulated cells and analyzed it by mass spectrometry for the presence of phosphorylated residues. This led to the identification of 13 serine and threonine phosphorylation sites, all of which are located in the linker between the C-terminal DEP domain and the PDZ domain (Figure S3A). Interestingly, many of the phosphorylation sites fall within "proline-directed" motifs like those in 4E-BP1 (*24*) which are known to be phosphorylated by mTOR (*25-27*). Extensive characterization of DEPTOR from serum-stimulated cells supported the notion that DEPTOR is heavily phosphorylated in an mTOR-dependent manner (Figures S3B-D). We changed all 13 phosphorylation sites to alanine to generate a non-phosphorylatable mutant protein that we call DEPTOR 13xS/T->A. In serum-stimulated cells the mutant protein did not undergo a mobility shift on SDS-PAGE (Figure S3E). When overexpressed, neither wild-type nor 13xS/T->A DEPTOR decreased in expression upon serum stimulation of cells (compare Figures 4B and S3E), suggesting that the machinery that degrades DEPTOR is readily saturated. Consistent with this, stable and modest 2-5 fold overexpression of epitope-tagged wild-type DEPTOR severely inhibited the loss of endogenous DEPTOR that normally occurs upon serum stimulation (Figure S3F). Because overexpression of DEPTOR impaired the regulation its expression (Figure S3E-F), we focused on other functions for DEPTOR phosphorylation that could be relevant to DEPTOR turnover and, in particular, examined the potential role of DEPTOR phosphorylation on regulating the DEPTOR-mTOR interaction. Compared to wild-type DEPTOR, the 13xS/T->A DEPTOR mutant bound better

to mTOR within mTORC1 and mTORC2 (Figure 5A). These results suggest that the phosphorylation of DEPTOR promotes its release from mTOR and correlates with its loss. In addition, experiments described below indicate that DEPTOR phosphorylation is necessary to reverse the inhibitory effects of DEPTOR on mTORC2 activity.

DEPTOR Overexpression Inhibits mTORC1 but Activates PI3K/Akt Signaling

Because our loss-of-function experiments indicate that DEPTOR is an mTOR inhibitor, we hypothesized that DEPTOR overexpression should suppress both the mTORC1 and mTORC2 pathways. Indeed, transient overexpression of wild-type DEPTOR, but not a control protein, in MEFs reduced the phosphorylation of T389 of co-expressed S6K1, an established mTORC1 substrate, to a similar degree as overexpression of PRAS40, a known mTORC1 inhibitor (Figure 5B). DEPTOR overexpression also strongly inhibited mTORC1 in MEFs lacking TSC2 or rictor (Figure 5B). Overexpression of just the PDZ domain of DEPTOR, the region of DEPTOR that binds mTOR (Figure 1H), but not of the tandem DEP domains of DEPTOR, also inhibited mTORC1 signaling (Figure 5B).

In contrast to the expected effects we observed with regards to mTORC1, DEPTOR overexpression led to an apparent increase instead of inhibition of mTORC2 signaling as monitored by Akt S473 phosphorylation (Figures 5C and Figure S4). We suspected that because DEPTOR overexpression inhibits mTORC1, it relieves the inhibitory feedback signal normally transmitted from mTORC1 to PI3K. This would lead to hyperactive PI3K signaling, which then overcomes the direct inhibitory effects of DEPTOR on mTORC2, just as the hyperactive rheb found in TSC2 null cells can overcome the inhibitory effects of PRAS40 on mTORC1 (*7*). Consistent with this interpretation, overexpression of DEPTOR, like that of PRAS40, not only caused an increase in the phosphorylation of Akt at S473 but also at T308, the PDK1-catalyzed site which serves as a read-out of PI3K activity (*28*) (Figure 5C and Figure S4). The

activation of Akt by DEPTOR overexpression was not observed in the absence of serum, as expected from the known requirement for growth factors for mTORC1 to PI3K feedback signaling (*29*) (Figure 5D). As was the case with wild-type DEPTOR, overexpression of the non-phosphorylatable DEPTOR mutant inhibited mTORC1 signaling (Figure 5B) and triggered feedback activation of PI3K as detected by T308 phosphorylation of Akt (Figure 5C). However, unlike wild-type DEPTOR, the 13xS/T->A DEPTOR mutant did not promote Akt phosphorylation on S473, indicating that PI3K activation cannot activate mTORC2 when DEPTOR cannot be phosphorylated (Figure 5C).

We propose that the effects of DEPTOR overexpression on the mTOR pathway—inhibition of mTORC1 signaling but activation of mTORC2 signaling—result from DEPTOR-mediated inhibition of mTORC1, which then leads to the hyperactivation of PI3K and Akt. In agreement with this model, in many cell types treatment with rapamycin or overexpression of PRAS40 (Figure 5C) has similar effects on mTOR signaling as DEPTOR overexpression (*19, 29*). However, both rapamycin and PRAS40 are predominantly mTORC1 inhibitors, while our loss of function data indicates that DEPTOR inhibits mTORC1 and mTORC2. To gain evidence that a dual mTORC1 and mTORC2 inhibitor can also lead to a stable cell state characterized by inhibition of mTORC1 signaling but and activation of PI3K/mTORC2/Akt signaling we explored the time- and dose-dependent effects of the mTOR inhibitor Torin1 (*30*). As expected, acute Torin1 treatment of cells for 10 minutes led to a dose-dependent inhibition of both mTORC1 and mTORC2 signaling, as monitored by S6K1 and Akt phosphorylation, respectively (Figure 5E). By 48 hours of Torin1 treatment, however, mTORC1 signaling was still inhibited but was now accompanied by increased T308 and S473 Akt phosphorylation and IRS-1 levels, molecular phenotypes consistent with the loss of the inhibitory feedback signal from mTORC1 to the PI3K pathway (Figure 5E). At a higher concentration (250 nM) of Torin1, Akt T308 phosphorylation and IRS-1 expression were very high indicating that, at this dose, PI3K signaling was still hyperactive. However, like overexpression of a non-phosphorylatable DEPTOR mutant (Figure 5C), the higher dose of Torin1 eliminated Akt S473

phosphorylation, revealing that mTORC2 was now fully inhibited. PP242, a distinct ATP-competitive inhibitor of mTOR (*23*), had similar time- and dose-dependent effects on mTOR and PI3K signaling as Torin1 (Figure S5). Thus, because of the inhibitory feedback signal from mTORC1 to the PI3K pathway, partial mTOR inhibition caused by either DEPTOR overexpression or chemical inhibitors leads to an asymmetrical state of mTOR signaling characterized by an inhibition of mTORC1 but an activation of mTORC2-dependent outputs.

In a Subset of Multiple Myelomas DEPTOR Overexpression is Necessary for Akt Activation and Cell Survival

The dynamic nature of DEPTOR expression and the interesting consequences of DEPTOR overexpression on mTORC1 and PI3K/mTORC2/Akt signaling prompted us to examine the levels of DEPTOR mRNA in databases of transcriptional profiles of human tumors and cancer cell lines. Consistent with mTORC1 and mTORC2 being active in many cancers (reviewed in (*3*)), the levels of DEPTOR mRNA were significantly lower in most cancer types compared to the normal tissues from which they are derived (Figure 6A, Table S1). Anomalously, this was not the case for Multiple Myelomas (MM), a malignancy of antibody-producing plasma cells (reviewed in (*31*)), in which the DEPTOR mRNA is overexpressed (Figure 6A, Table S1).

To expand upon these findings, we measured DEPTOR mRNA levels in a collection of 581 human Multiple Myelomas and found that 28% (160/581) of the MMs had mRNA levels that were 4-fold or greater than those in normal plasma cells (see methods and Table S1). Multiple Myelomas can be grouped into two broad types: (1) hyperdiploid MMs, which are associated with multiple trisomies of 8 chromosomes and bi-allelically deregulate Cyclin D1/D2 mRNA expression, and (2) non-hyperdiploid MMs, which mono-allelically deregulate Cyclin D1/D3, c-MAF/MAFB, or FGFR3/MMSET expression through translocation events involving these genes (*32*) (In Figure 6B these two types are referred to as "Bi-allelic deregulation" and "Translocation"). We noted that many of the MMs with high levels of DEPTOR mRNA were of the non-hyperdiploid type and had

translocations involving the genes for Cyclin D1 or D3, or, in particular, for the c-MAF or MAFB transcription factors (Table S1). In these MMs, the mean level of DEPTOR mRNA is significantly higher than in those without the translocations (Figure 6B).

We next examined DEPTOR mRNA and protein expression and mTORC1 and PI3K/mTORC2/Akt signaling in a set of MM cell lines. Many MM cell lines, particularly those with c-MAF/MAFB translocations, have levels of DEPTOR protein and mRNA expression that are many folds greater than those found in non-MM cancer cell lines, such as HeLa and PC3 cells (Figures 6D, S6A-B, and Table S1). Consistent with our exogenous DEPTOR overexpression studies (Figure 5), DEPTOR expression across the cell lines correlated positively with the phosphorylation of Akt on T308 and S473 (PDK1/PI3K and mTORC2 outputs, respectively), but negatively with S6K1 T389 phosphorylation (an mTORC1 output) (Figure 6C). The sole exception was the □47 cell line, which is one of the few MM cell lines that lack PTEN and thus has high levels of S6K1 and Akt phosphorylation (Figure 6C). Remarkably, the MM cell lines with high DEPTOR expression had levels of S473, and, particularly, T308 Akt phosphorylation comparable to those in the PTEN-null □47 cell line.

As PTEN inactivation and PI3K-activating mutations are rare in MM (*33*) (Kuehl et al., unpublished), we considered the possibility that overexpression of endogenous DEPTOR might also be a mechanism to promote activation of PI3K and Akt and cell survival in a subset of human MMs. To test this, we used RNAi to suppress the very high levels of DEPTOR expression in 8226 and OCI-MY5 Multiple Myeloma cell lines to levels comparable to those in HeLa cells (Figure 6D). DEPTOR suppression led to an increase in mTORC1 activity as detected by S6K1 T389 phosphorylation, IRS1 levels, and IRS1 phosphorylation, but to a drop in PI3K/PDK1 and mTORC2 outputs as measured by T308 and S473 Akt phosphorylation, respectively (Figure 6E). Even though the DEPTOR knockdown decreased the cellular levels of phospho-S473 Akt, it caused an increase in the in vitro kinase activity of mTORC2 isolated from the DEPTOR knockdown cells (Figure S7), a result consistent with DEPTOR being a negative regulator of

mTORC2 kinase activity (Figure 2D). DEPTOR suppression had similar inhibitory effects on T308 and S473 Akt phosphorylation in OCI-MY5 cells except that in this cell line IRS-1 was not detected and decreased Akt phosphorylation instead correlated instead with a loss of PDGFR-□ levels (Figure 6E, see also Figure S8). Lastly, co-knockdown of raptor with DEPTOR partially reversed the effects of the DEPTOR knockdown on T308 and S473 Akt phosphorylation, suggesting that mTORC1 activation mediates the reduction in PI3K signaling seen in the 8226 cells upon a reduction in DEPTOR expression (Figure S9).

Consistent with the pro-survival role of PI3K/Akt signaling, suppression of DEPTOR in 8226 cells abolished cell proliferation over a 7-day culture period (Figure 6F) and caused apoptosis as detected by the presence of numerous cell fragments in the culture media (Figure 6G) and increased cleaved caspase-3 and PARP (Figure 6H). Thus, in a subset of Multiple Myeloma cell lines, high expression of DEPTOR contributes to Akt activation and is an endogenous mechanism for maintaining cell survival.

Because PI3K/mTORC2/Akt signaling represses DEPTOR mRNA levels (Figures 4F-G and Figures S2A-B), we wondered how certain Multiple Myeloma cells can keep DEPTOR at elevated levels in the face of hyperactive PI3K signaling. DEPTOR mRNA levels are highest in MM tumors and cell lines in which chromosomal translocations cause the overexpression of c-MAF or MAFB. Moreover, a transcriptional profiling study shows that DEPTOR is highly induced upon forced MAFB overexpression (*34, 35*). To test if deregulated overexpression of c-MAF or MAFB drives DEPTOR expression, we used RNAi to reduce c-MAF expression in 8226 cells, a MM cell line with a translocation involving the c-MAF gene (*36*). Indeed, loss of c-MAF substantially diminished DEPTOR mRNA and protein levels and, by activating mTORC1 and inhibiting mTORC2 outputs, recapitulated the effects of a DEPTOR knockdown on the mTOR pathway (Figure 6I, 6J). As expected, the knockdown of c-MAF decreased the expression of the mRNA for Integrin β7, a known c-MAF target (Figure 6I). These results are consistent with deregulated overexpression of c-

MAF or MAFB driving DEPTOR expression to high levels and, thus, hyperactivating PI3K signaling.

DISCUSSION

Our loss of function data indicate that DEPTOR inhibits both the mTORC1 and mTORC2 pathways. However, by inhibiting mTORC1, DEPTOR overexpression relieves mTORC1-mediated inhibition of PI3K, causing an activation of PI3K and, paradoxically, of mTORC2-dependent outputs, like Akt.

mTOR interacts with DEPTOR via its PDZ domain and so far there is no information about the function of the tandem DEP domains the protein also contains. In other proteins DEP domains mediate protein-protein interactions (*37, 38*), but in numerous DEPTOR purifications we have failed to identify additional DEPTOR-interacting proteins besides the known components of mTORC1 and mTORC2 (data not shown). Therefore, based on our current evidence, DEPTOR appears dedicated to mTOR regulation, and we propose that in vertebrates it is likely to be involved in regulating other outputs of the mTOR signaling network besides the growth and survival pathways we have examined. The mTOR complexes and DEPTOR negatively regulate each other, suggesting the existence of a feedforward loop in which the loss of DEPTOR leads to an increase in mTOR activity, which then further reduces DEPTOR expression. This type of regulatory circuit should result in DEPTOR expression being tightly coupled to mTOR activity, and, interestingly, we have noted that DEPTOR mRNA levels strongly anti-correlate with cell size, a readout of mTORC1 activity (Figure S6B).

We find that about 28% of human Multiple Myelomas (MM) overexpress DEPTOR. Our results are consistent with a published survey of 67 MM tumors and 43 MM cell lines, in which 21% were shown to possess copy number gains and associated expression increases of the genes within a 6 Mb region of chromosome 8q24 that contains DEPTOR (*39*). Furthermore, it appears that deregulated overexpression of c-MAF and MAFB is an additional, perhaps even

more prevalent, mechanism for increasing DEPTOR expression in MMs. The related c-MAF and MAFB transcription factors are expressed--frequently as the result of chromosomal translocations--in a large fraction of MMs, but not in the plasma cells from which they are derived (reviewed in (*40*)). Consistent with c-MAF playing a key role in promoting DEPTOR expression, a knockdown of c-MAF in a MM cell line having a c-MAF translocation decreases the expression of DEPTOR and mimics the effects of a DEPTOR knockdown on mTOR and PI3K signaling. The levels of the DEPTOR and c-MAF or MAFB mRNAs highly correlate with each other (*35*) and, importantly, DEPTOR expression correlates with poor survival in patients with Multiple Myeloma (*39*).

In many Multiple Myeloma cell lines DEPTOR is massively overexpressed compared to the levels found in other cancer cell lines, such as HeLa cells. In these cells, the great overexpression of DEPTOR inhibits mTORC1 growth signaling and drives outputs dependent on PI3K. Interestingly, a reduction in DEPTOR expression to the lower levels seen in non-Multiple Myeloma cell lines causes cell death via apoptosis. This suggests that a pharmacologically induced reduction in DEPTOR expression or disruption of the DEPTOR-mTOR interaction could have therapeutic benefits for the treatment of Multiple Myeloma. There has been progress in developing small molecule inhibitors of protein-protein interactions mediated by PDZ domains (*41, 42*), so it is conceivable that blockers of the DEPTOR-mTOR interaction could be made.

Although a number of other cancer cell lines have high levels of DEPTOR (data not shown), as a class only Multiple Myelomas appear to consistently overexpress it. Besides activating PI3K/Akt signaling, DEPTOR overexpression in MM cells may provide these cells with benefits that are not relevant in other cancer types or perhaps even detrimental. For example, the high demand that MM cells place on the protein synthesis machinery to produce large amounts of immunoglobulins (reviewed in (*43*)), causes a significant ER stress which renders these cells susceptible to apoptosis-induction via agents which induce further ER stress, such as proteasome inhibitors (*44, 45*). DEPTOR overexpression, by partially inhibiting protein synthesis through the suppression of mTORC1, may

reduce the levels of ER stress below the threshold that triggers apoptosis. In contrast, in other cancer cells in which ER stress is not a significant factor, DEPTOR overexpression may be selected against because reduced rates of protein synthesis may not be tolerated. That mTORC1-stimulated protein synthesis leads to ER stress is already appreciated as TSC1 or TSC2 null cells have increased sensitivity to ER stress-induced death (*46*).

It is curious that DEPTOR is overexpressed mostly in MMs characterized by chromosomal translocations instead of those which are hyperdiploid because of aneuploidy (Figure 6B) (*32*). Elevated DEPTOR expression might be tolerated better in the non-hyperdiploid MMs because aneuploidy itself increases sensitivity to conditions, like mTORC1 inhibition, that interfere with protein synthesis (*47*). Moreover, the state of high mTORC2 and low mTORC1 signaling that our work indicates some MM cells prefer, cannot be achieved by mutations that activate PI3K signaling, perhaps explaining why Multiple Myelomas exhibit low rates of PTEN-inactivating or PI3K-activating mutations (*33*)(Kuehl et al., unpublished).

FIGURE LEGENDS

Figure 1. DEPTOR is an mTOR-Interacting Protein

(A) Silver stain of SDS-PAGE analysis of mTOR immunoprecipitates prepared from HEK-293E cells.

(B) Schematic representation of structural features of human DEPTOR and its mouse and chicken orthologues.

(C) Endogenous mTOR, raptor, and rictor co-immunoprecipitate with epitope-tagged DEPTOR. FLAG immunoprecipitates from HEK-293E cells expressing FLAG-DEPTOR, FLAG-PRAS40, or FLAG-tubulin were analyzed by SDS-PAGE followed by silver staining.

(D) Interaction of endogenous DEPTOR with endogenous mTORC1 and mTORC2 is sensitive to high salt-containing buffers. mTOR, raptor, rictor, or actin immunoprecipitates were prepared from HEK-293E cells, washed with buffers containing indicated amounts of NaCl and analyzed by SDS-PAGE followed by immunoblotting for indicated proteins.

(E) Endogenous DEPTOR co-immunoprecipitates endogenous mTOR. DEPTOR immunoprecipitates were prepared from HeLa cells, washed in a buffer containing 150 mM NaCl, and analyzed as in (D).

(F) DEPTOR interacts with mTOR and not mLST8/GβL. Indicated cDNAs in expression vectors were co-expressed in HEK-293T cells,
cell lysates prepared, and used to prepare anti-HA immunoprecipitates and anti-myc immunoprecipitates. Both immunoprecipitates and cell lysates were analyzed as in (D).

(G) Myc-tagged mTOR, its indicated fragments, or rap2a were co-expressed in HEK-293T cells with FLAG-DEPTOR, and anti-myc immunoprecipitates were analyzed as in (D).

(H) The PDZ domain of DEPTOR interacts with mTOR. FLAG-tagged DEPTOR, its fragments, or metap2 were co-expressed in HEK-293T cells with myc-mTOR, and anti-FLAG immunoprecipitates were analyzed as in (D). Asterisks (*) indicate non-specific bands.

(I) Schematic indicating the regions of mTOR and DEPTOR that mediate their interaction. The abbreviations for and residues that define known mTOR domains are: HEAT Repeats, 1-1382; FAT, 1383-2014; R (FKBP12-Rapamycin Binding), 2015-2114; KD (PI3K-like Kinase Domain), 2115-2431; C (FATC), 2432-2549.

Figure 2. DEPTOR Depletion in Cells Activates mTORC1 and mTORC2 signaling and In Vitro Kinase Activities

(A) Knockdown of DEPTOR activates the mTORC1-S6K1 pathway. HeLa cells or p53-/- MEFs were infected with lentiviruses expressing shRNAs targeting the indicated genes. Cell lysates were analyzed by immunoblotting for the levels of the indicated proteins and phosphorylation states.

(B) Knockdown of DEPTOR activates mTORC1 kinase activity towards S6K1 and 4E-BP1. HeLa cells were infected with lentiviruses expressing shRNAs targeting the indicated genes. mTOR immunoprecipitates were prepared from cell lysates (1 mg total protein) and analyzed for mTORC1 kinase activity toward S6K1 and 4E-BP1 and for levels of mTOR, raptor, and DEPTOR.

(C) Knockdown of DEPTOR activates the mTORC2-Akt pathway. The experiment was performed as in (A) except that Akt phosphorylation and levels were measured.

(D) Knockdown of DEPTOR activates mTORC2 kinase activity towards Akt1. The experiment was performed as in (B) except that mTORC2 activity towards Akt was measured.

Figure 3. DEPTOR Depletion Increases Cell Size and Protects Cells from Apoptosis Induced by Serum Deprivation

(A) Knockdown of DEPTOR increases cell size in an mTORC1-dependent fashion. Cell size distributions (graphs) and S6K1 phosphorylation (immunoblot) are shown for HeLa cells stably expressing shRNAs targeting DEPTOR or luciferase. Where indicated, cells were pre-treated with 100 nM rapamycin or vehicle before infection. 72 hours after infection, cell size was measured using a Coulter counter.

(B) A knockdown of DEPTOR has similar effects on cells size as a TSC2 knockdown. p53 null MEFs were infected with shRNAs and cell size measured as in (A).
(C) DEPTOR knockdown protects against apoptosis induced by serum withdrawal. HeLa cells expressing shRNAs targeting luciferase or DEPTOR were grown in media containing the indicated concentrations of serum for 30 hours. Cell lysates were then analyzed by immunoblotting for the levels of the indicated proteins and phosphorylation states.
(D) mTOR inhibition re-sensitizes DEPTOR knockdown cells to apoptosis induced by serum withdrawal. HeLa cells expressing shRNAs targeting luciferase or DEPTOR were serum deprived for 30 hours in the presence of 100 nM rapamycin, 250 nM Torin1, or vehicle. Cell lysates were then analyzed as in (C).
(E) Rictor but not raptor inhibition re-sensitizes DEPTOR knockdown cells to apoptosis induced by serum withdrawal. HeLa cells co-expressing shRNAs targeting luciferase or DEPTOR along with shRNAs targeting luciferase or rictor or raptor were serum deprived for 30 hours. Cell lysates were then analyzed as in (C).
(F) SGK1 inhibition re-sensitizes DEPTOR knockdown cells to apoptosis induced by serum withdrawal. HeLa cells co-expressing shRNAs targeting luciferase or DEPTOR along with shRNAs targeting luciferase or SGK1 were analyzed as in (C).

Figure 4. mTOR Negatively Regulates DEPTOR Protein and mRNA Expression

(A) Serum starvation and stimulation regulates DEPTOR protein expression. HeLa cells were serum starved for 30 hours and stimulated with serum (10% final concentration) for the indicated times. Cell lysates were analyzed by immunoblotting for the levels of indicated proteins and phosphorylation states.
(B) DEPTOR amounts in mTORC1 and mTORC2 correlate with its expression within cells. HeLa cells were serum starved for 30 hours and stimulated with serum (10% final concentration) for the indicated times. Cell lysates and raptor

and rictor immunoprecipitates were analyzed by immunoblotting for indicated proteins.

(C) DEPTOR protein expression is downregulated in cancer cell lines with constitutive mTOR signaling. Cell lines were seeded at equal density and grown in the presence or absence of serum for 30 hours and cell lysates analyzed as in (A).

(D) DEPTOR protein expression is downregulated in PTEN null or TSC2 null MEFs. Indicated MEF lines were seeded at equal density and grown in the presence or absence of serum for 30 hours and cell lysates analyzed for levels of DEPTOR, PTEN, TSC2, and raptor. An asterisk (*) indicates a non-specific band.

(E) Rapamycin treatment partially and Torin1 treatment fully rescues the serum-induced decrease in DEPTOR protein. HeLa cells were serum-deprived for 30 hours, and then stimulated with serum in the presence of 100 nM rapamycin, 250 nM Torin1, or vehicle for the specified times. Cell lysates were analyzed as in (A).

(F) Regulation of DEPTOR protein and mRNA expression. HeLa cells were serum-deprived for 30 hours, and then stimulated with serum in the presence of 100 nM rapamycin, 10 uM of MG132, 250 nM Torin1, or vehicle for the specified times. Cell lysates were analyzed by immunoblotting for the levels of indicated proteins and phosphorylation states. DEPTOR mRNA was measured by qRT-PCR and normalized to GADPH mRNA levels. Error bars indicate standard deviation for n=3.

(G) Reductions in raptor or rictor expression increase DEPTOR protein and mRNA levels. Five days after transductions with raptor or rictor shRNA-expressing lentiviruses, HeLa cells were lysed and analyzed as in (A). DEPTOR mRNA was prepared and analyzed as in (F).

Figure 5. DEPTOR Overexpression Inhibits mTORC1 but Activates PI3K/Akt Signaling

(A) The 13xS/T->A DEPTOR mutant binds mTORC1 and mTORC2 more tightly than wild-type DEPTOR. HEK-293T cells were transfected with 500 ng of

expression vectors encoding the indicated FLAG-tagged proteins for 48 hours. Raptor or rictor immunoprecipitates were prepared from cell lysates, washed with buffers containing 150 mM NaCl, and analyzed along with cell lysates by immunoblotting for indicated proteins.

(B) Overexpression of DEPTOR inhibits T389 phosphorylation of S6K1. HeLa cells or the indicated p53-/- MEFS were cotransfected with expression plasmids encoding HA-GST-S6K1 as well as the indicated FLAG-tagged proteins. Cell lysates were prepared 24 hours after transfection and were analyzed by immunoblotting for the levels of the indicated proteins and phosphorylation states.

(C) Overexpression of DEPTOR activates T308 and S473 Akt1 phosphorylation. HeLa cells were cotransfected with expression plasmids encoding HA-GST-Akt1 as well as the indicated FLAG-tagged proteins. Cell lysates were analyzed as in (B).

(D) Overexpression of DEPTOR activates T308 and S473 Akt1 phosphorylation only in serum-replete cells. HeLa cells were transfected as in (B), serum starved for 24 hours and stimulated for the indicated times and cell lysates were analyzed as in (B).

(E) Partial inhibition of mTOR with Torin1 inhibits S6K1 phosphorylation but activates PI3K/mTORC2/Akt signaling. HeLa cells were treated with the specified concentrations of Torin1 or vehicle for either 10 minutes or 48 hours and cell lysates were analyzed as in (B).

Figure 6. DEPTOR is Overexpressed in a Subset of Multiple Myeloma Cells and in these Cells Activates PI3K/Akt signaling and Promotes Cell Survival

(A) DEPTOR mRNA expression is downregulated in most cancers, yet is up-regulated in Multiple Myelomas. Relative DEPTOR mRNA expression in various cancer types versus matched unaffected tissue was collated from publicly available microarray studies. For all studies shown, $p<0.05$ for DEPTOR mRNA downregulation or upregulation by one-tailed T-test.

(B) DEPTOR mRNA is mostly highly expressed in the subset of Multiple Myelomas which possess Cyclin D1/D3 or c-MAF/MAFB translocations. DEPTOR mRNA levels were normalized by the summed mean values of the housekeeping genes GAPDH, β-actin, and FIP (7 total probe-sets). Error bars indicate standard error for n=7. The differences in mean DEPTOR mRNA levels between plasma cells and MMs with Cyclin D1, Cyclin D3, or c-MAF/MAFB translocations are significant to at least $p<0.005$.

(C) Human Multiple Myeloma cell lines with high DEPTOR protein expression have activated PI3K and suppressed mTORC1 signaling. Cell lysates were analyzed by immunoblotting for the levels of the indicated proteins and phosphorylation states. Cell lines with known translocations of c-MAF or MAFB are indicated.

(D) RNAi-mediated knockdown of DEPTOR in 8226 and OCI-MY5 cells reduces DEPTOR expression to levels similar to those in HeLa cells. Five days after transductions with shRNA-expressing lentiviruses, cells were lysed and as in (C).

(E) DEPTOR suppression in 8226 and OCI-MY5 cells activates mTORC1 signaling, inhibits IRS-1 or PDGFR-β expression, and reduces PI3K/mTORC2/Akt signaling. Five days after transduction with shRNA-expressing lentiviruses, cells were lysed and analyzed as in (C).

(F) DEPTOR suppression markedly decreases 8226 cell number. Cell number was measured at indicated time points with a Coulter Counter. Error bars indicate mean ± standard deviation for n=3 samples per time point.

(G) Representative 20x light microscopy images of 8226 cells expressing shRNAs targeting DEPTOR, GFP, or luciferase at day 8 post-infection.

(H) DEPTOR suppression causes apoptosis. Three days after transduction with shRNA-expressing lentiviruses, 8226 cells were lysed and analyzed as in (C).

(I) A reduction in c-MAF expression decreases DEPTOR mRNA levels. Five days after transduction of 8226 cells with lentiviruses expressing the indicated shRNAs, DEPTOR and Integrin β7 mRNA levels were measured by qRT-PCR and normalized to GADPH mRNA levels. Error bars indicate standard deviation for n=3.

(J) A c-MAF knockdown activates mTORC1 and downregulates PI3K signaling. Five days after transductions with shRNA-expressing lentiviruses, lysates of 8226 cells were analyzed as in (C).

Figure S1. Similar to a Reduction in Raptor Expression, a Reduction in DEPTOR Expression Protects Cells from Apoptosis Induced by Serum Withdrawal.

HT-29 cells expressing shRNAs targeting DEPTOR, raptor, or luciferase were serum starved for 6 hours. Cell lysates were analyzed by immunoblotting for the levels of indicated proteins and phosphorylation states.

Figure S2. PTEN Positively Regulates DEPTOR mRNA Expression.

(A) PTEN Loss Reduces DEPTOR mRNA Expression. HeLa, PC3, and U87 cells were seeded at equal density. 48 hours after seeding DEPTOR mRNA was determined by qRT-PCR from total RNA samples and normalized to GADPH mRNA levels. Error bars indicate mean ± standard deviation for n=3 per condition.

(B) Expression of an shRNA targeting PTEN in HeLa cells reduces DEPTOR mRNA expression. Five days after transductions with an shRNA-expressing lentivirus, cells were lysed and analyzed by immunoblotting for PTEN levels. DEPTOR mRNA was prepared and analyzed as in (A)

Figure S3. Further Characterization of DEPTOR Phosphorylation and its Functions.

(A) Schematic representation of the location of phosphorylation sites identified in DEPTOR by mass spectrometry. All 13 phosphorylation sites were mutated to alanine as described in the methods.

(B) DEPTOR gel mobility is increased by Calf Intestinal Phosphatase (CIP) treatment. Immunoprecipitated wild-type recombinant DEPTOR was incubated without CIP or with active or heat-inactivated CIP for 30 minutes and analyzed by SDS-PAGE followed by immunoblotting.

(C) mTOR inhibitors decrease the recognition of DEPTOR by a phospho-specific antibody. Serum-replete HEK-293T cells expressing FLAG-DEPTOR were treated with vehicle, 50 nM rapamycin, or 250 nM Torin1 for 16 hours. Immunoblotting was performed for the indicated proteins and phosphorylation states. A phospho-specific antibody designed against phospho-S877 raptor cross-reacts with DEPTOR and was used to detect phospho-DEPTOR.
(D) Proline-directed DEPTOR phosphorylation sites serines 244, 265, 293, and 299 are dephosphorylated in the presence of Torin1. Serum-replete HEK-293T cells expressing FLAG-DEPTOR were treated with vehicle or 250nM Torin1 for 16 hours. After immunopurification from cell lysates, the extent of phosphorylation at each of the indicated sites was measured using mass spectrometry as described in the methods.
(E) Elimination of the DEPTOR phosphorylation sites impairs the serum-induced mobility shift seen in SDS-PAGE analyses of wild-type DEPTOR. HeLa cells were transfected with 50 ng of the indicated plasmids expressing FLAG-DEPTOR. Three days later, cells were starved for serum for 30 hours and, where indicated, stimulated with serum for the specified times. Cell lysates were analyzed by immunoblotting for levels of recombinant DEPTOR and, as a loading control, mTOR. Arrows indicate serum-induced mobility shifts of wild-type and 13xS/T->A mutant FLAG-DEPTOR.
(F) Overexpression of recombinant wild-type DEPTOR blocks serum-induced degradation of recombinant and endogenous DEPTOR. Myc-tagged DEPTOR was induced by treatment with 10 ng/ml doxycycline in Tet-On HeLa cells. Two days post-induction, non-induced, and induced cells were serum starved for 30 hours and stimulated with serum for the specified times. Cell lysates were analyzed by immunoblotting for the levels of the indicated proteins.

Figure S4. Overexpression of DEPTOR Activates Phosphorylation of T308 and S473 of Akt1 in a Dose-Dependent Manner.

p53-/- MEFs cells were cotransfected with expression plasmids encoding HA-GST-Akt1 (200 ng) as well as 200 ng or 2 □g of the indicated FLAG-tagged

proteins. Cell lysates were prepared 24 hours after transfection and were analyzed by immunoblotting for the levels of the indicated proteins and phosphorylation states.

Figure S5. Effects of Prolonged Inhibition of mTOR with the ATP Competitive Inhibitor PP242 on mTORC1 and PI3K/mTORC2/Akt Signaling.
HeLa cells were treated with the specified concentrations of PP242 or vehicle for either 1 hour or 48 hours. Cell lysates were prepared and analyzed by immunoblotting for the levels of the indicated proteins and phosphorylation states.

Figure S6. DEPTOR Expression across Human Cancer Cell lines Anti-Correlates with Cell Size.
(A) Indicated cell lines were seeded at equal density and 48 hours later cell lysates were prepared and analyzed by immunoblotting for DEPTOR. mTOR expression was used as a loading control. Multiple Myeloma cell lines with or without c-MAF/MAFB translocations are indicated where known.
(B) DEPTOR mRNA levels anti-correlate with cell size across a variety of human cell lines. Mean values of DEPTOR mRNA levels and cell diameter are shown in Table S1. Cell size was measured using a Coulter Counter. Non-Multiple Myeloma cell lines (PC3, HEK-293T, and HeLa) are indicated by red squares. Multiple Myeloma cell lines are indicated by black squares.

Figure S7. A Reduction in DEPTOR Expression in 8226 Cells Activates the In Vitro Kinase Activity of mTORC2 Despite Decreasing Akt S473 Phosphorylation in Cells.
8226 cells were infected with lentiviruses expressing shRNAs targeting GFP or DEPTOR. Six days post-infection, mTOR immunoprecipitates were prepared from cell lysates (0.2 mg total protein) and analyzed for mTORC1/2 kinase activities toward S6K1 and Akt1 and for levels of mTOR and DEPTOR.

Figure S8. A Reduction in TSC2 Expression Increases mTORC1 Signaling but Represses PDGFRβ Protein Levels.

OCI-MY5 cells were infected with a control shRNA or an shRNA targeting TSC2. Five days after infection, cell lysates were analyzed for the indicated protein levels and phosphorylation states.

Figure S9. Raptor Knockdown Restores PI3K Signaling in DEPTOR knockdown 8226 Cells. 8226 cells co-expressing shRNAs targeting luciferase or DEPTOR along with shRNAs targeting luciferase or raptor were lysed five days after infection and cell lysates were analyzed for the indicated protein levels and phosphorylation states.

Table S1. DEPTOR mRNA Expression Analysis in Human Cancers

(A) Figure 6A worksheet. Listing of primary references used to generate meta-analysis of DEPTOR mRNA expression in human cancers.

(B) Figure 6B worksheet. Raw data for DEPTOR and housekeeping mRNA expression in MM tumor samples and plasma cells.

(C) Figure S6B worksheet. Raw data for DEPTOR mRNA expression and cell size measurements in Multiple Myeloma cell lines.

Fig.1

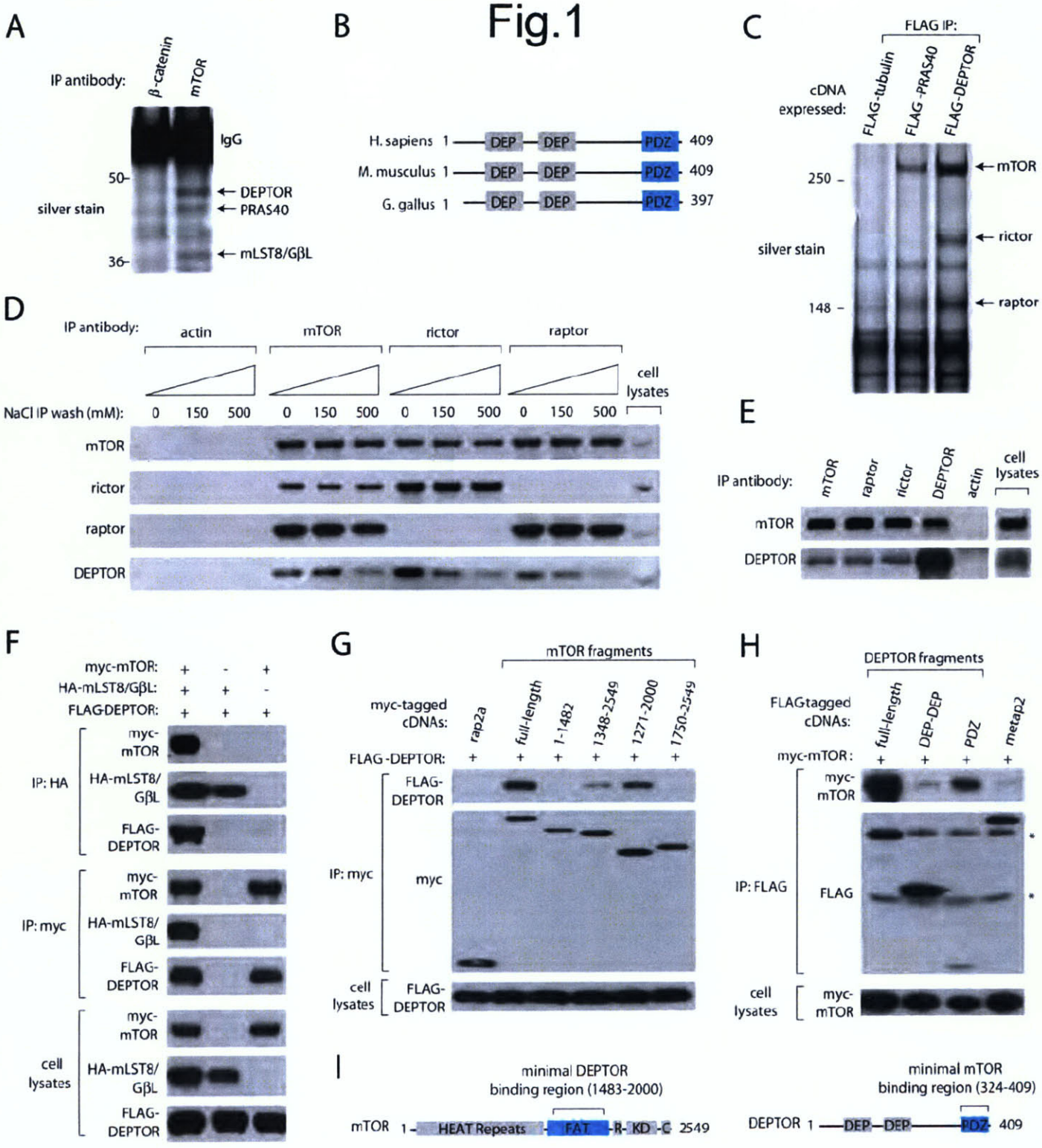
A
IP antibody:
β-catenin
mTOR
IgG
50–
DEPTOR
PRAS40
silver stain
36–
mLST8/GβL
B
H. sapiens 1 DEP DEP PDZ 409
M. musculus 1 DEP DEP PDZ 409
G. gallus 1 DEP DEP PDZ 397
C
FLAG IP:
cDNA expressed:
FLAG-tubulin
FLAG-PRAS40
FLAG-DEPTOR
250 –
mTOR
rictor
silver stain
148 –
raptor
D
IP antibody:
actin
mTOR
rictor
raptor
cell lysates
NaCl IP wash (mM):
0 150 500 0 150 500 0 150 500 0 150 500
mTOR
rictor
raptor
DEPTOR
E
IP antibody:
mTOR
raptor
rictor
DEPTOR
actin
cell lysates
mTOR
DEPTOR
F
myc-mTOR: + - +
HA-mLST8/GβL: + + -
FLAG-DEPTOR: + + +
IP: HA
myc-mTOR
HA-mLST8/GβL
FLAG-DEPTOR
IP: myc
myc-mTOR
HA-mLST8/GβL
FLAG-DEPTOR
cell lysates
myc-mTOR
HA-mLST8/GβL
FLAG-DEPTOR
G
mTOR fragments
myc-tagged cDNAs:
rap2a
full-length
1-1482
1348-2549
1271-2000
1750-2549
FLAG-DEPTOR: + + + + + +
IP: myc
FLAG-DEPTOR
myc
cell lysates
FLAG-DEPTOR
H
DEPTOR fragments
FLAG-tagged cDNAs:
full-length
DEP-DEP
PDZ
metap2
myc-mTOR: + + + +
IP: FLAG
myc-mTOR
FLAG
*
*
cell lysates
myc-mTOR
I
minimal DEPTOR binding region (1483-2000)
mTOR 1 – HEAT Repeats – FAT – R – KD – C 2549
minimal mTOR binding region (324-409)
DEPTOR 1 DEP DEP PDZ 409

Fig.2

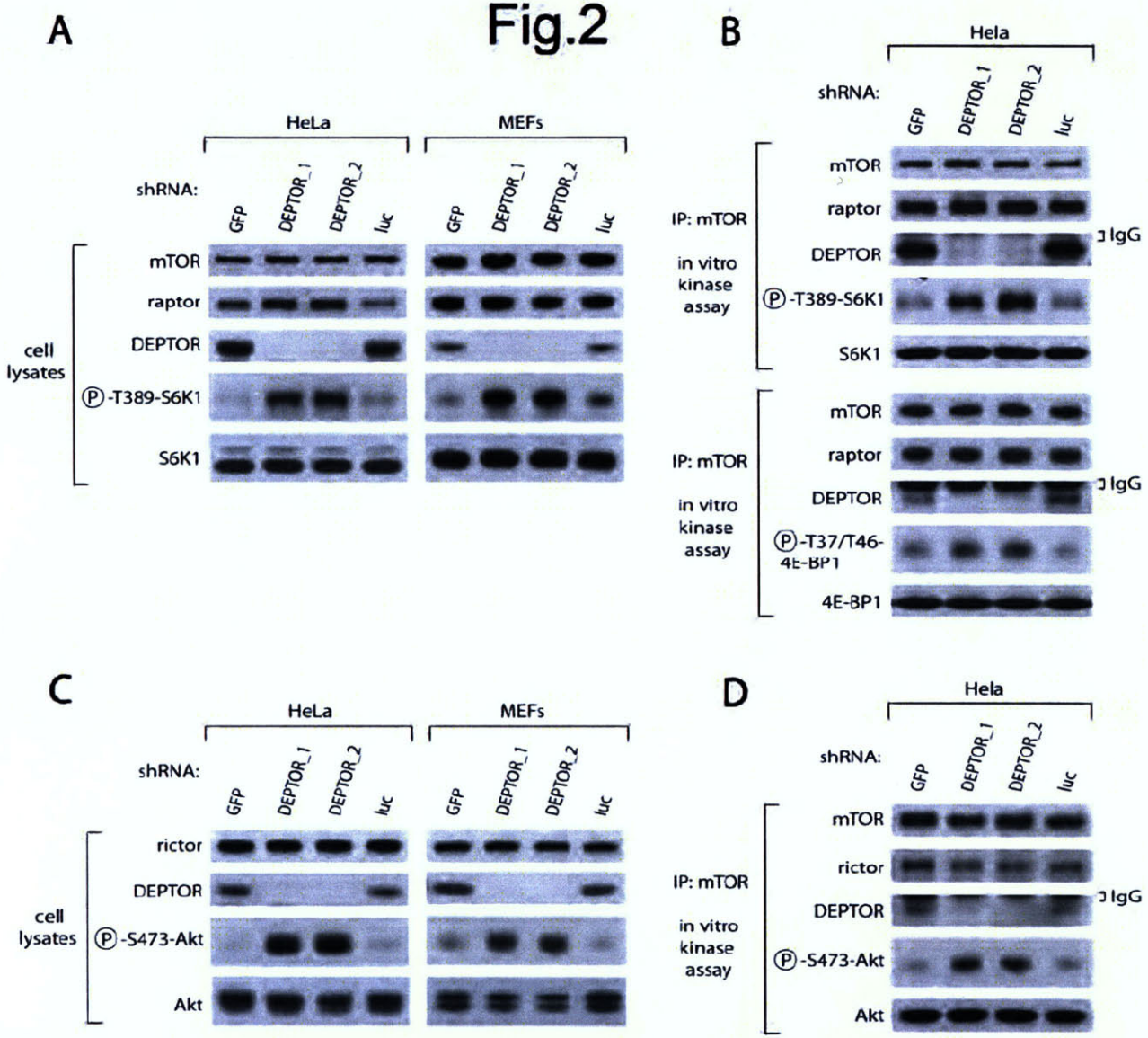
A
HeLa
MEFs
shRNA:
GFP
DEPTOR_1
DEPTOR_2
luc
cell lysates
mTOR
raptor
DEPTOR
Ⓟ-T389-S6K1
S6K1
B
Hela
shRNA:
GFP
DEPTOR_1
DEPTOR_2
luc
IP: mTOR
in vitro kinase assay
mTOR
raptor
DEPTOR
Ⓟ-T389-S6K1
S6K1
IgG
IP: mTOR
in vitro kinase assay
mTOR
raptor
DEPTOR
Ⓟ-T37/T46-4E-BP1
4E-BP1
IgG
C
HeLa
MEFs
shRNA:
GFP
DEPTOR_1
DEPTOR_2
luc
cell lysates
rictor
DEPTOR
Ⓟ-S473-Akt
Akt
D
Hela
shRNA:
GFP
DEPTOR_1
DEPTOR_2
luc
IP: mTOR
in vitro kinase assay
mTOR
rictor
DEPTOR
Ⓟ-S473-Akt
Akt
IgG

Fig.3

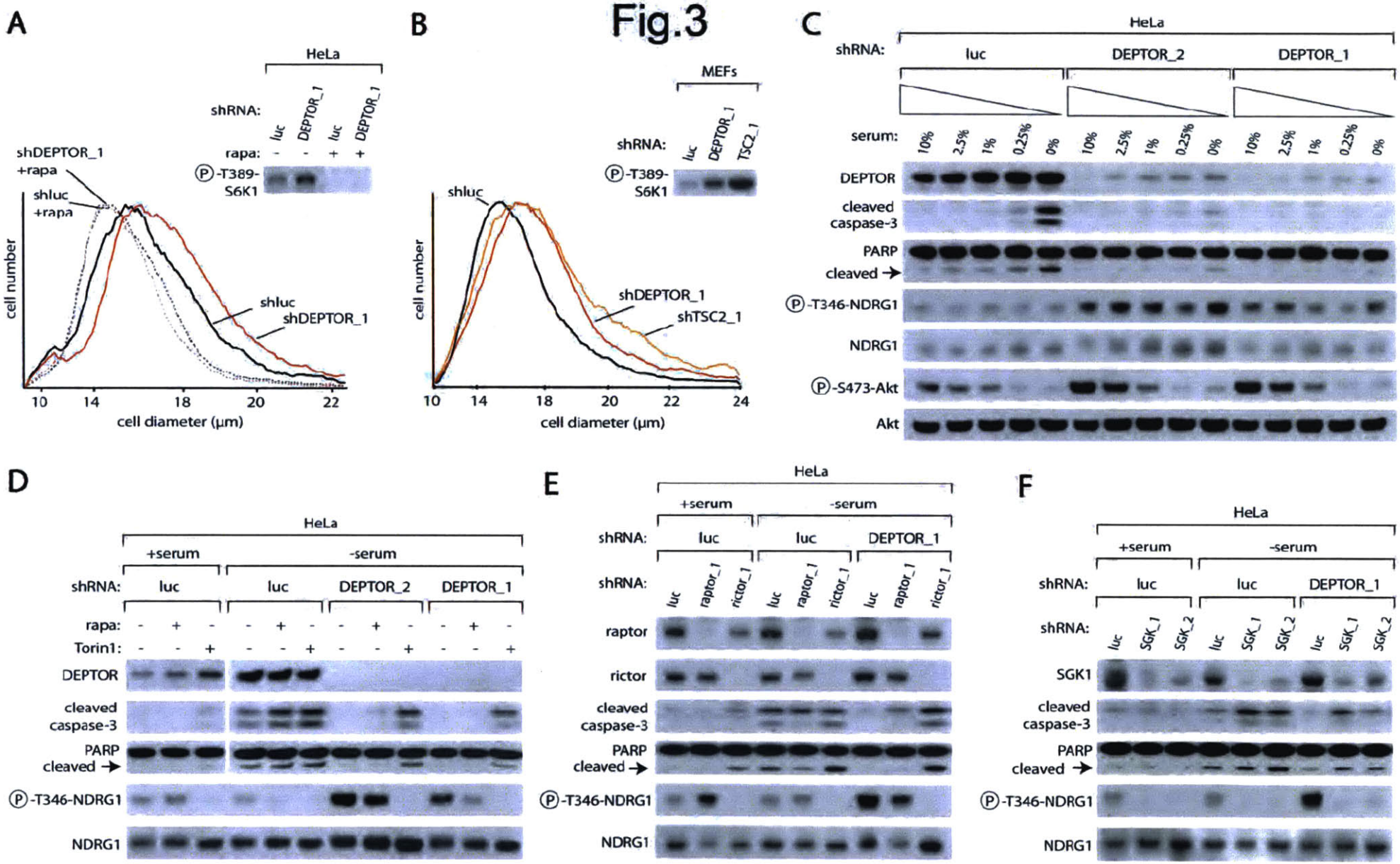
A
HeLa
shRNA:
luc
DEPTOR_1
luc
DEPTOR_1
rapa:
- - + +
Ⓟ-T389-S6K1
shDEPTOR_1 +rapa
shluc +rapa
shluc
shDEPTOR_1
cell number
10 14 18 20 22
cell diameter (μm)
B
MEFs
shRNA:
luc
DEPTOR_1
TSC2_1
Ⓟ-T389-S6K1
shluc
shDEPTOR_1
shTSC2_1
cell number
10 14 18 20 22 24
cell diameter (μm)
C
HeLa
shRNA:
luc
DEPTOR_2
DEPTOR_1
serum:
10% 2.5% 1% 0.25% 0% 10% 2.5% 1% 0.25% 0% 10% 2.5% 1% 0.25% 0%
DEPTOR
cleaved caspase-3
PARP cleaved
Ⓟ-T346-NDRG1
NDRG1
Ⓟ-S473-Akt
Akt
D
HeLa
+serum
-serum
shRNA:
luc
luc
DEPTOR_2
DEPTOR_1
rapa:
- + - - + - - + - - + -
Torin1:
- - + - - + - - + - - +
DEPTOR
cleaved caspase-3
PARP cleaved
Ⓟ-T346-NDRG1
NDRG1
E
HeLa
+serum
-serum
shRNA:
luc
luc
DEPTOR_1
shRNA:
luc raptor_1 rictor_1 luc raptor_1 rictor_1 luc raptor_1 rictor_1
raptor
rictor
cleaved caspase-3
PARP cleaved
Ⓟ-T346-NDRG1
NDRG1
F
HeLa
+serum
-serum
shRNA:
luc
luc
DEPTOR_1
shRNA:
luc SGK_1 SGK_2 luc SGK_1 SGK_2 luc SGK_1 SGK_2
SGK1
cleaved caspase-3
PARP cleaved
Ⓟ-T346-NDRG1
NDRG1

Fig.4

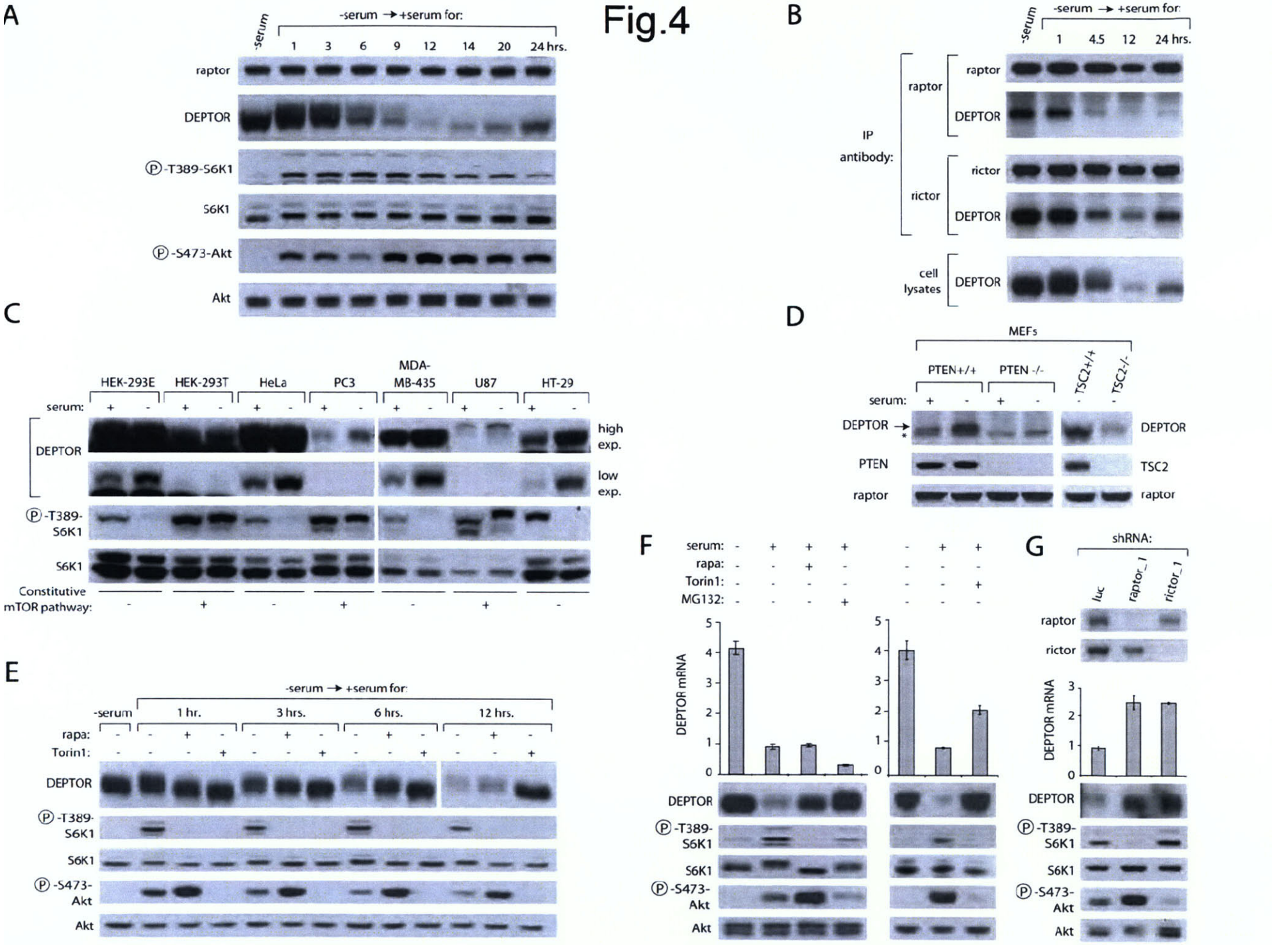
A
-serum
-serum → +serum for:
1 3 6 9 12 14 20 24 hrs.
raptor
DEPTOR
Ⓟ-T389-S6K1
S6K1
Ⓟ-S473-Akt
Akt
B
-serum
-serum → +serum for:
1 4.5 12 24 hrs.
IP antibody:
raptor
raptor
DEPTOR
rictor
rictor
DEPTOR
cell lysates
DEPTOR
C
HEK-293E HEK-293T HeLa PC3 MDA-MB-435 U87 HT-29
serum: + - + - + - + - + - + - + -
DEPTOR
high exp.
low exp.
Ⓟ-T389-S6K1
S6K1
Constitutive mTOR pathway: - + - + - + -
D
MEFs
PTEN+/+ PTEN -/- TSC2+/+ TSC2-/-
serum: + - + - - -
DEPTOR
*
PTEN
raptor
DEPTOR
TSC2
raptor
E
-serum → +serum for:
-serum 1 hr. 3 hrs. 6 hrs. 12 hrs.
rapa: - - + - - + - - + - - + -
Torin1: - - - + - - + - - + - - +
DEPTOR
Ⓟ-T389-S6K1
S6K1
Ⓟ-S473-Akt
Akt
F
serum: - + + + - + +
rapa: - - + - - - -
Torin1: - - - - - - +
MG132: - - - + - - -
DEPTOR mRNA
0 1 2 3 4 5
DEPTOR
Ⓟ-T389-S6K1
S6K1
Ⓟ-S473-Akt
Akt
G
shRNA:
luc raptor_1 rictor_1
raptor
rictor
DEPTOR mRNA
0 1 2 3
DEPTOR
Ⓟ-T389-S6K1
S6K1
Ⓟ-S473-Akt
Akt

Fig.5

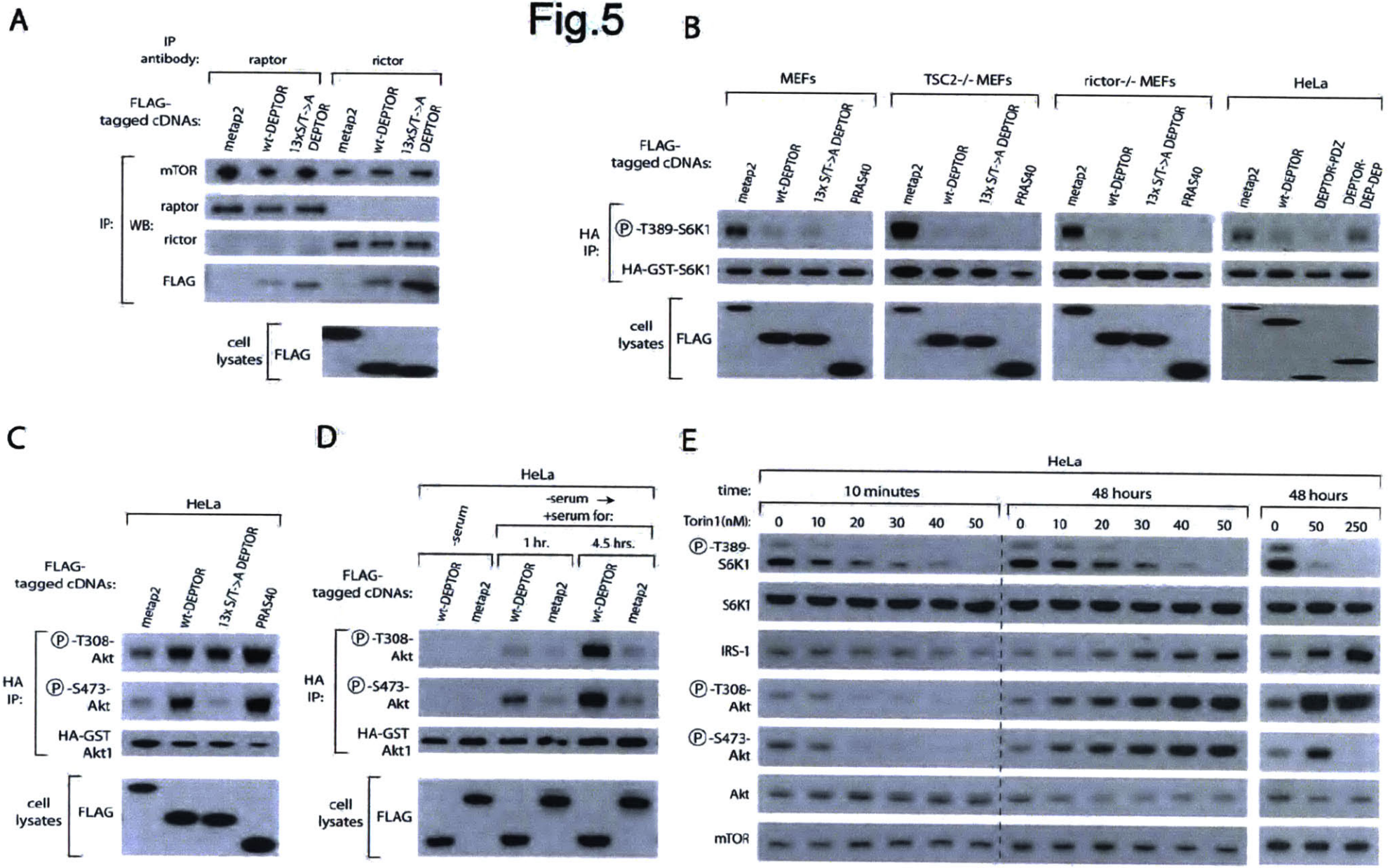
A
IP antibody:
raptor
rictor
FLAG-tagged cDNAs:
metap2
wt-DEPTOR
13xS/T->A DEPTOR
IP: WB:
mTOR
raptor
rictor
FLAG
cell lysates
FLAG
B
MEFs
TSC2-/- MEFs
rictor-/- MEFs
HeLa
FLAG-tagged cDNAs:
metap2
wt-DEPTOR
13x S/T->A DEPTOR
PRAS40
DEPTOR-PDZ
DEPTOR-DEP-DEP
HA IP:
Ⓟ-T389-S6K1
HA-GST-S6K1
cell lysates
FLAG
C
HeLa
FLAG-tagged cDNAs:
metap2
wt-DEPTOR
13x S/T->A DEPTOR
PRAS40
HA IP:
Ⓟ-T308-Akt
Ⓟ-S473-Akt
HA-GST Akt1
cell lysates
FLAG
D
HeLa
-serum
-serum → +serum for:
1 hr.
4.5 hrs.
FLAG-tagged cDNAs:
wt-DEPTOR
metap2
HA IP:
Ⓟ-T308-Akt
Ⓟ-S473-Akt
HA-GST Akt1
cell lysates
FLAG
E
HeLa
time:
10 minutes
48 hours
48 hours
Torin1(nM):
0
10
20
30
40
50
0
50
250
Ⓟ-T389-S6K1
S6K1
IRS-1
Ⓟ-T308-Akt
Ⓟ-S473-Akt
Akt
mTOR

Fig.6

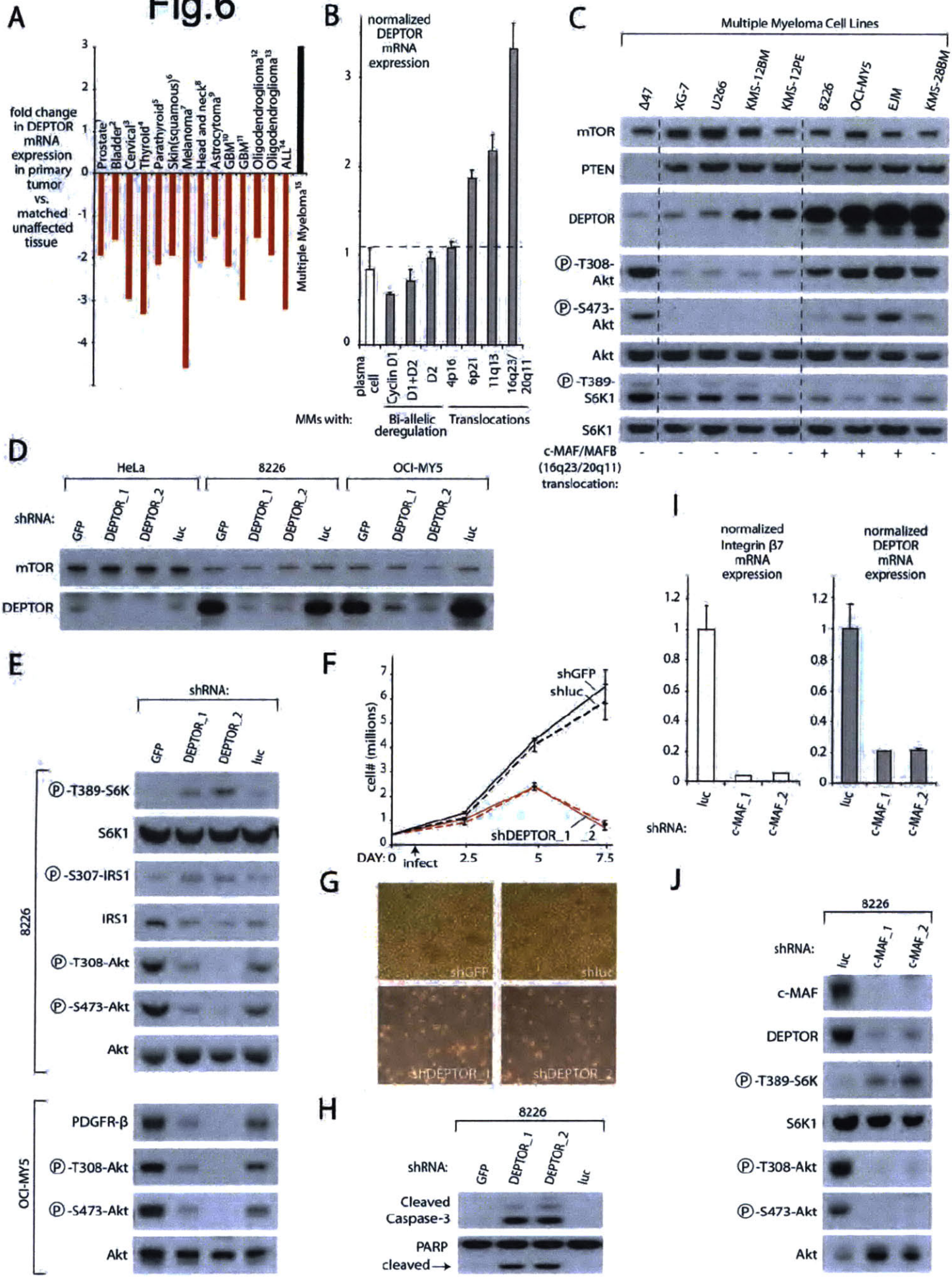
A
fold change in DEPTOR mRNA expression in primary tumor vs. matched unaffected tissue
Prostate
Bladder[2]
Cervical[3]
Thyroid[4]
Parathyroid[5]
Skin(squamous)[6]
Melanoma[7]
Head and neck[8]
Astrocytoma[9]
GBM[10]
GBM[11]
Oligodendroglioma[12]
Oligodendroglioma[13]
ALL[14]
Multiple Myeloma[15]
B
normalized DEPTOR mRNA expression
plasma cell
Cyclin D1
D1+D2
D2
4p16
6p21
11q13
16q23/ 20q11
MMs with:
Bi-allelic deregulation
Translocations
C
Multiple Myeloma Cell Lines
Δ47
XG-7
U266
KMS-12BM
KMS-12PE
8226
OCI-MY5
EJM
KMS-28BM
mTOR
PTEN
DEPTOR
Ⓟ-T308-Akt
Ⓟ-S473-Akt
Akt
Ⓟ-T389-S6K1
S6K1
c-MAF/MAFB (16q23/20q11) translocation:
D
HeLa
8226
OCI-MY5
shRNA:
GFP
DEPTOR_1
DEPTOR_2
luc
mTOR
DEPTOR
E
shRNA:
GFP
DEPTOR_1
DEPTOR_2
luc
8226
Ⓟ-T389-S6K
S6K1
Ⓟ-S307-IRS1
IRS1
Ⓟ-T308-Akt
Ⓟ-S473-Akt
Akt
OCI-MY5
PDGFR-β
Ⓟ-T308-Akt
Ⓟ-S473-Akt
Akt
F
cell# (millions)
shGFP
shluc
shDEPTOR_1
_2
DAY: 0
infect
2.5
5
7.5
G
shGFP
shluc
shDEPTOR_1
shDEPTOR_2
H
8226
shRNA:
GFP
DEPTOR_1
DEPTOR_2
luc
Cleaved Caspase-3
PARP cleaved→
I
normalized Integrin β7 mRNA expression
normalized DEPTOR mRNA expression
luc
c-MAF_1
c-MAF_2
shRNA:
J
8226
shRNA:
luc
c-MAF_1
c-MAF_2
c-MAF
DEPTOR
Ⓟ-T389-S6K
S6K1
Ⓟ-T308-Akt
Ⓟ-S473-Akt
Akt

Fig.S1

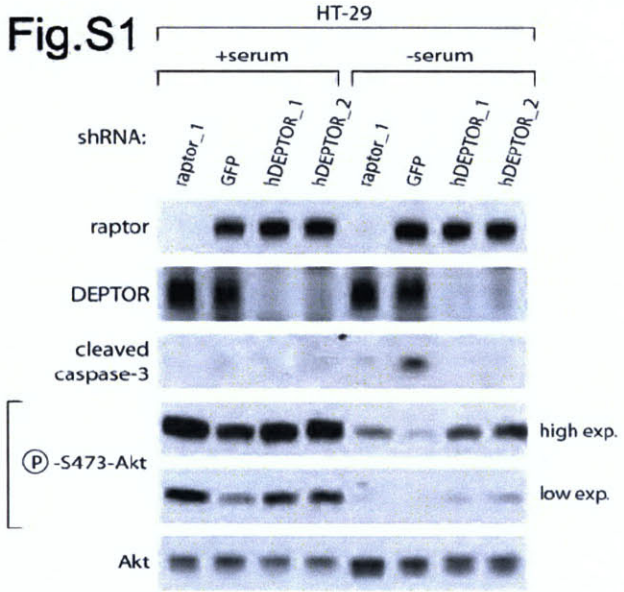
HT-29
+serum
-serum
shRNA:
raptor_1
GFP
hDEPTOR_1
hDEPTOR_2
raptor_1
GFP
hDEPTOR_1
hDEPTOR_2
raptor
DEPTOR
cleaved
caspase-3
Ⓟ-S473-Akt
high exp.
low exp.
Akt

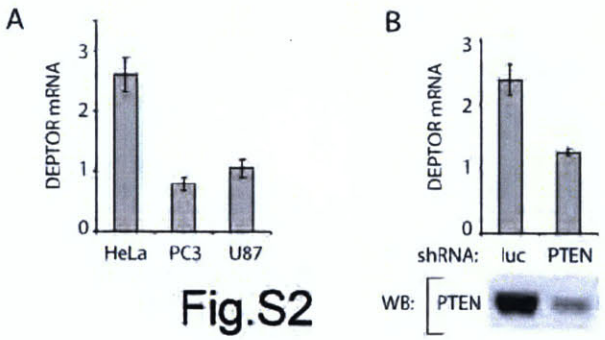
A
DEPTOR mRNA
3
2
1
0
HeLa
PC3
U87
B
DEPTOR mRNA
3
2
1
0
shRNA:
luc
PTEN
WB:
PTEN

Fig.S2

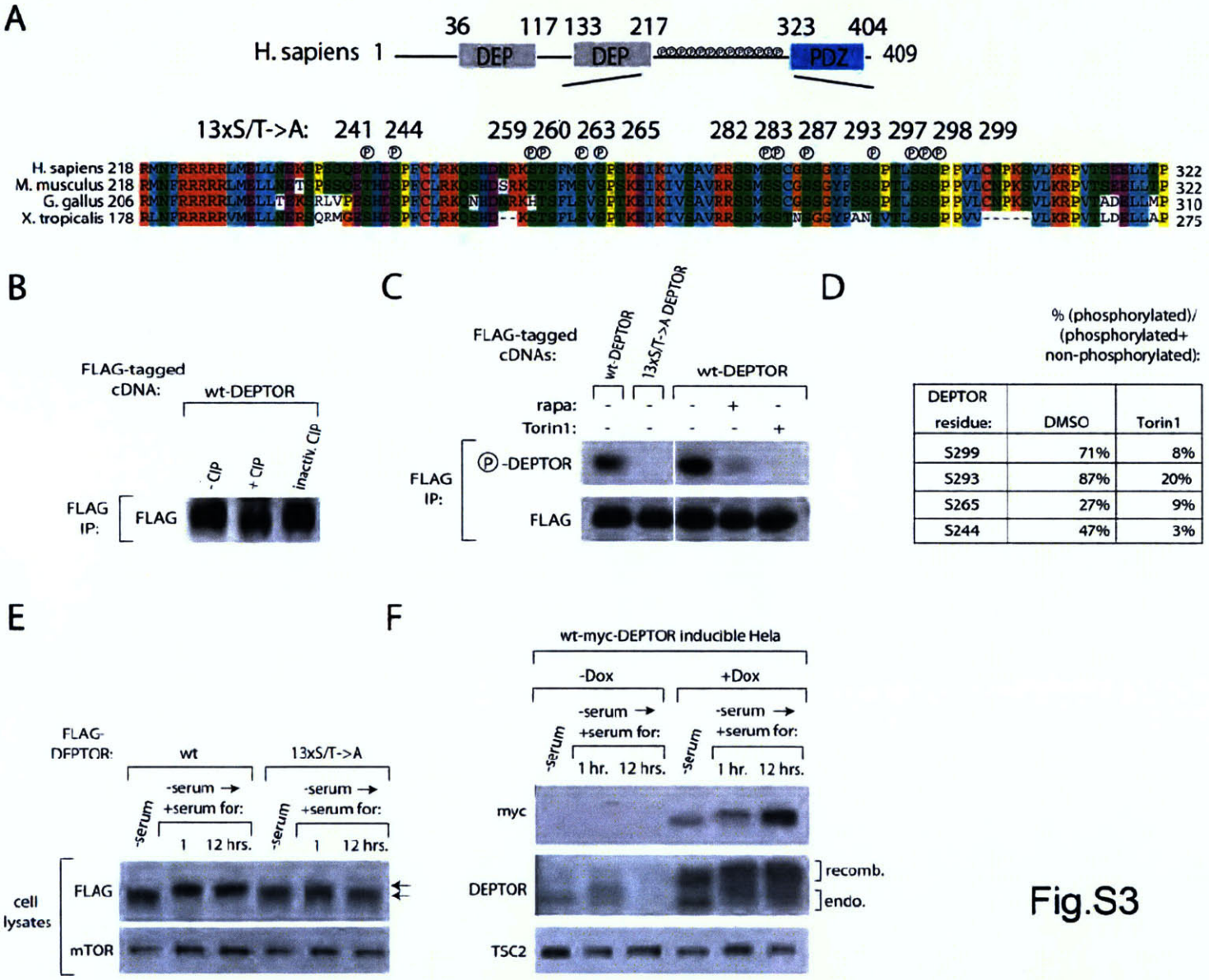
A
H. sapiens 1
36
117 133
217
323
404
409
DEP
DEP
PDZ
13xS/T->A:
241 244
259 260 263 265
282 283 287 293 297 298 299
H. sapiens 218
M. musculus 218
G. gallus 206
X. tropicalis 178
322
322
310
275
B
FLAG-tagged cDNA:
wt-DEPTOR
- CIP
+ CIP
inactiv. CIP
FLAG IP:
FLAG
C
FLAG-tagged cDNAs:
wt-DEPTOR
13xS/T->A DEPTOR
wt-DEPTOR
rapa:
Torin1:
FLAG IP:
-DEPTOR
FLAG
D
% (phosphorylated)/ (phosphorylated+ non-phosphorylated):
DEPTOR residue:
DMSO
Torin1
S299 71% 8%
S293 87% 20%
S265 27% 9%
S244 47% 3%
E
FLAG-DEPTOR:
wt
13xS/T->A
-serum →
+serum for:
-serum
1
12 hrs.
cell lysates
FLAG
mTOR
F
wt-myc-DEPTOR inducible Hela
-Dox
+Dox
-serum →
+serum for:
-serum
1 hr.
12 hrs.
myc
DEPTOR
recomb.
endo.
TSC2

Fig.S3

Fig.S4

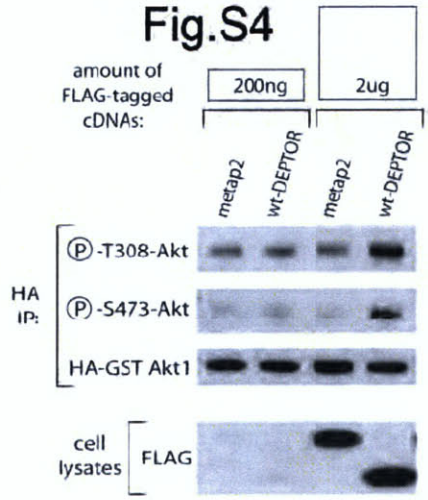
amount of FLAG-tagged cDNAs:
200ng
2ug
metap2
wt-DEPTOR
metap2
wt-DEPTOR
HA IP:
Ⓟ-T308-Akt
Ⓟ-S473-Akt
HA-GST Akt1
cell lysates
FLAG

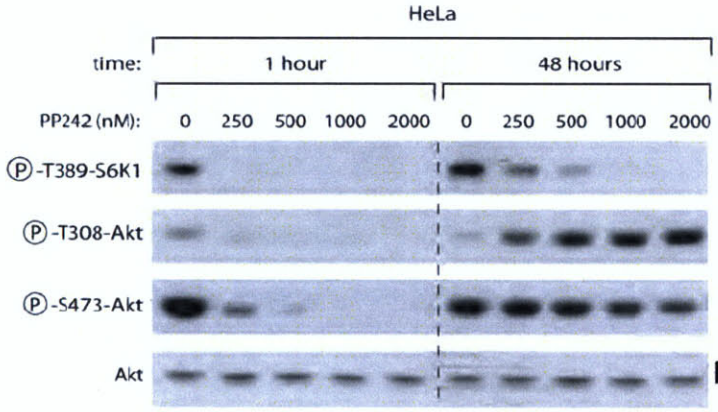
HeLa
time:
1 hour
48 hours
PP242 (nM):
0 250 500 1000 2000 0 250 500 1000 2000
Ⓟ-T389-S6K1
Ⓟ-T308-Akt
Ⓟ-S473-Akt
Akt

Fig.S5

Fig.S6

A

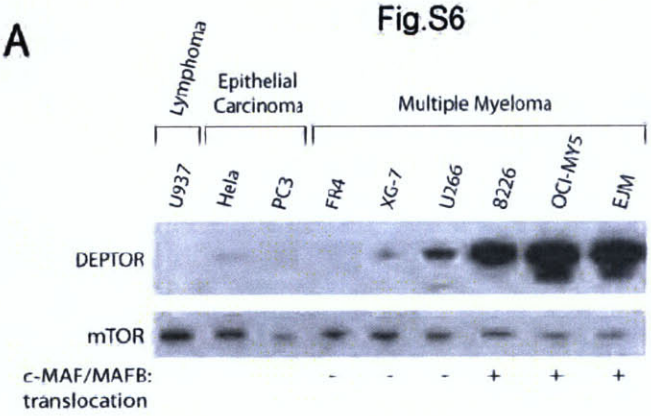
Lymphoma
Epithelial Carcinoma
Multiple Myeloma
U937
Hela
PC3
FR4
XG-7
U266
8226
OCI-MY5
EJM
DEPTOR
mTOR
c-MAF/MAFB: translocation
- - - + + +

B

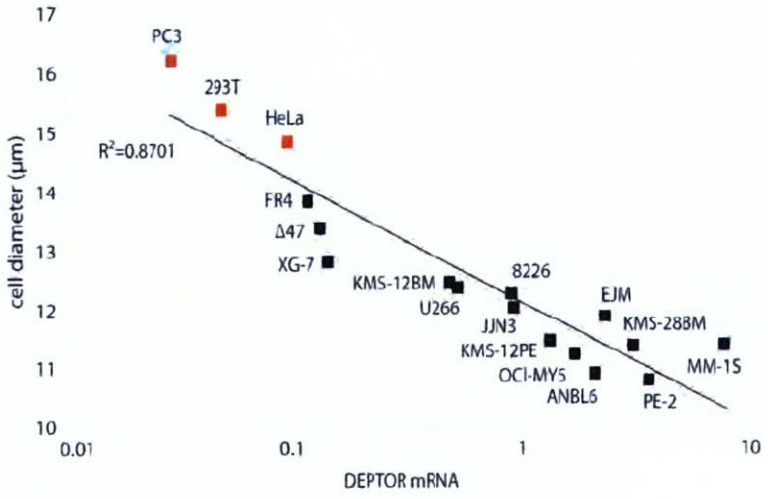
cell diameter (μm)
17
16
15
14
13
12
11
10
PC3
293T
HeLa
R²=0.8701
FR4
Δ47
XG-7
KMS-12BM
U266
8226
JJN3
KMS-12PE
OCI-MY5
ANBL6
EJM
KMS-288M
MM-1S
PE-2
0.01
0.1
1
10
DEPTOR mRNA

Fig.S7

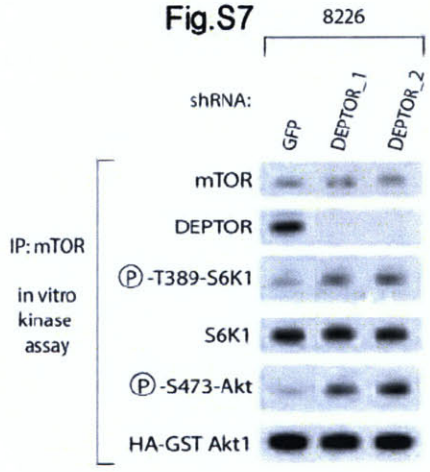
8226
shRNA:
GFP
DEPTOR_1
DEPTOR_2
IP: mTOR
in vitro kinase assay
mTOR
DEPTOR
Ⓟ-T389-S6K1
S6K1
Ⓟ-S473-Akt
HA-GST Akt1


Fig.S8
OCI-MY5
shRNA:
GFP
TSC2_1
TSC2
PDGFR-β
Ⓟ-T389-S6K1
S6K1

Fig.S9


8226
shRNA:
luc
DEPTOR_1
shRNA:
luc
raptor_1
luc
raptor_1
raptor
DEPTOR
Ⓟ-T389-S6K1
Ⓟ-T308-Akt
Ⓟ-S473-Akt

REFERENCES

1. D. D. Sarbassov, S. M. Ali, D. M. Sabatini, *Curr Opin Cell Biol* **17**, 596 (Dec, 2005).
2. D. A. Guertin, D. M. Sabatini, *Cancer Cell* **12**, 9 (Jul, 2007).
3. D. M. Sabatini, *Nat Rev Cancer* **6**, 729 (Sep, 2006).
4. B. D. Manning *et al.*, *Genes Dev* **19**, 1773 (Aug 1, 2005).
5. H. Zhang *et al.*, *J Clin Invest.* **117**, 730 (2007).
6. V. Bliskovsky *et al.*, *Proc Natl Acad Sci U S A.* **100**, 14982 (2003).
7. Y. Sancak *et al.*, *Mol Cell* **25**, 903 (Mar 23, 2007).
8. S. Chen, H. E. Hamm, *Dev Cell.* **11**, 436 (2006).
9. P. Jemth, S. Gianni, *Biochemistry.* **46**, 8701 (2007).
10. H. Dudek *et al.*, *Science* **275**, 661 (1997).
11. M. Tewari *et al.*, *Cell.* **81**, 801 (1995).
12. S. R. Datta, A. Brunet, M. E. Greenberg, *Genes Dev* **13**, 2905 (Nov 15, 1999).
13. M. Tessier, J. R. Woodgett, *J Cell Biochem.* **98**, 1391 (2006).
14. F. Hong *et al.*, *Mol Cell.* **30**, 701 (2008).
15. J. M. Garcia-Martinez, D. R. Alessi, *Biochem J* **17**, 17 (2008).
16. J. T. Murray *et al.*, *Biochem J.* **384**, 477 (2004).
17. C. C. Thoreen *et al.*, *J Biol Chem* **15**, 15 (2009).
18. J. E. Skeen *et al.*, *Cancer Cell.* **10**, 269 (2006).
19. D. D. Sarbassov *et al.*, *Mol Cell* **22**, 159 (Apr 21, 2006).
20. A. Carracedo, P. P. Pandolfi, *Oncogene.* **27**, 5527 (2008).
21. S. Tsubuki *et al.*, *Biochem Biophys Res Commun.* **196**, 1195 (1993).
22. A. Y. Choo, S. O. Yoon, S. G. Kim, P. P. Roux, J. Blenis, *Proc Natl Acad Sci U S A.* **105**, 17414 (2008).
23. M. E. Feldman *et al.*, *PLoS Biol.* **7**, e38. (2009).
24. A. C. Gingras *et al.*, *Genes Dev* **15**, 2852 (2001).
25. G. J. Brunn *et al.*, *Science* **277**, 99 (1997).
26. P. E. Burnett, R. K. Barrow, N. A. Cohen, S. H. Snyder, D. M. Sabatini, *PNAS* **95**, 1432 (1998).

27. A. C. Gingras *et al.*, *Genes Dev* **13**, 1422 (1999).
28. D. R. Alessi, *Biochem Soc Trans* **29**, 1 (2001).
29. K. E. O'Reilly *et al.*, *Cancer Res* **66**, 1500 (Feb 1, 2006).
30. C. C. Thoreen *et al.*, *J Biol Chem*, 16 (2009).
31. W. M. Kuehl, P. L. Bergsagel, *Nat Rev Cancer.* **2**, 175 (2002).
32. P. L. Bergsagel *et al.*, *Blood.* **106**, 296 (2005).
33. H. Chang *et al.*, *Leuk Res.* **30**, 262 (2006).
34. E. M. Hurt *et al.*, *Cancer Cell.* **5**, 191 (2004).
35. E. van Stralen *et al.*, *Exp Hematol.* **37**, 78 (2009).
36. M. Chesi *et al.*, *Blood.* **91**, 4457 (1998).
37. D. R. Ballon *et al.*, *Cell.* **126**, 1079 (2006).
38. A. Yu *et al.*, *Dev Cell.* **12**, 129 (2007).
39. D. R. Carrasco *et al.*, *Cancer Cell.* **9**, 313 (2006).
40. A. Eychene, N. Rocques, C. Pouponnot, *Nat Rev Cancer* **14**, 14 (2008).
41. M. I. Daw *et al.*, *Neuron.* **28**, 873 (2000).
42. N. Fujii *et al.*, *Cancer Res.* **67**, 573 (2007).
43. M. Shapiro-Shelef, K. Calame, *Curr Opin Immunol.* **16**, 226 (2004).
44. A. H. Lee, N. N. Iwakoshi, K. C. Anderson, L. H. Glimcher, *Proc Natl Acad Sci U S A.* **100**, 9946 (2003).
45. S. Meister *et al.*, *Cancer Res.* **67**, 1783 (2007).
46. U. Ozcan *et al.*, *Mol Cell.* **29**, 541 (2008).
47. E. M. Torres *et al.*, *Science.* **317**, 916 (2007).
48. M. P. Stokes *et al.*, *Proc Natl Acad Sci U S A.* **104**, 19855 (2007).
49. D. D. Sarbassov, D. A. Guertin, S. M. Ali, D. M. Sabatini, *Science* **307**, 1098 (Feb 18, 2005).
50. F. Zhan *et al.*, *Blood.* **99**, 1745 (2002).

EXPERIMENTAL PROCEDURES

Materials

Reagents were obtained from the following sources: rabbit polyclonal antibodies to DEPTOR (09-463), raptor (09-217), Akt (05-591), and phospho-S877 raptor (09-107) from Upstate/Millipore; mouse monoclonal antibody to DEPTOR from Novus Biologicals; mouse monoclonal antibodies to rictor and raptor from Assay Designs; antibodies to mTOR, □-catenin, actin, S6K1, c-MAF, as well as HRP-labeled anti-mouse, anti-goat, and anti-rabbit secondary antibodies from Santa Cruz Biotechnology; antibodies to phospho-T389 S6K1, phospho-T37/T46 4E-BP1, phospho-S473 Akt/PKB, phospho-T308-Akt, phospho-T346-NDRG1, phospho-S307-IRS-1, IRS-1, PTEN, TSC2, 4E-BP1, cleaved caspase-3, PARP, PDGFR-β, and the c-MYC epitope from Cell Signaling Technology; antibodies to rictor, HA, c-MYC from Bethyl Laboratories; Flag M2 affinity gel, Flag M2 antibody and SGK1 antibodies, ATP, and SYBR Green JumpStart Taq ReadyMix from Sigma Aldrich; mouse monoclonal antibody to mTOR and recombinant IL-6 from BD Pharmingen; protein G Sepharose and anti-sheep secondary antibody from Pierce; DMEM from SAFC Biosciences; rapamycin from LC Labs; MG-132 from Biomol; PreScission protease from Amersham Biosciences; pTREQ Tet-On vector from Clontech; Adenoviral CRE and GFP from University of Iowa Gene Transfer Vector Core; FuGENE 6 and Complete Protease Cocktail from Roche; 4E-BP1 from A.G. Scientific; SuperScript II Reverse Transcriptase, Platinum Pfx Polymerase, SimplyBlue Coomassie G, Silverquest Staining kit, and inactivated fetal calf serum (IFS) from Invitrogen. An antibody to NDRG1 was kindly provided by Dario Alessi (University of Dundee, UK). We have found that the phospho-S877 raptor antibody also recognizes immunoprecipitated phosphorylated DEPTOR and can be used to read out the DEPTOR phosphorylation state.

Cell Lines and Cell Culture

HEK-293E cells were kindly provided by John Blenis (Harvard Medical School). HeLa, HEK-293E, HEK-293T, HT-29, U87, PC3, MD-MBA-435, and MEFs were cultured in DMEM with 10% Inactivated Fetal Bovine Serum (IFS). The Human Multiple Myeloma cell lines: FR4, XG-7, U266, KMS-12BM, KMS-12PE, PE2, 8226, OCI-MY5, KMS-28BM were provided by the Kuehl lab. The EJM, MM-1S, JJN-3, and Δ47 Human Multiple Myeloma cell lines were kindly provided by Ken Anderson (Dana Farber Cancer Institute). Human Multiple Myeloma cell lines were cultured in RPMI-1640 with 10% Fetal Bovine Serum (FBS) supplemented with 2 mM glutamine. XG-7 cells were additionally supplemented with 2 ng/ml IL-6. TSC2-/-, p53-/- and TSC2+/+, p53-/- MEFs were kindly provided by David Kwitakowski (Harvard Medical School). PTEN LoxP/LoxP MEFs were generated from PTEN LoxP/LoxP mice kindly provided by Hong Wu (UCLA). To produce PTEN -/- and PTEN +/+ MEFs, 1 □l of Adenoviral CRE or Adenoviral GFP at a titer of $1X10^{10}$ PFU/mL was added to 500,000 PTEN LoxP/LoxP MEFs. Cell lysates were generated 5 days post-infection. The HeLa cell line with doxycycline-inducible DEPTOR expression was generated by retroviral transduction of HeLa that were previously modified to express rtTA with an inducible DEPTOR cDNA.

cDNA Manipulations, Mutagenesis, and Sequence Alignments

The cDNA for DEPTOR (NCBI gene symbol: DEPDC6) in the pCMV6-XL4 vector was obtained from Origene. The DEPTOR cDNA was amplified by PCR and the product subcloned into the Sal 1 and Not 1 sites of pRK5, the Xho I and Not I sites of pMSCV, or the BsiWI and BstB I sites of pTREQ. All constructs were verified by DNA sequencing. The DEPTOR cDNA in pRK5 was mutagenized using the QuikChange XLII mutagenesis kit (Stratagene) with oliogonucleotides obtained from Integrated DNA Technologies. NCBI Blosum62 Blast searches were used to identify blocks of similar sequence between DEPTOR orthologues. Amino acid sequence alignment of the phosphorylated region of DEPTOR was performed using ClustalX v1.81.

Mass Spectrometric Analysis

mTOR or FLAG immunoprecipitates prepared from 30 million HEK-293E cells were resolved by SDS-PAGE, Coomassie G-stained, and gel bands were excised and processed as described in (*7*). In 4 independent experiments, a total of 12 peptides corresponding to DEPTOR were identified while no DEPTOR peptides were identified in control purifications.

DEPTOR phosphorylation sites were identified by mass spectrometry of trypsin digested FLAG-DEPTOR purified from HEK-293E or HEK-293T cells stably or transiently over-expressing FLAG-DEPTOR. All putative phosphorylated residues on DEPTOR (highlighted in **BOLD**) were detected on the following peptides (amino acid position according to NCBI DEPDC6 Protein Sequence NP_073620):

234 KSPSSQE**T**HD**S**PFCLR 249

257 K**ST**SFM**S**V**S**PSK 268

278 RSSM**SS**CGS**S**GYFSS**S**PTL**SSS**PPVLCNPK 311

Label-free quantification of DEPTOR phosphorylation sites were performed using BioWorks Rev3.3 software following methodology utilized in (*48*).

Mammalian Lentiviral shRNAs

Lentiviral shRNAs to human raptor, rictor, and mTOR were previously described (*49*). All other shRNAs were obtained from the collection of The RNAi Consortium (TRC) at the Broad Institute (Moffat et al., 2006). These shRNAs are named with the numbers found at the TRC public website: (http://www.broad.mit.edu/genome_bio/trc/publicSearchForHairpinsForm.php)

Human DEPTOR_1 shRNA: TRC candidate; NM_022783.1-877s1c1

Human DEPTOR_2 shRNA: TRC candidate; NM_022783.1-1101s1c1

Human TSC2_1 shRNA: TRCN0000040178; NM_000548.2-4551s1c1

Human PTEN_1 shRNA: TRCN0000002746; NM_000314.x-1320s1c1

Mouse DEPTOR_1 shRNA: TRCN0000110157; NM_145470.1-1164s1c1

Mouse DEPTOR_2 shRNA: TRCN0000110159; NM_145470.1-1165s1c1

Mouse TSC2_1 shRNA: TRCN0000042727; NM_011647.1-1843s1c1
Human SGK1_1 shRNA: TRCN0000040175; NM_005627.2-964s1c1
Human SGK1_2 shRNA: TRCN0000040176; NM_005627.2-252s1c1
Human c-MAF_1 shRNA: TRCN0000000255; NM_005360.x-1839s1c1
Human c-MAF_2 shRNA: TRCN0000000257; NM_005360.x-1067s1c1

shRNA-encoding plasmids were co-transfected with the Delta VPR envelope and CMV VSV-G packaging plasmids into actively growing HEK-293T using FuGENE 6 transfection reagent as previously described (*49*). Virus containing supernatants were collected at 48 hours after transfection, filtered to eliminate cells, and target cells (e.g., 300,000 HeLa cells or 500,000 8226 cells) infected in the presence of 8 □g/ml polybrene. For 8226 cells, infected cells were spun at 300g for 1.5 hours before incubating at 37°C for 24 hours. For all cell types, 24 hours after infection, the cells were split into fresh media (e.g., DMEM/10%IFS for HeLa/MEFs; RPMI/10%FBS for 8226/OCI-MY5), selected with 1 □g/ml puromycin. Five days post-infection, shRNA-expressing cells were analyzed or split again and analyzed 2-3 days later. For adherent cell lines, shRNA-expressing cells were analyzed at 50-75% confluence.

Cell Lysis and Immunoprecipitations

All cells were rinsed with ice-cold PBS before lysis. All cells, with the exception of those used to isolate mTOR-containing complexes, were lysed with Triton-X 100 containing lysis buffer (40 mM HEPES [pH 7.4], 2 mM EDTA, 10 mM sodium pyrophosphate, 10 mM sodium glycerophosphate, 150 mM NaCl, 50 mM NaF, 1% Triton-X 100, and one tablet of EDTA-free protease inhibitors [Roche] per 25 ml). The soluble fractions of cell lysates were isolated by centrifugation at 13,000 rpm for 10 min in a microcentrifuge. For immunoprecipitations, primary antibodies were added to the lysates and incubated with rotation for 1.5 hr at 4°C. A 50% slurry of protein G Sepharose (60 µl) was then added, and the incubation continued for an additional 1 hr. Immunoprecipitated proteins were denatured by the addition of 20 µl of sample

buffer and boiling for 5 min, resolved by 4%–12% SDS-PAGE, and analyzed by immunoblotting as described (Kim et al., 2002). To observe gel mobility shifting in DEPTOR, 8% Tris Glycine gels (Invitrogen) were used. For all other applications, 4-12% Bis-Tris gels (Invitrogen) were used. For immunoprecipitations of mTOR containing complexes, cells were lysed in ice-cold CHAPS-containing lysis buffer lacking added NaCl (40 mM HEPES [pH 7.4], 2 mM EDTA, 10 mM pyrophosphate, 10 mM glycerophosphate, 0.3% CHAPS, and one tablet of EDTA-free protease inhibitors [Roche] per 25 ml). Immunoprecipitates were washed once each in the CHAPS lysis buffer and twice with CHAPS lysis buffer containing 150 mM NaCl such that the immunopurified material would be rinsed in a solution with a phyisiologically-relevant salt concentration. When specified, the latter two washes contained 0 mM or 500 mM NaCl.

In Vitro Kinase Assay For mTORC1 and mTORC2 Activities

For kinase assays, immunoprecipitates were washed once in CHAPS lysis buffer followed by two additional washes in CHAPS lysis buffer containing 150 mM NaCl. Immunoprecipitates were then washed twice in 25 mM HEPES (pH 7.4), 20 mM KCl. Kinase assays were performed as described (7).

cDNA Transfection-based Experiments

To examine the effects on mTOR signaling of DEPTOR overexpression, 500,000 HeLa; 300,000 p53-/- or rictor -/-, p53-/-; or 200,000 TSC2-/-, p53-/- regularly passaged (every 2-3 days) cells were plated in 6 cm culture dishes in DMEM/10%IFS. 12 hours later, cells were transfected with the pRK5-based cDNA expression plasmids indicated in the figures in the following amounts: 2 □g for all FLAG tagged cDNAs and 200 ng of HA-GST S6k1 or Akt1. All cells were lysed at 50-75% confluence 24 hours after transfection.

Gene Expression and Mutation Analysis in Human Cancers and Cancer Cell Lines

For quantification of DEPTOR, Integrin β7, and GAPDH mRNA expression in HeLa, PC3, or 8226 cell lines, total RNA was isolated from cells grown in the indicated conditions and reverse-transcription was performed. The resulting cDNA was diluted in DNase-free water (1:25) before quantification by real-time PCR. mRNA transcript levels were measured using Applied Biosystems 7900HT Sequence Detection System v2.3 software. Data are expressed as the ratio between the expression of DEPTOR or Integrin β7 and the housekeeping gene GAPDH. The following primers were used for quantitative real-time PCR:
DEPTOR (H. sapiens):
Forward: TTTGTGGTGCGAGGAAGTAA
Reverse: CATTGCTTTGTGTCATTCTGG
GAPDH (H. sapiens):
Forward: CTCTCTGCTCCTCCTGTTCGAC
Reverse: TGAGCGATGTGGCTCGGCT
Integrin β7 (H. sapiens):
Forward: TGGAGCGCTGCCAGTCACCATT
Reverse: CGTCTGAAGTGAACACCAGCAGC

For meta-analysis of DEPTOR mRNA expression in human cancers, "DEPDC6" was searched in NCBI GEO and Oncomine gene expression data repositories. Only those studies where data from primary human tumors could be compared with matched unaffected tissue were considered further. Fold change in DEPTOR mRNA was measured by taking the quotient of the mean level of DEPTOR mRNA in unaffected tissue versus that of the tumor sample. Statistical significance was measured by one-tailed, unequal variance T test. Only those studies with $p<0.05$ were included in the final analysis.

RNA isolation from primary Multiple Myelomas has been described (*50*). Normalized DEPTOR mRNA expression was clustered according to the translocation/Cyclin D groups classified in (*32*). The Multiple Myeloma gene expression data used in this study was generated on an Affymetrix U133_Plus_2 platform and can be found in its entirety in the NCBI GEO database with the

following identifiers: GSE2658 for 559 newly diagnosed, untreated tumors and GSE5900 for 22 normal plasma cells, 12 smoldering myeloma, and 44 MGUS. Human Myeloma cell line mRNA data have been deposited in an MMRC genomics portal website that is sponsored by the MMRF (www.broad.mit.edu/mmgp).

PTEN mutation status in human cancer cell lines can be found at the following URL: http://www.sanger.ac.uk/genetics/CGP/CellLines/.

Live Cell Imaging

8226 cells grown in 12 well dishes were imaged at 20x magnification using a Canon Powershot 5 Megapixel digital camera.

ACKNOWLEDGEMENTS

The authors thank Thijn Brummelkamp for reviewing the manuscript and the following for technical assistance: Leslie Brents, Stephen Carr, Jake Jaffe, Xana Frias, Heather Keys, Stephanie Kinkel, Doug McMillin, Jan Reiling, Eric Spooner, Ed Van Veen, and Marcel Van Vugt. We thank members of the Sabatini lab for helpful discussions. This work was supported by grants from the National Institutes of Health (R01 AI47389 and R01 CA103866) to D.M.S.; awards from the Keck Foundation and LAM Foundation to D.M.S.; a fellowship from the American Diabetes Association to T.R.P.; a fellowship from the Canadian Institutes of Health Research to M.L.; and a fellowship from the American Cancer Society to S.A.K. N.S.G. is funded in part by the Dana Farber Cancer Institute High-Tech Research Fund. D.M.S. is an investigator of the Howard Hughes Medical Institute. None of the authors have a conflict of interest related to the work reported in this manuscript.

Chapter 4

The Rag GTPases Bind Raptor and Mediate Amino Acid Signaling to mTORC1

Reprinted from Science Magazine:

Yasemin Sancak [1], Timothy R. Peterson [1], Yoav D. Shaul [1], Robert A. Lindquist [1], Carson C. Thoreen [1], Liron Bar-Peled [2], David M. Sabatini [3].
The Rag GTPases Bind Raptor and Mediate Amino Acid Signaling to mTORC1. *Science.* 2008 Jun 13;320(5882):1496-501.

[1] Whitehead Institute for Biomedical Research and Massachusetts Institute of Technology Department of Biology, Nine Cambridge Center, Cambridge, MA 02142, USA.; MIT Center for Cancer Research, 77 Massachusetts Avenue, Cambridge, MA 02139, USA.
[2] Whitehead Institute for Biomedical Research and Massachusetts Institute of Technology Department of Biology, Nine Cambridge Center, Cambridge, MA 02142, USA.
[3] Whitehead Institute for Biomedical Research and Massachusetts Institute of Technology Department of Biology, Nine Cambridge Center, Cambridge, MA 02142, USA.; MIT Center for Cancer Research, 77 Massachusetts Avenue, Cambridge, MA 02139, USA.; Broad Institute, Seven Cambridge Center, Cambridge, MA 02142, USA.

Experiments in Figure 1 were performed by Y.S.
Experiments in Figure 2 were performed by Y.S.
Experiments in Figure 3A, 3B, 3C, 3D, 3E, 3F, 3G were performed by Y.S.
Experiments in Figure 3H were performed by R.L.
Experiments in Figure 4 were performed by T.R.P
Experiments in Figure 5 were performed by T.R.P

Summary

The multiprotein mTORC1 protein kinase complex is the central component of a pathway that promotes growth in response to insulin, energy levels, and amino acids, and is deregulated in common cancers. We find that the Ragproteins—a family of four related small guanosine triphosphatases (GTPases)—interact with mTORC1 in an amino acid–sensitive manner and are necessary for the activation of the mTORC1 pathway by amino acids. A Rag mutant that is constitutively bound to GTP interacted strongly with mTORC1, and its expression within cells made themTORC1 pathway resistant to amino acid deprivation. Conversely, expression of a GDP-bound Rag mutant prevented stimulation of mTORC1 by amino acids. The Rag proteins do not directly stimulate the kinase activity of mTORC1, but, like amino acids, promote the intracellular localization of mTOR to a compartment that also contains its activator Rheb.

Introduction

The mTOR complex 1 (mTORC1) branch of the mammalian target of rapamycin (mTOR) pathway is a major driver of cell growth in mammals and is deregulated in many common tumors (*1*). It is also the target of the drug rapamycin, which has generated considerable interest as an anticancer therapy. Diverse signals regulate the mTORC1 pathway, including insulin, hypoxia, mitochondrial function, and glucose and amino acid availability. Many of these are integrated upstream of mTORC1 by the tuberous sclerosis complex (TSC1-TSC2) tumor suppressor, which acts as an important negative regulator of mTORC1 through its role as a guanosine triphosphatase (GTPase)–activating protein (GAP) for Rheb, a small guanosine triphosphate (GTP)–binding protein that potently activates the protein kinase activity of mTORC1 (*2*). Loss of either TSC protein causes hyperactivation of mTORC1 signaling, even in the absence of many of the upstream signals that are normally required to maintain pathway activity. A notable exception is the amino acid supply, as the mTORC1 pathway remains sensitive to amino acid starvation in cells lacking either TSC1 or TSC2 (*3*–*5*).

The mechanisms through which amino acids signal to mTORC1 remain mysterious. It is a reasonable expectation that proteins that signal the availability of amino acids to mTORC1 are also likely to interact with it, but, so far, no good candidates have been identified. Because most mTORC1 purifications rely on antibodies to isolate mTORC1, we wondered if in previous work antibody heavy chains obscured, during SDS–polyacrylamide electrophoresis (SDS-PAGE) analysis of purified material, mTORC1-interacting proteins of 45 to 55 kD. Indeed, using a purification strategythat avoids this complication (*6*), we identified the 44-kD RagC protein as copurifying with overexpressed raptor, the defining component of mTORC1 (*7*–*10*).

RagC is a Ras-related small GTP-binding protein and one of four Rag proteins in mammals (RagA, RagB, RagC, and RagD). RagA and RagB are very similar to each other and are orthologs of budding yeast Gtr1p, whereas RagC and RagD are similar and are orthologs of yeast Gtr2p (*11*–*13*). In yeast and in human cells, the Rag and Gtr proteins function as heterodimers consisting of one Gtr1p-like (RagA or RagB) and one Gtr2p-like (RagC or RagD) component (*14*, *15*). The finding that RagC copurifies with raptor was intriguing to us because, in yeast, Gtr1p and Gtr2p regulatethe

intracellular sorting of the Gap1p amino acid permease (*16*) and microautophagy (*17*), processes modulated by amino acid levels and the TOR pathway (*18*–*20*). The Gtr proteins have been proposed to act downstream or in parallel to TORC1 in yeast because their overexpression induces microautophagy even in the presence of rapamycin, which normally suppresses it (*17*).

Results

To verify our identification of RagC as an mTORC1-interacting protein, we expressed raptor with different pairs of Rag proteins in human embryonic kidney (HEK)-293T cells. Consistent with the Rags functioning as heterodimers, raptor copurified with RagA-C orRagB-C, but not with RagA-B or the Rap2A control protein (Fig. 1A). Because the nucleotide loading state of most GTP-binding proteins regulates their functions, we generated RagB, RagC, and RagD mutants predicted (14, 16, 17) to be restricted to the GTP- or guanosine diphosphate (GDP)–bound conformations (for simplicity, we call these mutants RagBGTP, RagBGDP, etc.) (6). When expressed with mTORC1 components, Rag heterodimers containing RagBGTP immunoprecipitated with more raptor and mTOR than did complexes containing wild-type RagB or RagBGDP (Fig. 1B). The GDP-bound form of RagC increased the amount of copurifying mTORC1, so that RagBGTP-CGDP recovered the highest amount of endogenous mTORC1 of any heterodimer tested (Fig. 1C). Giving an indication of the strength of the mTORC1-RagBGTP-CGDP association, in this same assay, we could not detect coimmunoprecipitation of mTORC1 with Rheb1 (Fig. 1C), an established interactor and activator of mTORC1 (1). When expressed alone, raptor, but not mTOR, associated with RagBGTPDGDP, which suggests that raptor is the key mediator of the Rag-mTORC1 interaction (Fig. 1D). Consistent with this, rictor, an mTOR-interacting protein that is only part of mTORC2 (1), did not copurify with any Rag heterodimer (Fig. 1C and fig. S1). Last, highly purified raptor interacted in vitro with RagB-D and, to a larger extent, with RagBGTP-DGDP, which indicates that the Rag-raptor interaction is most likely direct (Fig. 1E).

We tested whether various Rag heterodimers affected the regulation of the mTORC1 pathway within human cells. In HEK-293T cells, expression of the RagBGTP-

DGDP heterodimer, which interacted strongly with mTORC1, not only activated the pathway, but also made it insensitive to deprivation for leucine or total amino acids, as judged by the phosphorylation state of the mTORC1 substrate T389 of S6K1 (Fig. 2, A and B). The wild-type RagB-C heterodimer had milder effects than RagB-GTPCGDP, making the mTORC1 pathway insensitive to leucine deprivation, but not to the stronger inhibition caused by total amino acid starvation (Fig. 2, A and B). Expression of RagBGDPDGTP, a heterodimer that did not interact with mTORC1 (Fig. 1, C and D), had dominant negative effects, as it eliminated S6K1 phosphorylation in the presence, as well as absence, of leucine or amino acids (Fig. 2, A and B). Expression of RagBGDP alone also suppressed S6K1 phosphorylation (fig. S2). These results suggest that the activity of themTORC1 pathway under normal growth conditions depends on endogenous Rag function.

To verify the actions of the Rags in a more physiological setting than that achieved by transient cDNA transfection, we generated HEK- 293T cell lines stably expressing Rheb1, RagB, or RagBGTP (attempts to generate lines stably expressing RagBGDP failed). Under normal growth conditions, these cells were larger than control cells and had higher levels of mTORC1 pathway activity (Fig. 3A). Unlike transient Rheb1 overexpression (Fig. 2, A and B), stable expression did not make the mTORC1 pathway insensitive to leucine or amino acid starvation (Fig. 3, B and C), consistent with evidence that transiently overexpressed Rheb may have nonphysiological consequences on amino acid signaling to mTORC1 (4, 5). Stable expression of a Rheb1GTP mutant was also unable to make the mTORC1 pathway resistant to amino acid deprivation (fig. S3). In contrast, stable expression of RagBGTP eliminated the sensitivity of the mTORC1 pathway to leucine or total amino acid withdrawal, whereas that of wild-type RagB overcame sensitivity to leucine but not to amino acid starvation (Fig. 3, B and C). Thus, transient or stable expression of the appropriate Rag mutants is sufficient to put the mTORC1 pathway into states that mimic the presence or absence of amino acids.

To determine if the Rag mutants affect signaling to mTORC1 from inputs besides amino acids, we tested whether in RagBGTP-expressing cells themTORC1 pathway

was resistant to other perturbations known to inhibit it. This was not the case, as oxidative stress, mitochondrial inhibition, or energy deprivation still reduced S6K1 phosphorylation in these cells (fig. S4).Moreover, in HEK-293E cells, expression of RagBGTP-DGDP did not maintain mTORC1 pathway activity in the absence of insulin (Fig. 2C). Expression of the dominant-negative RagBGDP-DGTP heterodimer did, however, block insulin-stimulated phosphorylation of S6K1 (Fig. 2C), as did amino acid starvation (Fig. 2D). Thus, although RagBGTP expression mimics amino acid sufficiency, it cannot substitute for other inputs that mTORC1 normally monitors. This evidence for a primary role of the Rag proteins in amino acid signaling to mTORC1 raised the question of where, within the pathway that links amino acids to mTORC1, the Rag proteins might function. The existence of the Rag-mTORC1 interaction (Fig. 1), the effects on amino acid signaling of the Rag mutants (Figs. 2 and 3), and the sensitivity to rapamycin of the S6K1 phosphorylation induced by RagBGTP (fig. S4), strongly suggested that the Rag proteins function downstream of amino acids and upstream of mTORC1. To verify this, we took advantage of the established finding that cycloheximide reactivates mTORC1 signaling in cells starved for amino acids by blocking protein synthesis and thus boosting the levels of the intracellular amino acids sensed by mTORC1 (21–23). Thus, if the Rag proteins act upstream of amino acids, cycloheximide should overcome the inhibitory effects of the RagBGDP-CGTP heterodimer on mTORC1 signaling, but if they are downstream, cycloheximide should not reactivate the pathway. The results were clear: cycloheximide treatment of cells reversed the inhibition of mTORC1 signaling caused by leucine deprivation, but not that caused by expression of RagBGDP-CGTP (fig. S5). Given the place- ment of the Rag proteins downstream of amino acids and upstream of mTORC1, we determined whether amino acids regulate the RagmTORC1 interaction within cells. Initial tests using transiently coexpressed Rag proteins and mTORC1 components did not reveal any regulation of the interaction. Because we reasoned that pronounced overexpression might overcome the normal regulatory mechanisms that operate within the cell, we developed an assay (6), based on a reversible chemical cross-linker, that allows us to detect the interaction of stably expressed FLAG-tagged Rag proteins with endogenous mTORC1. With this approach, we readily found that amino acids, but not

insulin, promote the Rag-mTORC1 interaction when we used either FLAG-tagged RagB or RagD to isolate mTORC1 from cells (Fig. 3D and fig. S6A). As the GTP-loading state of the Rag proteins also regulates the Rag-mTORC1 interaction (Fig. 1), we determined whether amino acids modulate the amount of GTP bound to RagB. Indeed, amino acid stimulation of cells increased the GTP loading of RagB (Fig. 3E). Consistent with this, amino acids did not further augment the already high level of interaction between mTORC1 and the RagBGTP mutant (Fig. 3D).

To determine whether the Rag proteins are necessary for amino acids to activate them TORC1 pathway, we used combinations of lentivirally delivered short hairpin RNAs (shRNAs) to suppress RagA and RagB or RagC and RagD at the same time. Loss of RagA and RagB also led to the loss of RagC and RagD and vice versa, which suggests that, within cells, the Rag proteins are unstable when not in heterodimers (Fig. 3F). In cells with a reduction in the expression of all the Rag proteins, leucine stimulated phosphorylation of S6K1 was strongly reduced (Fig. 3G). The role of the Rag proteins appears to be conserved in Drosophila cells as double-stranded RNA–mediated suppression of the Drosophila orthologs of RagB or RagC eliminated amino acid–induced phosphorylation of dS6K (Fig. 3H). Consistent with amino acids being necessary for activation of mTORC1 by insulin, a reduction in Rag expression also suppressed insulin-stimulated phosphorylation of S6K1 (fig. S6B). Thus, the Rag proteins appear to be both necessary and sufficient for mediating amino acid signaling to mTORC1.

Unlike Rheb (24, 25), the Rag heterodimers did not directly stimulate the kinase activity of mTORC1 in vitro (fig. S7), so we considered the possibility that the Rag proteins regulate the intracellular localization of mTOR. mTOR is found on the endomembrane system of the cell, including the endoplasmic reticulum, Golgi apparatus, and endosomes (26, 27). The intracellular localization of endogenous mTOR, as revealed with an antibody that we validated recognizes mTOR in immunofluorescence assays (fig. S8), was strikingly different in cells deprived of amino acids than in cells starved and briefly restimulated with amino acids (Fig. 4A and fig. S11) or growing in fresh complete media (fig. S9). In starved cells, mTOR was in tiny

puncta throughout the cytoplasm, whereas in cells stimulated with amino acids for as little as 3 min, mTOR localize to the perinuclear region of the cell, to large vesicular structures, or to both (Fig. 4A). Rapamycin did not block the change in mTOR localization induced by amino acids (Fig. 4A), which indicated that it is not a consequence of mTORC1 activity but rather may be one of the mechanisms that underlies mTORC1 activation. The amino acid–induced change in mTOR localization required expression of the Rag proteins and of raptor (Fig. 4, B and C), and amino acids also regulated the localization of raptor (fig. S10).

In cells overexpressing RagB, Rheb1, or Rheb1GTP, mTOR behaved as in control cells, its localization changing upon amino acid stimulation from small puncta to the perinuclear region and vesicular structures (Fig. 4D). In contrast, in cells overexpressing the RagBGTP mutant that eliminates the amino acid sensitivity of the mTORC1 pathway, mTOR was already present on the perinuclear and vesicular structures in the absence of amino acids, and became even more localized to them upon the addition of amino acids (Fig. 4D). Thus, there is a correlation, under amino acid–starvation conditions, between the activity of the mTORC1 pathway and the subcellular localization of mTOR, which implies a role for Rag-mediated mTOR translocation in the activation of mTORC1 in response to amino acids.

We failed to find an established marker of the endomembrane system that colocalized with mTOR in amino acid–starved cells. However, in cells stimulated with amino acids, mTOR in the perinuclear region and on the large vesicular structures overlapped with Rab7 (Fig. 5A), which indicated that a substantial fraction of mTOR translocated to the late endosomal and lysosomal compartments in amino acid–replete cells. In cells expressing RagBGTP, mTOR was present on the Rab7-positive structures even in the absence of amino acids (Fig. 5B). The perinuclear region and vesicular structures on which mTOR appears after amino acid stimulation are similar to the Rab7-positive structures where green fluorescent protein (GFP)– tagged Rheb localizes in human cells (28, 29). Unlike mTOR, however, amino acids did not appreciably affect the localization of Rheb, as GFP-Rheb1 colocalized with Discosoma red fluorescent protein (DsRed)–labeled Rab7 (DsRed- Rab7) in the presence or absence of amino acids (Fig. 5C). Unfortunately, it is currently not possible to compare, in the same cells, the

localization of endogenous mTOR with that of Rheb, because the signal for GFP-Rheb or endogenous Rheb is lost after fixed cells are permeabilized to allow access to intracellular antigens (28, 29). Nevertheless, given that both mTOR and Rheb are present in Rab7-positive structures after amino acid stimulation, we propose that amino acids might control the activity of the mTORC1 pathway by regulating, through the Rag proteins, the movement of mTORC1 to the same intracellular compartment that contains its activator Rheb (see model in Fig. 5D). This would explain why activators of Rheb, like insulin, do not stimulate the mTORC1 pathway when cells are deprived of amino acids and why Rheb is necessary for amino acid–dependent mTORC1 activation (4) (fig. S12). When Rheb is highly overexpressed, some might become mislocalized and inappropriately encounter and activate mTORC1, which could explain why Rheb overexpression, but not loss of TSC1 or TSC2, makes the mTORC1 pathway insensitive to amino acids (4, 5).

Discussion

In conclusion, the Rag GTPases bind raptor, are necessary and sufficient to mediate amino acid signaling to mTORC1, and mediate the amino acid–induced relocalization of mTOR within the endomembrane system of the cell. Given the prevalence of cancer-linked mutations in the pathways that control mTORC1 (1), it is possible that Rag function is also deregulated in human tumors.

Figure legends

Fig. 1. Interaction of Rag heterodimers with recombinant and endogenous mTORC1 in a manner that depends on the nucleotide binding state of RagB. In (**A**) through (**D**) HEK-293T cells were transfected with the indicated cDNAs in expression vectors, cell lysates were prepared, and lysates and hemagglutinin (HA)– or FLAG-tagged immunoprecipitates were analyzed by immunoblotting for the amounts of the specified recombinant or endogenous proteins. (**E**) In vitro binding of purified FLAG-raptor with wild-type RagB-D or $RagB^{GTP}$-D^{GDP}.

Fig. 2. Effects of overexpressed $RagB^{GTP}$-containing heterodimers on the mTORC1 pathway and its response to leucine, amino acids, or insulin. Effects of expressing the indicated proteins on the phosphorylation state of coexpressed S6K1 in response to deprivation and stimulation with (**A**) leucine, (**B**) total amino acids, or (**C**) insulin. Cell lysates were prepared from HEK-293T cells deprived for 50 min of serum and of (A) leucine or (B) amino acids and, then, where indicated, stimulated with leucine or amino acids for 10 min. HEK-293E cells (C) were deprived of serum for 50 min and, where indicated, stimulated with 150 nM insulin for 10 min. Lysates and FLAG-immunoprecipitates were analyzed for the levels of the specified proteins and the phosphorylation state of S6K1. (**D**) Effects of amino acid deprivation on insulin-mediated activation of mTORC1. HEK-293E cells were starved for serum and amino acids or just serum for 50 min, and where specified, stimulated with 10 or 150 nM insulin. Cell lysates were analyzed for the level and phosphorylation state of S6K1.

Fig. 3. Insensitivity of the mTORC1 pathway to amino acid deprivation in cells stably expressing $RagB^{GTP}$. (**A**) Cell size distributions (graphs) and S6K1 phosphorylation (immunoblot) of cells stably expressing RagB, Rheb1, Rag^{GTP}, or Rap2A. Mean cell diameters (μm) ± SD are Rap2A, 16.05 ± 0.07; Rheb1, 16.79 ± 0.06; RagB, 16.40 ± 0.08; and $RagB^{GTP}$, 16.68 ± 0.06 ($n = 4$ and $P < 0.0008$ for all comparisons to Rap2A-expressing cells). HEK-293T cells transduced with lentiviruses encoding the specified proteins were deprived for 50 min for serum and (**B**) leucine or (**C**) total amino acids,

and, where indicated, restimulated with leucine or amino acids for 10 min. Cell lysates were analyzed for the levels of the specified proteins and the phosphorylation state of S6K1. (**D**) Amino acid–stimulated interaction of the Rag proteins with mTORC1. HEK-293T cells stably expressing FLAG-tagged RagB, RagD, or $RagB^{GTP}$ were starved for amino acids and serum for 50 min and, where indicated, restimulated with amino acids for 10 min. Cells were then processed with a chemical cross-linking assay, and cell lysates and FLAG immunoprecipitates were analyzed for the amounts of the indicated proteins. (**E**) Effects of amino acid stimulation on GTP loading of RagB. Values are means ± SD for $n = 3$ ($P < 0.02$ for increase in GTP loading caused by amino acid stimulation). (**F**) Abundance of RagA, RagB, RagC, and RagD in HeLa cells expressing the indicated shRNAs. (**G**) S6K1 phosphorylation in HeLa cells expressing shRNAs targeting RagC and RagD. Cells were deprived of serum and leucine for 50 min, and, where indicated, were restimulated with leucine for 10 min. (**H**) Effects of double-stranded RNA (dsRNA)–mediated knockdowns of *Drosophila* orthologs of RagB or RagC on amino acid–induced phosphorylation of dS6K.

Fig. 4. Rag-dependent regulation by amino acids of the intracellular localization of mTOR. (**A**) HEK-293T cells were starved for serum and amino acids for 50 min or starved and then restimulated with amino acids for the indicated times in the presence or absence of rapamycin. Cells were then processed in an immunofluorescence assay to detect mTOR (green), costained with 4',6'-diamidino-2-phenylindole (DAPI) for DNA content (blue), and imaged. Of these cells, 80 to 90% exhibited the mTOR localization pattern shown. (**B**) and (**C**) mTOR localization in HEK-293T cells expressing the indicated shRNAs and deprived and restimulated with amino acids as in (A). Immunoblot of raptor expression levels. (**D**) mTOR localization in HEK-293T cells stably expressing RagB, Rheb1, $RagB^{GTP}$, or $Rheb1^{GTP}$ and deprived and restimulated with amino acids as in (A).

Fig. 5. Amino acids promote the localization of mTOR to a Rab7-positive compartment that also contains Rheb. (**A**) mTOR and Rab7 localization in cells deprived or stimulated with amino acids. HEK-293T cells transiently transfected with a cDNA for DsRed-Rab7

were starved for serum and amino acids for 50 min and, where indicated, stimulated with amino acids for 10 min. Cells were then processed to detect mTOR (green), Rab7 (red), and DNA content (blue), and imaged. Two examples are shown of mTOR localization in the presence of amino acids. (**B**) HEK-293T cells stably expressing $RagB^{GTP}$ and transiently transfected with a cDNA for DsRed-Rab7 were treated and processed as in (A). (**C**) Rheb1 and Rab7 localization in cells deprived or stimulated with amino acids. HEK-293T cells transiently transfected with 1 to 2 ng of cDNAs for GFP-Rheb1 and DsRed-Rab7 were treated as in (A), processed to detect Rheb1 (green), Rab7 (red), and DNA content (blue), and imaged. (**D**) Model for role of Rag GTPases in signaling amino acid availability to mTORC1.

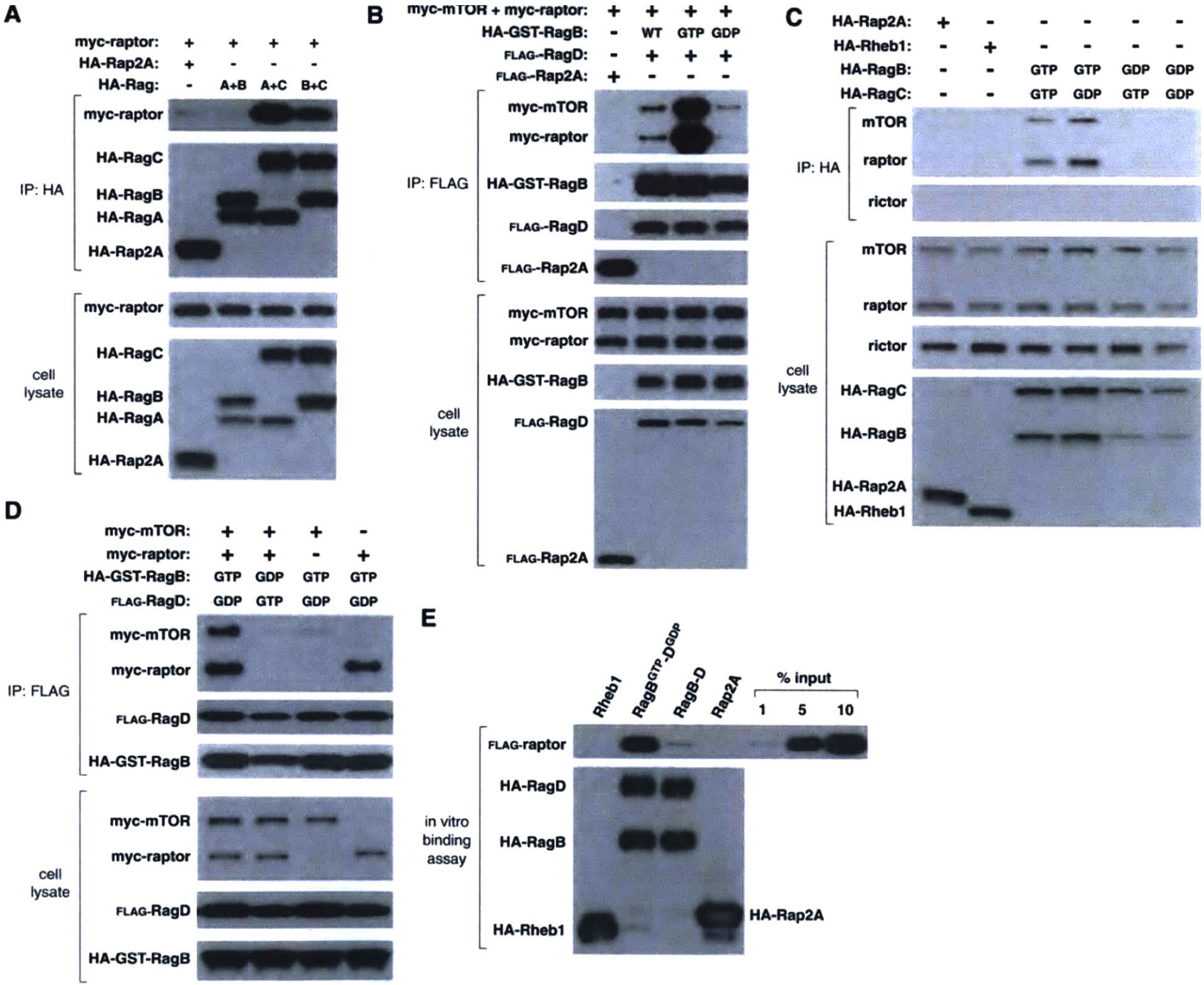
A
myc-raptor: + + + +
HA-Rap2A: + - - -
HA-Rag: - A+B A+C B+C
IP: HA
myc-raptor
HA-RagC
HA-RagB
HA-RagA
HA-Rap2A
cell lysate
myc-raptor
HA-RagC
HA-RagB
HA-RagA
HA-Rap2A
B
myc-mTOR + myc-raptor: + + + +
HA-GST-RagB: - WT GTP GDP
FLAG-RagD: - + + +
FLAG-Rap2A: + - - -
IP: FLAG
myc-mTOR
myc-raptor
HA-GST-RagB
FLAG-RagD
FLAG-Rap2A
cell lysate
myc-mTOR
myc-raptor
HA-GST-RagB
FLAG-RagD
FLAG-Rap2A
C
HA-Rap2A: + - - - - -
HA-Rheb1: - + - - - -
HA-RagB: - - GTP GTP GDP GDP
HA-RagC: - - GTP GDP GTP GDP
IP: HA
mTOR
raptor
rictor
cell lysate
mTOR
raptor
rictor
HA-RagC
HA-RagB
HA-Rap2A
HA-Rheb1
D
myc-mTOR: + + + -
myc-raptor: + + - +
HA-GST-RagB: GTP GDP GTP GTP
FLAG-RagD: GDP GTP GDP GDP
IP: FLAG
myc-mTOR
myc-raptor
FLAG-RagD
HA-GST-RagB
cell lysate
myc-mTOR
myc-raptor
FLAG-RagD
HA-GST-RagB
E
Rheb1
RagB GTP-D GDP
RagB-D
Rap2A
% input
1 5 10
FLAG-raptor
in vitro binding assay
HA-RagD
HA-RagB
HA-Rheb1
HA-Rap2A

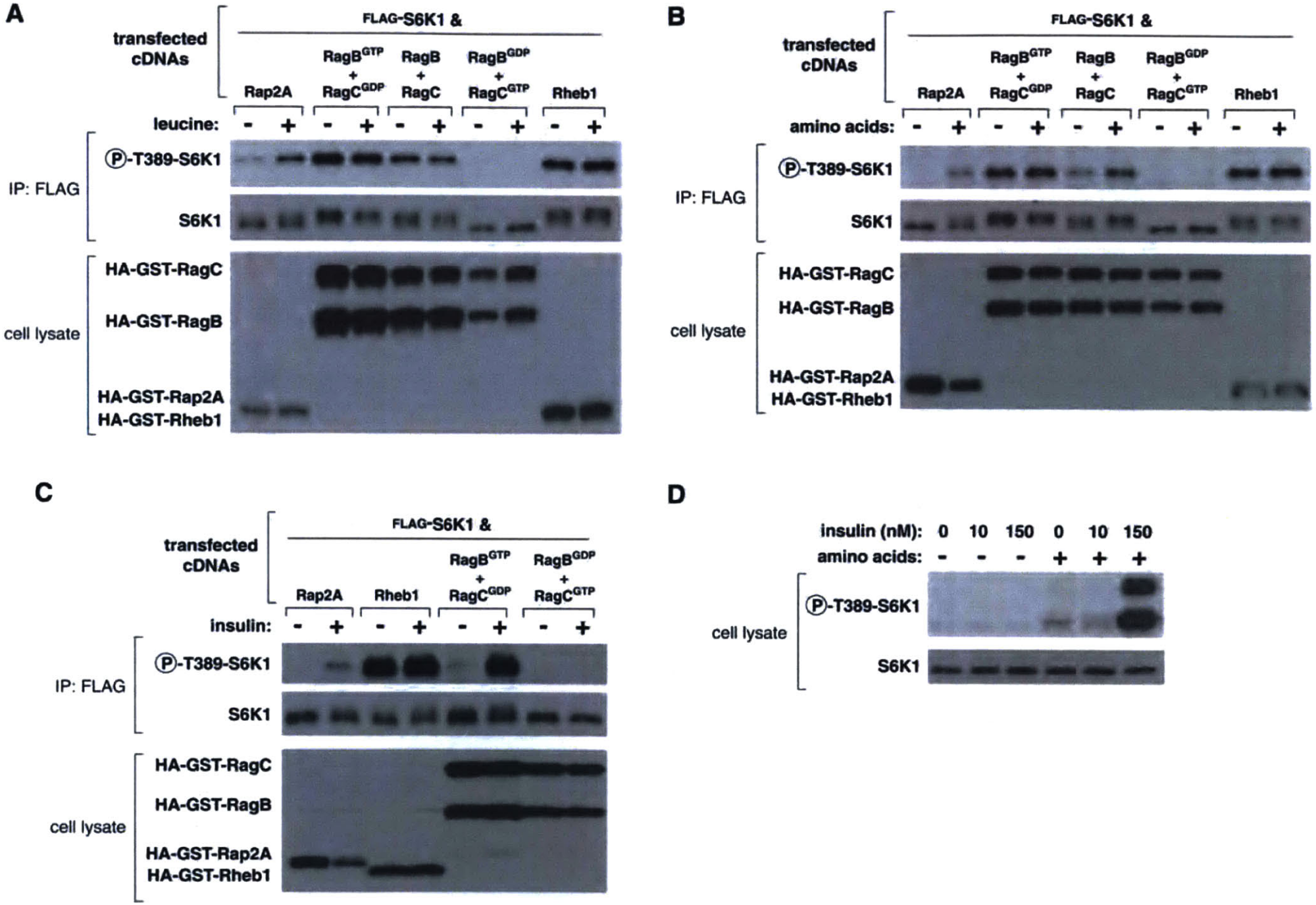
A
transfected cDNAs
FLAG-S6K1 &
Rap2A
RagB^GTP + RagC^GDP
RagB + RagC
RagB^GDP + RagC^GTP
Rheb1
leucine: - + - + - + - + - +
IP: FLAG
Ⓟ-T389-S6K1
S6K1
cell lysate
HA-GST-RagC
HA-GST-RagB
HA-GST-Rap2A
HA-GST-Rheb1
B
transfected cDNAs
FLAG-S6K1 &
Rap2A
RagB^GTP + RagC^GDP
RagB + RagC
RagB^GDP + RagC^GTP
Rheb1
amino acids: - + - + - + - + - +
IP: FLAG
Ⓟ-T389-S6K1
S6K1
cell lysate
HA-GST-RagC
HA-GST-RagB
HA-GST-Rap2A
HA-GST-Rheb1
C
transfected cDNAs
FLAG-S6K1 &
Rap2A
Rheb1
RagB^GTP + RagC^GDP
RagB^GDP + RagC^GTP
insulin: - + - + - + - +
IP: FLAG
Ⓟ-T389-S6K1
S6K1
cell lysate
HA-GST-RagC
HA-GST-RagB
HA-GST-Rap2A
HA-GST-Rheb1
D
insulin (nM): 0 10 150 0 10 150
amino acids: - - - + + +
cell lysate
Ⓟ-T389-S6K1
S6K1

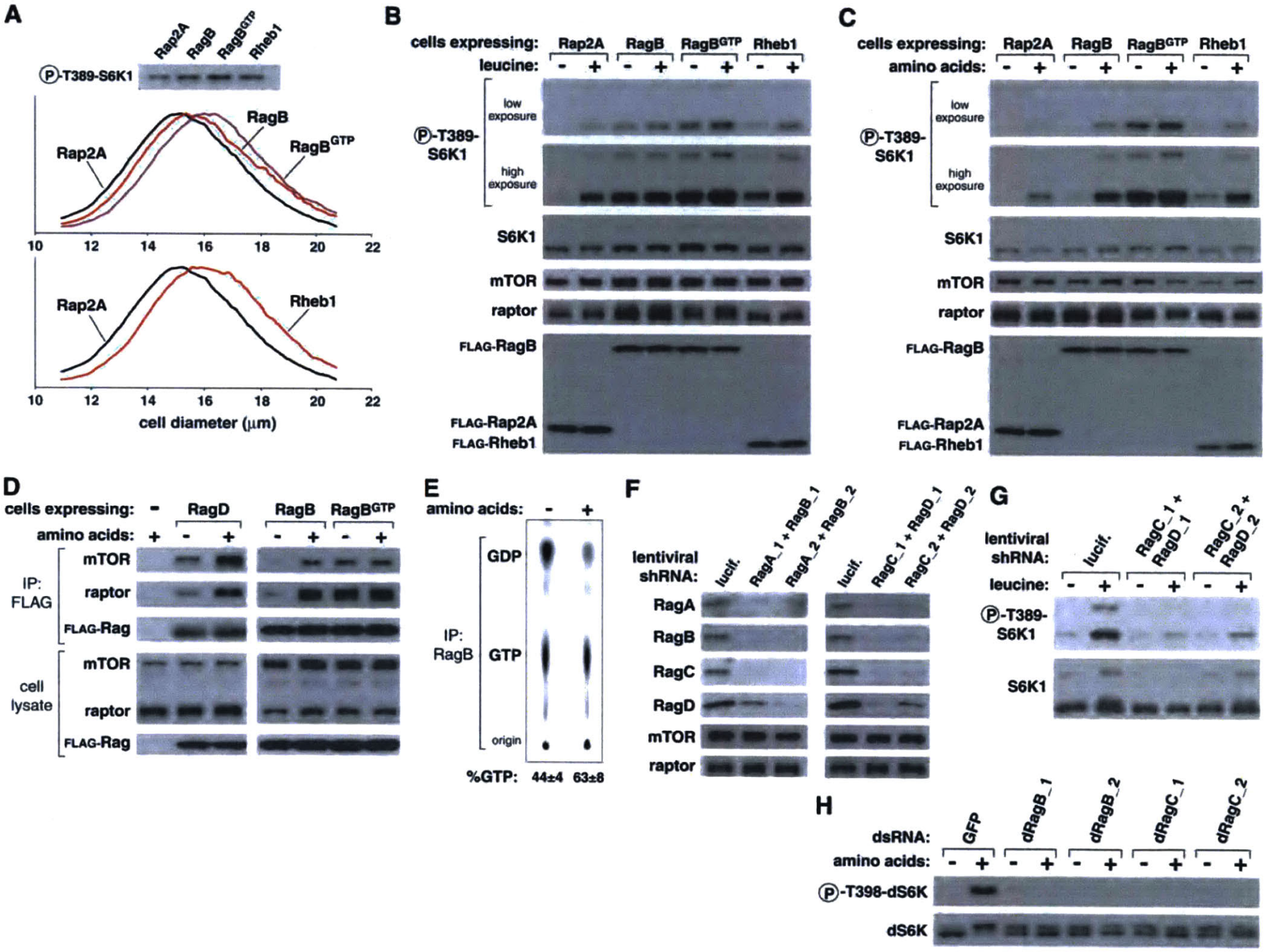
A
Rap2A
RagB
RagBGTP
Rheb1
Ⓟ-T389-S6K1
RagB
RagBGTP
Rap2A
Rheb1
10 12 14 16 18 20 22
cell diameter (μm)
B
cells expressing: Rap2A RagB RagBGTP Rheb1
leucine: - + - + - + - +
Ⓟ-T389-S6K1
low exposure
high exposure
S6K1
mTOR
raptor
FLAG-RagB
FLAG-Rap2A
FLAG-Rheb1
C
cells expressing: Rap2A RagB RagBGTP Rheb1
amino acids: - + - + - + - +
Ⓟ-T389-S6K1
low exposure
high exposure
S6K1
mTOR
raptor
FLAG-RagB
FLAG-Rap2A
FLAG-Rheb1
D
cells expressing: - RagD RagB RagBGTP
amino acids: + - + - + - +
IP: FLAG
mTOR
raptor
FLAG-Rag
cell lysate
mTOR
raptor
FLAG-Rag
E
amino acids: - +
IP: RagB
GDP
GTP
origin
%GTP: 44±4 63±8
F
lentiviral shRNA: lucif. RagA_1 + RagB_1 RagA_2 + RagB_2 lucif. RagC_1 + RagD_1 RagC_2 + RagD_2
RagA
RagB
RagC
RagD
mTOR
raptor
G
lentiviral shRNA: lucif. RagC_1 + RagD_1 RagC_2 + RagD_2
leucine: - + - + - +
Ⓟ-T389-S6K1
S6K1
H
dsRNA: GFP dRagB_1 dRagB_2 dRagC_1 dRagC_2
amino acids: - + - + - + - + - +
Ⓟ-T398-dS6K
dS6K

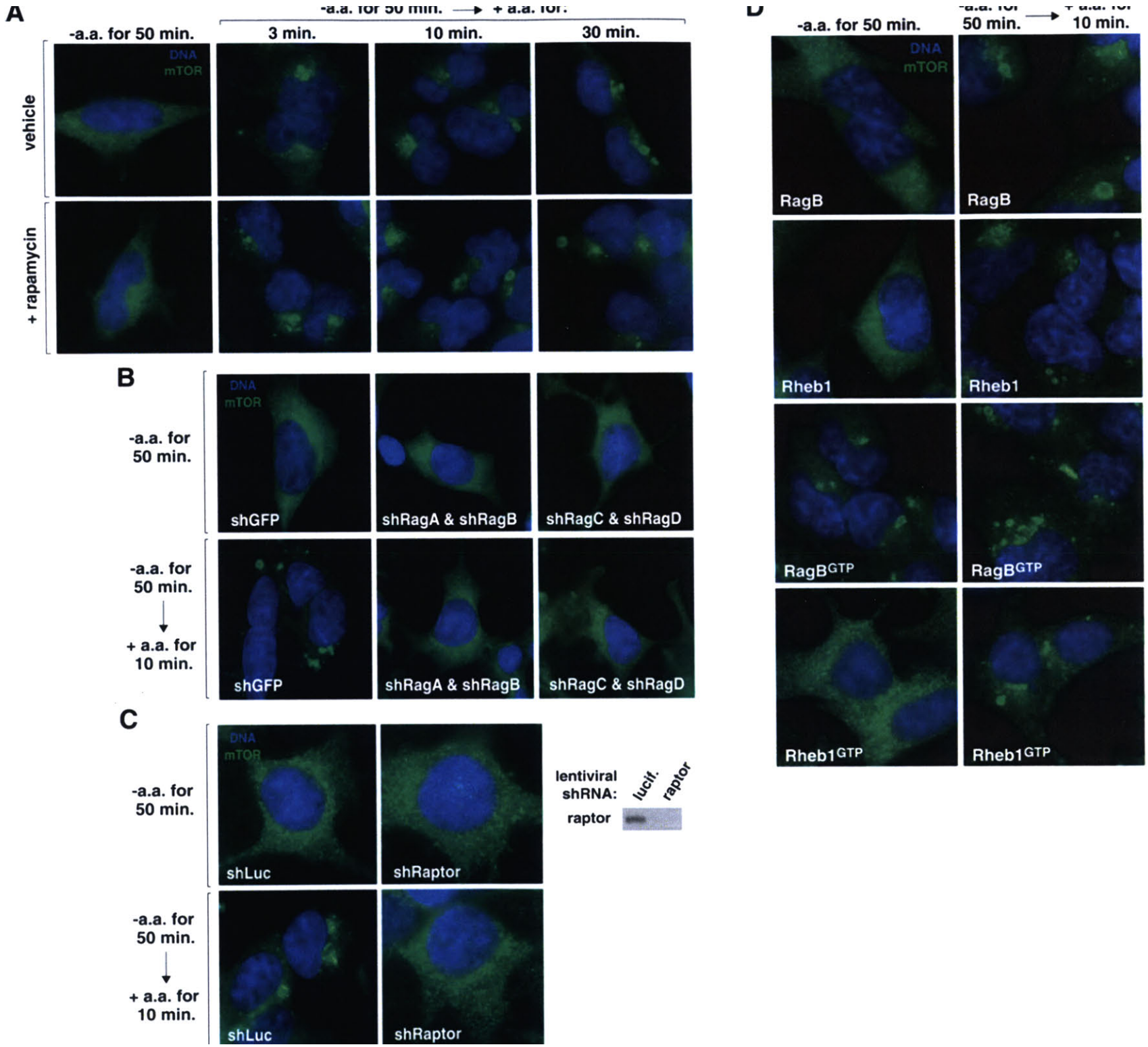
A
-a.a. for 50 min.
+ a.a. for
-a.a. for 50 min.
3 min.
10 min.
30 min.
DNA
mTOR
vehicle
+ rapamycin
B
-a.a. for 50 min.
shGFP
shRagA & shRagB
shRagC & shRagD
-a.a. for 50 min.
+ a.a. for 10 min.
C
-a.a. for 50 min.
shLuc
shRaptor
lentiviral shRNA:
lucif.
raptor
raptor
-a.a. for 50 min.
+ a.a. for 10 min.
D
-a.a. for 50 min.
50 min.
10 min.
RagB
Rheb1
RagB^GTP
Rheb1^GTP

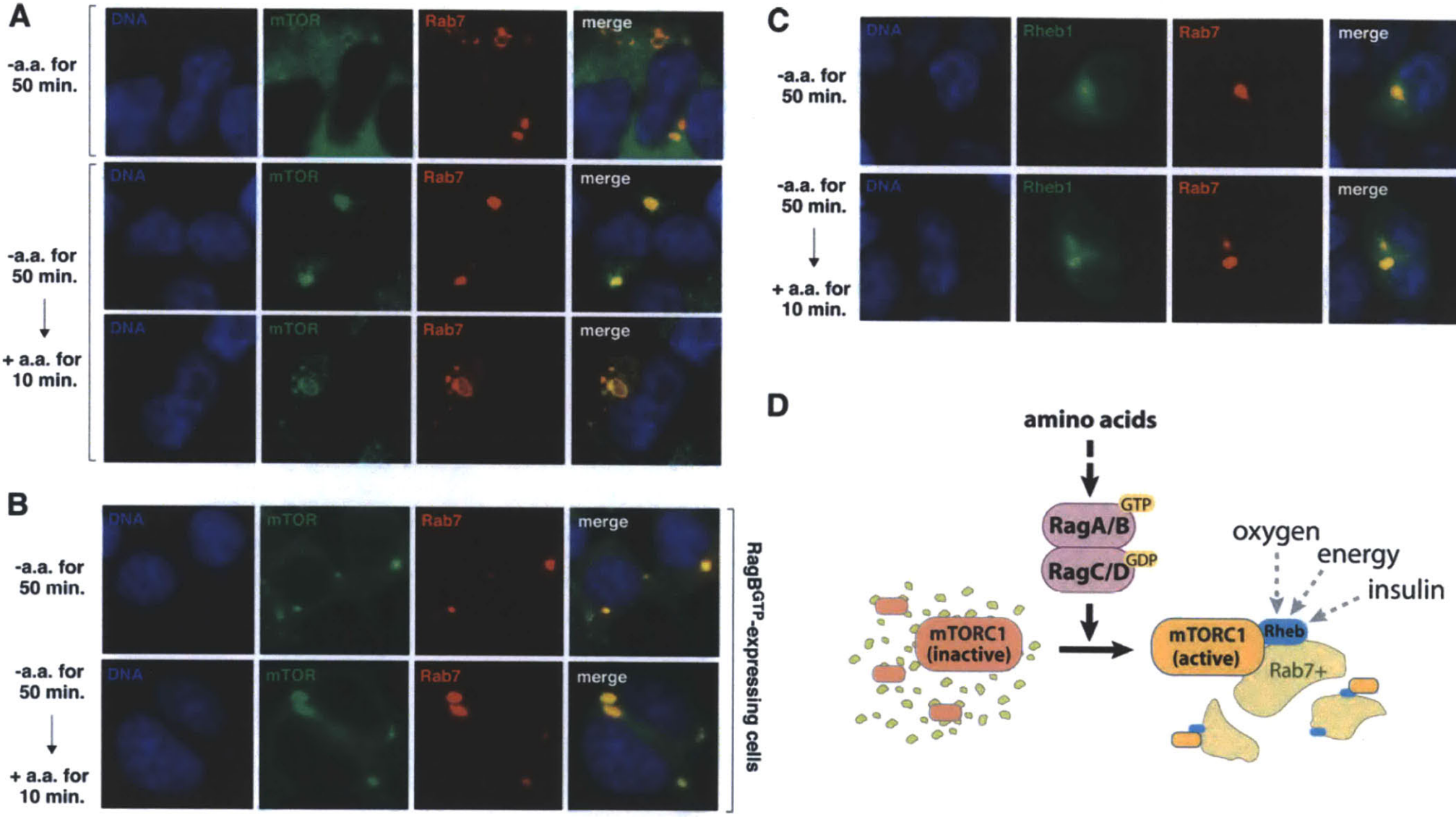
A
-a.a. for 50 min.
-a.a. for 50 min.
+ a.a. for 10 min.
DNA
mTOR
Rab7
merge
B
-a.a. for 50 min.
-a.a. for 50 min.
+ a.a. for 10 min.
RagB^GTP-expressing cells
C
-a.a. for 50 min.
-a.a. for 50 min.
+ a.a. for 10 min.
Rheb1
D
amino acids
RagA/B
GTP
RagC/D
GDP
mTORC1 (inactive)
mTORC1 (active)
oxygen
energy
insulin
Rheb
Rab7+

Figure S1

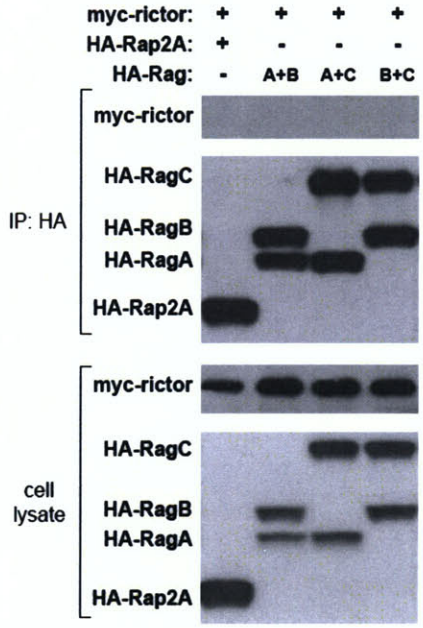

Fig. S1. Rag heterodimers do not interact with rictor. HEK-293T cells were transfected with the indicated cDNAs in expression vectors, cell lysates prepared, and lysates and HA-immunoprecipitates analyzed for the levels of the specified proteins. This experiment was performed side-by-side with that shown in Figure 1A and is displayed here for space reasons.

Figure S2

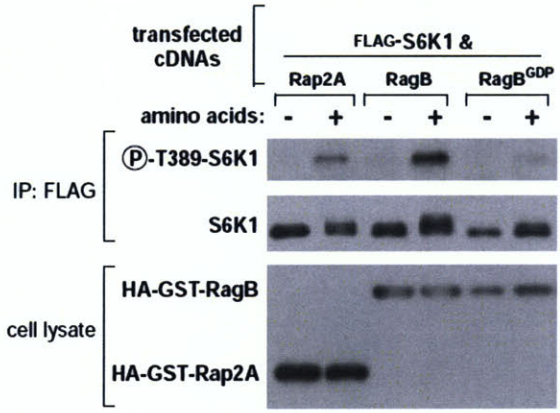

Fig S2. Expression of RagB^{GDP} alone suppresses endogenous mTORC1 signaling. Cell lysates were prepared from HEK-293T cells transfected with the indicated cDNAs and deprived for 50 minutes of serum and amino acids, and where indicated, stimulated with amino acids for 10 minutes. Lysates and FLAG-immunoprecipitates were analyzed for the levels of the specified proteins and the phosphorylation state of S6K1.

Figure S3

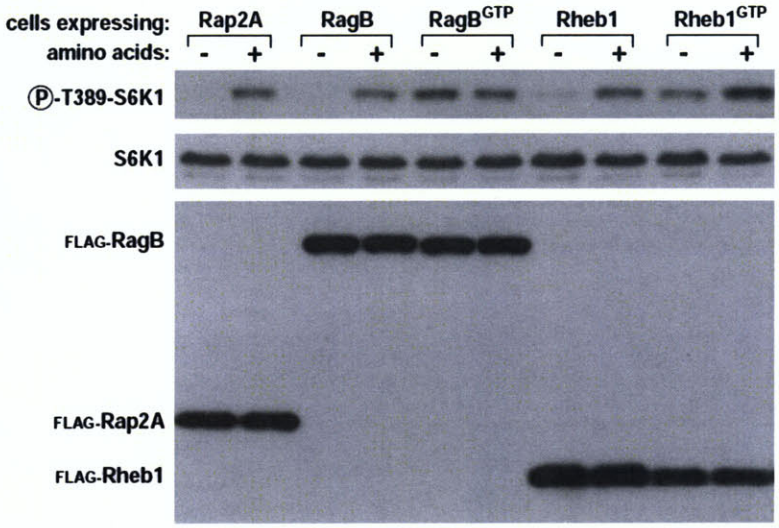

Fig S3. Stable expression of Rheb1 or Rheb1^{GTP} does not eliminate the sensitivity of the mTORC1 to amino acids. HEK-293T cells stably expressing the indicated proteins were deprived of serum and amino acids for 50 minutes, and where indicated, stimulated with amino acids for 10 minutes. Lysates were analyzed for the levels of the specified proteins and the phosphorylation state of S6K1.

Figure S4

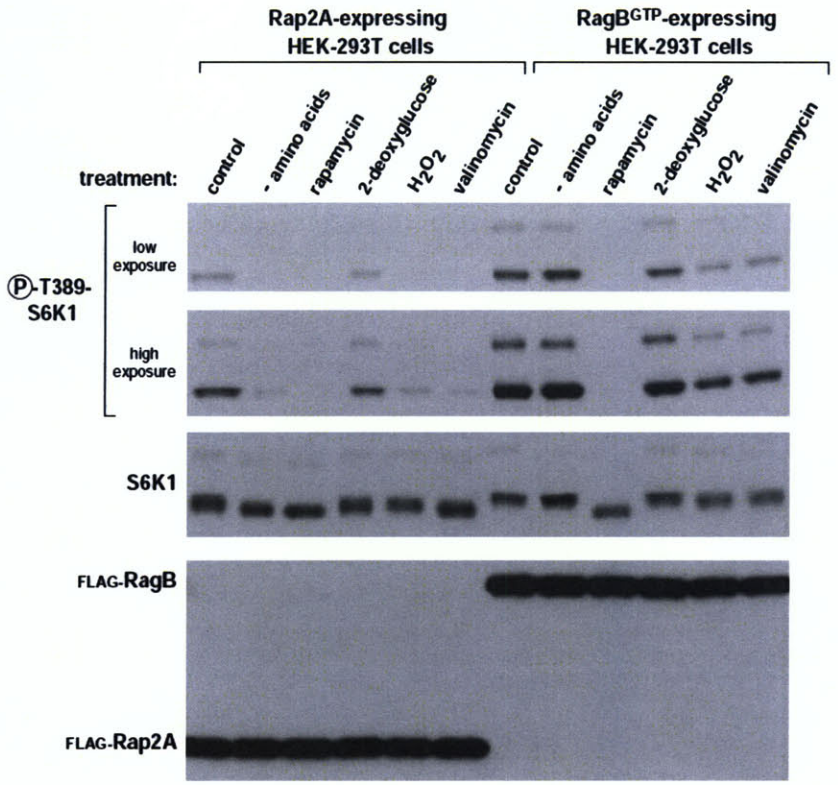

Fig. S4. Effects of various insults on mTORC1 signaling in cells expressing $RagB^{GTP}$. HEK-293T cells stably expressing Rap2A or $RagB^{GTP}$ and growing in full media were untreated (control), or deprived of amino acids for 30 minutes, or treated for 30 minutes with 20 nM rapamycin, 100 mM 2-deoxyglucose (energy deprivation), 1 mM H_2O_2 (oxidative stress), or 1 μM valinomycin (mitochondrial proton gradient inhibition). Cell lysates were prepared and analyzed for the levels of the specified proteins and the phosphorylation state of S6K1.

Figure S5

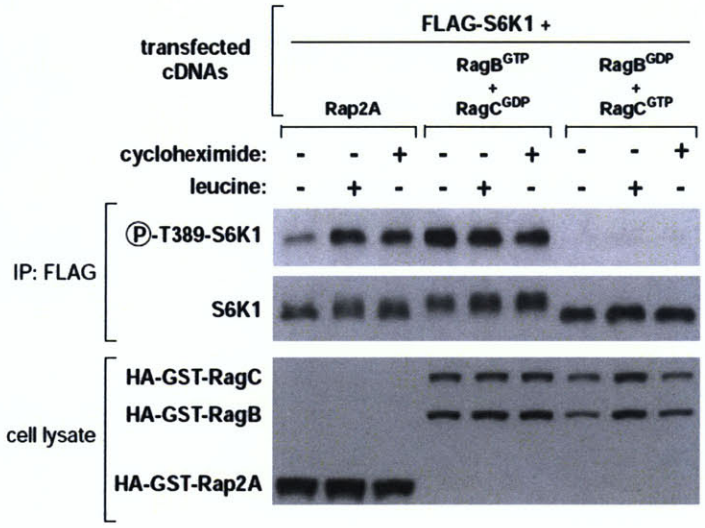

Fig. S5. Inhibition of protein synthesis with cycloheximide does not prevent $RagB^{GDP}$-C^{GTP} from inhibiting the mTORC1 pathway. HEK-293T cells were transfected with the indicated cDNAs in expression vectors, and starved for 50 minutes for serum and leucine, and, where indicated, stimulated with leucine or 10 μg/ml cycloheximide for 20 minutes. Cell lysates and FLAG-immunoprecipitates were analyzed for the levels of the specified proteins and the phosphorylation state of S6K1.

Figure S6

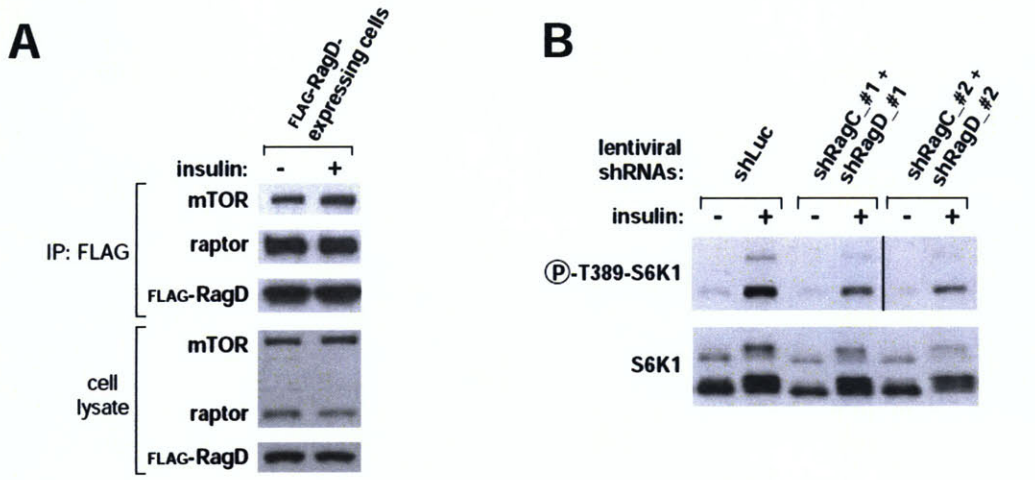

Fig. S6. (A) Insulin does not increase the interaction between mTORC1 and the Rag proteins. Hela cells stably expressing FLAG-RagD were starved for serum for 50 minutes and, where indicated, stimulated with 100 nM insulin for 10 minutes. Cells were then processed with a chemical cross-linking assay and cell lysates and FLAG-immunoprecipitates analyzed for the levels of the indicated proteins. **(B)** Knockdowns of RagC and RagD suppress insulin-stimulated phosphorylation of S6K1. HeLa cells expressing shRNAs targeting RagC and RagD were prepared as in Figure 3. Cells were deprived of serum for 50 minutes, and, where indicated, re-stimulated with 100 nM insulin for 10 minutes. Cell lysates were prepared and analyzed for the levels and phosphorylation state of S6K1.

Figure S7

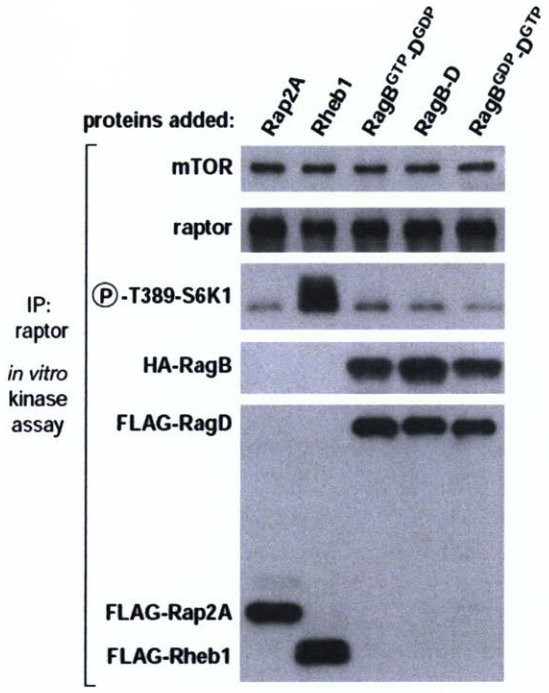

Fig. S7. Rag heterodimers do not activate the in vitro kinase activity of mTORC1 in assays in which Rheb1 does. In vitro kinase assays containing 300 ng of each of the indicated proteins or Rag heterodimers were performed as described in the methods using mTORC1 immunopurified from HEK-293T cells with a raptor antibody. Rap2A, Rheb1, and the Rag heterodimers were expressed in HEK-293T cells and purified under conditions where the endogenous nucleotides remained bound.

Figure S8

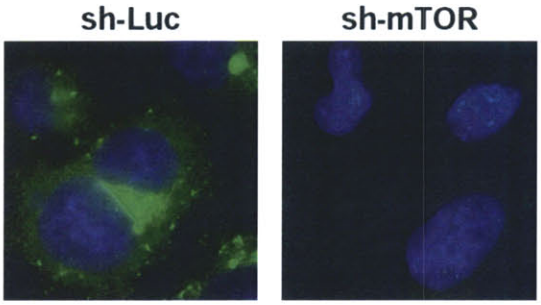

Fig. S8. Validation that an mTOR antibody detects mTOR in an immunofluorescence assay. HEK-293T cells expressing a control shRNA (sh-Luc) or an shRNA targeting mTOR (sh-mTOR) that is known to reduce mTOR expression (see methods) were processed in an immunofluorescence assay with an mTOR antibody (green) and co-stained with DAPI for DNA content (blue).

Figure S9

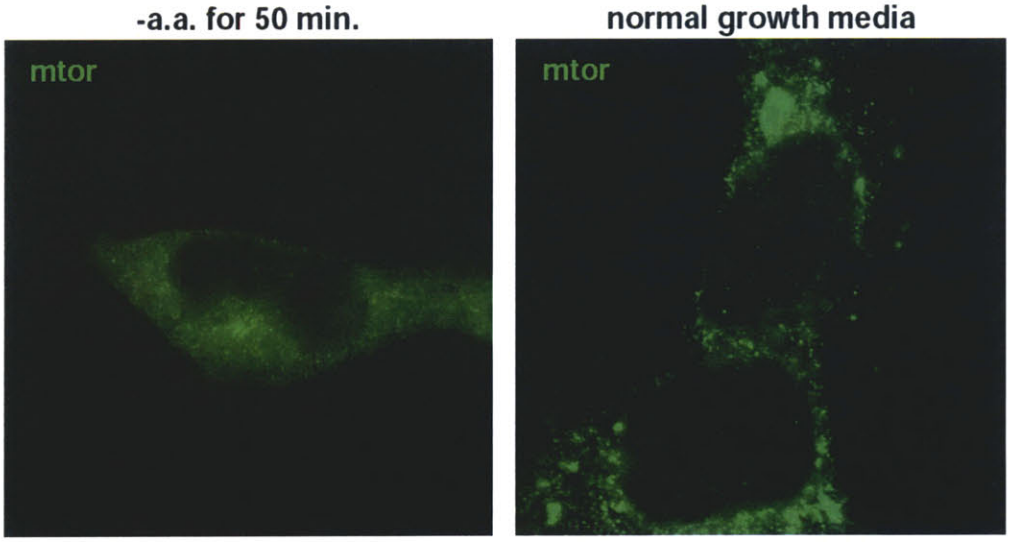

Fig. S9. Localization of mTOR in HEK-293T cells growing in normal growth media. Where indicated, cells were deprived of amino acids for 50 minutes. For cells growing in normal media, the media was replaced with fresh media 1 hour before processing. Cells were processed in an immunofluorescence assay with an mTOR antibody (green) and imaged.

Figure S10

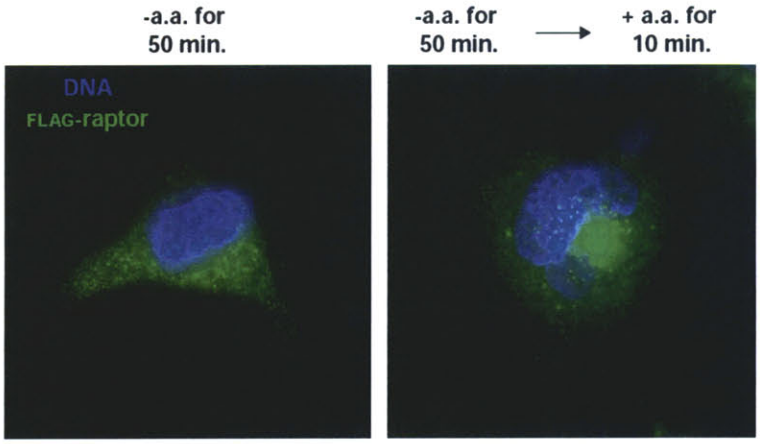

Fig. S10. Raptor localization in cells deprived or stimulated with amino acids. HEK-293T cells stably expressing FLAG-raptor were deprived of serum and amino acids for 50 minutes, and where indicated, stimulated with amino acids for 10 minutes. Cells were processed in an immunofluorescence assay with a FLAG antibody (green), co-stained with DAPI for DNA content (blue), and imaged.

Figure S11

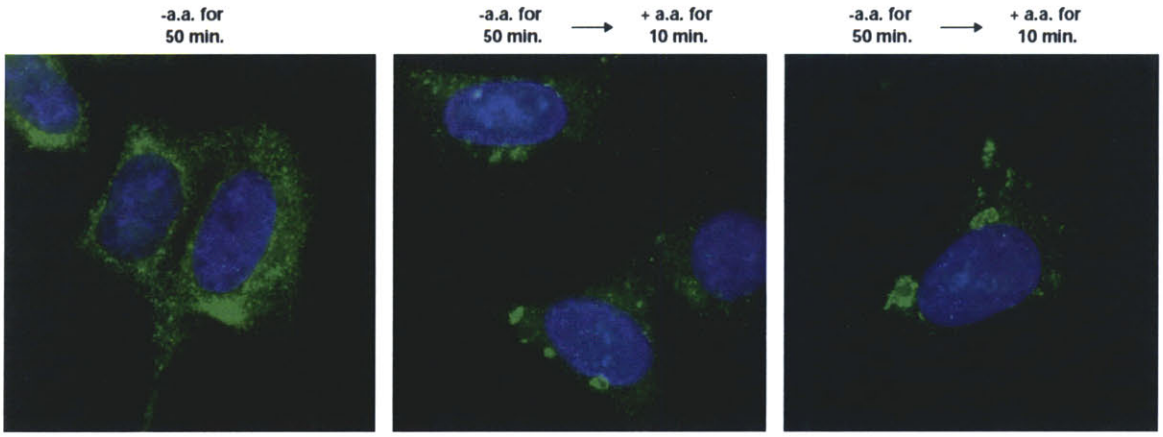

Fig. S11. mTOR localization in HeLa cells starved and stimulated for amino acids as in Figure 4. Cells were processed in an immunofluorescence assay with an mTOR antibody (green) and co-stained with DAPI for DNA content (blue).

Figure S12

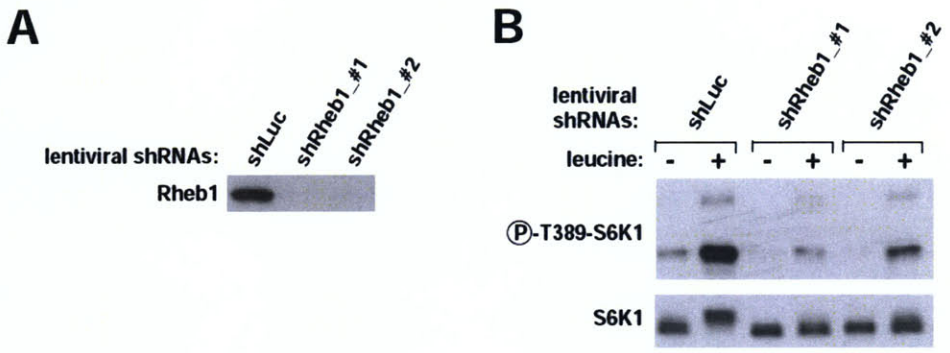

Fig. S12. Rheb is necessary for leucine to activate the mTORC1 pathway. **(A)** Validation that the two independent shRNAs targeting Rheb1 reduce its expression. Immunoblot analysis of Rheb1 in HEK-293T cells expressing the indicated shRNAs. **(B)** Cells from (A) were deprived of serum and leucine for 50 minutes, and, where indicated, re-stimulated with leucine for 10 minutes. Cell lysates were prepared and analyzed for the levels and phosphorylation state of S6K1.

References and Notes

1. D. A. Guertin, D. M. Sabatini, Cancer Cell 12, 9 (2007).

2. D. D. Sarbassov, S. M. Ali, D. M. Sabatini, Curr. Opin. Cell Biol. 17, 596 (2005).

3. M. P. Byfield, J. T. Murray, J. M. Backer, J. Biol. Chem. 280, 33076 (2005).

4. T. Nobukuni et al., Proc. Natl. Acad. Sci. U.S.A. 102, 14238 (2005).

5. E. M. Smith, S. G. Finn, A. R. Tee, G. J. Browne, C. G. Proud, J. Biol. Chem. 280, 18717 (2005).

6. Materials and methods are available as supporting material on Science Online.

7. D.-H. Kim et al., Cell 110, 163 (2002).

8. R. Loewith et al., Mol. Cell 10, 457 (2002).

9. K. P. Wedaman et al., Mol. Biol. Cell 14, 1204 (2003).

10. K. Hara et al., Cell 110, 177 (2002).

11. M. Bun-Ya, S. Harashima, Y. Oshima, Mol. Cell. Biol. 12, 2958 (1992).

12. A. Schurmann, A. Brauers, S. Massmann, W. Becker,
H. G. Joost, J. Biol. Chem. 270, 28982 (1995).

13. E. Hirose, N. Nakashima, T. Sekiguchi, T. Nishimoto, J. Cell Sci. 111, 11 (1998).

14. N. Nakashima, E. Noguchi, T. Nishimoto, Genetics 152, 853 (1999).

15. T. Sekiguchi, E. Hirose, N. Nakashima, M. Ii, T. Nishimoto, J. Biol. Chem. 276, 7246 (2001).

16. M. Gao, C. A. Kaiser, Nat. Cell Biol. 8, 657 (2006).

17. F. Dubouloz, O. Deloche, V. Wanke, E. Cameroni, C. De Virgilio, Mol. Cell 19, 15 (2005).

18. J. B. Kunz, H. Schwarz, A. Mayer, J. Biol. Chem. 279, 9987 (2004).

19. K. J. Roberg, N. Rowley, C. A. Kaiser, J. Cell Biol. 137, 1469 (1997).

20. E. J. Chen, C. A. Kaiser, J. Cell Biol. 161, 333 (2003).

21. A. Beugnet, A. R. Tee, P. M. Taylor, C. G. Proud, Biochem. J. 372, 555 (2003).

22. G. R. Christie, E. Hajduch, H. S. Hundal, C. G. Proud, P. M. Taylor, J. Biol. Chem. 277, 9952 (2002).

23. D. J. Price, R. A. Nemenoff, J. Avruch, J. Biol. Chem. 264, 13825 (1989).

24. Y. Sancak et al., Mol. Cell 25, 903 (2007).

25. X. Long, Y. Lin, S. Ortiz-Vega, K. Yonezawa, J. Avruch, Curr. Biol. 15, 702 (2005).

26. R. M. Drenan, X. Liu, P. G. Bertram, X. F. Zheng, J. Biol. Chem. 279, 772 (2004).
27. M. Mavrakis, J. Lippincott-Schwartz, C. A. Stratakis, I. Bossis, Autophagy 3, 151 (2007).
28. K. Saito, Y. Araki, K. Kontani, H. Nishina, T. Katada, J. Biochem. 137, 423 (2005).
29. C. Buerger, B. DeVries, V. Stambolic, Biochem. Biophys.
Res. Commun. 344, 869 (2006).
30. Supported by grants from the NIH (R01 CA103866 and AI47389), Department of Defense (W81XWH-07-0448), and W.M. Keck Foundation to D.M.S. as well as an EMBO fellowship to Y.D.S. We thank T. Kang for the preparation of FLAG-raptor and members of the Sabatini lab for helpful suggestions.

Experimental procedures

Materials

Reagents were obtained from the following sources: antibody to raptor from Upstate/Millipore; HRP-labeled anti-mouse, anti-goat, and anti-rabbit secondary antibodies from Santa Cruz Biotechnology; antibodies to phospho-T389 S6K1, S6K1, RagA, RagB, RagC and RagD, mTOR, rictor, phospho-T398 dS6K, and the myc epitope from Cell Signaling Technology; an antibody to the HA tag from Bethyl laboratories; an antibody to RagB from Novus Biologicals; Cellulose PEI TLC plates, RPMI, FLAG M2 affinity gel, FLAG M2 antibody, ATP, cycloheximide, valinomycin, H_20_2, 2-deoxyglucose, amino acids, and human recombinant insulin from Sigma Aldrich; DSP, protein G-sepharose, and immobilized glutathione beads from Pierce; DMEM from SAFC Biosciences; FuGENE 6 and Complete Protease Cocktail from Roche; Alexa 488 or Texas-Red-X conjugated secondary antibodies, Schneider's media, Express Five Drosophila-SFM, and Inactivated Fetal Calf Serum (IFS) from Invitrogen; and amino acid-free RPMI, amino acid- and phosphate- free RPMI, and amino acid-free Schneider's media from US Biological. The dS6K antibody was a generous gift from Mary Stewart (North Dakota State University).

Cell lines and tissue culture

HEK-293E, HEK-293T, and HeLa cells were cultured in DMEM with 10% IFS. In HEK-293E, but not HEK-293T, cells the mTORC1 pathway is strongly regulated by serum and insulin (*1*). The HEK-293E cell line was kindly provided by John Blenis (Harvard Medical School).

Leucine or amino acid starvation and stimulation of cells

Almost confluent cultures in 10 cm culture plates were rinsed with leucine-free RPMI once, incubated in leucine-free RPMI for 50 minutes, and stimulated with 52 µg/ml leucine for 10 minutes. For amino acid starvation, cells in 10 cm culture dishes or coated glass cover slips were rinsed with and incubated in amino acid-free RPMI for 50 minutes, and stimulated with a 10X amino acid mixture for 3-30 minutes as indicated in the figures. After stimulation, the final concentration of amino acids in the media was the same as in RPMI. Cells were processed for biochemical or immunofluorescence assays as described below. The 10X amino acid mixture was prepared from individual amino acid powders.

Cell lysis, immunoprecipitations, and kinase assays

Cells were rinsed once with ice-cold PBS and lysed in ice-cold lysis buffer (40 mM HEPES [pH 7.4], 2 mM EDTA, 10 mM pyrophosphate, 10 mM glycerophosphate, and 0.3% CHAPS or 1% Triton X-100, and one tablet of EDTA-free protease inhibitors (Roche) per 25 ml). The soluble fractions of cell lysates were isolated by centrifugation at 13,000 rpm for 10 minutes by centrifugation in a microfuge. For immunoprecipitations, primary antibodies were added to the lysates and incubated with rotation for 1.5 hours at 4°C. 60 µl of a 50% slurry of protein G-sepharose was then added and the incubation continued for an additional 1 hour. Immunoprecipitates were washed three times with lysis buffer containing 150 mM NaCl. Immunoprecipitated proteins were denatured by the addition of 20 µl of sample buffer and boiling for 5 minutes, resolved by 8%–16% SDS-PAGE, and analyzed by immunoblotting as described (*2*). For FLAG and GST purifications, immobilized glutathione or Flag M2 affinity resins were washed with lysis buffer 3 times. 20 µl of a 50% slurry of the resins was then added to pre-cleared cell lysates and incubated with rotation for 2 hours at 4°C. Finally, the beads were washed 3 times with lysis buffer containing 150 mM NaCl. For elution of FLAG-tagged proteins, beads were incubated in elution buffer (50 mM HEPES pH 7.4, 500 mM NaCl, 0.5% CHAPS, 50

μg/μl FLAG peptide) for 30 min at 30 °C. Elution of proteins from glutathione beads and kinase assays were performed as previously described (*1*).

cDNA manipulations and mutagenesis

The cDNAs for human RagA, RagB, RagC and RagD were obtained from Open Biosystems. The cDNAs were amplified by PCR and the products were subcloned into Sal I and Not I sites of HA-GST-pRK5, HA-pRK5 and FLAG-pRK5. The cDNAs were mutagenized using the QuickChange XLII mutagenesis kit (Stratagene) with oligonucleotides obtained from Integrated DNA Technologies. All constructs were verified by DNA sequencing. The Rag mutants used in our experiments are: $RagB^{GTP}$ = Q99L RagB; $RagB^{GDP}$ = T54L RagB; $RagC^{GTP}$ = Q120L RagC; $RagC^{GDP}$ = S75L RagC; $RagD^{GTP}$ = Q121L RagD; and $RagD^{GDP}$ = S77L RagD. $Rheb1^{GTP}$ = Q64L Rheb1.

FLAG-tagged wild type and mutant RagB and RagD cDNAs or GFP-tagged Rheb1 were amplified by PCR and cloned into the Age I and Bam HI sites of a modified pLKO.1 vector having a CMV promoter (pLJM1). After sequence verification, these plasmids were used, as described below, in transient cDNA transfections or to produce the lentiviruses needed to generate cell lines stably expressing the proteins. An expression plasmid encoding DsRed-Rab7 was obtained from Addgene.

cDNA transfection-based experiments

For co-transfection experiments, 2 million HEK-293T or HEK-293E cells were plated in 10 cm culture dishes. 24 hours later, cells were transfected with the prk5-based cDNA expression plasmids indicated in the figures in the following amounts: 500 ng myc-mTOR (*3*); 50 ng myc- or HA-raptor (*2*); 100 ng myc-rictor (*4*); 100 ng HA-GST-, HA- or FLAG-tagged Rap2A (*1*); 100 ng HA-GST-, HA-, or FLAG-tagged Rheb1 (*1*); 100 ng HA-tagged RagA; 100 ng HA-GST- or HA-tagged RagB; 100 ng HA-GST- or HA-tagged RagC; 100 ng HA-GST- or FLAG-tagged RagD; 1 ng of FLAG-S6K1. Transfection mixes were taken up to a total of 2 μg of DNA using empty pRK5.

In-cell cross-linking assay

DSP was dissolved in DMSO to a final concentration of 250 mg/ml to make a 250X stock solution for the in-cell cross-linking assay. HEK-293T cells stably expressing FLAG-tagged RagB, $RagB^{GTP}$, or RagD and growing in 10 cm culture dishes were starved for amino acids or starved and then stimulated as described above. At the end of the starvation or stimulation period, cells were rinsed once with cold PBS and incubated with 4 ml of PBS containing 1 mg/ml DSP for 7 minutes at room temperature. The cross-linking reaction was quenched by adding 1M Tris pH 8.5 to a final concentration of 100 mM followed by a 1-minute incubation. The cells were rinsed once with ice cold PBS, and lysed with RIPA buffer (40 mM HEPES [pH 7.4], 2 mM EDTA, 10 mM pyrophosphate, 10 mM glycerophosphate, 1% sodium deoxycholate, 1% NP40, 0.1% SDS, and one tablet of EDTA-free protease inhibitors per 25 ml). FLAG-immunoprecipitates were prepared as described above.

Identification of RagC as a raptor-associated protein

FLAG-raptor was immunoprecipitated with the FLAG M2 affinity gel from 30 million HEK-293T cells stably expressing FLAG-raptor. Proteins eluted with the FLAG peptide from the affinity matrix were resolved by SDS-PAGE, stained with silver, and the 45-55 kD region of the gel excised and digested with trypsin overnight. The resulting peptides were separated by liquid chromatography (NanoAcquity UPLC, Waters) using a self-packed Jupiter 3 micron C18 column. The eluting peptides were mass analyzed prior to collisionally induced dissociation (CID) using a ThermoFisher LTQ linear ion trap mass spectrometer equipped with a nanospray

source. Selected mass values from the MS/MS spectra were used to search the human segment of the NCBI non-redundant protein database using Xcalibur Mass Spectrometry software (Thermo Fischer Scientific). In 4 independent purifications of FLAG-raptor performed as above, this procedure led to the identification of a total of 20 peptides matching RagC that were not present in control FLAG-tubulin samples.

Cell size determinations

To measure cell size, 2 million cells were plated into 10 cm culture dishes. 24 hours later the cells were harvested by trypsinization in a 4 ml volume, diluted 1:20 with counting solution (Isoton II Diluent, Beckman Coulter), and cell diameters determined using a particle size counter (Coulter Z2, Beckman Coulter) with Coulter Z2 AccuComp software.

Mammalian lentiviral shRNAs

TRC lentiviral shRNAs (*5*) targeting RagA, RagB, RagC and RagD were obtained from Sigma. The TRC number for each shRNA is as follows:

Human RagA shRNA #1: TRCN0000047305
Human RagA shRNA #2: TRCN0000047307
Human RagB shRNA #1: TRCN0000047308
Human RagB shRNA #2: TRCN0000047311
Human RagC shRNA #1: TRCN0000072874
Human RagC shRNA #2: TRCN0000072877
Human RagD shRNA #1: TRCN0000059533
Human RagD shRNA #2: TRCN0000059534

The shLuc and shGFP control shRNAs and the shRNAs targeting mTOR and raptor are previously described and validated (*6*). Lentiviral shRNAs targeting Rheb1 were cloned into LKO.1 vector as described (*6*). The target sequences for the Rheb1 shRNAs are:

Human Rheb1 shRNA#1: CCTCAGACATACTCCATAGAT
Human Rheb1 shRNA#2: TTATGTTGGTTGGGAATAAGA

shRNA-encoding plasmids were co-transfected with Delta VPR envelope and CMV VSV-G packaging plasmids into actively growing HEK-293T cells using FuGENE 6 transfection reagent as previously described (*6, 7*). Virus-containing supernatants were collected 48 hours after transfection, filtered to eliminate cells and target cells were infected in the presence of 8 μg/ml polybrene. 24 hours later, cells were selected with puromycin and analyzed on the 2nd or 3rd day after infection.

In vitro Rag-raptor binding assay

2 million HEK-293T cells were plated into 10 cm culture dishes. 24 hours later, the cells were transfected with 2 μg HA-GST-Rap2a, 2 μg HA-GST-Rheb1, or 2 μg HA GST-RagB together with 2 μg of HA GST-RagC (wild type or Rag mutants as indicated). 2 days after transfection, the cells were lysed in Rheb lysis buffer containing 1% Triton X-100 (*1*), and cleared lysates were incubated with glutathione beads for 1.5 hours at 4°C with rotation. The beads were washed 3 times with lysis buffer and two times with Rheb storage buffer (*1*). 1/4 of the glutathione beads were incubated with 300 ng of FLAG-raptor in Rheb lysis buffer with 0.3% CHAPS for 30 min at 4°C with rotation. The glutathione beads were washed twice with Rheb lysis buffer containing 0.3% CHAPS and proteins were denatured by the addition of 20 μl of sample buffer and boiling

for 5 minutes and analyzed by SDS-PAGE and immunoblotting. FLAG-raptor was purified from HEK-293T cells stably expressing FLAG-raptor. Following the affinity-tag purification, the protein was further purified as described (*1*) by gel filtration using a Superose 6 10/300GL column (GE Healthcare) to obtain FLAG-raptor that by silver and coomasie staining was 99% pure.

Determination of guanyl nucleotide binding state of RagB in cells

Determination of the guanyl nucleotides bound to RagB in cells was performed essentially as previously described for Rheb (*8*). HEK-293T cells were cultured in fibronectin coated 6-well dishes until confluent, rinsed once with phosphate-and serum-free DMEM, and then incubated in phosphate-and serum-free DMEM containing 1 mCi ^{32}P orthophosphate (Perkin Elmer) for 4 hours. After 4 hours, cells were rinsed once with serum-, amino acid-, and phosphate-free RPMI, incubated with serum-, amino acid-, and phosphate-free media containing 1 mCi ^{32}P orthophosphate for 50 minutes, and stimulated with amino acids as described above. After rinsing with ice-cold PBS, cells were lysed in 0.5 ml lysis buffer (50 mM HEPES KOH (pH 7.4), 100 mM NaCl, 1 mM KH_2PO_4, 1 mM ATP, 100 µM GDP, 100 µM GTP, 5 mM $MgCl_2$, 1% Triton X-100), and the lysate microcentrifuged for 10 minutes at 13,000 rpm at 4°C. The supernatant was incubated with 15 µl of RagB antibody (Novus Biologicals) for 1 hour at 4°C. 20 µl of protein G beads were added to the lysates and the incubation continued for another 45 minutes. The beads were washed 8 times with wash buffer (50 mM HEPES KOH [pH 7.4], 500 mM NaCl, 5 mM $MgCl_2$, 0.5% Triton X-100, 0.005% SDS) and bound nucleotides were eluted in 23 µl of elution buffer (10 mM EDTA, 2 mM DTT, 0.2% SDS, 0.5 mM GDP, 0.5 mM GTP) at 60 °C for 10 minutes. 15 µl of the eluate was transferred to a clean tube. 60 µl of methanol and then 30 µl of chloroform were added to the tube, each addition followed by brief vortexing and microcentrifugation. After the addition of 45 µl of water, the samples were vortexed vigorously, microcentrifuged for 1 minute at 13,000 rpm and the aqueous phase transferred to a clean tube. Using a speedvac the samples were dried and then re-suspended in 15 µl of deionized water. Samples were spotted on PEI cellulose TLC plates and the plates developed with 1.2 mM ammonium formate and 0.8 mM HCl, and the radioactivity detected with a phosphoimager. After background subtraction, the intensities of the GTP and GDP spots were determined. The percent of GTP nucleotide was calculated using the following formula: [(GTP/3)/((GTP/3) + (GDP/2))] X 100%.

Immunofluorescence assays

150,000 HEK-293T cells were plated on fibronectin-coated glass coverslips in 12-well tissue culture plates. 24 hours later cells were starved for and stimulated with amino acids as described above, rinsed with PBS once and fixed for 5 minutes with 4% paraformaldehyde in PBS warmed to 37°C. The coverslips were rinsed twice with PBS and permealized with 0.2% Triton X-100 in PBS for 15 minutes. After rinsing twice with PBS, the coverslips were blocked for one hour in blocking buffer (0.25% BSA in PBS) and incubated with primary antibody in blocking buffer overnight at 4°C, rinsed twice with blocking buffer and incubated with secondary antibodies (diluted in blocking buffer 1:1000) for one hour at room temperature in dark. The coverslips were mounted on glass slides using Vectashield (Vector Laboratories) and imaged with a 63X objective using epifluorescence microscopy.

Where indicated, 1-2 ng of plasmids encoding GFP-Rheb1 or dsRed-Rab7 were transfected per well of a 12-well dish.

***Drosophila* cell experiment**

dsRNA transfection and amino acid starvation and stimulation

5 million S2 cells were plated in 6-cm culture dishes in 5 ml of Express Five SFM media. Cells were transfected with 1 μg of dsRNA per million cells. 4 days later, cells were rinsed once with amino acid-free Schneider's medium, and starved for amino acids by replacing the media with amino acid-free Schneider's medium for 1.5 hours. To stimulate with amino acids, the amino acid-free medium was replaced with complete Schneider's medium for 20 minutes. Cells were then washed with ice cold PBS twice, lysed, and processed as described (*1*). The pH of the amino acid free media was made to match that (pH 6.70) of an opened bottle of full Schneider's media.

Design and synthesis of dsRNAs

The control GFP dsRNA has been described (*4*). Other dsRNAs were designed to target all known transcripts of the target *Drosophila* gene. In order to minimize off-target effects, we used the DRSC tool at http://flyrnai.org/RNAi_find_frag_free.html and excluded regions of 19-mer-or-greater identity to any *Drosophila* transcripts. The Drosophila genome encodes for one RagA/B-like gene (CG11968) and one RagC/D-like gene (CG8707). We designed and tested two distinct dsRNAs to each gene. Synthesis of dsRNAs was performed as previously described (*4*) using the primers indicated below.

Primer sequences (including underlined 5' and 3' T7 promoter sequences)

dRagB (CG11968) dsRNA_1 forward primer:
GAATTAATACGACTCACTATAGGGAGACGCTCCATTATCTTTGCTAACTATAT

dRagB (CG11968) dsRNA_1 reverse primer:
GAATTAATACGACTCACTATAGGGAGACATCAAACACATAAATCAGCACTTC

dRagB (CG11968) dsRNA_2 forward primer:
GAATTAATACGACTCACTATAGGGAGAATAGAGCGCGACATCCATTACTAC

dRagB (CG11968) dsRNA_2 reverse primer:
GAATTAATACGACTCACTATAGGGAGACTTGATGATGTTGGACACCTTTT

dRagC (CG8707) dsRNA_1 forward primer:
GAATTAATACGACTCACTATAGGGAGAGAGTCGACCAGTAAGATCGTGAA

dRagC (CG8707) dsRNA_1 reverse primer:
GAATTAATACGACTCACTATAGGGAGATGTAGTCATCCTTGGCATCG

dRagC (CG8707) dsRNA_2 forward primer:
GAATTAATACGACTCACTATAGGGAGAAGTTCGAGGTGTTTATACACAAGGT

dRagC (CG8707) dsRNA_2 reverse primer:
GAATTAATACGACTCACTATAGGGAGAAAGATGGAGTGGTCGTATATGGAG

References for Experimental procedures

1. Y. Sancak et al., *Mol Cell* 25, 903-15 (2007).
2. D.-H. Kim et al., *Cell* 110, 163-175 (2002).
3. P. E. Burnett, R. K. Barrow, N. A. Cohen, S. H. Snyder, D. M. Sabatini, *PNAS* 95, 1432-1437 (1998).
4. D. D. Sarbassov et al., *Curr Biol* 14, 1296-302 (2004).
5. J. Moffat et al., *Cell* 124, 1283-98 (2006).
6. D. D. Sarbassov, D. A. Guertin, S. M. Ali, D. M. Sabatini, *Science* 307, 1098-101 (2005).
7. S. M. Ali, D. M. Sabatini, *J Biol Chem* 280, 19445-8 (2005).
8. X. Long, Y. Lin, S. Ortiz-Vega, K. Yonezawa, J. Avruch, *Curr Biol* 15, 702-13 (2005).

Chapter 5

mTORC1 regulates cytokinesis through activation of Rho-ROCK signaling

Timothy R. Peterson[1], Van Veen E[2], Van Vugt MA[2], Thoreen CC[1], David M. Sabatini[1].

[1]Whitehead Institute for Biomedical Research, Howard Hughes Medical Institute, and Massachusetts Institute of Technology, Department of Biology, Nine Cambridge Center, Cambridge, MA 02142.
[2]MIT Center for Cancer Research, 77 Massachusetts Avenue, Cambridge, MA 02139.

Experiments in Figure 1 were performed by T.R.P.
Experiments in Figure 2 were performed by T.R.P. and assisted by E.V.
Experiments in Figure 3 were performed by T.R.P.
Experiments in Figure 4 were performed by T.R.P.

Summary

Understanding the mechanisms by which cells coordinate their size with their ability to divide has long attracted the interest of biologists. The Target of Rapamycin (TOR) pathway is becoming increasingly recognized as a master regulator of cell size, however less is known how TOR activity might be coupled with the cell cycle. Here, we establish that mTOR complex 1 (mTORC1) promotes cytokinesis through activation of a Rho GTPase-Rho Kinase (ROCK) signaling cascade. Hyperactivation of mTORC1 signaling by depletion of any of its negative regulators: TSC1, TSC2, PTEN, or DEPTOR, induces polyploidy in a rapamycin-sensitive manner. mTORC1 hyperactivation-mediated polyploidization occurs by a prolonged, but ultimately failed attempt at abcission followed by re-fusion. Similar to the effects of ROCK2 overexpression, these mTORC1-driven aberrant cytokinesis events are accompanied by increased Rho-GTP loading, extensive plasma membrane blebbing, and increased actin-myosin contractility, all of which can be rescued by either mTORC1 or ROCK inhibition. These results provide evidence for the existence of a novel mTORC1-Rho-ROCK pathway during cytokinesis and suggest that mTORC1 might play a critical role in setting the size at which a mammalian cell divides.

Introduction

Key to the proper transition of cells through the cell cycle is their passage through multiple signaling 'checkpoints'. One of the first insights into the existence and function of one of these checkpoints was the isolation and characterization of a mutation in the Wee1 gene. Wee1 mutant cells were shown to abrogate a previously unknown to exist cell size checkpoint strikingly, undergoing cell division at half the size of wild-type cells (*1*). Since this discovery, our understanding of the mechanisms controlling cell size and cell division have rapidly, though separately, evolved. The Rho pathway has emerged as a central player in controlling the actin-myosin-based contractile events required for cytokinesis (*2, 3*). Regarding the regulation of cell size, the TOR signaling

pathway has received considerable attention, in particular for its role in controlling the G1 growth phase of the cell cycle. Though it has largely become known as a controller of protein synthesis and the G1 program, it has also long been clear that TOR has a second, distinct essential function involving the cell-cycle dependent organization of the cytoskeleton (*4*). Mutations in TOR2 do not arrest cells in G1 as is the case with rapamycin treated cells, but rather cause arrest at multiple points in the cell cycle (*5*) accompanied by profound actin cytoskeletal disorganization (*4*). That the lethality of a TOR2 mutation could be rescued by overexpression of components of the Rho pathway hinted at the relationship between these pathways during the cell cycle (*6*). However, the importance of such a coupling during cell division still remains largely unknown. To address this question, we have investigated the involvement of mTOR signaling in cytokinesis. We find that mTORC1 hyperactivation causes prolonged cytokinesis due to Rho-ROCK hyperactivity and is associated with increased polyploidy, a condition thought to underlie the malignancy of certain cancers.

Results

The mTOR pathway is repressed through the actions of multiple upstream inhibitory proteins including TSC1, TSC2, PRAS40, PTEN, and REDD1 (*7*). We recently identified a novel negative regulator of the mTOR pathway, DEPTOR, which binds mTOR and inhibits both mTORC1 and mTORC2 signaling pathways (*8*). In characterizing DEPTOR function, we noticed that its depletion in cells by RNAi promoted their multinucleation (Fig. 1A-B). To quantify this phenomenon, we measured the DNA content of DEPTOR knockdown cells compared with control cells. The results were clear; DEPTOR knock-down increased the percentage of 8N cells relative to those of control knockdown cells (Fig. 1C). Because DEPTOR depletion activates both the mTORC1 and mTORC2 pathways, we sought to determine whether either of these pathways might be responsible for mediating the effects of DEPTOR on ploidy. First, we knocked down known regulators of mTORC1 and/or mTORC2: raptor, rictor, mTOR, TSC1, TSC2, and PTEN and measured their DNA content. Similar to that of DEPTOR knockdown cells, cells with knockdown of any of the negative regulators of mTOR:

TSC1, TSC2, or PTEN increased the percentage of 8N cells relative to control knockdown cells (Fig. 1C). Fittingly, the increased >4N DNA content of TSC1 knockdown was similar to those seen in a different cell type with complete loss of TSC1 (*9*). That neither mTORC1 nor mTORC2 inactivation by knockdown or raptor or rictor, respectively increased the percentage of 8N cells is consistent with DEPTOR being a negative regulator of mTOR signaling (Fig. 1C). Finally, treatment of DEPTOR or TSC2 knock-down cells with rapamycin, which only significantly inhibits mTORC1 and not mTORC2 in the cells we assessed (*8*), fully reduced the percentage of 8N cells (Fig. 1C) suggesting that deregulation of mTORC1 is responsible for effects of mTOR on polyploidy.

To explore at which point in their cell cycle mTORC1-hyperactivated cells became polyploid, we visually monitored individual knockdown cells over time. Both wild-type and DEPTOR knockdown cells progressed through interphase and through early stages of mitosis similarly (Fig. 2A). However, upon daughter cell separation, the surface of DEPTOR knockdown cells, unlike control cells, began to bleb massively and this was subsequently followed after a prolonged period of blebbing by fusion of their membranes and the creation of one cell containing both daughter nuclei (Fig. 2A). The same prolonged period of surface blebbing pattern was also observed in cells deficient in TSC1, TSC2, or PTEN but not in rictor knockdown cells (Fig. 2B-C) suggesting that blebbing-associated multinucleation is due to hyperactivation of mTORC1 and not mTORC2 (either directly or indirectly through the well-characterized mTORC1-PI3K feedback loop(*10*)). To strengthen the claim that this aberrant surface blebbing was mediated by mTORC1, we treated DEPTOR knock-down cells with rapamycin immediately preceding the point at which they began to separate into two daughter cells. Rapamycin treatment dramatically reduced the time required for the separation of DEPTOR-deficient daughter cells as well as the time of their surface blebbing (Fig. 2B, 2D). Correlating with the degree of polyploidy, these results suggest that surface blebbing-associated cytokinesis defects in DEPTOR deficient cells are the result of mTORC1 hyperactivation. During cytokinesis, cytoskeletal rearrangements are critical for physically separating cells after their duplication (*11*). Both microtubules and the actin are core components of the cytoskeleton driving this process (*11*), therefore we

assessed their morphology with or without mTORC1 hyperactivation during multiple stages of cell cycle. Control and DEPTOR knockdown cells had similar cortical actin positioning and assembly of their α-tubulin-containing spindles in mitosis (Fig. 2E). However, in cytokinesis, while control daughter cells had symmetrical actin cortices, in DEPTOR depleted cells, their actin architecture was grossly disorganized and appeared to be forming blebbing patterns similar to that which we observed in DEPTOR depleted cells by light microscopy (Fig.2A-B, 2E).

Actin-myosin contractility provides critical mechanical force to promote cell cleavage in cytokinesis and is known to be coordinated by many Rho-GTP-dependent kinases which regulate this contractility by phosphorylating myosin light chain 2 (MLC2) (*12*). To test a role for mTORC1 in regulating actin-myosin contractility, we first confirmed in our cell system that the MLC2 phosphorylating kinase, Rho kinase 2 (ROCK2), regulates the morphology of the actin cytoskeleton (*13*). While overexpression of kinase dead ROCK2 did not strongly perturb the actin cytoskeleton compared with overexpression of a control protein, overexpression of wild-type ROCK2 produced strong actin blebbing much like that we had seen with DEPTOR knockdown cells (Fig. 2E, 3A). As expected, ROCK2 overexpression also increased S19 MLC2 phosphorylation (Fig. 3B). To test whether DEPTOR regulated ROCK signaling during cytokinesis, we measured MLC2 phosphorylation in DEPTOR and control knockdown cells. Typical of metazoan cells in cytokinesis, we detected prominent S19 MLC2 phosphorylation in control cells that was reduced by inhibition of ROCK activity (Fig. 3C) (*14, 15*). On the other hand, DEPTOR depleted cells, had substantially elevated levels of S19 MLC2 phosphorylation compared with control cells (Fig. 3C). That the effects of DEPTOR loss of S19 MLC2 phosphorylation were strongly reduced by ROCK inhibition (Fig. 3C) suggests that DEPTOR loss activates ROCK signaling.

Because it is possible that DEPTOR knockdown activates ROCK signaling independent of its effects on mTORC1, we tested whether mTORC1 inhibition would reverse the effects of DEPTOR depletion on MLC2 phosphorylation. Indeed, treating DEPTOR knockdown cells with either rapamycin or a concentration of Torin1 which only potently inhibits mTORC1 signaling (*8*) reduced S19 MLC2 phosphorylation (Fig. 3D). We next sought to determine whether the effects of DEPTOR on ROCK activity were

direct. Because ROCK is activated by binding to the active, GTP-bound form of Rho (*16*) and because TOR is known to regulate Rho GEF activity (*6*), we tested whether DEPTOR knockdown regulates ROCK by altering the Rho-GTP/GDP state. DEPTOR knockdown cells had higher levels of Rho-GTP than control cells and this increased activity was reduced by rapamycin (Fig. 3E). These results are consistent with mTORC1 activating ROCK upstream of ROCK itself by promoting Rho activity. Because ROCK directly phosphorylates many substrates besides MLC2, we checked whether other ROCK outputs were also regulated by manipulation of mTORC1. Mypt1 is the targeting subunit for the S19 MLC2 phosphatase and is known to be inhibited in its activity by phosphorylation at its T696 site by ROCK (*17, 18*). DEPTOR knockdown increased and mTOR knockdown decreased Mypt1 T696 phosphorylation consistent with mTORC1 positively regulating ROCK activity toward this substrate (Fig. 3F). Another target of ROCK pathway is Cofilin. Cofilin is an F-actin severing protein which is inhibited through its S3 phosphorylation by the ROCK-activated kinase, LIMK1 (*19*). Consistent with the effects of DEPTOR knockdown on MLC2 and Mypt1 phosphorylation, S3 cofilin phosphorylation was increased by DEPTOR knockdown above the levels seen in control knockdown in multiple cell types (Fig. 3F-G). In total, these results suggest that Rho-ROCK signaling toward multiple effector pathways is positively regulated by mTORC1.

To better define how DEPTOR-mTORC1 controls Rho-ROCK activity, we assessed DEPTOR localization in cells undergoing cytokinesis. We detected DEPTOR throughout the cell, though it was clearly enriched at the centrosomes and the cleavage furrow, two subcellular localizations, which interestingly are also enriched for ROCK and RhoA, respectively (Fig. 4A) (*20, 21*). Previously, we have shown that DEPTOR phosphorylation state and levels are regulated by growth factors in an mTOR-dependent manner (*8*), therefore we assessed whether DEPTOR was also regulated in a cell cycle-dependent manner. Arresting cells in mitosis with nocodazole, a microtubule disrupting agent (*22*), significantly impaired the gel mobility of the DEPTOR protein, and this gel mobility was restored when nocodazole was removed from the media (Fig. 4B). This suggests that DEPTOR might be regulated by phosphorylation during completion of the cell cycle. Because DEPTOR phosphorylation is known to regulate its ability to

repress mTOR signaling (*8*), we wanted to determine we might be able to overcome this reduction in DEPTOR function during cytokinesis by inducing its overexpression. To do this, we measured histone phosphorylation, which regulates and provides a convenient marker of mitotic progression (*23*). While nocodazole increased the percentage of phosphorylated S10 Histone H3 (p-H3) positive control and DEPTOR overexpressing cells similarly, release from mitotic arrest was slower in DEPTOR overexpressing cells than control cells (Fig. 4C-D). In summary, this data suggests that DEPTOR is regulated both post-translational and by localization during the later stages of the cell cycle and that inactivation or hyperactivation of mTORC1 signaling both prolong the time necessary to complete cytokinesis.

Discussion

Here we find that increased mTORC1 causes polyploidy due to defective cytokinesis that is correlated with increased Rho-ROCK-mediated phosphorylation of multiple effectors including MLC2, Mypt1, and Cofilin. While there is some evidence that mTOR regulates Rho-dependent processes in mammalian cells (*24, 25*), our work, to our knowledge, is the first to demonstrate that mTORC1 regulates cytokinesis via activation of Rho-ROCK signaling. One question still remaining is whether mTORC1 and not mTORC2 controls all mTOR-dependent, Rho signaling processes. Recently, it has been argued that, on the contrary, many of the effects of mTOR on the actin cytoskeleton are due to regulation of TORC2 and not TORC1 signaling (*24*). While our work does not directly address these claims, there is precedence with other TOR-dependent outputs that TORC1 and TORC2 might overlap in function more than is readily appreciated. In yeast, Sch9 is a target of TORC1 and controls longevity in a manner analogous to one of its homologs in higher organisms, Akt, which is an mTORC2, and not mTORC1, substrate (*26-28*). Also, loss-of-function alleles of LST8, a component of both TORC1 and TORC2, regulates rapamycin-sensitive, GAP1 permease sorting in yeast, but in mammals, does not only significant impair mTORC1 function and rather is essential for mTORC2-Akt activity (*29, 30*).

Future studies will undoubtedly be needed to better understand the mechanisms by which TOR regulates Rho function. Recently, it has been shown that rapamycin downregulates the translation of ROCK1(*31*). Whereas, our data suggests that mTORC1 also regulates the Rho pathway upstream of ROCK (Fig. 3E). Because TOR is known to regulate numerous effectors by their phosphorylation (*32*), one interesting possibility stemming from our work is to test whether mTORC1 regulates the phosphorylation state of a Rho-GAP or Rho-GEF. By answering this as well as other questions of how TOR and Rho work, it is exciting to consider that understanding of one of biology's central questions 'how cell size is coordinated with cell division' will be closer in reach.

Figure Legends

Fig. 1. mTORC1 hyperactivation causes polyploidy. (A) and (B) HeLa cells were infected with lentivirus expressing shRNAs targeting DEPTOR or GFP. Cells were then analyzed by immunoblotting for the levels of the specified proteins (A) or processed in an immunofluorescence assay to detect α-tubulin (green), costained with DAPI for DNA content (blue), and imaged (B). (C) HeLa cells pretreated with 100nM rapamycin or vehicle were infected with lentivirus expressing the indicated shRNAs, stained with propidium iodide, and analyzed for DNA content by flow cytometry. ≥ 20,000 cells were analyzed for each condition. Error bars indicate standard error for n=3.

Fig. 2. mTORC1 hyperactivation distorts the actin cytoskeleton and prolongs cytokinesis.
(A) and (B) HeLa cells were infected with lentivirus expressing shRNAs targeting DEPTOR, TSC2, or GFP were analyzed by light microscopy (10x). Images were captured once per minute. (C) and (D) All images from (A) and (B) were visually inspected and manually counted to determine the % of cells blebbing and time of blebbing in minutes. ≥ 50 cells were analyzed for each sample. Error bars indicated standard error for n=3. (E) HeLa cells were infected with lentivirus expressing a shRNA targeting DEPTOR or GFP. Cells were then processed in an immunofluorescence assay to detect α-tubulin (green), actin (red), costained with DAPI for DNA content (blue), and imaged.

Fig. 3. mTORC1 hyperactivation activates Rho-ROCK signaling. (A) HeLa cells transfected with the indicated cDNAs were processed in an immunofluorescence assay to detect FLAG (red), actin (green), costained with DAPI for DNA content (blue), and imaged. (B) HEK-293T cells transfected with the indicated cDNAs were analyzed by immunoblotting for S19 MLC2 phosphorylation. (C) HeLa cells were infected with lentivirus expressing shRNAs targeting DEPTOR or GFP, treated for 10 minutes with 10μM of Y-27632 or vehicle, and processed in an immunofluorescence assay to detect α-tubulin (green), S19 MLC2 phosphorylation (red), costained with DAPI for DNA

content (blue), and imaged. (D) HeLa cells were infected with lentivirus expressing shRNAs targeting DEPTOR or GFP, treated for 10 minutes with 100nM rapamycin, 50μM Torin1, 10μM of Y-27632, or vehicle and processed in an immunofluorescence assay to detect S19 MLC2 phosphorylation and imaged. (E) HeLa cells were infected with lentivirus expressing shRNAs targeting DEPTOR or GFP, treated for 10 minutes with 100nM rapamycin or vehicle, immunoprecipitation of Rhotekin binding proteins was performed, and immunoprecipitates and lysates were analyzed by immunoblotting for the indicated levels of the specified proteins. (F) HeLa cells were infected with lentivirus expressing the indicated shRNAs were analyzed by immunoblotting for the phosphorylation states of the specified proteins. (G) Indicated p53-/- MEFs were generated and analyzed as in (F).

Fig. 4. Further characterization of DEPTOR during cytokinesis. (A) HeLa cells were processed in an immunofluorescence assay to detect DEPTOR (green), costained with DAPI for DNA content (blue), and imaged. (B) HeLa cells were treated with 100ng/μl nocodazole or vehicle for 16 hours and released for the indicated times, cell lysates were prepared and analyzed by immunoblotting for DEPTOR or mTOR. (C) and (D) HeLa cells treated as in (B) were processed in an immunofluorescence assay to detect phosphorylated S10 Histone H3 (pink), myc-DEPTOR (green), costained with DAPI for DNA content (blue), and imaged. Three images for each condition were analyzed by image analysis software (CellProfiler) and mean measurements are shown in (C). Representative images are shown in (D). (E) Depiction of mTORC1-DEPTOR activity during the cell cycle.

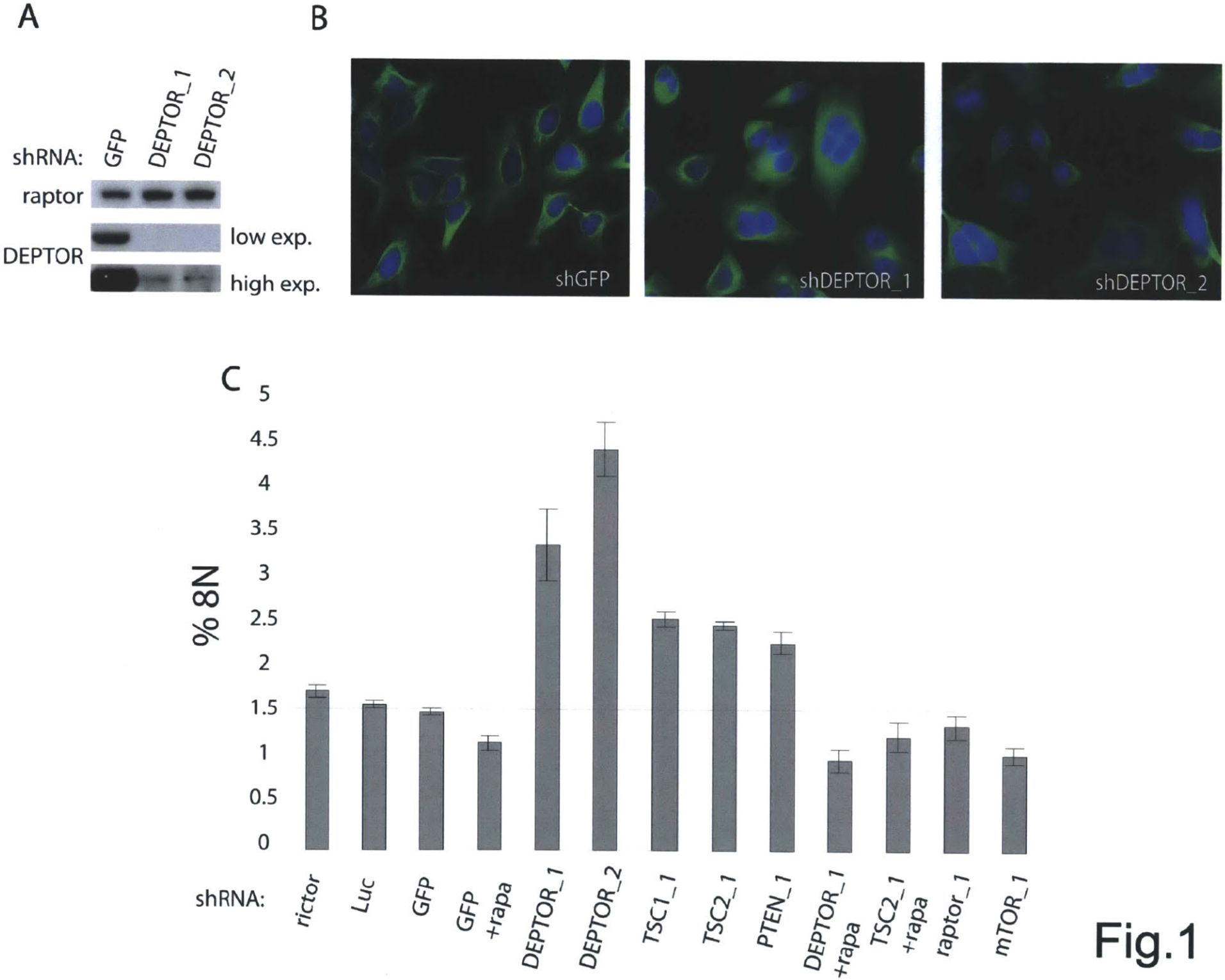
A
shRNA:
GFP
DEPTOR_1
DEPTOR_2
raptor
DEPTOR
low exp.
high exp.
B
shGFP
shDEPTOR_1
shDEPTOR_2
C
% 8N
5
4.5
4
3.5
3
2.5
2
1.5
1
0.5
0
shRNA:
rictor
Luc
GFP
GFP +rapa
DEPTOR_1
DEPTOR_2
TSC1_1
TSC2_1
PTEN_1
DEPTOR_1 +rapa
TSC2_1 +rapa
raptor_1
mTOR_1

Fig.1

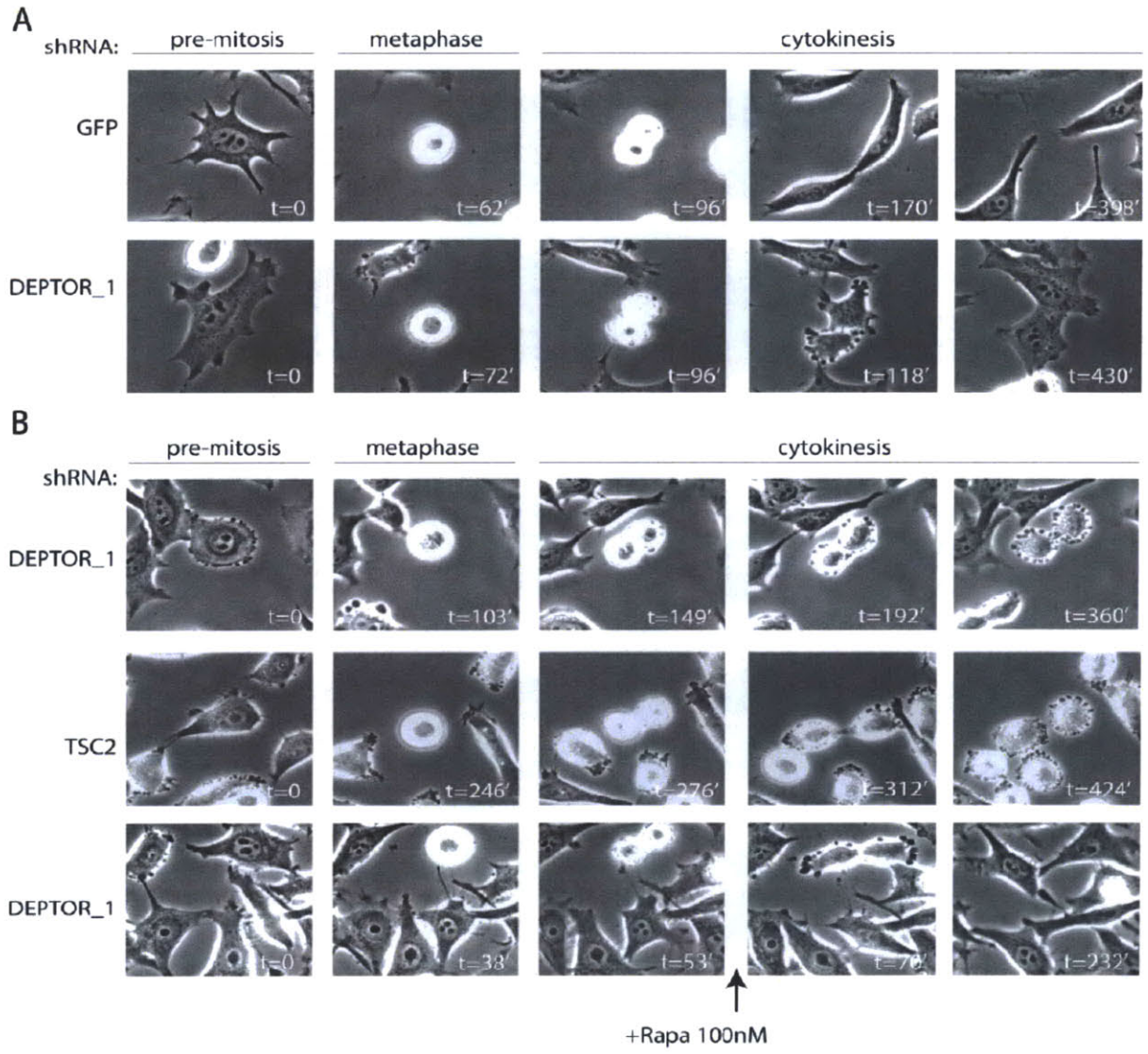
A
shRNA:
pre-mitosis
metaphase
cytokinesis
GFP
t=0
t=62′
t=96′
t=170′
t=398′
DEPTOR_1
t=0
t=72′
t=96′
t=118′
t=430′
B
shRNA:
pre-mitosis
metaphase
cytokinesis
DEPTOR_1
t=0
t=103′
t=149′
t=192′
t=360′
TSC2
t=0
t=246′
t=276′
t=312′
t=424′
DEPTOR_1
t=0
t=38′
t=53′
t=232′
+Rapa 100nM

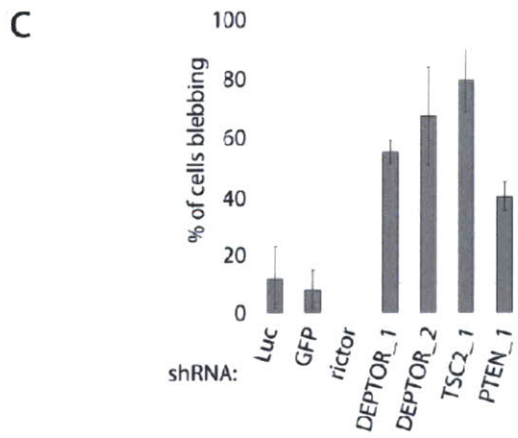
C
% of cells blebbing
100
80
60
40
20
0
shRNA:
Luc
GFP
rictor
DEPTOR_1
DEPTOR_2
TSC2_1
PTEN_1

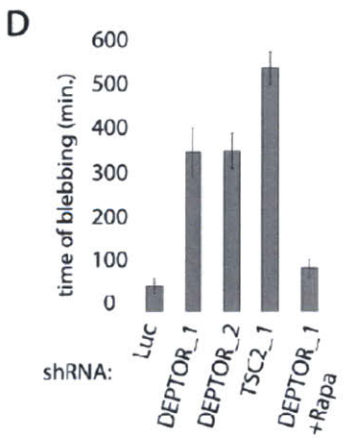
D
time of blebbing (min.)
600
500
400
300
200
100
0
shRNA:
Luc
DEPTOR_1
DEPTOR_2
TSC2_1
DEPTOR_1 +Rapa

Fig.2

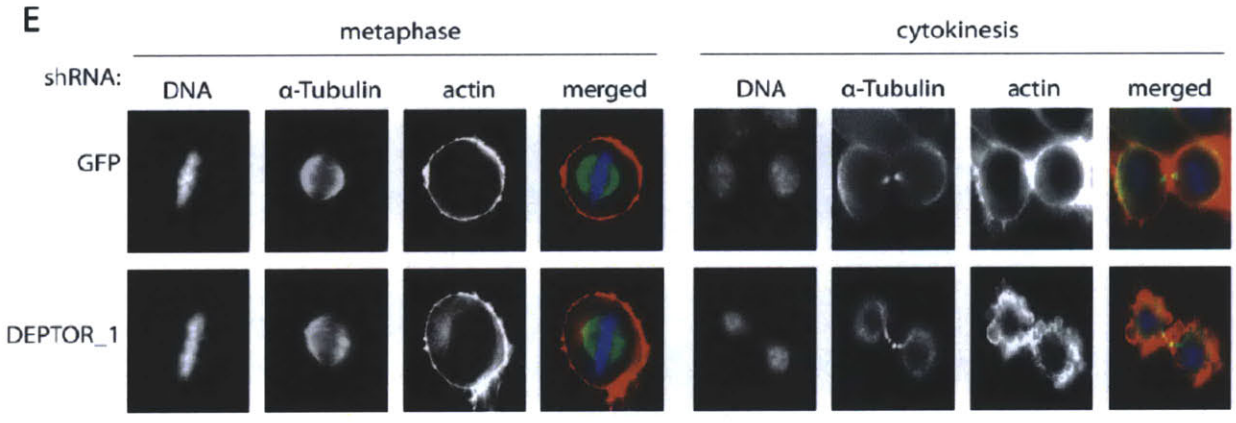
E
metaphase
cytokinesis
shRNA:
DNA
α-Tubulin
actin
merged
DNA
α-Tubulin
actin
merged
GFP
DEPTOR_1

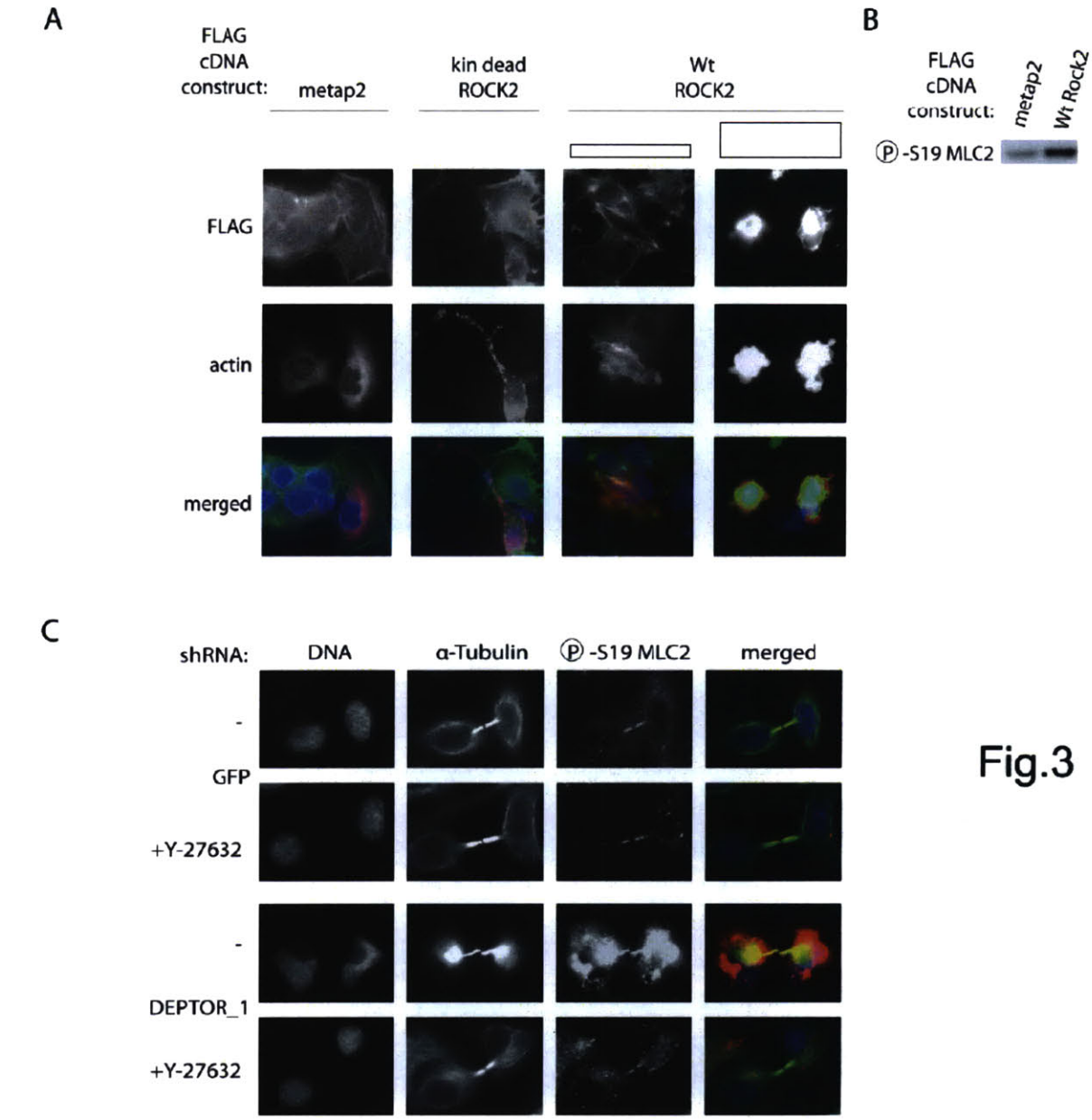
A
FLAG cDNA construct:
metap2
kin dead ROCK2
Wt ROCK2
FLAG
actin
merged
B
FLAG cDNA construct:
metap2
Wt Rock2
Ⓟ-S19 MLC2
C
shRNA:
DNA
α-Tubulin
Ⓟ-S19 MLC2
merged
-
GFP
+Y-27632
-
DEPTOR_1
+Y-27632
D
shRNA:
GFP
DEPTOR_1
tx:
dmso
Y-27632 1μm
dmso
rapa 100nM
Torin1 50nM
Y-27632 1μM
Ⓟ-S19 MLC2
E
shRNA:
GFP
DEPTOR_1
rapa:
- + - +
Rhotekin:
Rho-GTP
total Rho
cell lysates:
DEPTOR
raptor
F
Hela
shRNA:
GFP
mTOR_1
DEPTOR_2
DEPTOR_1
Ⓟ-T696 Mypt1
Ⓟ-S19 MLC2
Ⓟ S3 Cofilin
G
p53-/- MEFs
shRNA:
GFP
DEPTOR_1
DEPTOR_2
Luc
DEPTOR
Ⓟ S3 Cofilin
total Cofilin

Fig.3

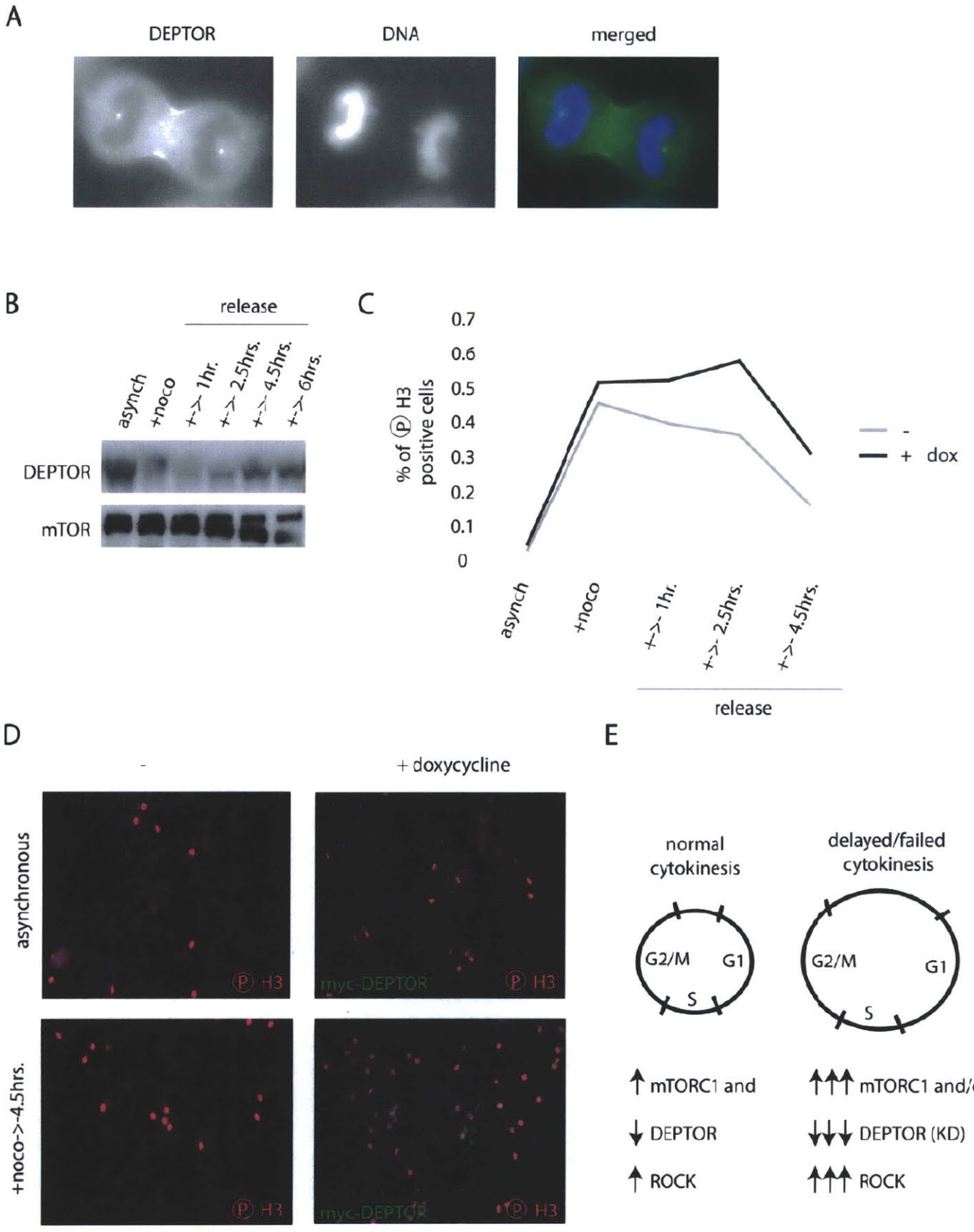
A
DEPTOR
DNA
merged
B
release
asynch
+noco
+->- 1hr.
+->- 2.5hrs.
+->- 4.5hrs.
+->- 6hrs.
DEPTOR
mTOR
C
% of Ⓟ H3 positive cells
0.7
0.6
0.5
0.4
0.3
0.2
0.1
0
asynch
+noco
+->- 1hr.
+->- 2.5hrs.
+->- 4.5hrs.
release
-
+ dox
D
-
+ doxycycline
asynchronous
+noco->-4.5hrs.
Ⓟ H3
myc-DEPTOR
E
normal cytokinesis
delayed/failed cytokinesis
G2/M
G1
S
↑ mTORC1 and
↓ DEPTOR
↑ ROCK
↑↑↑ mTORC1 and/or
↓↓↓ DEPTOR (KD)
↑↑↑ ROCK

Fig.4

References

1. P. Nurse, *Nature* **256**, 547 (Aug 14, 1975).
2. M. Glotzer, *Science* **307**, 1735 (Mar 18, 2005).
3. S. J. Heasman, A. J. Ridley, *Nat Rev Mol Cell Biol* **9**, 690 (Sep, 2008).
4. A. Schmidt, J. Kunz, M. N. Hall, *Proc Natl Acad Sci U S A* **93**, 13780 (Nov 26, 1996).
5. J. Kunz *et al.*, *Cell* **73**, 585 (May 7, 1993).
6. A. Schmidt, M. Bickle, T. Beck, M. N. Hall, *Cell* **88**, 531 (Feb 21, 1997).
7. A. Efeyan, D. M. Sabatini, *Curr Opin Cell Biol* **22**, 169 (Apr).
8. T. R. Peterson *et al.*, *Cell* **137**, 873 (May 29, 2009).
9. A. Astrinidis, W. Senapedis, E. P. Henske, *Hum Mol Genet* **15**, 287 (Jan 15, 2006).
10. S. H. Um *et al.*, *Nature* **431**, 200 (Sep 9, 2004).
11. F. A. Barr, U. Gruneberg, *Cell* **131**, 847 (Nov 30, 2007).
12. F. Matsumura, *Trends Cell Biol* **15**, 371 (Jul, 2005).
13. Y. Wang *et al.*, *Circ Res* **104**, 531 (Feb 27, 2009).
14. H. Kosako *et al.*, *Oncogene* **19**, 6059 (Dec 7, 2000).
15. S. O. Dean, J. A. Spudich, *PLoS ONE* **1**, e131 (2006).
16. K. Riento, A. J. Ridley, *Nat Rev Mol Cell Biol* **4**, 446 (Jun, 2003).
17. K. Kimura *et al.*, *Science* **273**, 245 (Jul 12, 1996).
18. M. Ito, T. Nakano, F. Erdodi, D. J. Hartshorne, *Mol Cell Biochem* **259**, 197 (Apr, 2004).
19. M. Maekawa *et al.*, *Science* **285**, 895 (Aug 6, 1999).
20. V. Chevrier *et al.*, *J Cell Biol* **157**, 807 (May 27, 2002).
21. W. M. Zhao, G. Fang, *J Biol Chem* **280**, 33516 (Sep 30, 2005).
22. M. De Brabander, J. De May, M. Joniau, G. Geuens, *Cell Biol Int Rep* **1**, 177 (Mar, 1977).
23. E. M. Bradbury, R. J. Inglis, H. R. Matthews, *Nature* **247**, 257 (Feb 1, 1974).
24. E. Jacinto *et al.*, *Nat Cell Biol* **6**, 1122 (Nov, 2004).

25. S. F. Tavazoie, V. A. Alvarez, D. A. Ridenour, D. J. Kwiatkowski, B. L. Sabatini, *Nat Neurosci* **8**, 1727 (Dec, 2005).
26. J. Urban *et al.*, *Mol Cell* **26**, 663 (Jun 8, 2007).
27. P. Fabrizio, F. Pozza, S. D. Pletcher, C. M. Gendron, V. D. Longo, *Science* **292**, 288 (Apr 13, 2001).
28. D. D. Sarbassov, D. A. Guertin, S. M. Ali, D. M. Sabatini, *Science* **307**, 1098 (Feb 18, 2005).
29. E. J. Chen, C. A. Kaiser, *J Cell Biol* **161**, 333 (Apr 28, 2003).
30. D. A. Guertin *et al.*, *Dev Cell* **11**, 859 (Dec, 2006).
31. R. Fox *et al.*, *Embo J* **26**, 505 (Jan 24, 2007).
32. A. Huber *et al.*, *Genes Dev* **23**, 1929 (Aug 15, 2009).
33. M. Amano *et al.*, *Genes Cells* **3**, 177 (Mar, 1998).

Experimental procedures

Materials

Reagents were obtained from the following sources: Rho Assay Reagent (Rhotekin RBD agarose), and antibodies to DEPTOR, raptor, Rho, phospho-T696 Mypt1 from Millipore; mouse monoclonal DEPTOR antibody from Novus Biologicals; antibodies to phospho-S10 Histone H3, mTOR, actin, as well as HRP-labeled secondary antibodies from Santa Cruz Biotechnology; antibodies to mTOR, phospho-S19 MLC2, phospho-S3 Cofilin, Cofilin, and the c-MYC epitope from Cell Signaling Technology; α-tubulin antibodies, Y-27632, and nocodazole from Sigma Aldrich; DMEM from SAFC Biosciences; rapamycin from LC Labs; PreScission protease from Amersham Biosciences; pTREQ Tet-On vector from Clontech; FuGENE 6 and Complete Protease Cocktail from Roche; Alexa Fluor 488 and 568 Phalloidin, Propidium Iodide, and inactivated fetal calf serum (IFS) from Invitrogen. Torin1 was kindly provided by Nathaniel Gray (Harvard medical School).

Cell Lines and Cell Culture

HeLa, HEK-293T, and MEFs were cultured in DMEM with 10% Inactivated Fetal Bovine Serum (IFS). p53-/- MEFs were kindly provided by David Kwitakowski (Harvard Medical School). The HeLa cell line with doxycycline-inducible DEPTOR expression was generated by retroviral transduction of HeLa that were previously modified to express rtTA with an inducible DEPTOR cDNA (*8*).

cDNA Manipulations, Mutagenesis, and Sequence Alignments

The cDNAs for DEPTOR and metap2 was previously described. The cDNA for full-length wild-type ROCK2 was kindly provided by K. Kaibuchi (*33*).

Mammalian Lentiviral shRNAs

Lentiviral shRNAs to the indicated human and mouse genes were previously described (*8, 28*) .

shRNA-encoding plasmids were co-transfected with the Delta VPR envelope and CMV VSV-G packaging plasmids into actively growing HEK-293T using FuGENE 6 transfection reagent as previously described (*28*). Virus containing supernatants were collected at 48 hours after transfection, filtered to eliminate cells, and target cells infected in the presence of 8 μg/ml polybrene. For all cell types, 24 hours after infection, the cells were split into fresh media, selected with 1 μg/ml puromycin. Five days post-infection, shRNA-expressing cells were analyzed or split again and analyzed 2-3 days later. All shRNA-expressing cells were analyzed at 50-75% confluence.

Cell Lysis and Immunoprecipitations

All cells were rinsed with ice-cold PBS before lysis. All cells were lysed with Triton-X 100 containing lysis buffer (40 mM HEPES [pH 7.4], 2 mM EDTA, 10 mM sodium pyrophosphate, 10 mM sodium glycerophosphate, 150 mM NaCl, 50 mM NaF, 1% Triton-X 100, and one tablet of EDTA-free protease inhibitors [Roche] per 25 ml). The soluble fractions of cell lysates were isolated by centrifugation at 13,000 rpm for 10 min in a microcentrifuge. For measurement of the Rho-GTP loading state, Rho Assay Reagent was used according to the manufacturer's protocol (Millipore). To observe gel mobility shifting in DEPTOR, 8% Tris Glycine gels (Invitrogen) were used. For all other applications, 4-12% Bis-Tris gels (Invitrogen) were used.

cDNA Transfection

To examine the effects of ROCK2 overexpression on endogenous S19 MLC2 phosphorylation, 500,000 HEK-293T were plated in 6 cm culture dishes in DMEM/10% IFS. 24 hours later, cells were transfected with 1 μg of the indicated pRK5-based cDNA expression plasmids. All cells were lysed at 50-75% confluence 24 hours after transfection.

Immunofluorescence Assays

25,000-100,000 cells were plated on fibronectin-coated glass coverslips in 12-well tissue culture plates, rinsed with PBS once and fixed for 15 minutes with 4% paraformaldehyde in PBS warmed to 37°C. The coverslips were rinsed three times with

PBS and permeabilized with 0.2% Triton X-100 in PBS for 15 minutes. After rinsing three times with PBS, the coverslips were blocked for one hour in blocking buffer (0.25% BSA in PBS), incubated with primary antibody in blocking buffer overnight at 4°C, rinsed twice with blocking buffer, and incubated with secondary antibodies (diluted in blocking buffer 1:1000) and/or Phalloidin for one hour at room temperature in the dark. The coverslips were then rinsed twice more in blocking buffer and twice in PBS, mounted on glass slides using Vectashield containing DAPI (Vector Laboratories), and imaged with a 10x or 63X objective using epifluorescence microscopy. Quantification of the percentage of p-H3 positive cells was performed with CellProfiler (www.cellprofiler.org) using 10x images. After illumination correction, the nuclei were automatically identified using the DAPI staining. P-H3 positive cells were defined by threshold intensity. The percentage of p-H3 positive cells was then determined by the quotient of the total number of nuclei above that threshold intensity divided by total number of nuclei in the field.

Live Cell Imaging

HeLa cells were plated on glass-bottom dishes (MatTek). Cells were imaged with an ORCA-ER camera (Hammamatsu) attached to a Nikon TE2000 microscope. All images were collected, measured, and compiled with the aid of Metamorph imaging software (Molecular Devices) and Adobe Photoshop. For time-lapse imaging, cells were kept at 37°C with the aid of a Solent incubation chamber (Solent Inc.).

Fluorescence Activated Cell Sorting

Exponentially growing cells were treated as indicated, trypsinized, washed once in ice-cold PBS and fixed overnight in 1 ml 70% ethanol on ice. Cells were washed once in PBS and incubated in PBS containing 70 µM propidium iodide and 10 mg/ml RNAse A at 37°C for 30 minutes. Flow cytometry analysis was performed using a Becton-Dickinson FACScan machine and CellQUEST DNA Acquisition software.

Acknowledgements

The authors thank Glenn Paradis for technical assistance. We thank members of the Sabatini lab for helpful discussions. This work was supported by fellowships from the American Diabetes Association and Ludwig Cancer Fund to T.R.P.; D.M.S. is an investigator of the Howard Hughes Medical Institute and is additionally supported by grants from the National Institutes of Health and awards from the Keck Foundation and LAM Foundation; None of the authors have a conflict of interest related to the work reported in this manuscript.

Chapter 6

Future Directions

Summary

The mTORC1 pathway controls cell growth, survival, and proliferation by spatially and temporally orchestrating many key aspects of cell metabolism. In the work describe here, we have investigated the localization of mTORC1-dependent pathways that control lipid and protein synthesis as well as those that regulate the cell cycle. We identify that mTORC1 regulates cholesterol and lipid homeostasis by regulating the cytoplasmic-nuclear localization of the phosphatidic acid phosphatase, lipin 1. In a growth factor- and nutrient-dependent manner, mTORC1 and GSK3 phosphorylate lipin 1 which promotes its cytoplasmic retention. However, in the absence of mTORC1 and GSK3 activity, lipin 1 accumulates in the nucleus where it downregulates SREBP target gene expression by altering the structure of the lamin A-containing nuclear matrix and sequestering SREBP in it. We also have examined how mTORC1 controls the cytoskeletal machinery that drives the fission of daughter cells upon completion of the cell cycle. As part of this effort, we identified a novel mTOR interacting protein, DEPTOR, which negatively regulates mTORC1 and mTORC2, but paradoxically activates PI3K/mTORC2 signaling when overexpressed. Hyperactivation of mTORC1 caused by DEPTOR depletion hyperactivates Rho-Rho Kinase-dependent, actin-myosin contractility during cytokinesis and ultimately leads to polyploidy. Lastly, we have shed light on the long-standing question of how amino acids activate mTORC1 signaling towards the translational regulator, S6K1. We identify that mTORC1 relocalizes from the cytosol to a Rab7-containing endomembrane compartment upon amino acid stimulation of cells where it becomes juxtaposed to the mTORC1-activating GTPase, Rheb. We also find that this relocalization, which requires the canonical mTORC1 component, raptor, and mTORC1 signaling, are both dependent on a novel heterodimer GTPase complex, Rag A/B/C/D. The following discussion explores some of the new questions that have emerged from this work.

Phosphatidic acid: a key signaling lipid for both cholesterol synthesis and mTORC1 activity?

We find that lipin 1, a phosphatase for the phospholipid, phosphatidic acid (PA), requires its catalytic activity to regulate SREBP target gene expression (Chapter 2, Fig.3D). Similarly, the catalytic activity of the lipin 1 *S. cerevisiae* homolog, Pah1, has been previously shown to be required for its effects on neutral lipid biosynthesis and gene expression (*1*). These results suggest that the levels of the substrate of lipin 1, PA and as well as its product, diacylgycerol (DAG), are conserved, key regulatory molecules in sterol- and lipogenesis production. While DAG is readily appreciated as a rate-limiting substrate in triacylglycerol synthesis (*2*), the role for PA as a signaling intermediate in sterol synthesis and SREBP function is less well known. While the 'sensing' of cholesterol abundance in the endoplasmic reticulum (ER) by the SREBP escort protein, SCAP, has long been known to be a crucial part of the mechanism for controlling SREBP cleavage (*3*), more recent work presents a distinct view for how the SREBP pathway may be thought to be regulated (*4*). Unlike in mammalian cells, where most of the pioneering studies on the SREBP pathway were performed, insect cells, such as the widely utilized drosophila S2 cell line, do not produce sterols and the major targets of SREBP in these cells are not cholesterol biosynthetic genes, but rather those that promote saturated fatty acid formation (*4*). More surprisingly, it was shown it these cells that phospholipids such as phosphatidylethanolamine (PE), and not cholesterol, are the major controllers of SREBP cleavage (*5*). These results suggest that the cleavage of SREBP, rather than necessarily being tied to the presence or absence of cholesterol per se, might be controlled by the levels of different components of internal membranes in different organisms, and that 'membrane integrity' might be a more general term to describe what is being sensed by this pathway.

Another indication of the potential importance of phospholipids in regulating cholesterol homeostasis comes from a recent study in yeast on the function of Pah1 phosphorylation. In a gain-of function screen, Han et al. identified the PA-generating, CTP-dependent, diacylglycerol kinase 1 (DGK1) as a gene whose overexpression rescues the lethality caused by inositol deprivation of cells harboring a constitutively

dephosphorylated Pah1 mutation (*6, 7*). That overexpressing DGK1 restored PA levels in these Pah1 mutant cells and that this particular phospholipid is required for proper nuclear membrane proliferation, which is an essential feature of cell division (*8*), highlights the importance of PA in eukaryotic cells (*7*). Though the authors did not explicitly address the relationship between PA and cholesterol levels in this study, one hypothesis following from their work for how low levels of nuclear PA might inhibit cholesterol synthesis could be that the SREBP transcriptional machinery is particularly sensitive to the physical space provided to it in the nucleus. Our work suggesting that mTORC1 inhibition or constitutively dephosphorylated lipin 1 promotes the binding of lamin A with a SREBP response element (Fig. S5C-D) is consistent with this hypothesis. Furthermore, it has recently been shown that deletion of the Pah1 phosphatase regulatory subunit, spo7, promotes expansion of the nuclear membrane (*9*). Considering that this expansion is specifically filled by the nucleolus and that TORC1 is a key regulator of ribosome biogenesis which is a process that primarily takes place in the nucleolus (*9, 10*), it is tempting to consider that sterol biosynthesis might concurrently be controlled in this same nuclear subcompartment by the PA hydrolyzing activity of lipin 1.

While we have mainly focused on PA as being a downstream signal of mTORC1 acted on by nuclear lipin 1, PA is also believed to be a key phospholipid for promoting mTORC1 kinase activity (*11*). How might these two findings indicate the mutual interest of mTORC1 and lipin 1 in this particular phospholipid? Consider the following model based on the evidence we present or reference herein: in the absence of upstream signals to activate mTORC1 (e.g., amino acids), 1) mTORC1 resides in the cytosol where it does not contact PA and where it consequently is unable to phosphorylate lipin 1; 2) lipin 1 associates with nuclear membranes (as well as cytoplasmic membranes depending on how much mTORC1 activity is lost) where it hydrolyzes PA; and thus 3) mTORC1 is not inappropriately activated in the PA-depleted membrane environment where lipin 1 localizes. On the contrary, in the presence of an mTORC1-activating stimuli, 4) mTORC1 becomes associated with PA-containing cytoplasmic membranes; 5) this PA-containing membrane environment promotes the phosphorylation and redistribution of lipin 1 to the cytosol which; 6) preserves PA levels and mTORC1

activity in the local membrane environment where mTORC1 resides. Our work characterizing the localization of mTORC1 is consistent with it being translocated from the cytosol to cytoplasmic membranes upon activating stimuli such as amino acids (Chapter 4, Figs.4-5). Recent work by Harris et al. is consistent with lipin 1 translocating from the cytosol to endomembranes upon decreased mTORC1 activity (*12*). Additionally, we show that mTORC1 and lipin 1 can physically interact in cells in a Torin1-manner (Chapter 2, Fig. 2D, S2B), which is consistent with mTORC1 and lipin 1 co-localizing (at least transiently) to a shared compartment in a manner dependent on mTOR kinase activity. Future work aimed at determining the levels of PA in the membrane compartments where mTORC1 and lipin 1 jointly reside as well as in more precisely defining the cytosol/membrane localizations of mTORC1 and lipin 1 upon changes in mTORC1 activity will be required to further investigate this model.

How does mTORC1 regulate SREBP localization?

As previously discussed, SREBP is known to localize in the ER and upon intracellular cholesterol depletion, to translocate to the golgi and subsequently the nucleus where it binds sterol response element-containing DNA and transactivates cholesterol biosynthetic gene expression. We report that in the absence of mTORC1 signaling, SREBP1 relocalizes from presumably the ER and/or golgi to the nuclear periphery where it colocalizes with lamin A (Chapter 2, Fig. 5H). Our work, while leading to a preliminary explanation for how mTORC1 inhibition represses SREBP target gene expression, does not attempt to explain how mTORC1 signaling and cholesterol levels might be coordinated to determine SREBP localization. However, potentially placing already synthesized cholesterol upstream of mTORC1, previous work does indirectly suggest that mTORC1 might regulate the cleaved, mature form of SREBP at the level of its nuclear import-export.

Rapamycin has previously been shown to regulate the nuclear localization of multiple nutrient-regulated transcription factors (*16*). Nuclear transport of cargo is known to be controlled by the coordinated actions of multiple proteins, notably including the importins and the Ran GTPase (*13*). Suggesting a potential role of TORC1 in regulating nuclear transport through Ran, inactivation of the *S. cerevisiae* RagA/B homolog, Gtr1,

or overexpression of the *Schizosaccharomyces pombe* lipin 1 homolog, Ned1, both produce phenotypes consistent with mTORC1 inhibition promoting the Ran-GTP state (*14, 15*). Regarding the nuclear import of SREBP, it has been shown that reconstitution of permeabilized cells with co-injection of wild-type importin-β, the active GTP-bound form of Ran, and mature SREBP-2 promoted the full nuclear accumulation of SREBP-2 (*17*). On the other hand, co-expression of SREBP-2 and importin alone, promoted SREBP-2 accumulation at the nuclear rim, which is similar to that we detected with SREBP-1 after mTORC1 inhibition with Torin1 (Chapter 2, Fig. 5H). Based on the above results, we find it reasonable to speculate that SREBP localization might be dependent on mTORC1 regulating importin-β function and/or the Ran-GTP/GDP state.

Furthermore, regarding the function of importins, TOR-dependent phosphorylation of Gln3, a transcriptional activator of nitrogen catabolite repressible genes, is known to regulate its interaction with the importin, Srp1p, and thereby control its localization (*18*). SREBP is also known to be regulated by phosphorylation which is controlled by GSK3 (*19*), a kinase we show both to be regulated by mTORC1 and to regulate lipin 1 phosphorylation (Chapter 2, Fig.2E-F). Drawing analogy with Gln3, it is conceivable that mTORC1 controls SREBP localization by controlling the ability of GSK3 to phosphorylate it. If this were true, how then would lipin 1 participate in the regulation of SREBP phosphorylation-dependent localization? One way might be through lipin 1 controlling PA levels and therefore mTORC1-GSK3 activity. Because GSK3 phosphorylation of SREBP is known to regulate SREBP degradation, conceivably this turnover might be accomplished through piecemeal microautophagy of the nucleus, a process known to be under the control of TORC1 signaling (*20*). Alternatively, perhaps PA or DAG initiates a signaling cascade distinct from TORC1-GSK3 kinase activity which impinges on the importin-Ran nuclear transport cycle (*21*). Regardless, exploration of the understudied subject of nuclear signaling should provide a clearer picture of how SREBP localization might be controlled by mTORC1.

mTOR: the Target Of DEPTOR

While we learned that DEPTOR negatively regulates the mTOR pathway (Chapter 3), we still have few insights into its mechanism of action on mTOR. One

possibility warranting further consideration is whether the ability of DEPTOR to regulate mTOR depends on its association with a particular membrane environment. Our interest in this idea comes from a study of another DEP domain containing protein, Dishevelled, whose interaction with the Frizzled receptor and effects on planar cell polarity signaling require the interaction of its DEP domain with negatively charged phospholipids (*22*). During cytokinesis, it is known that the phosphatidylinositol, PIP3, and the lipid kinase which generates it, PI3K, are present on the leading edge of the daughter cells, while the PIP3 phosphatase, PTEN, and PIP2 accumulate at the cleavage furrow (*23*). Because we detect DEPTOR at the cleavage furrow (Chapter 4, Fig. 4A), one can reason that DEPTOR might dampen mTOR signaling during cytokinesis by having its interaction with mTOR being modulated by its concomitant interaction with PIP2. Experiments to assess whether DEPTOR binds to this lipid or other neutral or phospholipids in vitro would be a first pass at addressing this question.

Defining the affinity of DEPTOR and mTOR for certain phospholipids might also enable the development of increasingly physiological mTORC1 and/or mTORC2 *in vitro* kinase assays. We found that DEPTOR depletion from mTORC1 and mTORC2 complexes in cells increases their respective *in vitro* kinase activities (Fig. 3B, D). However, because we were unable to demonstrate specific binding of DEPTOR to mTORC1 or mTORC2 *in vitro* (data not shown), this precluded us from determining whether DEPTOR alone was sufficient to produce the changes in mTORC1 or mTORC2 kinase activities obtained from DEPTOR deficient cells. Our lab has previously shown that mTORC1 is activated by the non-ionic detergent, Triton X-100 (*24*). In future work, it would be interesting to determine whether certain natural lipids, such as PIP2, might facilitate a specific interaction of DEPTOR with mTOR *in vitro*. If this were the case, we could then test whether the presence of these lipids were required for DEPTOR to inhibit mTORC1 or mTORC2 *in vitro* kinase activities.

Lastly, we would like to understand better the importance of mTOR-dependent phosphorylation of DEPTOR on mTOR activity. Here, it might also prove valuable to draw analogy to the function of another DEP domain protein, Sst2, which regulates pheromone signaling in yeast (*25*). Sst2 docks to the pheromone receptor, Ste2, only when Ste2 is unphosphorylated, and this allows for the release of Sst2 upon receptor

densensitization and internalization (*25*). Similarly, perhaps DEPTOR phosphorylation by mTOR provides a densensitization mechanism whereby mTOR signaling could be downregulated once the level of DEPTOR phosphorylation reaches a certain threshold. Because Sst2 ultimately controls Ste2 localization, one could test this analogy by determining whether manipulation of DEPTOR function alters the localizations of mTORC1 and/or mTORC2 (*26*).

Why is the late endosome/lysosome key for mTORC1 pathway activity?

We identify a Rab7-positive compartment to which mTORC1 migrates upon amino acid stimulation where it comes into proximity with its activator, Rheb (Chapter 4, Fig.4,5). This result begs the following questions: 'what is unique about the Rab7-positive compartment?' and 'where is Rab7 in the cell?' Rab7 is a homolog of the yeast Ypt7, which is a GTPase that localizes to the late endosomes and mediates endosomal fusion with the vacuole (*27*). In yeast, it is known that TORC1 localizes to the vacuole (*28, 29*) and more recently, our lab has shown that mTORC1 localizes to lysosome, which is the mammalian vacuole equivalent (*30*). The vacuole/lysosome is an acidic organelle with both degradative and storage capabilities (*31*). Amongst the storage capabilities, the vacuole is known to accumulate amino acids, and in particular those that are neutral or possess basic charge (*32*). Of the basic amino acids, arginine has received particular notice because the levels of it and its derivatives are substantially altered in TOR1, TSC1, TSC2, and BHD null cells (*33*). Pointing to the importance of the vacuole as a nitrogen reserve, the vacuolar storage of arginine, the amino acid with the highest nitrogen content involves three separate transport mechanism (*32*). Key for TORC1 activation, nitrogen starvation through limitation of glutamine, is one way to promote the release of vacuolar arginine (*34, 35*). Importantly, this release is not a general response to amino acid starvation as it is not elicited by proline deprivation (*36*). Interestingly, arsenate, which disrupts ATP production by inhibiting glycolysis (by blocking 1, 3-biphosphoglycerate synthesis), also leads to arginine mobilization from the vacuole (*37*). That respiratory inhibitors or uncouplers similarly block vacuolar arginine release suggests that, in addition to glutamine, the vacuole might have an energy requirement for controlling arginine efflux (*37*).

How then might arginine occupy a unique role in promoting TOR signaling? Perhaps the answer lies in polyamine biology. Polyamines are direct products of arginine catabolism that are known to accumulate in/on endosomal membranes with low pH (*38*). Further aligning with a putative role in TORC1 signaling, polyamines, such as spermidine, are known to be potent inducers of autophagy and have an essential role in cell growth (*39, 40*). One hypothesis that could place polyamines upstream of TORC1 activity would be if they were to build-up on vacuolar/lysosomal membranes in the absence of TORC1-activating inputs such as glutamine such that they might disrupt the association of TORC1 with these membranes (i.e., as an result of arginine release from the vacuole and subsequent polyamine production). Better defining the amino acid flux and energy requirements that allow for the deposition and/or preservation of TORC1 on vacuolar/lysosomal membranes will be required to address this hypothesis.

Conclusions

By studying the geography of mTORC1 signaling, namely in the nucleus, on internal membranes, and of the actin cytoskeleton, we now have a better view of how mammalian cells control their growth. Rapamycin, a highly selective TOR inhibitor, has proven itself to be a trusty 'compass' in defining the cellular 'map' of TOR signaling we know today. Ironically, many of key findings we report here were instead made possible through use of a distinct class of mTOR inhibitor fronted by Torin1. For example, because Torin1, unlike rapamycin, inhibits both mTOR in mTORC1 and mTORC2, it was possible for us to demonstrate that DEPTOR functions as a negative regulator of both mTOR pathways. Additionally, because Torin1 inhibits mTORC1 more potently than rapamycin, we could readily detect that mTORC1 controls lipin 1 nuclear-cytoplasmic shuttling, which was a key initial insight in connecting lipin 1 to the regulation of the SREBP pathway. Considering the value of Torin1, a next step would be to put it to use in revisiting TOR signaling in other experimental models which have relied upon rapamycin until now. It is our expectation that these experiments should enable the identification of additional players in the TOR signaling as well as shed further insights on the players these compounds have already helped characterize, such

as DEPTOR and lipin 1. No doubt, charting the remaining territory of TOR signaling appears close at hand.

References

1. G. S. Han, S. Siniossoglou, G. M. Carman, *J Biol Chem* **282**, 37026 (Dec 21, 2007).
2. R. M. Bell, R. A. Coleman, *Annu Rev Biochem* **49**, 459 (1980).
3. X. Hua, A. Nohturfft, J. L. Goldstein, M. S. Brown, *Cell* **87**, 415 (Nov 1, 1996).
4. A. C. Seegmiller *et al.*, *Dev Cell* **2**, 229 (Feb, 2002).
5. I. Y. Dobrosotskaya, A. C. Seegmiller, M. S. Brown, J. L. Goldstein, R. B. Rawson, *Science* **296**, 879 (May 3, 2002).
6. G. S. Han, W. I. Wu, G. M. Carman, *J Biol Chem* **281**, 9210 (Apr 7, 2006).
7. G. S. Han, L. O'Hara, G. M. Carman, S. Siniossoglou, *J Biol Chem* **283**, 20433 (Jul 18, 2008).
8. B. Burke, J. Ellenberg, *Nat Rev Mol Cell Biol* **3**, 487 (Jul, 2002).
9. J. L. Campbell *et al.*, *Mol Biol Cell* **17**, 1768 (Apr, 2006).
10. F. M. Boisvert, S. van Koningsbruggen, J. Navascues, A. I. Lamond, *Nat Rev Mol Cell Biol* **8**, 574 (Jul, 2007).
11. Y. Fang, M. Vilella-Bach, R. Bachmann, A. Flanigan, J. Chen, *Science* **294**, 1942 (Nov 30, 2001).
12. T. E. Harris *et al.*, *J Biol Chem* **282**, 277 (Jan 5, 2007).
13. M. Stewart, *Nat Rev Mol Cell Biol* **8**, 195 (Mar, 2007).
14. N. Nakashima, N. Hayashi, E. Noguchi, T. Nishimoto, *J Cell Sci* **109 (Pt 9)**, 2311 (Sep, 1996).
15. Y. Tange, A. Hirata, O. Niwa, *J Cell Sci* **115**, 4375 (Nov 15, 2002).
16. T. Beck, M. N. Hall, *Nature* **402**, 689 (Dec 9, 1999).
17. E. Nagoshi, N. Imamoto, R. Sato, Y. Yoneda, *Mol Biol Cell* **10**, 2221 (Jul, 1999).
18. J. Carvalho, P. G. Bertram, S. R. Wente, X. F. Zheng, *J Biol Chem* **276**, 25359 (Jul 6, 2001).
19. A. Sundqvist *et al.*, *Cell Metab* **1**, 379 (Jun, 2005).
20. P. Roberts *et al.*, *Mol Biol Cell* **14**, 129 (Jan, 2003).

21. M. Okada, K. Ye, *RNA Biol* **6**, 12 (Jan-Mar, 2009).
22. M. Simons *et al.*, *Nat Cell Biol* **11**, 286 (Mar, 2009).
23. C. Janetopoulos, J. Borleis, F. Vazquez, M. Iijima, P. Devreotes, *Dev Cell* **8**, 467 (Apr, 2005).
24. D. H. Kim *et al.*, *Cell* **110**, 163 (Jul 26, 2002).
25. D. R. Ballon *et al.*, *Cell* **126**, 1079 (Sep 22, 2006).
26. T. W. Sturgill *et al.*, *Eukaryot Cell* **7**, 1819 (Oct, 2008).
27. H. Wichmann, L. Hengst, D. Gallwitz, *Cell* **71**, 1131 (Dec 24, 1992).
28. M. E. Cardenas, J. Heitman, *Embo J* **14**, 5892 (Dec 1, 1995).
29. W. K. Huh *et al.*, *Nature* **425**, 686 (Oct 16, 2003).
30. Y. Sancak *et al.*, *Cell* **141**, 290 (Apr 16).
31. S. C. Li, P. M. Kane, *Biochim Biophys Acta* **1793**, 650 (Apr, 2009).
32. D. J. Klionsky, P. K. Herman, S. D. Emr, *Microbiol Rev* **54**, 266 (Sep, 1990).
33. M. van Slegtenhorst *et al.*, *J Biol Chem* **282**, 24583 (Aug 24, 2007).
34. F. Dubouloz, O. Deloche, V. Wanke, E. Cameroni, C. De Virgilio, *Mol Cell* **19**, 15 (Jul 1, 2005).
35. T. L. Legerton, R. L. Weiss, *J Biol Chem* **259**, 8875 (Jul 25, 1984).
36. R. H. Davis, *Microbiol Rev* **50**, 280 (Sep, 1986).
37. C. Drainas, R. L. Weiss, *J Bacteriol* **150**, 770 (May, 1982).
38. D. Soulet, B. Gagnon, S. Rivest, M. Audette, R. Poulin, *J Biol Chem* **279**, 49355 (Nov 19, 2004).
39. R. A. Casero, Jr., L. J. Marton, *Nat Rev Drug Discov* **6**, 373 (May, 2007).
40. T. Eisenberg *et al.*, *Nat Cell Biol* **11**, 1305 (Nov, 2009).